nº de arquivo

“copyright”

ANA ZÉLIA ALMEIDA DE FRANÇA E MILLER

PRIMARY BIORECEPTIVITY OF LIMESTONES FROM THE MEDITERRANEAN BASIN TO PHOTOTROPHIC MICROORGANISMS

Dissertação apresentada para a obtenção do grau de Doutor em Conservação e Restauro pela Universidade Nova de Lisboa, Faculdade de Ciências e Tecnologia.

Lisboa

2010

The main results presented in this PhD thesis have been published or accepted for publication in international journals included in the Science Citation Index (SCI):

Macedo, M.F., Miller, A.Z., Dionísio, A., Saiz-Jimenez, C., 2009. Biodiversity of cyanobacteria and green algae on monuments in the Mediterranean Basin: an overview. Journal of Microbiology 155, 3476-3490.

Miller, A.Z., Laiz, L., Dionísio, A., Macedo, M.F., Saiz-Jimenez, C. 2009a. Growth of phototrophic biofilms from limestone monuments under laboratory conditions. International Biodeterioration and Biodegradation 63, 860-867.

Miller, A.Z., Laiz, L., Gonzalez, J.M., Dionisio, A., Macedo, M.F., Saiz-Jimenez, C., 2008. Reproducing stone monument photosynthetic-based colonization under laboratory conditions. Science of the Total Environmental 405, 278-285.

Miller, A.Z., Leal, N., Laiz, L., Rogerio-Candelera, M.A., Silva, R.J.C., Dionisio, A., Macedo, M.F., Saiz-Jimenez, C. 2010. Primary bioreceptivity of limestones used in Southern Europe monuments. In: Smith, B.J., Gomez-Heras, M., Viles, H.A., Cassar, J. (Eds), Limestone in the Built Environment: Present Day Challenges for the Preservation of the Past. Geological Society of London, Special Publications 331, 79-92.

Miller, A.Z., Dionísio, A., Laiz, L., Macedo, M.F., Saiz-Jimenez, C. 2009b. The influence of inherent properties of building limestones on their bioreceptivity to phototrophic microorganisms. Annals of Microbiology 59, 1-9.

Miller, A.Z., Rogerio-Candelera, M.A., Laiz, L., Wierzchos, J., Ascaso, C., Sequeira Braga, M.A., Hernández-Mariné, M., Maurício, A., Dionísio, A., Macedo, M.F., Saiz-Jimenez, C., 2010. Laboratory-induced endolithic growth in calcarenites: biodeteriorating potential assessment. Microbial Ecology (accepted).

ACKNOWLEDGEMENTS

This PhD was performed at Departamento de Conservação e Restauro, Faculdade de Ciências e Tecnologia – Universidade Nova de Lisboa (DRC-FCT-UNL), at Centro de Petrologia e Geoquímica, Instituto Superior Técnico (CEPGIST), and at Instituto de Recursos Naturales y Agrobiología de Sevilla – Consejo Superior de Investigaciones Científicas (IRNAS-CSIC). This multidisciplinary work would not have been possible without the financial support from the Fundação para a Ciência e a Tecnologia, Ministério da Ciência, Tecnologia e Ensino Superior (Portugal), (PhD grant SFRH/BD/21481/2005). It allowed not only to join expertise, knowledge and equipment, but also to make new contacts, and even friendships.

I would like to express my sincere gratitude to Dr. Maria Filomena Macedo, Auxiliary Professor of DCR-FCT-UNL, who has been my supervisor since the beginning of my PhD study. I am very grateful for her valuable contribution on the experimental design, helpful suggestions, important advice and constant encouragement during the course of this work.

I also wish to express my special gratitude to my co-supervisors Dr. Amélia Dionísio, Auxiliary Professor of Instituto Superior Técnico and member of CEPGIST, and Prof. Dr. Cesareo Saiz-Jimenez, Research Professor from IRNAS-CSIC, for the opportunity they gave me to work at their laboratories and for their invaluable assistance. They supported and provided many valuable suggestions that improved the quality of this study.

I would like to thank all people of the IRNAS-CSIC for all the help and the pleasant atmosphere. Special appreciation and gratitude are given to Dr. Leonila Laiz for her teaching, hospitality and friendship, as well as to Miguel Rogerio-Candelera for his essential collaboration in the digital image analysis, as well as constant encouragement, helpful suggestions and friendship.

Sincere thanks are also expressed to Prof. Dr. Carmen Ascaso and Dr. Jacek Wierzchos, both from Centro de Ciencias Medioambientales – CSIC (Madrid, Spain) for their hospitality and valuable collaboration in the scanning electron microscopy with back-scattered electron imaging (SEM-BSE) analysis.

I also would like to thank Prof. Dr. Mariona Hernández-Mariné from Facultat de Farmàcia, Universitat de Barcelona (Spain) and Dr. Mónica Roldán from Universidad Autónoma de Barcelona (Spain) for their hospitality and valuable collaboration in the taxonomic identification and confocal laser scanning microscopy examinations.

I am very grateful to Dr. Rui Silva (CENIMAT, FCT-UNL) for the SEM analysis performed at CENIMAT. I also would like to express my keen appreciation to Elin Figueiredo (DCR-FCT-UNL) for her help in this analysis, as well as for her support and friendship.

I also would like to express my appreciation and gratitude to Dr. António Maurício and Dr. Amália Sequeira Braga from CEPGIST for their special and helpful collaboration in the laboratory-induced endolithic growth analyses and data discussion.

I would like to thank Inês Gomes, Dr. Nuno Leal and all my colleagues from DCR-FCT-UNL for the support, collaboration and the pleasant time we shared. Special gratitude goes to Prof. Dr. Fernando Pina from DCR-FCT-UNL for the valuable suggestions and advices during this work.

I also thank many other people who helped me during sampling and experimental work, as well as their valuable comments.

To my friends, I would like to thank their support, affection and also the good time they provided me in my life outside the PhD.

I would like to express my impassioned thanks to José María de la Rosa and his family for their kindness and affection, and for never letting me feel that I was away from my parents and country, during my stay in Seville.

Finally, my special appreciation and heartiest thanks goes to my parents, who always kept me away from family responsibilities and encouraged me to concentrate on my study. Without their help, mental support and encouragement, this study would not have been completed.

Thanks a million

Ana Zélia Miller

ABSTRACT

The conservation of historic buildings and monuments from cultural heritage is a major issue in modern societies, both from an economical and cultural point of view. The wide distribution of stone monuments and lithic works of art, and their cultural, artistic and religious importance emphasise the general need to safeguard this praiseworthy cultural heritage. This PhD thesis arises from the growing national and international interest on the biodeterioration of stone cultural heritage as one of the most complex areas of stone conservation and restoration.

This study aimed to evaluate the primary bioreceptivity of limestones widely used as building materials in European countries from the Mediterranean Basin. In the first instance, a review of the literature was achieved in order to compare and be acquainted with the most abundant cyanobacteria and green algae detected on stone monuments. *Gloeocapsa*, *Phormidium* and *Chroococcus*, among cyanobacteria, and *Chlorella*, *Stichococcus* and *Chlorococcum*, among chlorophyta, were the most widespread genera identified on outdoor stone monuments. Limestone and marble were the lithotypes presenting the greatest diversity of phototrophic microorganisms. In the second step, five green biofilms were collected from Orologio Tower in Martano (Italy), Santa Clara-a-Velha Monastery (Coimbra) and Ajuda National Palace (Lisbon), both in Portugal, and Seville and Granada Cathedrals from Spain. The biofilm samples were subsequently characterised by molecular biology techniques and cultivated under laboratory conditions. DNA-based molecular analysis of 16S rRNA gene fragments revealed that the biofilms from Orologio Tower and Santa Clara-a-Velha Monastery were dominated by the microalga *Chlorella*, whereas the cyanobacterium *Chroococcidiopsis* was the dominating genus from Ajuda National Palace. The biofilms from Seville and Granada Cathedrals (Spain) were both dominated by the cyanobacterium *Pleurocapsa*. DGGE analysis of the cultivated biofilms revealed a remarkable stability of the microbial components from the Coimbra biofilm. This multiple-species phototrophic culture was further used as inoculum for stone bioreceptivity experiments. Laboratory-based stone colonisations relied on the inoculation of five limestone types with the selected biofilm culture, incubation within a growth chamber and monitoring of photosynthetic biomass through different analytical approaches. Subsequently, the primary bioreceptivity of *Ançã* (CA) and *Lioz* (CL) limestones, *San Cristobal* (SC) and *Escúzar* (PF) stones

and *Lecce* stone (PL) was determined, evaluating the relationship between stone intrinsic properties and photosynthetic growth. The results were statistically analysed by means of principal component analysis (PCA) and analysis of variance (ANOVA) in an attempt to determine their bioreceptivity to phototrophic microorganisms and to evaluate the direct relationships between stone bioreceptivity and petrophysical properties. *Escúzar* stone followed by *San Cristobal* stone showed the highest bioreceptivity, contrasting with the lowest bioreceptivity of *Lioz* limestone. *Ançã* and *Lecce* stones revealed moderate bioreceptivity. The petrophysical characteristics, water absorption by capillarity, surface roughness, as well as open porosity and water vapour permeability, were the keys for the microbial development on the stone samples. Finally, biogeochemical and biogeophysical deterioration were appraised on the lithotypes in which endolithic growth was detected. The results suggested chemical biocorrosion by active mineral dissolution and biomineralisation as a consequence of the inoculated phototrophic community.

The laboratory-based bioreceptivity experiments demonstrated that preliminary research is essential to make predictions and to choose the best conservation strategy concerning the potential bioreceptivity characteristics of the materials used in monuments. The high values of water absorption by capillarity and open porosity obtained for PF, SC and PL indicate great susceptibility to biodeterioration, which render them unsuitable for very humid outdoor environments if preventive treatments, such as the application of hydro-repellents, are not taking into account. The relative low values of water vapour permeability and open porosity of CA renders this lithotype less bioreceptive for microbial colonisation. The very compact nature of CL and its extremely low capillarity coefficient, open porosity, surface roughness and water vapour permeability constitute an impediment to microbial growth. It is expected that the diffusion of these data to the end-users of the field of cultural heritage, particularly, conservators/restorators, contribute to decision making on the lithotypes used in future construction, or will be used as guides for the design of conservation treatments.

Key words: Bioreceptivity, biodeterioration, limestones, cyanobacteria, green algae, photosynthetic biomass, endolithic growth.

LIST OF ABBREVIATIONS

DGGE	Denaturing Gradient Gel Electrophoresis
PCR	Polymerase Chain Reaction
APS	Ammonium persulfate
TAE	Tris-Acetate-EDTA buffer
EDTA	*Ethylene-diamine-tetra-acetic acid*
TEMED	N'-tetramethylethylenediamine
LB	Luria-Bertani medium
BLAST	Basic Local Alignment Search Tool
NCBI	National Center for Biotechnology Information
CA	*Ançã* limestone
CL	*Lioz* limestone
SC	*San Cristobal* stone
PF	*Escúzar* stone
PL	*Lecce* stone
Chl*a*	Chlorophyll *a*
DMSO	dimethyl-sulfoxide
Cps	counts per second
SEM	Scanning Electron Microscopy
SEM-BSE	SEM with Back-Scattered Electrons
SEM-SE	SEM with Secondary Electrons
SEM-EDS	SEM with Energy Dispersive X-ray Spectroscopy
CLSM	Confocal Laser Scanning Microscopy
XRD	X-Ray Diffraction

CONTENTS

ABSTRACT iv
LIST OF ABBREVIATIONS vi
CONTENTS vii

CHAPTER ONE

General Introduction 3
1.1. State of the art 3
1.1.1. Limestones as building materials 3
1.1.2. Biodeterioration of stone: definitions and history 8
1.1.3. Colonisation of stone by phototrophic microorganisms 11
1.1.4. The role of phototrophic microorganisms in the biodeterioration of limestones 17
1.1.5. Bioreceptivity of stone materials 22
1.1.6. Techniques applied for detection and identification of photosynthetic biofilms 26
1.1.6.1. Microscopy techniques 26
1.1.6.2. Molecular biology versus culture techniques 29
1.1.6.3. Photosynthetic biomass quantification techniques 35
1.1.6.4. Digital image analysis 37
1.2. Framework of the thesis 39
1.2.1. Research problems in the field of stone monuments conservation 39
1.2.2. Objectives 41
1.2.3. Work strategy 43

CHAPTER TWO

Biodiversity of cyanobacteria and green algae on monuments from the Mediterranean Basin: an overview 49
2.1. Introduction 49
2.2. Cyanobacteria on monuments 50
2.3. Green algae on monuments 60
2.4. Conclusions 64

CHAPTER THREE

Identification and growth of phototrophic biofilms from limestone monuments under laboratory conditions 67
3.1. Introduction 67
3.2. Materials and methods 68
3.2.1. Site description and biological sampling 68
3.2.2. Characterisation of natural phototrophic biofilms 72
3.2.2.1. DNA extraction 72
3.2.2.2. PCR amplification of 16S rDNA fragments 74
3.2.2.3. Analysis of PCR products by Denaturing Gradient Gel Electrophoresis (DGGE) 76
3.2.2.4. Construction of 16S rDNA clone libraries 76
3.2.2.5. Screening of 16S rDNA clone libraries by PCR and DGGE 77
3.2.2.6. Sequencing and identification of microorganisms by comparative sequence analyses 78
3.2.3. Biofilms enrichment and monitoring 79
3.3. Results 81
3.3.1. Microbial diversity of natural phototrophic biofilms as determined by molecular techniques 81
3.3.2. Monitoring of photosynthetic cultures 84
3.4. Discussion 91
3.5. Conclusions 94

CHAPTER FOUR

Reproducing stone monument photosynthetic-based colonisation under laboratory conditions 99
4.1. Introduction 99
4.2. Materials and methods 100
4.2.1. Experimental setup 100
4.2.2. Analysis of microbial community 101
4.2.2.1. Molecular biology techniques 101
4.2.2.2. Culture techniques 102
4.2.3. Stone colonisation experiment 103
4.3. Results 105

4.3.1. Natural green biofilm composition as determined by DGGE analysis 105
4.3.2. Biofilm composition as determined by culture techniques 108
4.3.3. Stone colonisation experiment 110
4.4. Discussion 112
4.5. Conclusions 115

CHAPTER FIVE

Primary bioreceptivity of limestones: the influence of their intrinsic properties on phototrophic colonisation 119
5.1. Introduction 119
5.2. Materials and methods 121
5.2.1. Studied lithotypes 121
5.2.2. Characterisation of the lithotypes 123
5.2.2.1. Petrographic examination 124
5.2.2.2. Petrophysical characterisation 124
5.2.2.3. Petrochemical characterisation 127
5.2.3. Stone bioreceptivity experiment 128
5.2.3.1. Inoculation and incubation of the stone samples 128
5.2.3.2. Monitoring of photosynthetic biomass during the incubation period 130
In vitro chlorophyll a quantification technique 130
In vivo chlorophyll a fluorescence technique 132
Digital image analysis 133
5.2.4. Post-experiment observations of phototrophic colonisation 134
5.2.4.1. Digital image analysis 134
5.2.4.2. Scaning electron microscopy analysis 135
5.2.5. Statistical analysis 135
5.3. Results 136
5.3.1. Limestone characteristics 136
5.3.1.1. Petrographic characteristics 136
5.3.1.2. Petrophysical characteristics 140
5.3.1.3. Petrochemical characteristics 145
5.3.2. Stone bioreceptivity experiment 147

5.3.2.1. Photosynthetic biomass quantified during 90 days of incubation 149
In vitro chlorophyll a quantification technique 149
In vivo chlorophyll a fluorescence technique 151
Digital image analysis 153
5.3.2.2. Post-experiment observations of phototrophic colonisation 155
Digital image analysis 155
Scanning electron microscopy analysis 158
5.3.2.3. Statistical Analysis 160
5.4. Discussion 162
5.4.1. Lithotypes characteristics 162
5.4.2. Stone bioreceptivity experiment 165
5.5. Conclusions 172

CHAPTER SIX

Appraisal of endolithic growth and its biodeteriorating potential on limestones 177
6.1. Introduction 177
6.2. Materials and methods 178
6.2.1. Investigated stone materials 178
6.2.2. Analysis of endolithic growth by microscopy techniques 179
6.2.2.1. Scanning electron microscopy 179
6.2.2.2. Confocal laser scanning microscopy 179
6.2.3. Biocalcarenite mineralogical and micromorphological characterisation 180
6.2.3.1. X-ray diffraction 180
6.2.3.2. SEM-EDS analysis 180
6.3. Results 181
6.3.1. Lithotypes colonisation by endolithic biofilms 181
6.3.2. Biocalcarenite mineralogical and micromorphological characteristics 188
6.3.2.1. X-ray diffraction 188
6.3.2.2. SEM-EDS analysis 189
6.4. Discussion 193
6.5. Conclusions 196

CHAPTER SEVEN

Concluding remarks 199
7.1. Conclusions 199
7.2. Further perspectives 205

RESUMO 209

REFERENCES 221

APPENDICES

Appendix one 251
Appendix two 253
Appendix three 257

FIGURE INDEX

Fig.1.1. Geological map of Western Europe..... 5
Fig. 1.2. SEM image showing green algae cells (arrows 1) adhered to Ançã limestone (arrow 2) and embedded in matrix of extracellular polymeric substances (arrow 3). 13
Fig. 1.3. Stone statue from Queluz National Palace (Portugal) showing green biofilms..... 17
Fig. 1.4. SEM image of *Scytomena julianum* mat. The calcified sheaths are composed of triradiate calcite crystals. 20
Fig. 1.5. Confocal microscope image of filaments of *Nostoc punctiforme* in the vegetative growth state (biofilm sample come from Nerja Cave, Málaga, Spain). Pigment fluorescence is shown as red colour, polysaccharides labelled with Con-A-AlexaFluor 488 as green colour, and nucleic acids stained with Hoechst 33258 as blue colour. 29
Fig. 1.6. Polymerase chain reaction (PCR).. 31
Fig. 1.7. Principle of DGGE.. 32
Fig. 1.8. Molecular cloning using a plasmid vector. 34
Fig. 1.9. Diagram of the experimental work performed to study the primary bioreceptivity of five different limestone types..... 45
Fig. 2.1. Percentage of lithotypes present in the monuments, statues and historic buildings reported in this study. 50
Fig. 2.2. *Gloeocapsa* sp. observed under optical microscope (1000x). 51
Fig. 2.3. Number of cyanobacteria taxa found on each lithotype..... 52
Fig. 2.4. *Klebsormidium flaccidum* biofilm on a terracotta statue, Cathedral of Seville. 54
Fig. 2.5. Light microscope micrograph of trichomes of *Borzia periklei*, composed of 4-8 cells. 55
Fig. 2.6. SEM micrograph of a biofilm induced *in vitro* on sandstone. *Gloeothece* cells and sheath..... 56
Fig. 2.7. Number of chlorophyte taxa found on each lithotype..... 61
Fig. 3.1. View of the outside limestone monuments studied..... 69
Fig. 3.2. 17th century engraving depicting the landing in Seville of *San Cristobal* stone from El Puerto de Santa María (Cadiz) with the help of a crane.....71

Fig. 3.3. Features of pCR®4-TOPO® and the sequence surrounding the TOPO® cloning site. 77
Fig. 3.4. Biofilms cultivation in BG11 liquid medium. 79
Fig. 3.5. DGGE profiles of 16S rRNA gene from the natural green biofilm collected from Orologio Tower, in Martano (natural sample), obtained after amplification using bacterial and cyanobacterial primers (Lanes “bact” and “cya”, respectively)..... 86
Fig.3.6. DGGE profiles of 16S rRNA gene from the natural green biofilm collected from Santa Clara-a-Velha Monastery (natural sample) and its liquid culture monitored during 90 days (Lanes 15, 30, 45, 60, 75 and 90, corresponding to the sampling days).. 87
Fig. 3.7. DGGE profiles of 16S rRNA gene from the natural green biofilm collected from Ajuda National Palace (natural sample) and its liquid culture monitored during 90 days (Lanes 15, 30, 45, 60, 75 and 90, corresponding to the sampling days).... 88
Fig. 3.8. DGGE profiles of 16S rRNA gene from the natural green biofilm collected from Cathedral of Seville (natural sample) and its liquid culture monitored during 90 days (Lanes 15, 30, 45, 60, 75 and 90, corresponding to the sampling days).. 89
Fig. 3.9. DGGE profiles of 16S rRNA gene from the natural green biofilm collected from Cathedral of Granada (natural sample) and its liquid culture monitored during 90 days (Lanes 15, 30, 45, 60, 75 and 90, corresponding to the sampling days) 90
Fig. 4.1. Scheme of the laboratory chamber used to assess the ability of phototrophic communities to colonise stone samples: 1 – Phototrophic liquid culture; 2 – Silicon tubing; 3 – Automatic pumps; 4 – Sprinklers; 5 – Outlet valve device; 6 – Control unit; 7 – Stone samples. 104
Fig. 4.2. Abundance graphical representation of the different microbial groups detected in the 16S rDNA clone libraries from Santa Clara-a-Velha Monastery (Coimbra, Portugal) green biofilm 107
Fig. 4.3. Abundance graphical representation of the green algae and fungi types detected in the 18S rDNA clone libraries from Santa Clara-a-Velha Monastery (Coimbra, Portugal) green biofilm 107
Fig. 4.4a. Light microscope micrograph of *Chlorella* sp. 108

Fig. 4.4b. Light microscope micrograph of *Chlorella* sp. 108
Fig. 4.4c. Light microscope micrograph of *Leptolyngbya* sp. 108
Fig. 4.4d. Light microscope micrograph of *Leptolyngbya* sp. 108
Fig. 4.4e. Light microscope micrograph of *Pleurocapsa* sp. 109
Fig. 4.4f. Light microscope micrograph of *Pleurocapsa* sp. 109
Fig. 4.5. DGGE fingerprints using cyanobacterial-specific primers of the isolated phototrophic strains identified by 16S rDNA amplification, DGGE, construction of clone libraries and sequence analyses. Accession numbers and similarity (%) of the closest related database entries are given between brackets..... 109
Fig. 4.6. Distribution pattern of the phototrophic biofilms developed on *Ançã* limestone samples during 90 days in a laboratory chamber. 110
Fig. 4.7. DGGE fingerprints using cyanobacterial-specific primers from samples of artificially colonising biofilms on *Ançã* limestone incubated in a laboratory chamber over three months (15, 30, 45, 60, 75, and 90 days). Lane I corresponds to the inoculum used to start the colonisation process of these stone samples. Lanes 15 to 90 represents the microbial communities' profiles of this stone colonisation experiment at the indicated sampling time. 112
Fig. 5.1. One representative sample of each studied lithotype: CA (*Ançã* limestone), CL (*Lioz* limestone), SC (*San Cristobal* stone), PF (*Escúzar* stone) and PL (*Lecce* stone)..... 119
Fig. 5.2. Scheme of the non-commercial incubation system: 1 – fluorescent lamp; 2 – Control unit; 3 – water pump; 4 – Silicon tubing for water circulation; 5 – Plastic grid; 6 – Stone samples. 130
Fig. 5.3. Spectrofluorometer (SPEX Fluorolog-3 FL3-22) fitted with a fibre-optic platform (Horiba Jobin Yvon F-3000) from Departamento de Química, Faculdade de Ciências e Tecnologia, Universidade Nova de Lisboa (Portugal). 132
Fig. 5.4. Multi-layer file of Ançã limestone samples (CA), elaborated by Adobe Photoshop© software. Adapted from Gomes (2008). 133
Fig. 5.5. One representative sample of each lithotype (CA – *Ançã* limestone, CL – *Lioz* limestone, SC – *San Cristobal* stone, PF – *Escúzar* stone, and PL – *Lecce* stone) selected for the stone bioreceptivity experiment. 138
Fig. 5.6. Photomicrograph of a thin section of CA lithotype (crossed polars). 139
Fig. 5.7. Photomicrograph of a thin section of CL lithotype (crossed polars)..... 139

Fig. 5.8. Photomicrograph of a thin section of SC lithotype (crossed polars).....139
Fig. 5.9. Photomicrograph of a thin section of PF lithotype (crossed polars). 139
Fig. 5.10. Photomicrograph of a thin section of PL lithotype (crossed polars). 139
Fig. 5.11. Open porosity of the studied lithotypes: CA (*Ançã* limestone), CL (*Lioz* limestone), SC (*San Cristobal* stone), PF (*Escúzar* stone) and PL (*Lecce* stone). The values correspond to average ± SD for 27 samples of each lithotype.....140
Fig. 5.12. Representative kinetics of water absorption by capillarity of the studied lithotypes: CA (*Ançã* limestone), CL (*Lioz* limestone) with enlarged inset, SC (*San Cristobal* stone), PF (*Escúzar* stone) and PL (*Lecce* stone).....141
Fig. 5.13. Visual impression (left image) and computed 3D surface topography (right image) of one representative measured area of *Ançã* limestone (CA).....144
Fig. 5.14. Visual impression (left image) and computed 3D surface topography (right image) of one representative measured area of *Lioz* limestone (CL).....144
Fig. 5.15. Visual impression (left image) and computed 3D surface topography (right image) of one representative measured area of *San Cristobal* stone (SC). 144
Fig. 5.16. Visual impression (left image) and computed 3D surface topography (right image) of one representative measured area of *Escúzar* stone (PF).....145
Fig. 5.17. Visual impression (left image) and computed 3D surface topography (right image) of one representative measured area of *Lecce* stone (PL).....145
Fig. 5.18. Upper view of one representative sample of each lithotype at the inoculation time and after 30, 60 and 90 days of incubation.....148
Fig. 5.19. Lateral views of the SC and PF samples depicting green colour appearance. 149
Fig. 5.20. Maximum concentration values of chl*a* (µg.cm^{-3}) present on the stone samples of CA, CL, SC, PF and PL lithotypes, measured by the *in vitro* chl*a* quantification technique after 30, 60 and 90 days of incubation.....150
Fig. 5.21. Intensities of chl*a* fluorescence obtained for each lithotype (excitation wavelength: 430 nm): A) Fluorescence intensity values of chl*a* at 684 nm measured immediately after inoculation (initial fluorescence), and after 30, 60 and 90 days of incubation. Each column corresponds to the mean value of an average of 15 measurements ± SD. B) Chl*a* fluorescence spectra measured after 90 days of incubation. Each lithotype spectrum is an average of 15 spectra.....152

Fig. 5.22. Thresholded areas obtained by ImageJ software for CA: A) After inoculation; B) After 45 days incubation; C) After 90 days incubation. The detected particles are then measured using ImageJ software. 154
Fig. 5.23. Sum of the stone surface areas covered by the biofilms, quantified by digital image analysis. 154
Fig. 5.24. CA sample micrograph (left) and false-colour image obtained by Principal Component Analysis (PC1, PC2, PC3) (right). The thin blue band with occasional occupations in the empty spaces is the photosynthetic biofilm. 156
Fig. 5.25. CL sample micrograph (left) and false-colour image obtained by Principal Component Analysis (PC1, PC2, PC3) (right), showing the biofilm as a thin blue band at the top of the image. 156
Fig. 5.26. SC sample micrograph (left) and false-colour image obtained by Principal Component Analysis (PC1, PC3, PC3) (right). The biofilm is presented as a blue band inside the stone sample. 157
Fig. 5.27. PF sample micrograph (left) and false-colour image obtained by Principal Component Analysis (PC1, PC3, PC3) (right), enhancing the extent of the endolithic biofilm (blue band). 157
Fig. 5.28. PL sample micrograph (left) and false-colour image obtained by Principal Component Analysis (PC1, PC3, PC3) (right). The biofilm is represented in dark red to black. 157
Fig. 5.29. Bands corresponding to the PC1, PC2 and PC3 of the original image of PL used in this work. 158
Fig. 5.30. SEM images of transversally cut fresh samples of CA lithotype after 90 days-incubation: a) phototrophic biofilm in external view; b) and c) details of image 5.30a. White arrows indicate EPS; empty arrows show mineral substratum; black arrows indicate microbial cells. 159
Fig. 5.31. SEM images of transversally cut samples of SC lithotype after 90 days-incubation: a) phototrophic biofilm in external view; b) and c) details of image 5.31a. White arrows indicate EPS; empty arrows show mineral substratum; black arrows indicate microbial cells. 159
Fig. 5.32. SEM images of transversally cut samples of PF lithotype after 90 days-incubation: a) phototrophic biofilm in external view; b) and c) details of image 5.32a. White arrows indicate EPS; empty arrows show mineral substratum; black arrows indicate microbial cells. 159

Fig. 5.33. SEM images of transversally cut samples of PL lithotype after 90 days-incubation: a) phototrophic biofilm in external view; b) and c) details of image 5.33a. White arrows indicate EPS; empty arrows show mineral substratum; black arrows indicate microbial cells. 160
Fig. 5.34. Correlation among the variables capillarity coefficient (Capillarity), surface roughness (R_a and R_z), open porosity (Porosity), water vapour permeability (Permeability), concentration of chl*a* (Chlorophyll) and chl*a* fluorescence (Fluorescence), and the factors (components). 161
Fig. 6.1. SEM-BSE image from PF lithotype depicting an interaction result between the inoculated phototrophic microorganisms and the substratum. It is particularly noticeable the endolithic activity creating small cavities (white arrows) in the calcite crystals. 182
Fig. 6.2. SEM-BSE images of phototrophic microorganisms in PF samples illustrating: A) epilithic microorganisms randomly scattered on the stone surface and the likely depths endolithic cells penetrating the stone through the accessible void spaces; B) detail from 6.2A showing compact cell aggregates of the endolithic colonisation; C) distribution map of Ca showing the dissolutions features of the calcite in the endolithic microhabitat analysed by EDS microanalytical Line-Scan analysis. 182
Fig. 6.3. SEM-BSE images from PF samples depicting: A) grains with cubic crystalline habit forming concentric or dispersed aggregates on the stone surface; and B) in the interior; C) enlarged view from image 6.3B. 183
Fig. 6.4. SEM-BSE images from SC samples showing randomly scattered cells within the pores of the calcarenite together with calcite grains. 184
Fig. 6.5. SEM-BSE images from SC samples showing: A) cubic crystalline aggregates within the calcite grains; B) close view of the cubic crystalline aggregates. 184
Fig. 6.6. SEM-BSE images from PL samples showing: A) the epilithic microbial colonisation, in which cells are distributed on the surface of the sample or very close to the surface; B) close view of the microbial cells showing disaggregation of the calcite grains. 185
Fig. 6.7. Three-channel maximum intensity projection of pigment fluorescence of unicellular phototrophic microorganisms in SC sample. It consists of a two-dimensional compound image of x-y optical selected section of acquisition. 186

Fig. 6.8. Three-dimensional extended focus projections in x-y, x-z and y-z views of a selected fragment of the PF sample. 187
Fig. 6.9. Three-dimensional extended focus projections in x-y, x-z and y-z views of a selected fragment of the PL sample. 187
Fig. 6.10. A) SEM image of non resin-cast samples of PF lithotype showing a biofilm deposition with Fe and Mn in its composition; B) EDS spectrum performed for this sample area. 190
Fig. 6.11. A) SEM image of a Mn oxide and clay minerals coating a calcareous (Ca) fissure in the PF lithotype; b) EDS spectrum obtained in position 1 from image 6.11A. 191
Fig. 6.12. SEM image of colonised PF lithotype presenting needle-like shaped goethite and very small iron-rich spherical particles, mostly likely ferrihydrite. 192
Fig. 6.13. SEM images of PF lithotype showing: A) calcite crystals coated by iron-oxyhydroxides and a globular aggregate of calcite grains surrounded by an iron-film; B) one globular aggregate of calcite grains with iron-rich coating and other porous round particle, likely biogeneous..... 192

TABLE INDEX

Table 2.1. Investigated monuments, statues and historic buildings in European countries from the Mediterranean Basin, and their bibliographic references. 57
Table 2.2. Cyanobacteria reported on stone monuments, statues and historic buildings in European countries from the Mediterranean Basin, on different substrata. 58
Table 2.3. Chlorophyta reported on stone monuments, statues and historic buildings in European countries from the Mediterranean Basin, on different substrata. 62
Table 3.1. Sampling areas and biofilm descriptions. 73
Table 3.2. Primers used in this study. 75
Table 3.3. Occurrence of prokaryotic microorganisms in the green biofilms of the studied monuments, detected by amplification using bacterial and cyanobacterial primers. 83
Table 4.1. Phylogenetic affiliations of eukaryotic microorganisms derived from the natural green biofilm of Santa Clara-a-Velha Monastery (Coimbra, Portugal). 106
Table 5.1. Quarry, location and monument of the five studied lithotypes. 122
Table 5.2. Major physical and chemical characteristics of the five lithotypes, together with the ANOVA results of open porosity (n = 27), capillarity water absorption coefficient (n = 27), water vapour permeability (n = 3), surface roughness (R_a and R_z) (n = 3 for each parameter) and stone suspension pH (n = 3). 143
Table 5.3. Chemical analysis in weight percent of the five lithotypes. Values are average ± SD (n = 3). 146
Table 5.4. ANOVA results obtained for the concentration of chl*a* present on the studied lithotypes after 30, 60 and 90 days of incubation. 151
Table 5.5. Intensity of chl*a* fluorescence values measured at 684 nm together with ANOVA results obtained for the five studied lithotypes after 30, 60 and 90 days of incubation. 153

CHAPTER ONE

General introduction

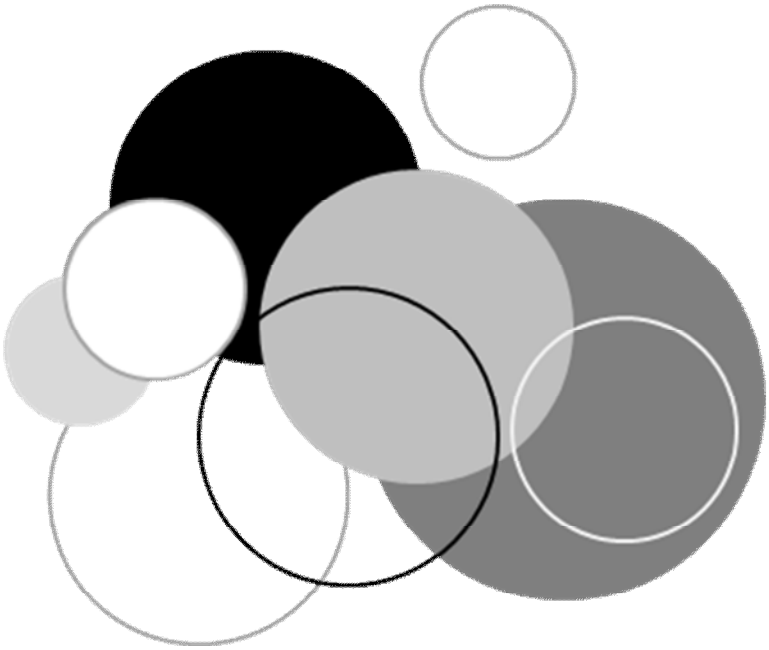

CHAPTER ONE

General introduction

1.1. State of the art

1.1.1. Limestones as building materials

The Mediterranean Basin countries are often recognised as the cradle of some of the world's most important cultural heritage in stone. The wide distribution of stone monuments and lithic works of art, and their cultural, artistic and religious importance emphasise the general need to safeguard this praiseworthy cultural heritage.

Stone materials have been used since the beginning of mankind for convenience, endurance and visual impact. Their selection for construction purposes has been invariably driven by questions of durability, availability, workability, cost and appearance. Despite the bewildering variety of stone types, carbonate rocks have been preferentially used as construction material in the architectural heritage of Mediterranean Basin region. Among them, limestones were prised for their attractive appearance, ease of quarrying, workability and exceedingly distribution across the Earth's surface.

Limestones are sedimentary rocks that contain 50% or more of calcium carbonate ($CaCO_3$) and possibly aragonite ($CaCO_3$); the essential carbonate minerals are calcite ($CaCO_3$), aragonite ($CaCO_3$) and dolomite ($CaMg(CO_3)_2$) (Chilingar et al., 1967). Aragonite is a polymorph of calcite, unstable at normal surface temperatures and pressures, which may change into calcite. Dolomite is calcium magnesium carbonate intimately associated with calcite since it is in most cases a replacement of calcite or aragonite. On the basis of chemical composition, particularly, Ca/Mg (weight) ratios, Chilingar et al. (1967) proposed the classification of limestones into the following types: highly dolomitic limestone, when the range in

Ca/Mg ratio is 4.74-16; dolomitic limestone when Ca/Mg ratio is between 16-60; slightly dolomitic limestone, when the range in Ca/Mg ratio is 60-105, and calcitic limestone when the Ca/Mg ratio is superior than 105. Although some limestones are very pure consisting almost wholly of one or more carbonate minerals, they may contain other minerals. The most common include silica (commonly quartz sand), silicates and clay. If present in amounts greater than 10% the limestone rock may be termed as siliceous limestone or argillaceous limestone. A system based on grain size is widely used recognising three categories: calcilutite (grains <62 μm), calcarenite (62 μm to 2 mm) and calcirudite (>2 mm) (Grabau, 1904, 1913; Powers, 1962). Other classification systems of carbonate rocks are currently used, which are based on the textural components (Leighton and Pendexter, 1962; Folk, 1962) and depositional texture (Dunham, 1962; Embry and Klovan, 1971).

About 75% of the Earth's surface is formed by sedimentary rocks, in which argillaceous rocks are the most abundant, occupying about 45% of the area; sandstones form about 30% and limestones about 28% (Dimes, 1998). Due to the availability of rocks and transport facilities, stonemasons trended to use the local stone materials for building construction. Thus, it is not surprising that memorials of our heritage are build of sedimentary rocks, being limestones and sandstones the predominant stone types used. Figure 1.1 depicts the geologic map of Western Europe, evidencing the presence of rocks from every age and almost every kind of rock. In the Southern Europe countries, especially in Spain and Italy, the broad distribution of tertiary sedimentary rocks explains the wide use of limestones in their architectural heritage. Great stages of geologic evolution are also setting in central Portugal, where extent layers of Cretaceous and Jurassic are quarried. In the north region of Lisbon, between Lameiras and Negrais, crops out one of the most traditional ornamental Portuguese stones, locally known as *Lioz* limestone (beige-white limestone). This rock is a Cretaceous fossiliferous limestone which owes its high value to its vivid colours and well known durability (Figueiredo et al., 2007). In the proximity of Coimbra (central Portugal), set in the northern branch of the Lusitanian Basin, layers dating from the Bajocian (Middle-Jurassic) are quarried for the *Ançã* limestone: an oolitic rock widely used in well known monuments in the region due to its workability and light colour.

Fig. 1.1 Geological map of Western Europe (http://www.discoveringfossils.co.uk/europe_geology.htm).

In what concerns the geology of Spain, a remarkable stone diversity is observed. It includes one of the most complete Palaeozoic sedimentary successions in Europe. In the North and West of the Peninsula, siliceous formations are seated on hard and durable crystalline rocks (granites, schist and gneiss) forming acid soils and poor in carbonates. Sedimentary rocks based on limestones and marls (argillaceous limestones) are seated on the heavily weathered Meseta (central Spain) that form the major agricultural zones. It constitutes the oldest and most complex geologic formation of the Iberian Peninsula. Some of the most remarkable Spanish cultural heritage built in limestone is found in Andalusia, where huge amounts of upper Miocene formations, such as *San Cristobal* and *Escúzar* stones, were quarried for the construction of the cathedrals of Seville, Jerez, Granada and the walls of the Alhambra Palace, etc.

Great creations like magnificent buildings or beautiful temples can also be admired in Italy, which has a rich geology from erupting volcanoes, with all kind of volcanic rocks, to sedimentary rocks seated in the Salento Peninsula (South-eastern Italy). In the historic city of Lecce (Southern Italy) crops out the city's main export, *Lecce* stone, because it is very soft and malleable, thus suitable for sculptures. This Tortonian (Miocene epoch) rock formation is extended throughout the Salentine Peninsula, particularly in the regions of Lecce, Corigliano d'Otranto, Melpignano, Cursi and Jerseys.

Portugal, Spain and Italy contain some of the best exposed outcrop geology in Europe, which provide huge amounts of limestone materials for construction purposes. Cretaceous and Jurassic formation outcrops from Portugal, and Miocene formations from Spain and Italy, provide some of the materials more frequently used in several important buildings that have been constructed in these countries. Unfortunately, we are confronted with some problems concerning their preservation. Physical and chemical weathering both in monument or in natural geological outcrops are observed, which induce stone disaggregation and decomposition resulting from material loss (Smith, 2003). Physical weathering can be caused specifically by salt crystallisation and freeze-thaw processes, as well as hydric, thermal and wet-dry cycling. Chemical weathering can essentially be understood as stone disintegration resulting from reactions induced on mineral constituents of rock by water, carbon dioxide and oxygen. Whereas rock weathering is essential for

pedogenesis, the deterioration of cultural heritage artefacts in stone represents an irretrievable loss to the history of mankind.

Deterioration of monument stones is a complex process influenced by the intrinsic properties of the stone materials (geological time, mineralogical composition, porosity, etc.) and by extrinsic factors, such as climatic conditions, atmospheric pollution and biological colonisation. Other factors, sometimes acting synergistically, include damage induced by quarrying, transport and stone preparation procedures, microclimatic conditions (affected by local urban geometry and building design), adjacent materials used, such as inappropriate jointing material and metal elements, etc. Unfortunately, there are even more factors contributing to stone deterioration: man destructive actions, lack of maintenance, and inappropriate conservation works carried out in the building. These factors are determined by the economical situation and lack of the knowledge and experience in the conservation of monument stones.

Limestones have been intensely studied in conservation, largely because they have been used in buildings and statuary all over the world and because they are mineralogically quite simple (Sabbioni, 2003). Several researches have studied the deterioration processes occurring on limestone surfaces (Maurício and Figueiredo, 2000; Maurício et al., 2005; Dionísio, 2007; Figueiredo et al., 2007). In many dense limestones, the rate of deterioration may be gradual and, given climatic conditions, largely predictable. However, there are many commonly limestone types which do not decay gradually, but instead experience episodic and sometimes catastrophic breakdown, especially in polluted urban environments. The increase of atmospheric contamination undoubtedly accelerates stone deterioration, especially on limestones where loss is primarily related to dissolution of calcium carbonate induced by the solvent action of acid rainwater. Its penetration into the pores hastens the rate of stone deterioration tremendously, first because water is itself an effective deteriorating agent, dissolving, hydrating and hydrolysing minerals, and, secondly because it holds in solution substances (carbonaceous particles, sulphur compounds, soluble salts) responsible for leaching of surfaces, pH reduction, dark crusts, efflorescences and subflorescences (Bell, 1993b; Camuffo, 1995; Ordóñez et al., 1997; Papida et al., 2000). In addition, the absorption of ground water through capillary rise transport organic acids which may also dissolve the sparingly soluble calcium carbonate (Drever and Stillings, 1997).

The problem of understanding the deterioration of limestones is compounded by the large range of stone varieties, with different textural, mineralogical and physical characteristics, and by their varying weathering responses under different climatic and environmental conditions. The interactions between these numerous and synergistically acting factors lead to a dynamic and complex process of physical, chemical and biological deterioration. Laboratory studies have demonstrated the combined process of physical, chemical and biological factors on the deterioration of stone (Badalyan et al., 1996; Papida et al., 2000). However, little research has been focused on the problem of microorganisms as agents of stone deterioration (biodeterioration). This study represents a multidisciplinary work focused on the biodeterioration susceptibility of different limestone types widely used in Portuguese, Spanish and Italian monuments.

1.1.2. Biodeterioration of stone: definitions and history

Within the last few years it has been widely accepted that rocks, either in natural geological outcrops or in stone monuments, are common habitats for a wide variety of microorganisms, such as bacteria, cyanobacteria, actinomycetes, algae, fungi and lichens. Krumbien (1983, 1988) studied the interactions between these microorganisms and the lithic substrata, reporting that microorganisms play an important and substantial role in all rock alteration processes. Aesthetical, physical and chemical changes are induced on the lithic substrata, where the formation of coloured patinas are visibly noticed (Urzì et al., 1991; Gorbushina et al., 1993; May et al., 1993; Sterflinger and Krumbein, 1997). In some natural environments, chemical and physical transformations in the materials can be seen as a necessary and positive process. A very practical example is the essential biotransfer process of rocks for soil formation (pedogenesis). However, when a rock is used as building material, these transformations induced by stone colonising microflora in association with other environmental agents are clearly seen as a negative or destructive process, both from cultural and economical viewpoints. Therefore, the comparison of the concepts “biodegradation” and “biodeterioration” leads to a consideration of the manifold relations between organisms and materials and to a systematisation of these fields of science (Hueck, 2001).

The term biodeterioration was defined about 45 years ago by Hueck (1965) as "*any undesirable change in the properties of a material caused by the vital activities of living organisms*". The term biodegradation is also of common use as a synonymous of biodeterioration. However, the definition of biodegradation with a negative, detrimental connotation is unjustified, according to Krumbein (1988). Biodegradation involves a positive or useful connotation in relation to ecology, waste management and environmental remediation. This concept is commonly used for the combined effects of erosion and weathering, i.e. the wearing down of the Earth's surface by physical, chemical and biological action, essential for pedogenesis (Krumbein, 1988). In geological nomenclature, weathering is the decomposition process of rocks, minerals and soils through direct contact with the atmosphere, and is a necessary process in most cases.

For a detailed historic review of these and related terms it is recommended the following literature: Krumbein (1966, 1988), Krumbein et al. (2003) and Gorbushina and Krumbein (2005).

The main processes of stone biodeterioration have gone through interesting theories related to the biogenic attack. For a long time, microbial effects on stones were described as physical, chemical or pollution derived processes. When considering the physical and chemical damage of a given monument, only stone characteristics and abiotic factors (e.g. rain, wind, relative humidity, sunlight, temperature, pollution, etc.) were taken into consideration. The research carried out by Krumbein (1966, 1988) demonstrated the catalytic power of rock biota in the natural process of rock decay, and the role of microorganisms in the partially or completely deterioration of stone materials used in cultural heritage assets. After recognition of the biological origin on the alteration of stone, an increasing awareness on the manifold aspects of stone biodeterioration yielded. A considerable number of investigations have begun to elucidate the role of microorganisms in the deterioration of building stone (Griffin et al., 1991; Bock and Sand, 1993; May et al., 1993; Koestler et al., 1996; Wakefield and Jones, 1998; Saiz-Jimenez, 1995, 1999). However, initial researches considered biodeterioration as a secondary deterioration problem, occurring only after an advanced state of deterioration predetermined by physical and chemical parameters (Griffin et al., 1991). In other words, abiotic factors were thought to condition stone surfaces exposed outdoors through fissure formations and enrichment of inorganic and organic nutrients. When the surface of

the lithic substratum had undergone this process of alteration, living organisms colonised the surface area. Furthermore, the effects of stone biodeterioration were thought to induce only an aesthetic problem, typically seen as an unacceptable appearance of staining of the stone surfaces by biogenic pigments (Urzì et al., 1991). Recently, several analytical approaches demonstrated that even in the early stages of stone exposure, primary biodeteriorating effects can be clearly defined (Koestler et al., 1996; Gaylarde and Morton, 1999). These studies also demonstrated that microorganisms are involved in the physical and chemical deterioration of stones (Saiz-Jimenez, 1999; Dornieden et al., 2000; Warscheid and Braams, 2000), and the rate and extent of microbial colonisation are strongly influenced by environmental parameters, such as, water availability, climatic conditions, and by petrologic parameters (e.g. mineralogical composition, porosity, roughness).

From the above mentioned investigations, it is clear that the concept of stone biodeterioration is now seen in a more holistic notion in which the biological deterioration is controlled by synergism/antagonism relationships among the colonising species and environmental factors (Koestler et al., 1996; Wakefield and Jones, 1998; Warscheid and Braams, 2000). Thus, stone biodeterioration cannot be considered as an isolated phenomenon. It generally occurs with other physical, chemical, or physicochemical deterioration processes, being difficult to attribute damage specifically to a single cause. Moreover, although microorganisms colonise permanently various materials, their damaging activity is not constant, but rather periodic and defined by the variety of different conditions as a result of the habitat in which they dwell.

Detailed literature, summarised by Warscheid and Braams (2000), Krumbein (2004) and Gorbushina and Krumbein (2005), gives an idea about the early phases and the later opinions changing with new findings.

Stone monuments can be a paradigm of a complex environment in which microorganisms can be confronted as it encompasses heterogeneity and dynamic in time and space. This heterogeneity of most cultural heritage substrata is linked to the numerous interrelationships among various biological populations and between these populations and the substratum, as well as other processes occurring in the surrounding environment. Thus, the study of stone biodeterioration involves complex and multidisciplinary approaches.

Over the years, scientific approaches and conservation strategies of stone biodeterioration have evolved to reach a high level of sophistication into a still growing scientific community. Yearbooks and symposium publications (e.g. Hougthon and Eggins, 1988; Rossmoore, 1991; Saiz-Jimenez, 2003) have been useful sources, where biodeterioration, biofilms and bioreceptivity and, obviously strategies to avoid and eliminate biological colonisation are the central focus.

1.1.3. Colonisation of stone by phototrophic microorganisms

It is amply recognised that microbial communities are truly ubiquitous in aquatic and terrestrial ecosystems as well as on man-made materials, including cultural heritage assets exposed outdoors. A high microbial diversity in the form of bacteria, cyanobacteria, algae, fungi, as well as lichens can find a suitable habitat for their growth both on rock surfaces and on monument stones. Photoautotrophic microorganisms (green microalgae, cyanobacteria and lichens) are particularly damaging of stone surfaces due to their ability to survive in inhospitable environments. They can develop on stone surfaces without any presence of organic matter (Tiano, 1998). Thus, photoautotrophic microorganisms have the greatest ecological importance as pioneer organisms in the colonisation of stone materials (Bock and Sand, 1993; Gómez-Alarcón et al., 1995; Lamenti et al., 2000; Tomaselli et al., 2000 a,b; Bellinzoni et al., 2003). Several investigations demonstrated that different stone materials, such as limestones, granites, sandstones and marbles, can promote significant microbial growth under oligotrophic conditions (Guillitte and Dreesen, 1995; Tiano et al., 1995; Prieto and Silva, 2005; Miller et al., 2006). In fact, these microorganisms can grow using the mineral components of a stone and sunlight as energy source. Their phototrophic mode of life allows their exposition to visible solar radiation becoming the dominant primary producers of environments that may be considered extreme, such as hotsprings, deserts, alkali lakes, polar areas (Bell, 1993b; Friedmann, 1982; Büdel et al., 2004), as well as, cultural heritage assets such as vertical surfaces of monuments (Saiz-Jimenez et al., 1990; Ortega-Calvo et al., 1991a; Ariño et al., 1997; Tomaselli et al., 2000b; McNamara et al., 2006). These ecosystems may often be considered “extreme” because of their exposure to high temperature, sun radiation and drought for long periods of time and

also to wide temperature variations and high salt concentrations (Daffonchio et al., 2000).

Taxonomically, cyanobacteria are an evolutionarily coherent group of photoautotrophic microorganisms within the eubacteria (Wilmotte, 1994; Castenholz, 2001). This group constitutes the only phototrophic prokaryotes capable of carrying out oxygenevolving, plantlike photosynthesis, and shares a common ancestry with the chloroplasts of higher plants and green algae (Nelissen et al., 1995). They conduct photosynthesis on specialised infolded cytoplasmic thylakoid membranes, rather than in chloroplasts. They can be found in a single cell, colonies of unicellular organisms or organised in filaments. The pigments are spread in a membrane system at the periphery of the cells, which have a mucilaginous sheath, often highly pigmented (Graham and Wilcox, 2000). They contain chlorophyll *a*, carotenoids (yellow/orange pigments), phycocyanin (blue pigment) and phycoerythrin (red pigment).

Green microalgae or Chlorophyta, are a diverse group of oxygenic photoautotrophic microorganisms within the eukaryotes, containing therefore a nucleus enclosed within a membrane, and conduct photosynthesis within chloroplasts. They may be unicellular, colonial or multicellular but typically consist of a relatively small number of cells. Chlorophyll *a* and *b* and carotenoid pigments are present, which occur in plastids (Graham and Wilcox, 2000).

Cyanobacteria and microalgae develop on stone surfaces forming biofilms composed of a mono- or multilayer of cells embedded in a hydrated extracellular polymeric matrix which hold the cells together (Morton et al., 1998; Warscheid, 2000; Roldan et al., 2003). These glue-like extracellular polymeric substances (EPS) secreted by the cells enhance the attachment of the biofilm community, allowing the adhesion of microbial cells to the lithic substratum (Cecchi et al., 2000; Wimpenny et al., 2000). The attachment of microorganisms on stone surfaces is regulated biologically by the microbial cell structure and their surface charge; it is physically controlled by the stone surface, which partially determines the availability of water, nutrients, niche possibilities, and thus the survivability of the microorganisms. Preferentially, phototrophic microorganisms adhere to humid stone surfaces, on rough or porous surfaces, cracks and fissures, where water is retained and evaporation is slow due to protection against winds or direct sunshine. Inoculation is more rapid when there are adjacent soils or overhanging vegetation from which

cyanobacteria and algae can be brought in by wind and rain (Saiz-Jimenez, 1999; Alakomi et al., 2004). Subsequent formation of surface covering biofilms improves the living conditions for the phototrophic microflora. Their slimy surfaces favour the adherence of nutritive airborne particles (dust, pollen, spores, oil-and coal-fired carbonaceous particles) and microorganisms from the atmosphere (Saiz-Jimenez, 1995; Koestler et al., 1996; Warscheid, 2000).

The use of sophisticated techniques, consisting mainly of microscopy analyses, illustrates the composition, function and structure of biofilms. These biofilms are composed of population or communities of different microorganisms (microalgae, cyanobacteria, bacteria and fungi) immobilised on the stone surface (substratum) and frequently embedded in an organic polymer matrix formed by EPS (Fig. 1.2).

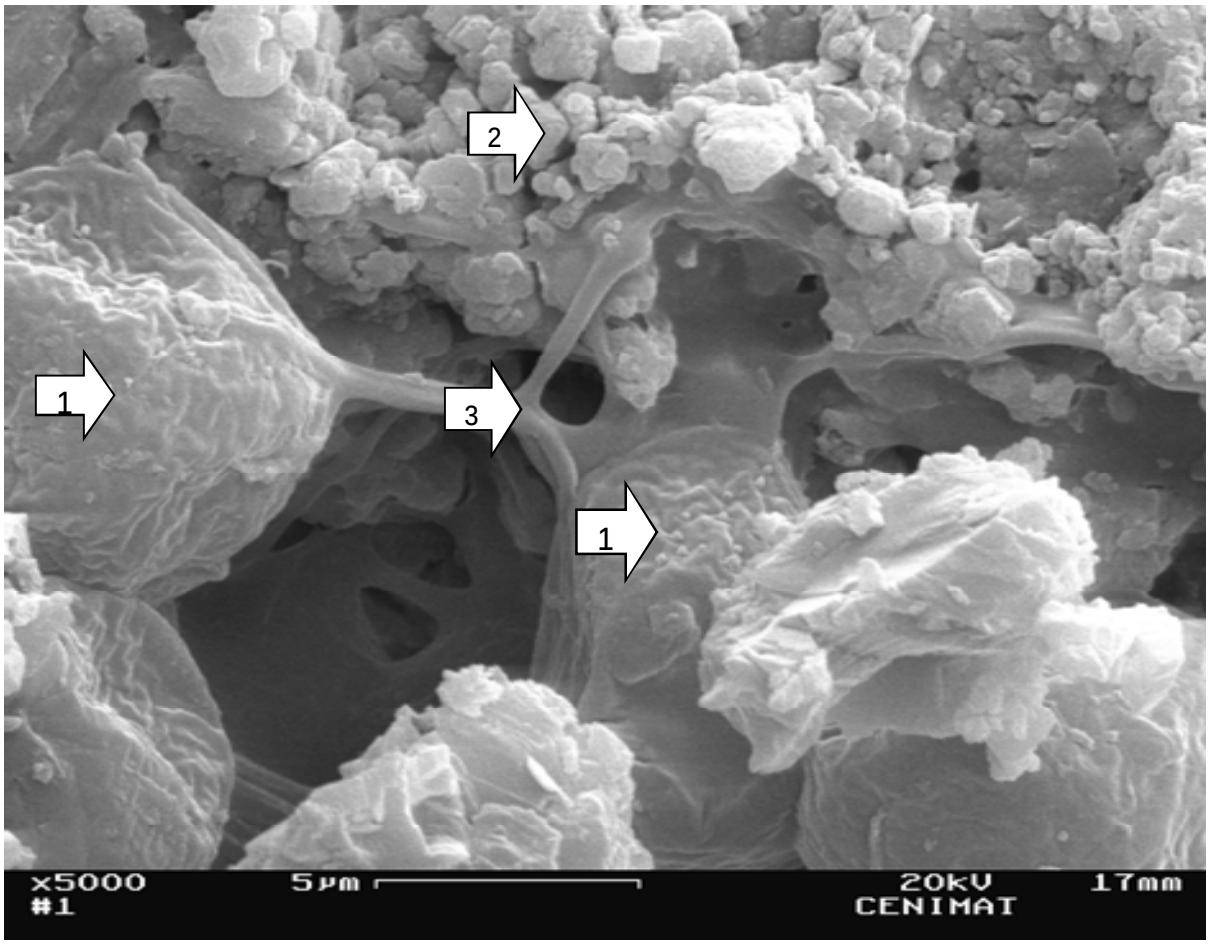

Fig. 1.2. SEM image showing green algae cells (arrows 1) adhered to Ançã limestone (arrow 2) and embedded in matrix of extracellular polymeric substances (arrow 3).

EPS may vary in chemical and physical properties, but consist mainly of polysaccharides with fatty acids, proteins and enzymes (Krumbein and Urzì, 1991; Kawaguchi and Decho, 2002; Young et al., 2008). It may also contain exoenzymes and inorganic inclusions such as clay particles and minerals (Wilderer and Characklis, 1989). Confocal laser scanning microscopy (CLSM) studies revealed that EPS are organised into complex exopolymeric matrix, which consists of a heterogeneous distribution of cells and cellular aggregates with void spaces or water channels (Costerton et al., 1995; Kawaguchi and Decho, 2002). Zhang et al. (1998) pointed out that the major component in the biofilm matrix is water - up to 97%. Mazor et al. (1996) showed that addition of 0.5 mg of *Microcoleus* sp. EPS per gram of sand retained approximately 30% of the water-holding capacity of the sand after 24h of desiccation at 55ºC, while sand samples without EPS dried out completely. Direct visual observation, either with CLSM (Neu and Lawrence, 1999; Kawaguchi and Decho, 2002; Roldán et al., 2004), scanning electron microscopy (SEM) (Hernandéz-Mariné et al., 2004; De los Ríos and Ascaso, 2005) or Fluorescent *In Situ* Hybridization (FISH) (Urzì and Albertano, 2001; Urzì et al., 2003), revealed the high biodiversity and distribution of phototrophic biofilms on stone surfaces. The top layer of biofilms is typically dominated by phototrophic microorganisms, such as cyanobacteria, green algae and diatoms, while underlying layers are composed by anoxygenic bacteria, such as green and purple sulfur bacteria (Martinez-Alonso et al., 2005).

According to their distribution pattern, the microorganisms that inhabit the rocks have been classified as epilithic and endolithic (Golubic et al., 1981). Epilithic microorganisms grow on the external surface of the rock, whereas endolithic microorganisms live in the interior of rocks, penetrating some millimetres into the rock pore system. Golubic et al. (1981) proposed a terminology which divides endolithic organisms into three groups: chasmoendolithic (colonising fissures and cracks), cryptoendolithic (colonising structural cavities within porous rocks) and euendolithic (penetrating actively into the interior of rocks and forming tunnels). Specialised euendolithic cyanobacteria penetrate and colonise the interior of limestone and dolomite rocks as well as loose sand-size particles, shell hash and other skeletal fragments. Generally, endolithic colonisation is a successful strategy of survival when surface environmental conditions are adverse for life on stone. The endolithic microhabitat gives protection from intense solar radiation and desiccation, and it

provides mineral nutrients, moisture and growth surfaces (Walker et al., 2005). The protection provided by the rock leads to the abundance of endolithic microorganisms in extreme environments, as cold and hot deserts, semiarid lands and even polar regions (Friedmann, 1982; Bell, 1993b; Walker et al., 2005). Microscopy techniques have also shown that penetration of growing organisms into rock and the diffusion of their excreted products may arise to depths of several millimetres (Saiz-Jimenez, 1999; Koestler, 2000; Salvadori, 2000; Pohl and Schneider, 2002; Barberousse et al., 2006; Young et al., 2008). Pohl and Schneider (2002) applied computerised image analysis to detect and quantify the biomass and depth of penetration of endolithic microorganisms into carbonate rock surfaces. They observed that the investigated natural carbonate rocks were endolithically colonised by lichens, cyanobacteria, algae and fungi. Phototrophic microorganisms from intensely insolated dry sites retreated to depths of 150-250 μm below the rock surface and revealed “cushions” of EPS oriented toward the surface, which protect them against intense light and provide water retention. In addition, these authors demonstrated that as soon as the endolithic biofilm was established it exerted an overall protective effect on the carbonate rocks. Salvadori (2000) examined by SEM the endolithic communities inhabiting stone Italian monuments and observed that euendolithic cyanobacteria and fungi could easily penetrate the calcite crystals of marble.

It is important to stress that phototrophic biofilms occur on contact surfaces at the interface between the solid substratum and the atmosphere. Thus, they are constantly subjected to adverse environmental conditions, such as, intense solar radiation, desiccation, temperature, moisture fluctuations, lack of nutrients, etc. Hence, the metabolic activity of phototrophic biofilms centres on retention of large amounts of water into its structure, protecting the cells from desiccation, fluctuating environmental conditions, as well as biocides, ultraviolet radiation, and prolonging their vegetative life (Prakash et al., 2003; Gorbushina, 2007). This leads to species characteristic of very different habitats and ecological requirements. Due to the presence of EPS, the biofilm incorporates large amounts of water into its structure ensuring the maintenance of moisture by balancing changes in humidity and temperature, which permits cyanobacteria and algae to resist drought periods (Gómez-Alarcón et al., 1995; Saiz-Jimenez, 1999; Schumann et al., 2005).

Summarised literature on the history, composition, structure and function of biofilms is presented by Christensen (1989), Costerton et al. (1994, 1995), Sutherland (2001) and Donlan (2002).

A number of factors influence the settlement, growth, distribution and metabolic activity of phototrophic biofilms on stone monuments, including i) intrinsic stone properties, such as geological origin, chemical composition, pore space structure and surface conditions that strongly influence water availability, nutrients and niche possibilities; ii) environmental parameters (e.g. solar radiation, temperature, water regime, wind, atmospheric pollution, etc.) iii) specific microclimatic parameters (e.g. orientation, exposure to shadow, permanent capillary humidity, etc.); iv) building maintenance. Yet clearly, the diversity and abundance of green algae and cyanobacteria are dependent on the availability of water allowing microorganisms to form biofilms on virtually any surface (Gorbushina, 2007). Water availability is one of the most important factors since all organisms need water for their metabolim. Bellinzoni et al. (2003) reported that the water factor, and in particular rain, represented the main limiting factor for the growth of phototrophic microflora in travertine walls. The shading of trees in Northern exposed surfaces reduced water evaporation favouring microflora growth. Ortega-Calvo et al. (1992) studying green biofilms on building stones from Spain and Northern Europe, showed that green algae only became dominant after the improvement of water retention properties to stone surfaces by pioneering cyanobacteria. Nevertheless, the stone surface has also several characteristics that are important in the attachment and development of phototrophic microorganisms. The extent of microbial colonisation appears to increase as the surface roughness increases. This is because shear forces are diminished, and total surface area is higher on rougher surfaces (Morton et al., 1998; Donlan, 2002). Tomaselli et al. (2000b) showed that high values of porosity and surface roughness played a greater role than mineral composition in promoting microbial establishment. Hernández-Mariné et al. (2001) examined phototrophic biofilms coating the limestone surface of the Puigmoltó sinkhole located in the East cost of the Iberian Peninsula, demonstrating that biofilms developed according to the decreasing irradiance; in the upper part of the sinkhole a discontinuous light green biofilm was formed with large amounts of EPS, whereas below 5 m in depth the biofilm occurred in patches and very few organisms were able to grow along the gradient of conditions.

1.1.4. The role of phototrophic microorganisms in the biodeterioration of limestones

The presence of cyanobacterial and algal biofilms on stone surfaces can be considered biodeteriogenic, simply because of the aesthetic damage they cause due to the formation of variously-coloured patinas (Ortega-Calvo et al., 1995). Most of these coloured patinas are produced by microbial organic pigments firmly bound to the stone particles (Urzì and Realini, 1998; Alakomi et al., 2004; Gorbushina, 2007). The consequence is the formation of greenish to blackish biofilm generated patinas, particularly evidenced on light colour limestones (Krumbein, 2004) (Fig. 1.3). Bartolini et al. (2004) studied phototrophic biofilms dwelling on carbonate monuments located in Appia Antica road (Rome, Italy), and observed that grey-black patinas were widespread distributed on stone surfaces exposed to sun radiation, while green patinas were more frequent in shaded areas.

Fig. 1.3. Stone statue from Queluz National Palace (Portugal) showing green biofilms.

Light radiation represents an important selective factor into ecosystems exposed for long time to solar radiation. In general, dark coloured algal/cyanobacterial biofilms are consequence of their protection against excessive light intensities. Cyanobacteria and green algae are able to modify their pigmentation, in order to optimise the photosynthetic process under unfavourable environmental conditions. For example, nitrogen-fixing cyanobacteria can take a yellow-brown colour when little nitrogen is available, leading to a dramatic reduction of chlorophyll *a* and phycocyanin and an increase of carotenoids. In other cases, it has been shown that the pigmentation changes in relation to light intensity, UV radiation, temperature and cells age. In very sunny environments, carotenoids are present in large amounts in the living microorganisms (Bartolini et al., 2004). Edwards et al. (2000) pointed out that scytonemin, a UV-protective pigment present in several cyanobacteria sheaths, may offer a selective advantage for epilithic organisms on stone surfaces because they filter UV rays.

The colour changes produced by phototrophic microorganisms on monumental stone materials have been seen as an unsightly and aesthetically detrimental effect (Fig. 1.3) (Urzì et al., 1991). Nevertheless, the occurrence of cyanobacteria and algae on stone monuments also induce physical and chemical biodeterioration (Anagnostidis et al., 1991; Griffin et al., 1991; Krumbein and Urzì, 1991; Ortega-Calvo et al., 1992, 1993b; Wakefield and Jones, 1998; Saiz-Jimenez, 1999; Warscheid and Braams, 2000; Crispim and Gaylarde, 2005; Zurita et al., 2005). It has been estimated that 20 to 30% of physicochemical deterioration of stone is a result of biological activity (Wakefield and Jones, 1998). Two types of biodeterioration can be considered: biogeophysical and biogeochemical deterioration. While the effects and extent of biogeochemical deterioration processes are controlled and determined by the chemistry of minerals and the binding cement of each rock, biogeophysical mechanisms are mostly regulated by the porous system of rocks, such as porosity and pore shape (Warscheid and Braams, 2000).

Biogeochemical deterioration is the direct action caused by the metabolic processes of organisms on the substratum. The biogenic release of corrosive acids is probably the best well known and most commonly investigated biogeochemical damage mechanism in inorganic materials. The process known as biocorrosion, involves the release of organic acids which can etch or solubilise stone minerals (Krumbien, 1988). The conversion of inorganic substances by redox reactions forms

acids that etch stone and contribute to salt formation (Griffin et al., 1991; Fernandes, 2006). For instance, aerobic phototrophic microorganisms produce respiratory carbon dioxide which becomes carbonic acid and contributes to dissolution of stone and soluble salt formation (Griffin et al., 1991; Wakefield and Jones, 1998). The development of algae on the Lions Fountain at the Alhambra Palace (Granada, Spain) favoured the neoformation of mineral products, particularly, calcite as a consequence of respiration and CO_2-fixing processes (Sarró et al., 2006). The microbial mobilisation of stone constituents brings the formation of secondary minerals (Gorbushina, 2007). Some organic acids exudated by phototrophic microorganisms act as chelating agents, which sequester metallic cations from stone, such as Ca^{2+}, Mg^{2+}, Fe^{3+} and $Mn^{2+,3+}$, and precipitate on polysaccharidic sheaths of the microorganisms in the form of salts (Albertano et al. 2000; Fernandes, 2006; Gorbushina, 2007). The precipitation of calcium salts on cyanobacterial cells were reported by several authors on limestone monuments (Fig. 1.4) (Ariño et al., 1997; Ascaso et al., 1998b; Zurita et al., 2005). The biomobilisation of iron and manganese as some of the metabolised elements readily redeposited have been described as an important factor in crust formation and stone deterioration (Krumbein, 1983). The production of organic acids such as lactic, oxalic succinic, acetic, glycoleic and pyruvic has been found and associated with the dissolution of calcite in calcareous stones (Danin and Caneva, 1990; Caneva et al., 1992). Endolithic cyanobacteria and algae may also induce biogeochemical deterioration though actively dissolution of carbonates to enable penetration into the substratum enhancing stone porosity (Griffin et al., 1991; Fernandes, 2006). These biogeochemical processes give rise to biogeophysical changes on the lithic substratum.

Biogeophysical deterioration can be defined as the mechanical damage caused by exerted pressure during biological growth resulting in surface detachment, superficial losses or penetration into the material increasing stone porosity (Griffin et al., 1991). Cyanobacterial and algal biofilms undergo large volume changes and exert considerable force through cycles of drying and moistening (Saiz-Jimenez, 1999). This can lead to the alteration of the stone's pore size distribution and resulting in changes of moisture circulation patterns and temperature response (Saiz-Jimenez, 1999; Warscheid and Braams, 2000). Furthermore, the formation of biofilms induced by cyanobacterial and algal growth alters capillary water uptake and gas

diffusion in the stone material and increases the deposition rate of acidic and nutritive aerosols impacting (bio)deterioration processes (Koestler et al., 1996).

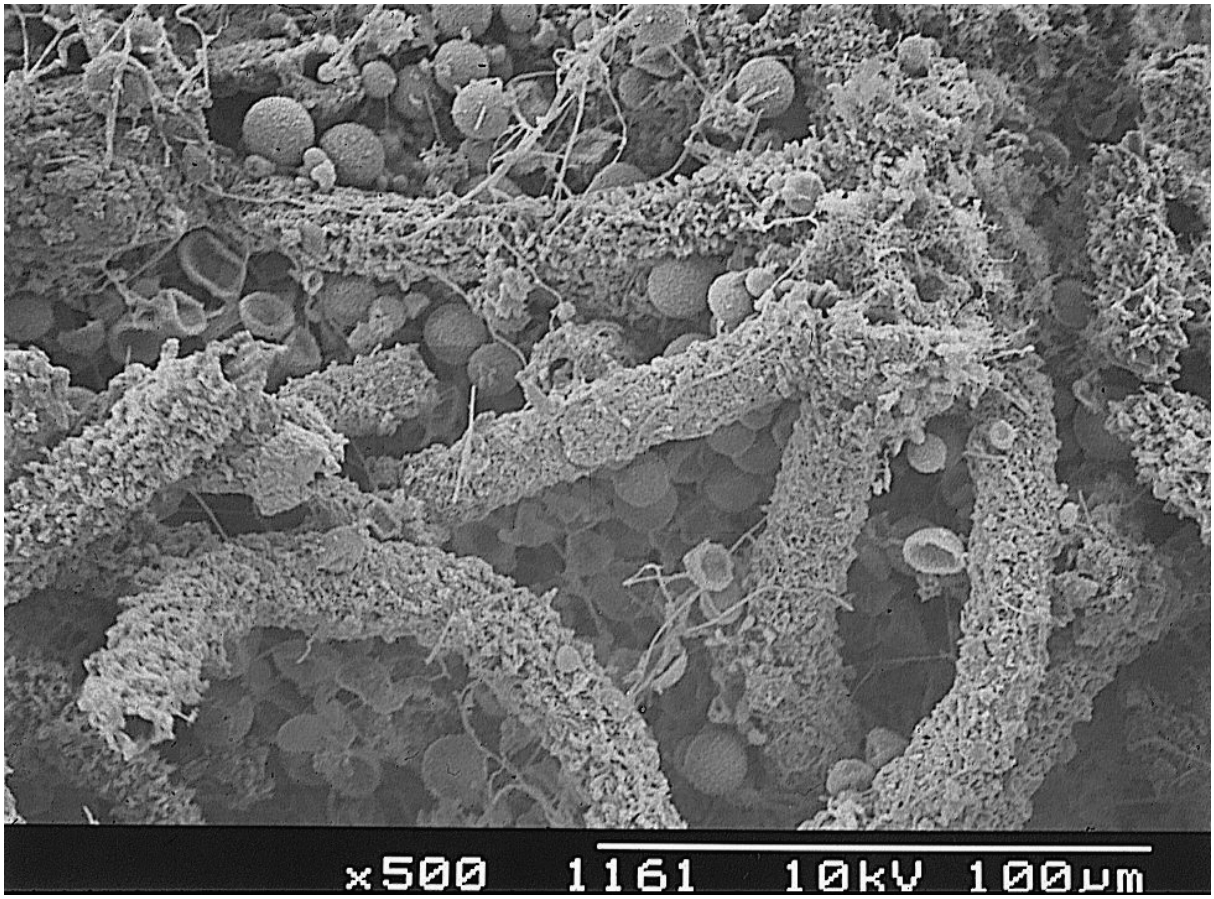

Fig. 1.4. SEM image of *Scytomena julianum* mat. The calcified sheaths are composed of triradiate calcite crystals.

A particular aspect of biogeophysical deterioration of stone monuments linked to endolithic microorganisms, is the periodic contraction and expansion of EPS inducing mechanical stress on the stone, particularly when the polymer penetrates into the pores, stimulating defoliation of the biofilm and the underlying substratum, evident at macroscopic scale (Saiz-Jimenez, 1999; Dornieden et al., 2000; Kemmling et al., 2004; Young et al., 2008). Krumbein and Urzì (1991) quoted the physical action of biofilms on and within marble demonstrating that stability and activity of water in polyionic gel matrix was crucial for the physical reactions and interactions between microbiota and rock matrix and rock porosity, giving rise to decomposition and detachment of grains, chips or scales in marbles.

Apart from direct deterioration of stone substrata, phototrophic biofilms play an indirect role in stone biodeterioration (Koestler et al., 1996). It was demonstrated that cyanobacterial and algal biofilms contribute indirectly to stone deterioration through the synergistic interactions with heterotrophic microorganisms such as fungi and bacteria. During the development of surface-covering phototrophic biofilms a succession of microorganisms occurs, beginning with the primary producers and basic mineral-degrading microorganisms and advancing to secondary consumers. The oxygenic photosynthetic activity of phototrophic microorganisms converts CO_2 into organic compounds that then become available for heterotrophic fraction, such as fungi and bacteria (Roeselers et al., 2006). Moreover, the accumulation of photosynthetic biomass on stone surfaces provides nutrients for the growth of other communities which graze on cyanobacterial and algal polysaccharides and cell debris (Albertano et al., 2000; Crispim and Gaylarde, 2005; McNamara and Mitchell, 2005; Fernandes, 2006). Therefore, the percursor function of the microbial biofilm has to be considered as one of the most important phenomena for biodeterioration impacts on stones. The detection and identification of these microorganisms are thus extremely important for future studies of biodeteriogenic processes and for the development of biodeterioration prevention and control methods.

A number of reviews give a comprehensive picture of the role of microorganisms in the deterioration of stone monuments (Warscheid et al., 1991; Ortega-Calvo et al., 1995; Tiano, 1998; Saiz-Jimenez, 1995, 1999; Warscheid and Braams, 2000; Fernandes, 2006; Gorbushina, 2007).

In recent years much emphasis has been placed upon the role of microorganisms present in biofilms responsible for stone biodeterioration. However, less attention has been paid to their accurate identification and ecology even though it may be of great interest and could provide useful information about general and applied microbiology. In fact, analysis of a microbial population can help to understand the steps of colonisation, microbial biodiversity and the relationship among the different populations on the surfaces and between microorganisms and mineral substratum. Moreover, the knowledge of the microorganisms colonising stone monuments is very important for the research of new sustainable treatments to eliminate and prevent the biodeterioration processes occurring on stone cultural heritage.

1.1.5. Bioreceptivity of stone materials

New ecology concepts, such as bioreceptivity, are currently emerging for cultural heritage studies. The concept of bioreceptivity was defined by Guillitte (1995) as "*the aptitude of a material to be colonised by one or several groups of living organisms*". The concept evidences an ecological relationship between substratum and colonising organisms. Another bioreceptivity description has also been introduced by Guillitte (1995) as "*the totality of materials properties that contribute to the establishment, anchorage and development of a microbial population, flora and fauna*". It is clear that the bioreceptivity concept expresses the colonisation potential as defined by the characteristics of the material. It is the combination of these potential and environmental conditions that allows colonisation to occur. In the study of rocks, this concept is of great usefulness since microorganisms are common inhabitants of rock surfaces and may act synergistically to deteriorate stone materials from cultural assets.

The biodeterioration effects on outdoor monuments are consequence of the bioreceptivity of the substratum. However, we must take into consideration that the chemical and physical characteristics of stone surfaces change over the time of exposure to weather. The initial mineral composition may be implemented with organic matter, contemporary the physical structure may change from almost smooth and polished to a rough finish surface with increase of stone porosity and mineral disaggregation. According to the different stages of stone deterioration, microbial colonisation of outdoor stone monuments may takes place from an earlier stage of stone deterioration to an advanced magnitude of stone deterioration. Guillitte (1995) defined different types of bioreceptivity according to the predetermined deterioration stage of the substratum. Thus, the "Primary or intrinsic bioreceptivity" is connected with the initial potential of colonisation of a sound stone. Then, following the evolution over time of surface characteristics under physical, chemical and biological factors, it becomes "Secondary bioreceptivity". The conservative and other treatments applied on stone induce "Tertiary bioreceptivity". Moreover, "Extrinsic bioreceptivity" can be defined when the stone colonisation is essentially due to the presence of settled matter not related with the beneath stone (Guillitte, 1995).

Guillitte (1995) not only defined the term but also proposed and demonstrated that bioreceptivity of a given material can be assessed by artificially inoculate the

material with the diaspores of the organism and incubate the specimens under environmental conditions that are optimal for the organism (growth chamber) (Guillitte and Dreseen, 1995). As a result, a specific “bioreceptivity index” can be determined and included in a bioreceptivity scale of each material. To achieve this outcome a multidisciplinary team must operates to choose the most suitable parameters for measuring bioreceptivity either for characterise stone properties or to quantify microbial mass. However, a methodological problem arises from this concept. Since many types of colonisation are part of a synergistic process and not all organisms present on exposed stone surfaces can develop on artificial conditions these studies are only indicatives. Taking this problem into account, it can be conjectured that the results reported in few laboratory-based experiments can be considered pertinent only for the stones used, the organisms tested and the incubation conditions applied (Guillitte, 1995; Guillitte and Dreesen, 1995).

Only recently, studies concerning the bioreceptivity of stone materials have been accomplished (Guillitte and Dreesen, 1995; Tiano et al., 1995; Silva et al., 1997; Urzì and Realini, 1998; Tomaselli et al., 2000b; Warscheid and Braams, 2000; Shirakawa et al., 2003; Prieto and Silva, 2005; Miller et al., 2006; Prieto et al., 2006; Camara et al., 2008). Within these studies, six assessed bioreceptivity of stone materials to phototrophic microorganisms through laboratory-based stone colonisation experiments (Guillitte and Dreesen, 1995; Tiano et al., 1995; Tomaselli et al., 2000b; Prieto and Silva, 2005; Miller et al., 2006; Prieto et al., 2006), and four of them included limestone materials (Guillitte and Dreesen, 1995; Tiano et al., 1995; Tomaselli et al., 2000b; Miller et al., 2006). Some attempted to develop standardised laboratory tests for assessing bioreceptivity based on several procedure steps (Shirakawa et al., 2003; Prieto and Silva, 2005). The experimental procedures rely on isolation of microorganisms, growth of isolated organisms, inoculation, incubation and quantification of biomass. In all of these experiments, single-species or a mixture of isolated strains was used for stone inoculation. However, in nature, microorganisms develop in more or less complex communities (Sand, 1997). On exposed stone surfaces they rarely grow as colonies comprising single species; rather they form complex microbial communities enclosed in a hydrated polysaccharide matrix (Costerton et al., 1995; Gorbushina, 2007). Thus, tests made with a single type of organism can become atypical, as the existence of competition and/or synergy between colonising microorganisms are not taken into account.

However, the practical approach developed by Guillitte and Dreesen (1995) showed that determining the bioreceptivity of materials from a mixture of species, such as cyanobacteria, heterotrophic bacteria, microfungi, green algae, diatoms, bryophytes, and placing them under optimal incubation conditions it was possible to simulate natural colonisation. Indeed, it was concluded that accelerated colonisation conditions allowed to distinguish different types of stone bioreceptivity and to relate these to precise characteristics of the materials.

The above mentioned experiments concerning bioreceptivity of limestones revealed that bioreceptivity is influenced by chemical and mineralogical composition, porosity, permeability and surface roughness. Guillitte and Dreesen (1995) reported that colonisation surface was correlated with the macroporosity, because this characteristic influenced the number of anchoring sites or attachment points for the diaspores. But once anchored, the development of the diaspores depended largely on the prevailing humidity. High porosity values of stone materials facilitate the spreading of microflora within the pore system, as macroporosity allows deep penetration of moisture into the material (Warscheid and Braams, 2000). While large-pore stones promote microbial colonisation only temporarily due to short water retention, small-pore stones linked to an important open capillarity favour permanent establishment due to longer water retention time (Warscheid et al., 1991; Guillitte and Dreesen, 1995).

Miller et al. (2006) reported that for the same experimental conditions and type of organisms used, differences in the bioreceptivity of stones are caused only by differences in their intrinsic properties. It was corroborated that the bioreceptivity of four Portuguese lithotypes (limestones, marble and granite) was mainly controlled by chemical composition of the substrata, rather than by physical characteristics. These findings are in contrast to the investigation of Tomaselli et al. (2000b), who demonstrated that high values of roughness and porosity determined the colonisation magnitude of five Italian lithotypes. Comparing the bioreceptivity of the assayed lithotypes of both studies, *Ançã* limestone had the highest primary bioreceptivity among the Portuguese lithotypes (Miller at al., 2006), and Pietra di Lecce and *Pietra di Vicenza*, which had the greatest values of porosity and roughness, expressed the highest degree of colonisation by phototrophic microorganisms (Tomaselli et al., 2000b).

In a study of the ability of phototrophic microorganisms to colonise 12 lithotypes, comprising marbles, limestones, dolostones, sandstones and granites, Tiano et al. (1995) also demonstrated that preferential colonisation was primarily correlated to petrophysical characteristics, especifically porosity and roughness, and secondarily to chemical composition of the assayed lithotypes. Also the stone pH controlled the colonisation process, rather than chemical composition. Regarding stone surface development, *Angera*, *Lecce* and *Vicenza* limestones presented the highest extent of colonisation.

From the above examples it is evident that limestones with high porosity values and surface roughness are more susceptible to phototrophic colonisation, facilitating the anchoring and spreading of microbial organisms into the stone material. Although high values of porosity linked to a large-pore system promote colonisation only temporarily, the development and death of successive pioneering generations will enrich and condition the lithic substratum with inorganic and organic nutrients for further development of heterotrophic microorganisms on stone surfaces. Then, with the progressive deterioration of the physical surface conditions, together with the accumulation of airborne particles and dust, a “soiling” effect is induced which allows the implantation and germination of vegetal reproductive bodies deposed from the air on surfaces. Thus, an ecological succession will progressively develop until a climax community is established. The ecological succession in a monument exemplify the importance of studying the bioreceptivity of a lithotype before using it as building stone in determined environmental conditions. The data obtained from these experiments provide architects, engineers and conservators/restorers with information on the colonisation risk and help them to select the appropriated stone materials to use in future construction and to design sustainable treatments and methodologies for conservation and restoration purposes.

The selection of appropriate type of stone for new buildings is one of the most important aspects in terms of durability to maintain the quality of stonework in lithic works of art exposed outdoors and buildings. The durability of these cultural heritage assets is a measure of its ability to resist deterioration and so to retain its original size, shape, strength, and appearance over an extensive period of time (Bell, 1993a; Ordóñez et al., 1997). Bioreceptivity, as well as, strength, hardness, density and appearance are stone properties that determine its durability and performance on buildings and works of art. Thus, bioreceptivity as a property influencing stone

durability is an important parameter for the estimation of the long-term evolution of monument's colonisation. The quality of a stone is ascertained approximately from a study of its geological origin, its physicochemical characteristics and from the results of tests and different laboratory-based experiments. Another important aspect is the way in which the extrinsic factors affect the stone materials, particularly the function and local of exposition, pollution and climatic conditions. The safeguard of cultural heritage has therefore a significant influence on the economy of nations rich in stone cultural assets, influencing two main socio-economic factors: the significant amount of human and financial resources needed to diagnostic and preserve important stone heritage and the improvement of both tourism and quality of life through a sustainable management of the artistic patrimony of the Mediterranean countries.

1.1.6. Techniques applied for detection and identification of photosynthetic biofilms

Stone monuments can be a paradigm of a complex environment with which microorganisms can be confronted as it encompasses heterogeneity and dynamic in time and space. The microbial flora of outdoor cultural assets can be exposed to a variety of different environmental conditions as a result of the habitat in which they dwell on. This heterogeneity of most stone cultural heritage poses particular problems for sampling and monitoring, as the representative sampling required is often difficult to obtain. These peculiarities are an example of the problems encountered with the methods used for the detection and identification of microorganisms dwelling on stone cultural assets.

1.1.6.1. Microscopy techniques

The identification of phototrophic microorganisms can be accomplished through direct observations of fresh sample material under the microscope. However, common microbial identification includes culture methods, which rely on isolation of microorganisms in culture media and subsequent identification of pure cultures. The culture of microorganisms is a cornerstone of microbial characterisation. Culture techniques were developed by Beijerinck and Winogradsky at the beginning of the

20th century to cultivate a variety of metabolically diverse microorganism from natural habitats. Microorganisms such as bacteria, cyanobacteria, algae and fungi are cultivated in a variety of culture media (liquid or solidified by the addition of agar), which contain nutrients indispensable to the growth of the microorganisms under investigation. After isolation procedures, the microorganism are morphologically characterised and taxonomically classified by direct observations of their phenotypic characteristics under the microscope. Taxonomic identification is drawn from comparisons with a number of literatures (e.g. Bourrelly, 1990; Komárek and Anagnostidis, 1999).

The application of microscopy techniques illustrates the diversity of microorganisms, but can also depict the function and structure of microbial biofilms. Analysis of microbial colonisation profile and microorganisms-mineral substratum interactions are important features for understanding the biodeterioration dynamics. Light microscopy and scanning electron microscopy are frequently used to monitor the colonisation progress and the relationships between microorganisms and certain deterioration phenomena. These techniques provide the best direct evidence of biofilm formation by imaging actual cells and permit to examine the microorganism-substratum interface and morphologically characterise the microbial species of this interface.

Several microscopy techniques have been used for the study of stone biodeterioration process by phototrophic microorganisms. The most common are the classical light microscopy (Ortega-Calvo et al., 1993b; Crispim et al., 2003; Miller and Macedo, 2006), scanning electron microscopy (SEM) (Ascaso et al., 2002; De los Ríos et al., 2004; De los Ríos and Ascaso, 2005), transmission electron microscopy (TEM) (Hernández-Mariné et al., 2001, 2004) and confocal laser scanning microscopy (CLSM) (Roldán et al., 2004; Wierzchos et al., 2004).

SEM creates magnified images with greater magnifications than light microscopy by using a particle beam of high-energy electrons to generate a variety of signals at the surface of solid samples. The three signals which provide the greatest amount of information in SEM are the secondary electrons, backscattered electrons, and X-rays. Scanning electron microscopy in secondary electron mode (SEM-SE) has been widely applied to morphologically characterise the biological elements of the microorganisms-substratum interface (Dornieden et al., 2000). Secondary electrons are emitted from the atoms occupying the sample surface, which produce a

contrast image determined by the sample morphology. SEM technique with backscattered electrons (SEM-BSE) is also widely used to identify phases based on qualitative chemical analysis and/or crystalline structure. Backscattered electrons are those which are reflected from atoms in the solid sample. The contrast image produced is determined by the atomic number of the elements in the sample. Thus, ultrastructural features inside the microorganisms can be examined (Wierzchos and Ascaso, 1994; Ascaso et al., 1998b), as well as their interaction with the mineral substratum (Ascaso et al., 1998a). The simultaneous application of the Energy Dispersive X-ray Spectroscopy (SEM-EDS) allows the chemical characterisation of mineral features. Interaction of the beam electrons with atoms in the sample causes shell transitions resulting in the emission of an X-ray, which has an energy characteristic of the element. Prieto et al. (1997) and Ascaso et al. (2002) applied SEM-EDS to morphologically, mineralogicallly and chemicallly characterise the effects produced by lichens on granite and limestone, respectively.

Conventional SEM preparation procedures include resin impregnation, sectioning and polishing. Non-conducting samples are then coated with a thin layer of carbon or gold. Biological samples require previous chemical fixation and dehydration, according to a method developed by Wierzchos and Ascaso (1994).

Other types of SEM have been applied to examine surface morphology and microorganism-substratum interface. For example, low-temperature SEM (LTSEM) has been applied to examine fractured deep-frozen samples, enabling observation of alterations related with the presence of water (Ascaso et al., 2002; De los Ríos and Ascaso, 2005). Environmental SEM (ESEM) has been used to examine fresh samples without modification or preparation (Welton et al., 2005; Sanchez-Moral et al., 2005; Cañaveras et al., 2006). TEM observations have also been applied to provide microbial cytological identification (size, shape and arrangement of organelles) and their relationships within the biofilms and with the substrata (Hernández-Mariné et al., 2004).

In addition to SEM examinations, the use of fluorochromes has been recently developed for CLSM application to cyanobacteria, and has provided valuable information on different types of phototrophic biofilms, their pigment properties, and presence of EPS structures (Hernández-Mariné et al., 2003; Roldán et al., 2004). CLSM is a technique for obtaining high-resolution optical images with depth selectivity. The key feature of confocal microscopy is its ability to acquire in-focus

images from selected depths, a process known as optical sectioning. Images are acquired point-by-point and reconstructed with a computer, allowing three-dimensional reconstructions of topologically-complex objects (Fig. 1.5).

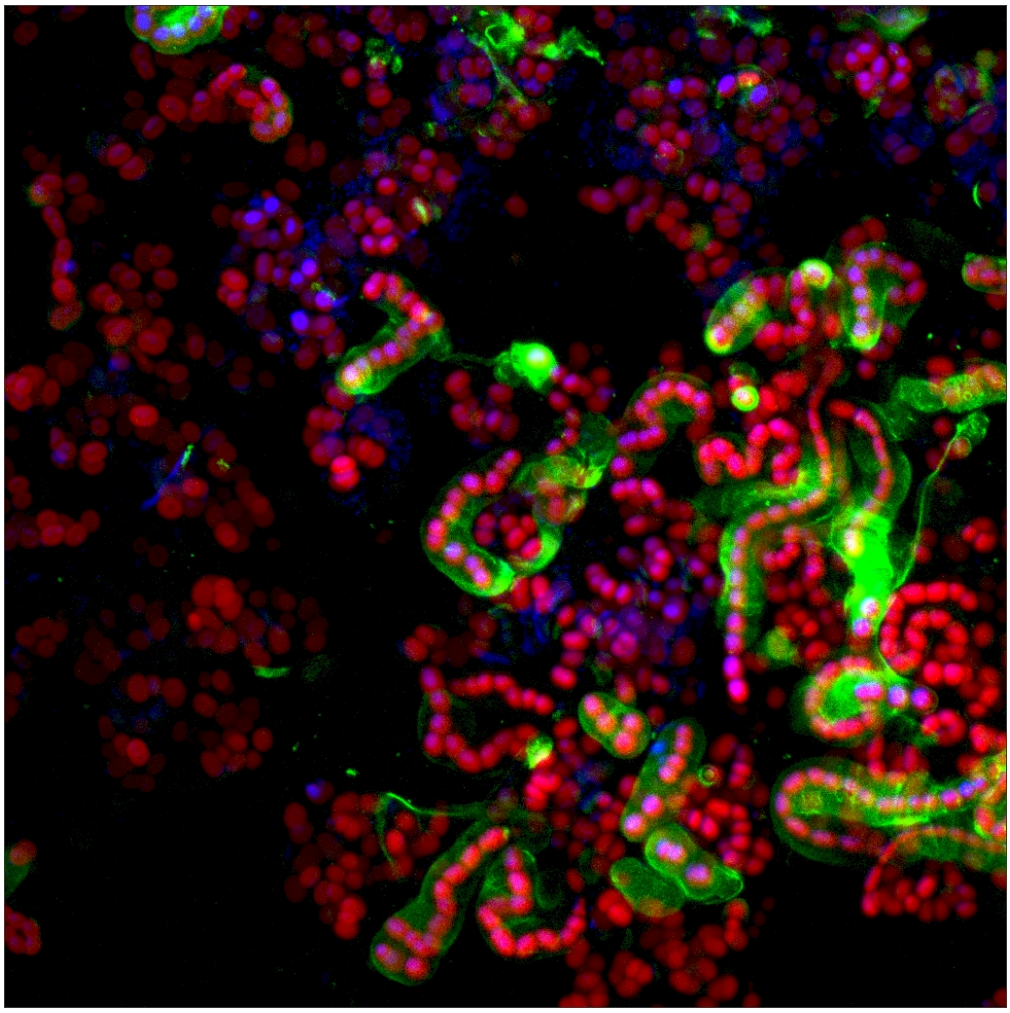

Fig. 1.5. Confocal microscope image of filaments of *Nostoc punctiforme* in the vegetative growth state (biofilm sample come from Nerja Cave, Málaga, Spain). Pigment fluorescence is shown as red colour, polysaccharides labelled with Con-A-AlexaFluor 488 as green colour, and nucleic acids stained with Hoechst 33258 as blue colour.

1.1.6.2. Molecular biology versus culture techniques

Classical culture methods have been used for the identification of biodeteriorating agents (Saiz-Jimenez et al., 1990; Ortega-Calvo et al., 1991a; Bellinzoni et al., 2003; Gaylarde and Gaylarde, 2005). These culture-based approaches are extremely useful for demonstrating the importance of microorganisms in biodeterioration processes and for understanding the physiology

and morphology of isolated microorganisms. However, they are not only time-consuming but also need relatively large amounts of sample, which may be particularly prominent when working with art objects, where only small quantities of sample material are available. Moreover, results do not necessarily provide complete information on the composition of microbial communities. This culture technique was questioned by several authors, on the grounds that some microorganisms are difficult to isolate and cultivate; only a small portion, typically far less than 1% of bacteria in the environment can be cultivated (Ward et al., 1990; Amann et al., 1995; Hugenholtz et al., 1998). There are many reasons for the failure of the usual culture strategies; the most common is that selective cultures fail to reproduce the conditions that particular microorganisms require for growth in their natural habitat. This conclusion has been confirmed in a variety of environments, including cultural heritage assets, where microorganisms are mostly members of a complex microbial consortium and depend on special nutrients (Gurtner et al., 2000; Laiz et al., 2003; Gonzalez and Saiz-Jimenez, 2004).

Recently, molecular biology methods are being introduced in the field of biodeterioration of cultural assets as culture-independent techniques based on the analysis of specific nucleic acids sequences (Muyzer et al., 1993). These culture-independent techniques enable the detection of slowly-growing, fastidious or unculturable microorganisms. Moreover, they only require little sample material in the range of 1 – 2 mg (Schabereiter-Gurtner et al., 2001), which is a big advantage in some specific environments such as cultural assets.

Molecular techniques are based on the detection of DNA genes encoding for the ribosomal RNA (rRNA). The most common is the 16S for prokaryotes and 18S for eukaryotes. The 16S rRNA gene (rDNA) is a good taxonomic tool due to its universal distribution and the fact that contains variable and highly conserved regions which allow distinguishing between organisms on all phylogenetic levels. In one of the most straightforward molecular methods used in analyses of microbial communities dwelling on monuments, the DNA is extracted from natural mixed microbial communities and amplified by PCR (Polymerase Chain Reaction) using primers[1] targeting the 16S rRNA gene. During PCR cycles of repeated heating and cooling are used for DNA melting and enzymatic replication of the DNA, generating 10^6-to-

[1] Short DNA fragments that serves as a starting point for DNA replication.

10^9 copies of the target DNA sequence. DNA amplification by PCR is schematically outlined in the diagram from Figure 1.6.

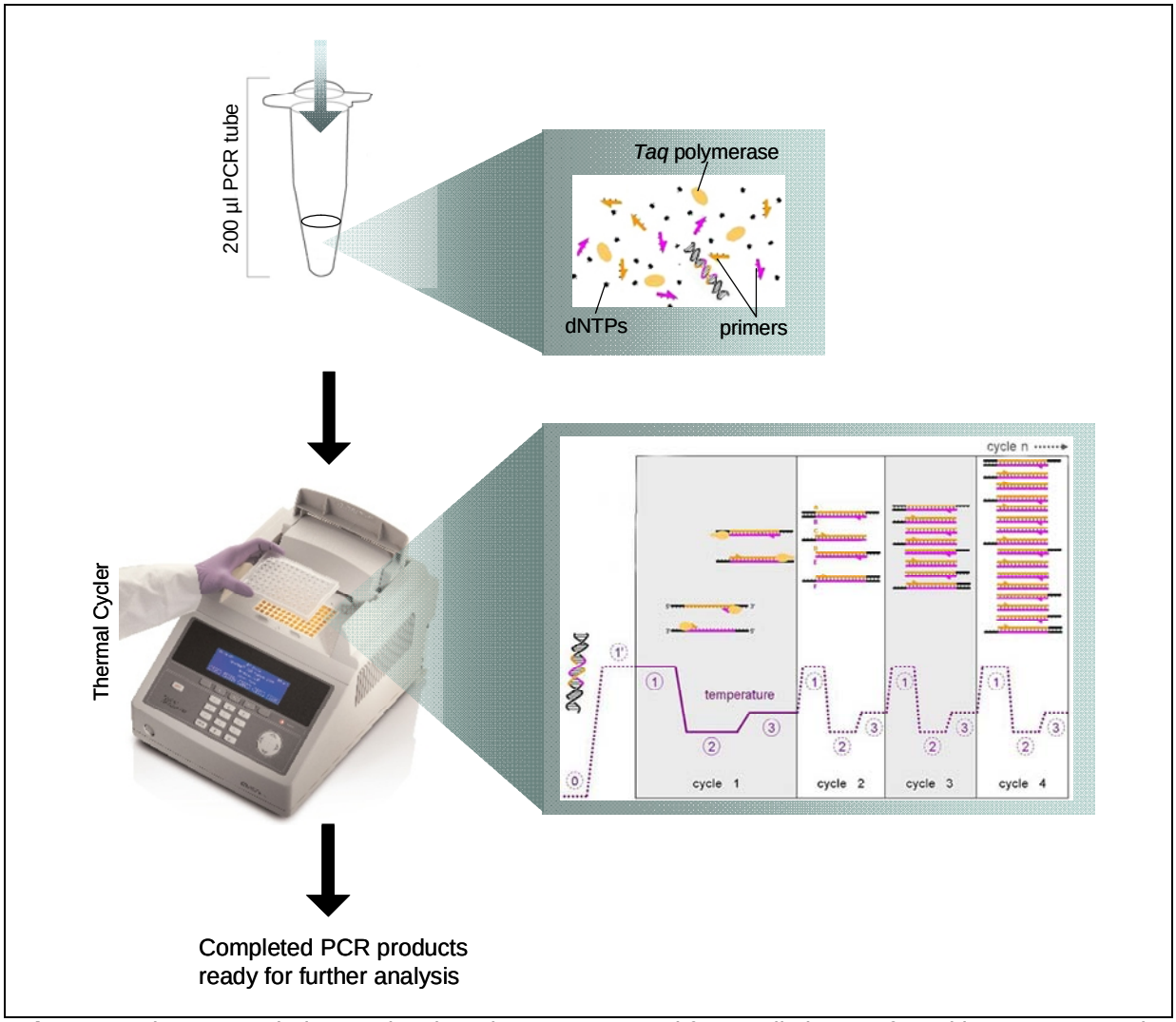

Fig. 1.6. Polymerase chain reaction (PCR). DNA extracted from cells is transferred into a 200 µL tube special for PCR. Two primers are added, each with a sequence complementary to that found in one strand at the end of the DNA region to be amplified. Nucleotides (dNTPs) and Taq polymerase are also added. In the first cycle, heating to 95ºC (temperature •) denatures the double-stranded DNA and subsequent cooling to 55-65ºC (temperature ❟) allows the primers to anneal to their complementary sequences in the target DNA. *Taq* polymerase extends each primer from 5' to 3', generating newly synthesised strands in both directions, which extend to the end of the original strands. The extension is performed at 72ºC (temperature ***f***). In the second cycle, the original and newly made DNA strands are denatured at 95ºC and primers are annealed to their complementary sequences at 55-65ºC. Each annealed primer again is extended by *Taq* polymerase. In the third cycle, two double stranded molecules are generated exactly equal to the target sequence. These two are doubled in the fourth cycle and are doubled again with each successive cycle.

In order to obtain a visualisation of the biodiversity present in the sample, the 16S rDNA PCR products are reamplified (nested PCR), and the resulting short length PCR amplified gene fragments are separated electrophoretically by DGGE (Denaturing Gradient Gel Electrophoresis). This technique separate 16S rDNA PCR products, all of the same length but with a different base pair composition, in an acrylamide gel system containing a gradient of denaturants (urea and formamide) (Muyzer et al., 1993). The denaturation of the double stranded DNA depends on the content of the GC (Guanine-Cytosine) and AT (Adenin-Thymin) base pairs. The increasing concentration of denaturants along the gel confers the double stranded DNA into single stranded DNA, decreasing their mobility (and thus their position in the gel). As a result, the community fingerprint or profile is obtained, which consists in a band pattern in which each band represents a microbial taxon from the original sample (Fig. 1.7). DGGE is one of the most used techniques to study natural microbial communities and is well suited to detect microbial community members dwelling on cultural heritage (Rölleke et al., 1996). The technique has the advantage to get phylogenetic sequence information of individual microbial members of the community by either excising individual DGGE bands from the gel, or by construction of clone libraries for further sequencing.

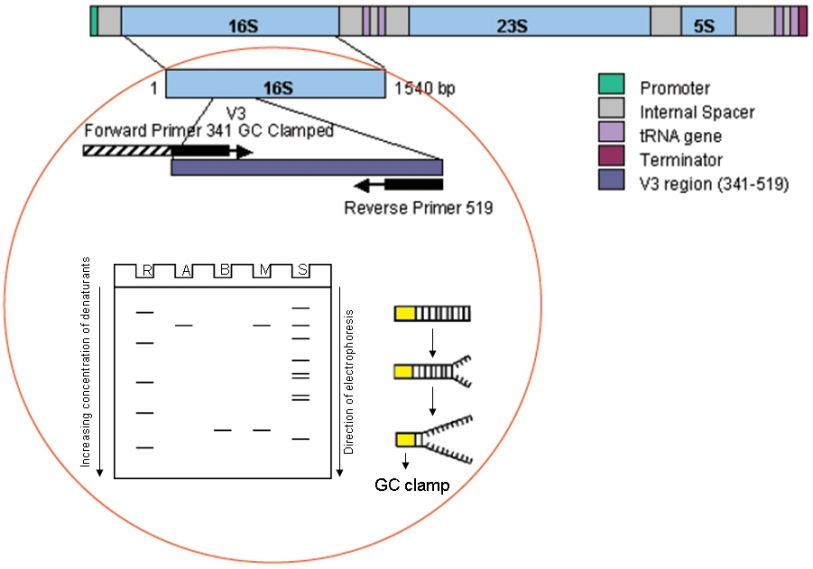

Fig. 1.7. Principle of DGGE. PCR products with the same length are electrophoretic separated depending on their GC-content. The increasing concentration of denaturants along the gel confers the double stranded DNA into single stranded DNA, decreasing their mobility (and thus their position in the gel). A GC clamp, attached to the 5' end of one of the PCR primers prevents complete denaturation of the double stranded DNA fragment since it is highly resistant to chemical denaturation. R: Reference pattern; A: Organism 1. A=T rich DNA; B: Organism 2. G≡C rich DNA; M: Mix of organisms 1 and 2; S: natural sample.

Construction of a clone library and sequencing can complement the information obtained from a community fingerprinting of the sample by allowing the identification of the microorganisms corresponding to each band visualised by DGGE. The resulting mixture of long PCR amplified fragments, originating from the different microorganisms in the sample, can be cloned by using commercially available kits. The basic procedure of molecular cloning involves the ligation of DNA fragments to a vector, transformation and screening of clones. Briefly, the DNA fragment produced by PCR is inserted into another DNA molecule that serves as vehicle or vector[2], which can replicates autonomously in host cells. When these two DNA of different origin are combined, the result is a recombinant DNA molecule, which is transferred to a host cell (usually *E*. *coli*). Within this cell, the recombinant DNA replicates, producing identical copies known as clones. As the host cells replicate, the recombinant DNA also replicates, creating a population of identical cells carrying the cloned sequence. Finally, the cloned DNA fragments can be recovered from the host cells and purified for further sequencing. The result is a clone library that can be screened by DGGE in order to identify potentially identical clones and minimise the amount of sequencing done (Fig. 1.8). By sequencing individual clones and comparing the obtained sequences with those present in very extensive and accessible international databases, it is possible to phylogenetically identify the corresponding microorganism without its cultivation. The information contained in any 16S rRNA gene sequence is enough to obtain an unambiguous identification of a microorganism at the genus level (Gonzalez and Saiz-Jimenez, 2004).

[2] Cloning vectors are carrier DNA molecules. The classic cloning vectors are plasmids, which are naturally occurring extrachromosomal double-stranded circular DNA molecules that carry an origin of replication and replicate autonomously within bacterial cells. Plasmid vectors are modified to contain a specific antibiotic resistance gene and a multiple cloning site.

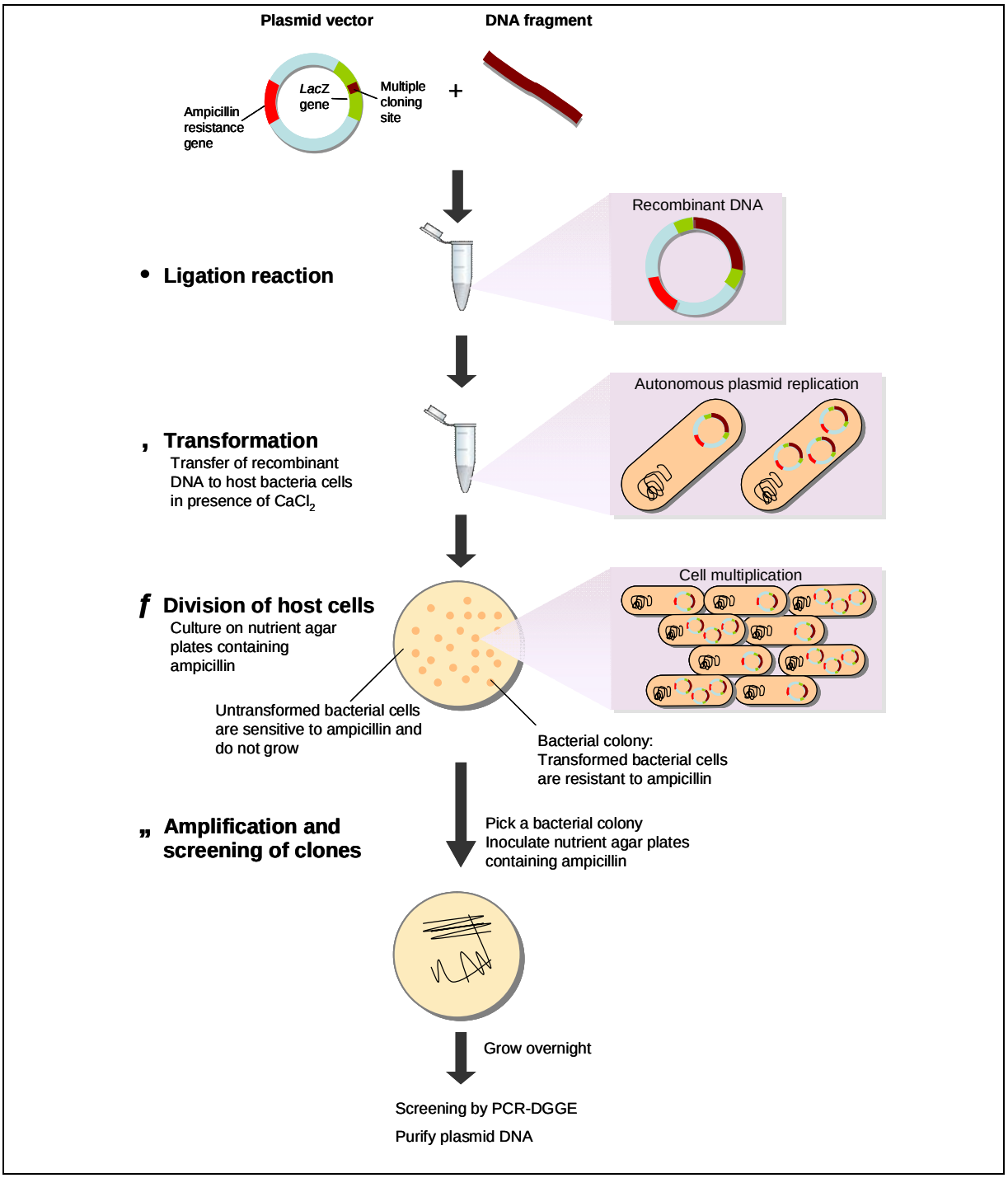

Fig. 1.8. Molecular cloning using a plasmid vector involves four major steps. 1) Ligation reaction. The plasmid vector and the DNA fragment are mixed together in a ligation reaction containing DNA ligase. The plasmid vector carries the ampicillin resistance gene and a multiple cloning site. 2) Transformation. Transfer of ligation reaction products to host bacteria, usually competent E. coli. Within each transformed host bacterium, there is autonomous multiplication of plasmid DNA. 3) Division of host cells. Bacteria are plated on a selective agar medium containing the antibiotic ampicillin. If foreign DNA is inserted into the multiple cloning site, bacterial colony containing recombinant plasmid DNA will appear. If there is no insertion of foreign DNA in the multiple cloning site, bacterial colony will not grow. 4) Amplification and screening of clones. A bacterial colony is used to inoculate agar medium containing ampicillin. After growing the bacteria overnight, the culture is harvested, bacterial cells are lysed, and the plasmid DNA is used for amplification by PCR-DGGE for the selection of clones to be sequenced. The selected plasmid DNA are purified and used for sequencing.

At present, the application of molecular techniques is filling the existing gap between the detection of cultured and uncultured microorganisms (Laiz et al., 2003). These techniques, especially those including the sequencing of genes encoding for 16S rRNA, have become a very important tool to study microbial communities dwelling on cultural heritage assets. The benefits are: i) the minimisation of sampling; ii) the optimisation of information on the type of microorganisms colonising different cultural heritage materials allowing to design effective treatments for eliminating active microbial communities, and iii) to analyse the potential health risks, such as toxic or bioreactive metabolites produced by the biological community colonising the objects undergoing restoration.

Microorganisms growing on cultural assets undergo a large variety of processes following their establishment, growth, death, physiological adaptation, conversion to unculturable cells, physical spread and gene transfer. Hence, the application of culture-dependent and culture-independent techniques has important differential characteristics but they are simultaneously complementary. For instance, the use of culture methods will assess the culturable part of the microbial population allowing the assessment of their morphology and physiology. On the other hand, the use of molecular biology techniques will yield information on the community members present, but it will not determine their viability or culturability. For a robust assessment of the type of microorganisms colonising monuments and cultural heritage assets, it is, therefore, often necessary to use both approaches.

1.1.6.3. Photosynthetic biomass quantification techniques

In addition to the identification of microorganisms present on a substratum, it is necessary to perform, when possible, quantitative analyses of the microbial biomass. It is not sufficient to know whether or not a microorganism is present, but also in what amounts it exists to determine its role in the deterioration process. Microbial biomass can be estimated by a variety of bulk techniques in which some cell constituent such as organic matter, protein, or chlorophyll is extracted and quantified from microbial communities. The biomass of cyanobacterial and algal communities dwelling on stone monuments can be quantified through chlorophyll *a* (chl*a*) quantification techniques. Chl*a* is a photosynthetic pigment present in all species that performs photosynthesis, including eukaryothic (algae) and prokaryotic (cyanobacteria)

organisms. This photosynthetic pigment harvests the light energy necessary for carbon reduction and forms approximately 1 to 2% of the dry weight from cyanobacteria and microalgae species (Banse, 1977). Thus, it is commonly used as a measure of phototrophic microorganisms biomass. Most methods of chlorophyll quantification are based on its extraction from disintegrated cells in an organic solvent and on its subsequent determination by spectrophotometry (Parsons and Strickland, 1963; Lorenzen, 1967), fluorometry (Yentsch and Menzel, 1963; Holm-Hansen et al., 1965) and high performance liquid chromatography (Goeyens et al., 1982; Wun and Lltsky, 1982). These methods have been widely used in limnological researches to determine chl*a* from different types of algae (phytoplankton, periphyton, marine or freshwater algae, etc.) and in monitoring programs with the purpose of ecosystem management (Macedo et al., 2000, 2001). However, these methods are time-consumimg, require large volume of samples and do not allow the repeated measurement in time of the same sampling unit, because of their destructive nature. To follow the temporal dynamics of a periphyton community using these methods, the mean value of biomass must be estimated from a relatively large number of samples at different times. Furthermore, in the case of cultural heritage samples, one of the disadvantages inherent to this method is the scaffolding and sampling procedure required, which takes more relevance when samples are collected from cultural heritage assets (thus a limitation in their number).

In recent years, a rapid, reliable and non-destructive chlorophyll determination method based on *in vivo* chlorophyll fluorescence were introduced in the analysis of monuments and historic buildings to detect phototrophic organisms (Cecchi et al., 2000; Tomaselli et al., 2002; Miller et al., 2006). This method allows rapid measurements of *in vivo* chl*a* fluorescence on solid substrata without sampling procedures and has been used to detect phototrophic microorganisms on monuments, monitor preventive treatments and to characterise different stone types (Cecchi et al., 2000; Tomaselli et al., 2002; Miller et al., 2006). Natural fluorescence is one of the key characteristics of chl*a*; this pigment absorbs light in all regions of the visible spectrum, showing maximum absorption in the blue-violet (about 430 nm) and red regions (around 660 nm) and emitting in a wavelength of about 680 nm when light excited at 430 nm (see appendix one). Fluorescence analysis can detect phototrophic microorganisms at an early stage of development when they are still not visually observed. Nowadays, a remote sensing analysis of stone monuments by

fluorescence lidar has been applied, which allows a fast, extensive monitoring of large surfaces and, in addition, an easy to read thematic mapping. This method was first investigated by Cecchi et al. (2000) for the detection of photosynthetic biodeteriogens growing both on stone surfaces from a monument and inoculated in the laboratory.

1.1.6.4. Digital image analysis

Digital image analysis techniques constitute a very useful set of tools allowing non destructive detection, monitoring and quantification of different elements included in digital images. As digital image, we understand every pictorial representation of the data obtained by a sensor, i.e., a device capable for detecting electromagnetic radiation, for converting it into a signal and for presenting it in a way suitable for study (Chuvieco Salinero, 2002).

The data obtained by a sensor is directly related to the materials reflectance, which is the percent of reflected radiation in its sensitivity wavelength range. These data are translated to numerical values and ordered in a matrix in which two Cartesian coordinates define the spatial position and a third coordinate defines the reflectance value. Digital images are usually multiband images, as for the Cartesian coordinates, is commonly available more than one reflectance coordinate. This set of two Cartesian coordinates and a third reflectance coordinate receives the name of band. A typical digital photographic image is composed of three bands, each one with encoded reflectance values of the intervals 400-500, 500-600, and 600-700 nm (Blue, Green and Red bands). As digital image analysis, we understand the set of mathematical operations that can be performed with this type of images.

The quantification and monitoring of phototrophic biofilms on surfaces by digital image analysis is easily performed by means of the simple counting of the pixels corresponding to the elements of interest from the digital photographs. Previously, it is necessary that the set of images used for the quantification is geometrically consistent. As photographs are product of a conical projection, they have not directly metrical properties. To correct this problem the geometry of the images must be remapped in order to elaborate ortophotographs. Photogrammetry, involving two or more images of the same object becomes necessary to perform this task. When the

photographed surface is flat enough it is possible to utilise single images for the geometrical rectification (Karras and Petsa, 1999; Schuhr and Kanngieser 1999, 2001, 2003). Easy-to-use software, such as Adobe Photoshop®, is available for the digital rectification of single photographs (Almagro, 2002).

Green patinas are a good indicator of the presence of phototrophic biofilms; however, these colour patinas are not always easily discernible from highly correlated images. The spectral behaviour of the different elements when registered in diverse wavelength intervals is quite similar, having the effect of masking them in the image, obtaining a high visual correlation. When the images fall into this category, we find two different options for image enhancement: i) conventional linear contrast stretching (Gillespie et al., 1986), i.e., contrast stretching by means of the expansion of the histogram, redefining the limits of the pixel values interval. With this approach, it is possible to obtain results enough good, although sacrificing the extreme values; and ii) decorrelation technique, which reduce the redundant data that mask the information in the image. This approach allows achieving the objective of the detection of masked elements inside the digital image, avoiding the loss of data. The most useful decorrelation technique is the Principal Components Analysis (PCA), which is a common multivariate statistical analysis technique developed at the beginning of 20th century by Pearson (1901) and widely used in the processing of remotely sensed images (Chuvieco Salinero, 2002). Basically, PCA consists in the calculation of uncorrelated linear combinations of the original data explaining amounts progressively reduced of data variation (Martínez Arias, 1999). As the analysis allows the reduction of the dataset, the redundant information can be securely avoided (Cetica et al., 2002). The application of this technique results in an improvement of the visualisation of the different elements included in the digital images. Applied to rock art studies, for example, PCA has revealed as a powerful tool to distinguish subtle differences, indistinguishable in conventional photographs (Vicent García et al., 1996), or to show motifs not visible at all (Mark and Billo, 2006). This approach has been used to improve the visualisation of rock art motifs in highly correlated images (Rogerio-Candelera, 2008), and to record separately different elements (of different nature and composition) present in mural paintings (Rogerio-Candelera et al., 2008a).

1.2. Framework of the thesis

1.2.1. Research problems in the field of stone monuments conservation

The present work was developed having the following problems under consideration:

1. The conservation of historic buildings and monuments from cultural heritage is a major issue in modern societies, both from an economical and cultural point of view. The wide distribution of stone cultural assets in the Mediterranean Basin countries, and their cultural, artistic and religious importance emphasises the potential social impact that biological damage can wreak on these cultural heritage. Part of the difficulties experienced on conservation interventions are caused by inaccuracy and inconsistency of conservation strategy designs. The knowledge of the microorganisms responsible for stone biodeterioration and the understanding of biodeterioration processes have a fundamental importance to define conservation strategies and new sustainable treatments, as well as to prevent further biodeterioration.
2. Portugal has played an important role in the world history and consequently numerous national monuments have been classified as World Heritage by UNESCO. These monuments are sensitive to deterioration and especially to biodeterioration. However, the biodeterioration of Portuguese stone monuments was not a major concern until recently. First studies date back from 90´s and addressed mainly the impact of lichens in granite and carbonate substrata (Aires-Barros and Maurício, 1995; Monte et al., 1996; Leite Magalhães et al., 1998; Romão et al., 2000; Ascaso et al., 1998b, 2002). Despite several international studies established that cultural heritage assets can be deteriorated by microorganisms, there is still a paucity of national knowledge in the field of stone conservation/restoration. Several interventions do not always take into account biodeterioration as an integral part of the global deterioration process due to the reduced national scientific knowledge. Consequently, conservation interventions

do not always obtain the expected result, and sometimes they even hasten the biodeterioration process.

3. Although colonising organisms dwelling on stone monuments have been described, less attention has been paid to their accurate identification. Precise characterisation of phototrophic biofilms associated with stone is crucial in order to prevent, eradicate or minimise microbial colonisation. There is a clear need for more extensive and multidisciplinary studies. In the particular case of Portugal, little if any attempt have been made regarding the identification of phototrophic biofilms. In fact, only a few studies were presented in international congresses (Miller and Macedo, 2006; Pereira de Oliveira et al., 2008, 2009).

4. The microbial ecology of weathered stone surfaces is poorly understood even though it may be of great interest and could provide useful information about general and applied microbiology. Analysis of phototrophic microorganisms, their role in the biodeterioration process as well as their geomicrobiological interactions can help to understand the steps of colonisation, microbial biodiversity, and the relationship among the different populations on the surfaces and between microorganisms and mineral substratum.

5. Most studies concerning microbial community composition applied classical culture methods, which detect only a small portion of microorganisms within the biological samples, are time-consuming and need relatively large amounts of sample material. This is particularly predicament when studying cultural assets. Recently, molecular biology techniques have been introduced in the field of cultural heritage as accurate and straightforward methodologies, which enable the unculturable microorganisms to be detected requiring very little amount of sample material. However, little if any attempt appear to have been made to the identification of stone colonising microorganisms by molecular techniques in the Portuguese context. Moreover, precise comparisons between phototrophic microorganisms dwelling on different stone monuments from countries with similar climatic conditions (e.g. Portugal, Spain and Italy) seem to be scarce.

6. Bioreceptivity is a new ecological concept currently emerging in the field of cultural heritage. However, the knowledge on the stone bioreceptivity and the influence of stone intrinsic properties on its bioreceptivity is still fragmentary and needs to be overcome. In what concerns bioreceptivity of Portuguese lithotypes, the first study was published in 2006 by Miller et al. (2006) and new publications were not noticed until now. It is, therefore, crucial to annihilate this drawback scenario and disseminate the bioreceptivity studies to end-users in order to provide them information on the colonisation risk and help for an appropriate selection of the lithotype for building purposes or for conservation and restoration interventions.

1.2.2. Objectives

The problems mentioned above have encouraged the development of this thesis, whose main objective was to evaluate the primary bioreceptivity of limestones widely used as building materials in European countries from the Mediterranean Basin. To achieve this goal some methodological/experimental issues were ought to be overcome through the following specific objectives:

1. To prepare a review of the literature concerning the phototrophic microorganisms dwelling on different and representative stone materials from historic buildings and monuments of the Mediterranean Basin, in order to compare and be acquainted with the most abundant cyanobacteria and green algae species detected on limestone materials.
2. To select five different limestone monuments from Portugal, Spain and Italy according to their cultural importance in the Mediterranean Basin, climate conditions similitude, availability of stone materials used in their constructions and presence of stone surfaces with green patina appearance.

3. To collect phototrophic biofilms from the five selected limestone monuments and to identify their major phototrophic components by molecular biology techniques.
4. To culture the natural phototrophic biofilms, composed mainly by cyanobacteria and algae, in order to monitor their evolution progression under laboratory conditions and to select a multiple-species phototrophic culture stable under laboratory conditions to be used for further limestone colonisation experiments.
5. To characterise petrographycally, petrophysically and petrochemically five different quarry limestone types used in the studied monuments in an attempt to further understand their primary bioreceptivity.
6. To inoculate quarry limestone samples, of the five lithotypes with the selected multi-species phototrophic culture and to incubate under optimal laboratory conditions during 90 days within an incubator chamber.
7. To monitor the phototrophic biofilms developing on the limestone samples during incubation by quantifying the biomass through different analytical approaches.
8. To evaluate the primary bioreceptivity of the five studied lithotypes and to assess the influence of petrophysical and petrochemical properties in their primary bioreceptivity.
9. To appraise the biodeterioration effects induced by the phototrophic microorganisms on the limestone types and to examine the interactions between the phototrophic microorganisms and the lithic substrata.
10. To disseminate the information obtained in this work to end-users, e.g. conservators/restorers, architects, engineers, and to diffusion molecular methodologies within the monumental conservation enterprises, especially in the case of Portugal. This involves contributions to conferences which central focus is the conservation of monuments and publications in international scientific journals.

1.2.3. Work strategy

The experimental work carried out for the study of bioreceptivity to phototrophic microorganisms of limestones from European countries of the Mediterranean Basin was achieved in six stages:

1. In the first instance, qualitative data establishing the presence of a large variety of cyanobacteria and green algae on stone monuments from the Mediterranean Basin have been synthesised in the second chapter in order to provide a quick way to compare the species dwelling on different monuments and to perceive correlations between microorganisms and stone types. About 45 case studies from 32 scientific papers published between 1976 and 2009 were analysed. Six distinct lithotypes were considered: marble, limestone, travertine, dolomite, sandstone and granite.
2. In the second step, five green biofilms were collected from the North outer surfaces of limestone monuments located in Portugal, Spain and Italy in order to characterise and compare phototrophic communities dwelling on the selected monuments by molecular biology techniques complemented with culture procedures. This study is presented in chapter three.
3. The third stage, also presented in chapter three, involved: i) the cultivation of large volumes of the five natural green biofilms and monitoring of their temporal evolution by DGGE, and ii) the determination and selection of the multiple-species phototrophic culture which represented an establishment of the microbial components present in the natural biofilm sample. This multiple-species community culture was obtained for further laboratory-based stone colonisation experiments since phototrophic microorganisms are pioneer inhabitants of stone materials.
4. The fourth step is attended in chapter four and consisted in a preliminary stone colonisation assay performed on *Ançã* limestone in order to evaluate the reliability of the selected phototrophic culture as inoculum for accelerated stone colonisation. This experiment relied on the inoculation of stone samples with the multiple-species culture and in their incubation in a laboratory chamber during three months.

5. The fifth experimental step comprised the primary bioreceptivity of five sound limestones obtained from the original quarries used for the construction of the studied stone monuments. Firstly, petrographic, petrophysical and petrochemical characterisation of the stone samples was accomplished, followed by their inoculation with the selected multiple-species phototrophic culture. Incubation was conducted inside a growth chamber during 90 days. Different analyses were carried out to monitor and determine which lithotype induced the best phototrophic growth. Thus, the bioreceptivity of the five limestones could be determined, together with statistical analyses, as well as the influence of the intrinsic stone properties in their bioreceptivity. The data are presented in chapter five.
6. Finally, a detailed study on the biodeterioration potential of cyanobacteria and algae, with particular reference to endolithic microorganisms is presented in chapter six. This stone biodeterioration appraisal was achieved through different microscopic techniques and X-ray diffraction analysis.

The experimental work performed in the thesis is schematically outlined in the diagram from Figure 1.9.

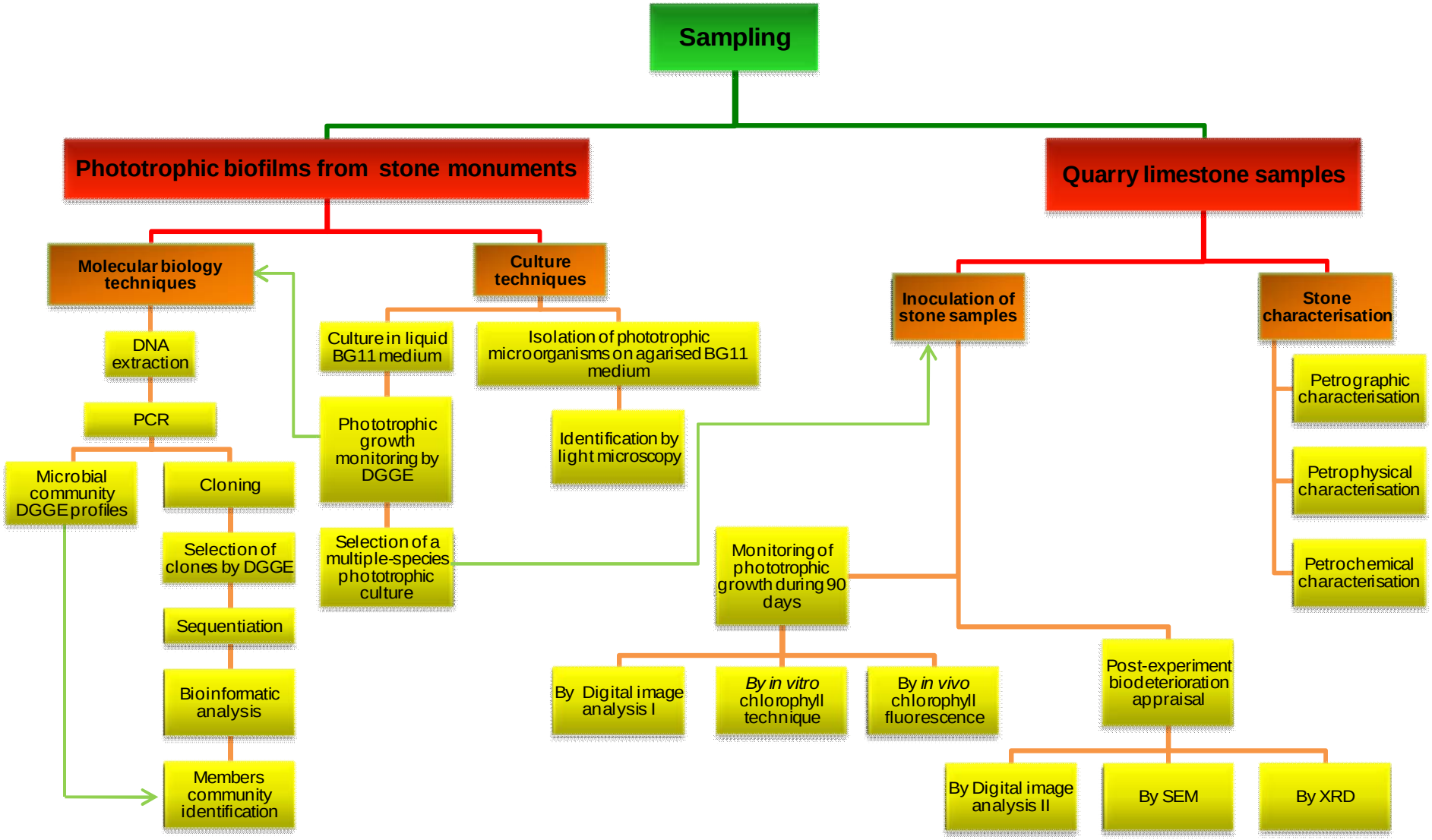

Fig. 1.9. Diagram of the experimental work performed to study the primary bioreceptivity of five different limestone types.

CHAPTER TWO

Biodiversity of cyanobacteria and green algae on monuments from the Mediterranean Basin: an overview

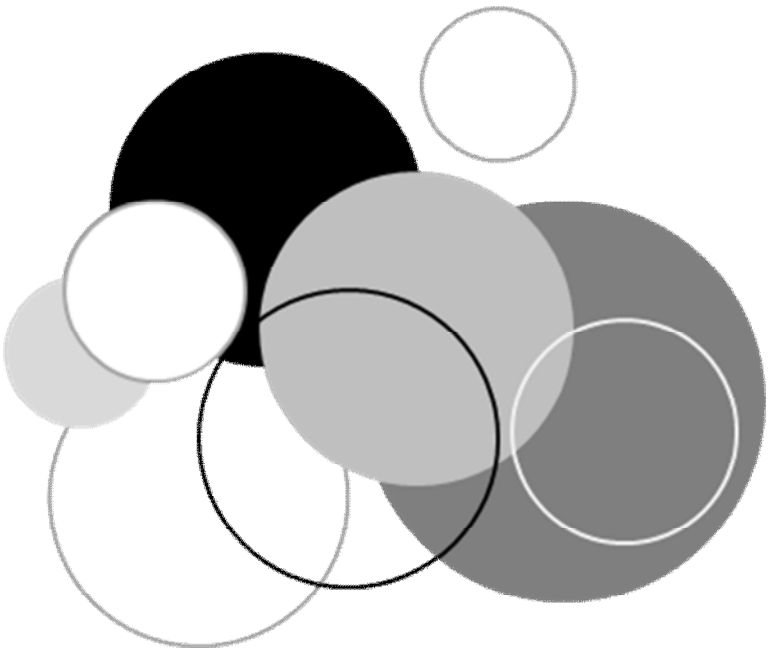

The main results presented in this chapter have been published in:

Macedo, M.F., Miller, A.Z., Dionísio, A., Saiz-Jimenez, C., 2009. Biodiversity of cyanobacteria and green algae on monuments in the Mediterranean Basin: an overview. Journal of Microbiology 155, 3476-3490.

CHAPTER TWO

Biodiversity of cyanobacteria and green algae on monuments from the Mediterranean Basin: an overview

2.1. Introduction

The extent and type of biological deterioration induced on different types of stone depend on the type of organisms found thereon. This review of the literature focus on the presence of cyanobacteria and green algae dwelling on stone monuments and lithic works of art. Microbial populations present in a stone substratum are usually the result of a successive colonisation by different microorganisms that has taken place over several years (Ortega-Calvo et al., 1991a; Lamenti et al., 2000; Crispim and Gaylarde, 2005). It is a process that comprises the capacity of a substratum to provide a protective niche on which microorganisms can develop. Identifying the microorganisms involved in biodeterioration is one of the most important steps in the study of the microbial ecology of monumental stones. It can help to understand the microbial biodiversity, phases of colonisation and the relationship among populations and between microorganisms and substrata.

Investigations which have been carried out on microbial communities on objects of art and monuments so far are mainly case studies. The results of all these studies have to be presented in a way that the data can be compared, and also to see correlations between microorganisms and certain deterioration phenomena. An inventory of the occurrence of cyanobacteria and green algae detected in stone monuments, statues and historic buildings from European countries of the Mediterranean Basin yielded by several authors was performed, indicating the type of microorganisms and from where they have been isolated (monument and substratum). Marble, limestone, travertine, dolomite, sandstone and granite were the six lithotypes considered in this work, corresponding to the lithotypes mainly used in the construction of buildings and monuments from the Mediterranean Basin. The

phototrophic microorganisms inventoried were almost entirely found on outdoor monuments located in the Mediterranean Basin area, belonging to the Mediterranean climate. This type of climate is characterised by mild and rainy winters, warm and dry summers and, usually, extended periods of sunshine throughout most of the year; temperatures during winter rarely reach freezing (except in areas with a high elevation), and snow is unusual.

This study is important since it gathers together data from the literature, useful for the study of biological colonisation in cultural heritage buildings. A growing database could offer a quick and powerful record, giving all-time opportunity of recognising any isolate of a biodeteriorating organism if already known from another site or type of cultural item. Such a library could on the long run, enable the conservators/restorers to choose methods for disinfecting/ sanitation of the objects which had proven value on a similar organism found earlier elsewhere. Moreover, this work provides a useful tool for laboratory-based stone colonisation experiments allowing for the selection of single-species or mixed community and/or stone substratum for ecological studies.

2.2. Cyanobacteria on monuments

Table 2.1 presents the monuments, statues and historic buildings reported in this study. Most of these works of art were built in limestone (32%) and marble (30%). Travertine (7%) and dolomite (2%) were the lithotypes less represented (Fig. 2.1).

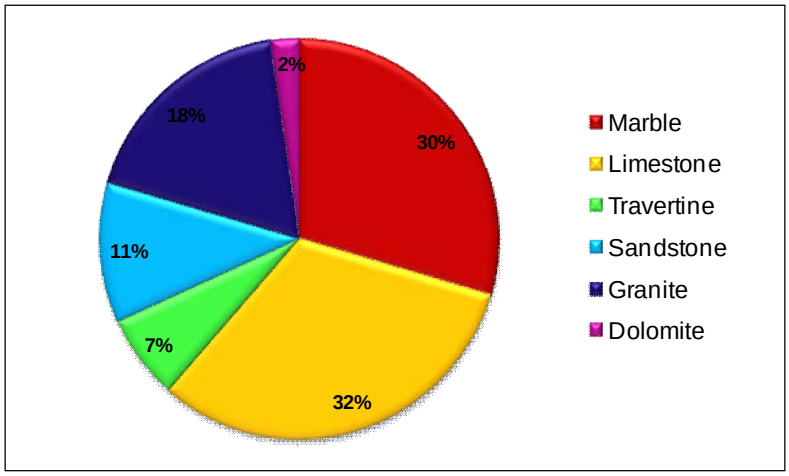

Fig. 2.1. Percentage of lithotypes present in the monuments, statues and historic buildings reported in this study.

Fig. 2.2. *Gloeocapsa* sp. observed under optical microscope (1000x).

Table 2.2 lists the cyanobacteria detected on monuments and works of art in the Mediterranean Basin, together with the substratum. The data on cyanobacteria occurring on stone monuments and works of art is rather wide. A total of 96 taxa of cyanobacteria were found. The genus *Gloeocapsa* (Fig. 2.2) was the most widespread, occurring in 20 of the 45 monuments reported, in all substrata and represented by 8 species. Cyanobacteria species from the genera *Phormidium* and *Chroococcus* were able to colonise 5 of the 6 stone substrata considered and they were represented by high species diversity: 8 species of *Phormidium* and 4 species of *Chroococcus* were reported. *Chroococcus* species were detected colonising 13 different monuments while *Phormidium* was found in 15 monuments. *Pleurocapsa* occurred in 13 monuments but only one species was identified while the genus *Scytonema* occurred with 5 species and colonising 8 different monuments. Therefore, we can consider that *Gloeocapsa*, *Phormidium* and *Chroococcus* are the most common cyanobacterial genera in the monuments of the Mediterranean Basin. This is in accordance with Ortega-Calvo et al. (1995) who stated that the most common species found on monuments located in Europe, America and Asia, belong to the genera *Gloeocapsa*, *Phormidium*, *Chroococcus* and *Microcoleus*. These

genera are ubiquitous and therefore their presence is not strictly related neither with a specific lithic substratum or climate. Tomaselli et al. (2000b) also found out that the data reported in the literature did not establish a clear relationship between organisms and the nature of the substratum. Nevertheless, these authors stated that *Phormidium tenue*, *P. autumnale* and *Microcoleus vaginatus* prefer siliceous substrata.

Figure 2.3 shows the number of cyanobacterial taxa present on each litothype. According to the literature reviewed in this study, marble and limestone were colonised by about the same number of taxa (56 and 55, respectively). Travertine was a lithotype present only in 7% of the monuments reported but it was colonised by a considerable number of taxa (23). Granite was colonised by very low number of different taxa (only 10) when compared with limestone or marble. According to Ortega-Calvo et al. (1995), granite, with a very low porosity and pH, is an unfavourable substratum for cyanobacteria. In fact, the colonisation of stones is closely correlated to porosity, roughness, hygroscopicity and capillarity water absorption that strongly influence water availability for microorganisms (Urzì and Realini, 1998; Prieto and Silva, 2005; Miller et al., 2006).

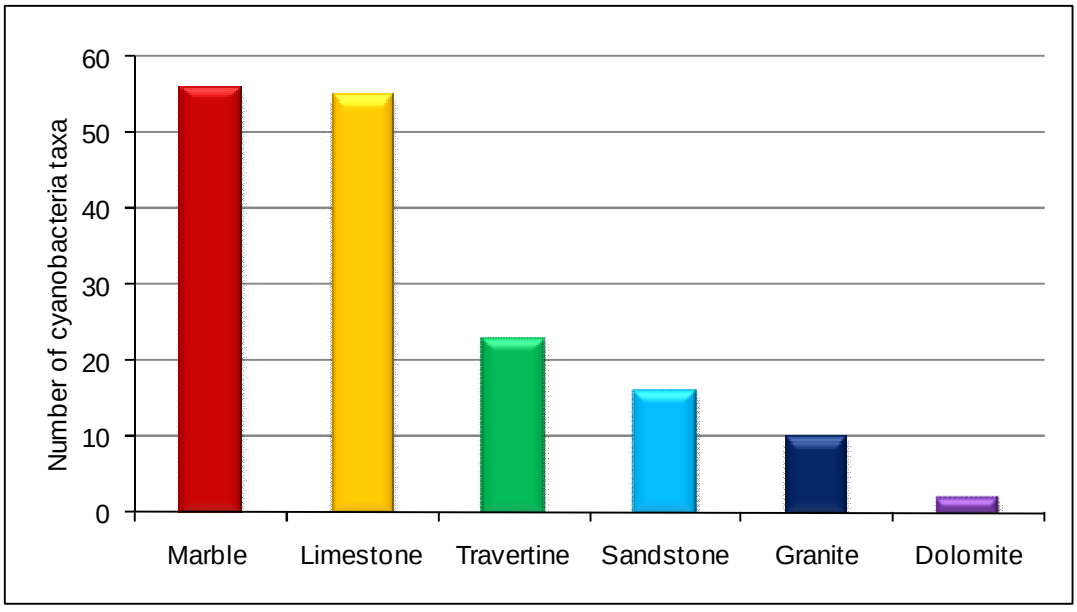

Fig. 2.3. Number of cyanobacteria taxa found on each lithotype.

A high number of taxa found on a substratum do not necessarily imply high bioreceptivity of that substratum, since many other environmental parameters play an important role in a successful colonisation (solar radiation, temperature, water regime, climate, etc.). In this study we attempted to select monuments subjected to similar climatic conditions (the Mediterranean climate), nevertheless specific microclimatic parameters (orientation, exposure to shadow, permanent capillary humidity, etc.) are generally missing in the available literature, and the extent microclimate determines colonisation is unknown. The microclimate determines the degree of colonisation, the type of community, and its specific composition. Monuments can create microclimatic differences between places that are very close. Ortega-Calvo et al. (1993b) observed that samples taken near ground level were characterised by the absence of cyanobacteria, which were however present in samples taken from places more exposed to sunlight. Detailed observations in different monuments subjected to lower humidity suggested that the formation of a photosynthetic biofilm developing on the stone surface is related substantially to the length of the period of wetness and the spatial orientation of the substratum (Fig. 2.4). In addition, the physicochemical characteristics of the materials favour the establishment of photosynthetic communities at depths that also depend on the external environmental factors, especially light, which influences the total biomass of the community (Saiz-Jimenez, 1995). Bellinzoni et al. (2003) assessed the correlation between biological growth and environmental factors on travertine. The biological colonisation showed a characteristic trend with the microclimate (orientation and presence or absence of trees).

Under the most extreme terrestrial climates, such as hot and cold deserts, endolithic cyanobacterial growth can occur and commonly inhabit the outer millimetres to inner centimetres of rocks exposed to such environments (Walker et al., 2005). The endolithic microhabitat gives protection from intense solar radiation and desiccation, and it provides mineral nutrients, rock moisture and growth surfaces (Friedmann, 1982; Bell, 1993a; Walker et al., 2005). However, very few studies report the presence of endolithic cyanobacteria in the monuments of the Mediterranean Basin. Pentecost (1992) observed that endolithic growth was often obscured by superficial algal growths, and subsequently overlooked.

Fig. 2.4. *Klebsormidium flaccidum* biofilm on a terracotta statue, Cathedral of Seville.

In this study, we noted the endolithic growth of *Phormidium*, *Plectonema*, *Chroococcopsis*, *Synechocystis* and *Synechococcus* on Ordem de São Francisco Church, Portugal. These cyanobacteria were found growing under a black patina in granite (Pereira de Oliveira, 2008; Pereira de Oliveira et al., 2008). *Phormidium* was also found growing under a black sulphated crust developed on limestone in the Cathedral of Seville, Spain (Saiz-Jimenez et al., 1991). Endolithic growth of *Hyella fontana* was observed in marble statues in Rome, Italy (Giaccone et al., 1976) and also in the Lindaraja Fountain, Granada (Spain) (Bolivar and Sanchez-Castillo, 1997).

Cyanobacteria can live in rock fissures and cracks and in cavities occurring in porous transparent rocks such as sandstones, granite and marble, but not in dense dark volcanic rocks. Chasmo- and endolithic cyanobacteria and chlorophyta were present in all samples examined from the marbles of the Parthenon and Propylaea Acropolis in Athens, Greece (Anagnostidis et al., 1991). Cryptoendolithic cyanobacteria such as *Chroococcidiopsis* live beneath rock surfaces together with cryptoendolithic lichen, fungi and bacteria. *Chroococcidiopsis* can survive extreme

cold, heat and arid conditions and it may be the single autotrophic organism most tolerant to environmental extremes (Graham and Wilcox, 2000).

The cyanobacterium *Borzia periklei,* a rare aerophitic species described and found on the marbles of the Parthenon, Greece (Anagnostidis and Komarek, 1988), is of particular interest. The second record was in the stuccos of the Roman town of Baelo Claudia, South Spain (Hernandez-Marine et al., 1997) (Fig. 2.5). The growth of this cyanobacterium on mortars suggests a good adaptation to carbonate environments. Mortars, not considered in this review, can provide niches which are suitable for relatively rare species or species peculiar to other, very specific, ecological niches. The high porosity and the mobilisation of salts, together with the humidity retained in the inner layers of the wall, facilitate the colonisation and growth of such organisms.

Fig. 2.5. Light microscope micrograph of trichomes of *Borzia periklei*, composed of 4-8 cells.

Most of the cyanobacteria mentioned in this review (e.g. *Gloeocapsa*, *Gloeothece*, *Phormidium*, *Chroococcus*, *Plectonema*, *Scytonema*, *Lyngbya* and *Microcoleus*) present a gelatinous sheath that acts as a reservoir of water, where it is bound through strong molecular forces, allowing these cyanobacteria to colonise the stone even when dry conditions prevail (Ortega-Calvo et al., 1991a). The sheath can

also play an important role in the substratum adhesion (Fig. 2.6). Sometimes sheaths may be pigmented. This is particularly evident in some cyanobacterial genera such as *Gloeocapsa* or *Scytonema* that show thick sheaths with intense colours being the expression of different ecological stages and environmental adaptations. Cyanobacteria can take a yellow-brown colour when the nitrogen is low due to a dramatic reduction in chlorophyll and phycocyanin and an increase in carotenoids. In other cases, it has been shown that pigmentation changes in response to environmental factors including light intensity, light quality, nutrient availability, temperature and the cells age. Bartolini et al. (2004), in a study carried out on monuments located on the Appia Antica road (Rome), observed that grey-black patinas represented a wide spread alteration on marble and travertine stone works exposed to sun irradiation, and the green patinas were more frequent on tufaceous materials and mortar in shaded areas. These coloured patinas cause aesthetic damage, giving an unsightly appearance of neglect to buildings, statues and monuments.

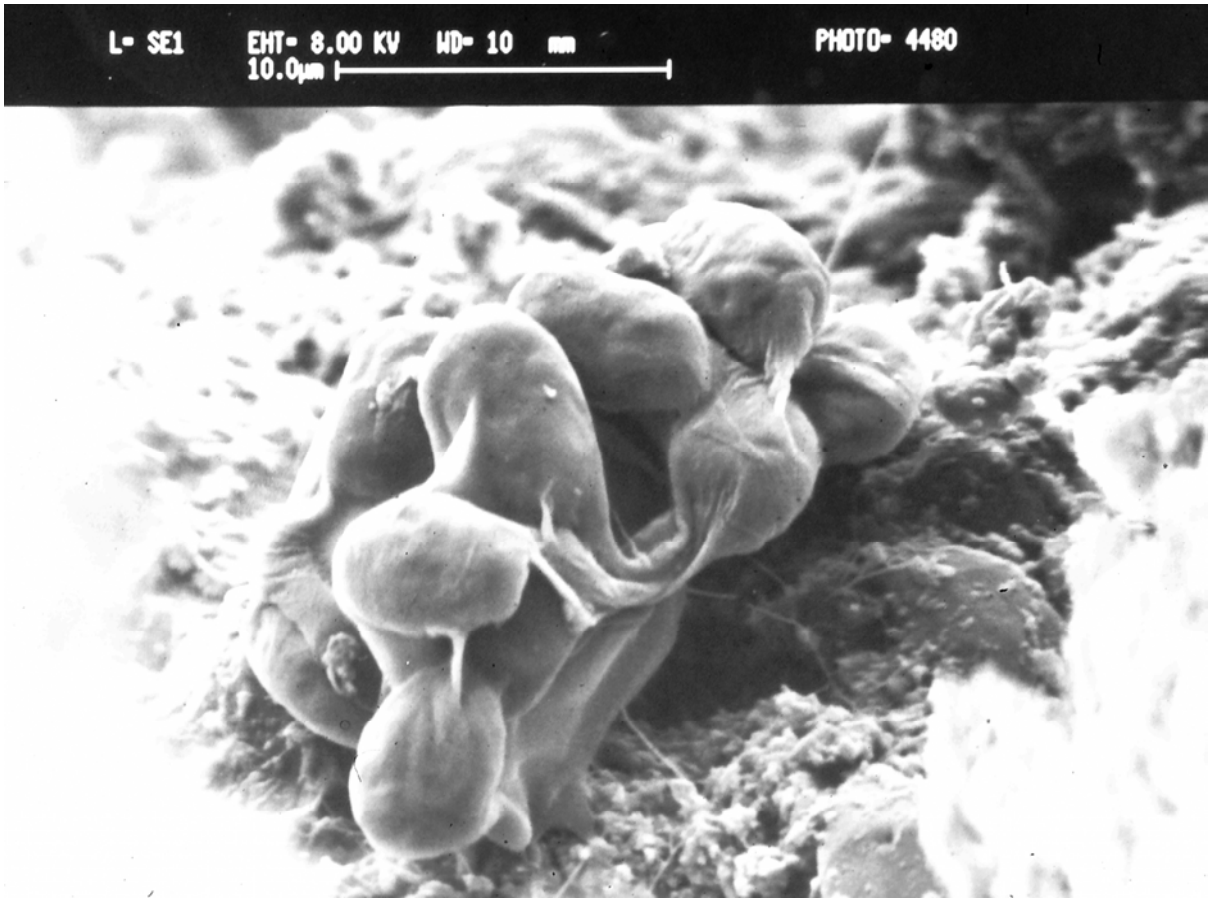

Fig. 2.6. SEM micrograph of a biofilm induced *in vitro* on sandstone. *Gloeothece* cells and sheath.

Table 2.1. Investigated monuments, statues and historic buildings in European countries from the Mediterranean Basin, and their bibliographic references.

No.	Monument	Reference
1	Ajuda National Palace, Lisbon (Portugal)	Miller et al. (2009b)
2	Bibatauín Fountain, Granada (Spain)	Zurita et al. (2005)
3	Boboli Garden statues, Florence (Italy)	Lamenti et al. (2000)
4	Brunelleschi Rotunda, Florence (Italy)	Tomaselli et al. (2000b)
5	Ca' d'Oro façade, Venice (Italy)	Salvadori et al. (1994)
6	Caestia Pyramid, Rome (Italy)	Caneva et al. (1992)
7	Carrascosa del Campo church, Cuenca (Spain)	Gómez-Alarcón et al. (1995)
8	Cathedral of Granada, Granada (Spain)	Miller et al. (2009b)
9	Cathedral of Seville, Seville (Spain)	Saiz-Jimenez et al. (1991)
9a	Cathedral of Seville, Seville (Spain)	Miller et al. (2009b)
10	Cathedral, SI. (Italy)	Tomaselli et al. (2000a)
11	Church of St. Cruz, Coimbra (Portugal)	Santos (2003)
12	Crypt, Church M. Favana, Lecce (Italy)	Tomaselli et al. (2000b)
13	Fontana dei Quattro Fiumi, Rome (Italy)	Ricci and Pietrini (1994)
14	Forte Belvedere, Florence (Italy)	Tomaselli et al. (2000b)
15	La Citadelle, Blaye (France)	Crispim et al. (2003)
16	La Mola quarry, Novelda –Alicante (Spain)	Ascaso et al. (2004)
17	Largo da Paço Building, Braga (Portugal)	Leite Magalhães and Sequeira Braga (2000)
18	Leaning Tower, Pisa (Italy)	Tomaselli et al. (2000b)
19	Fountains of the Alhambra, Granada (Spain)	Bolívar and Sánchez-Castillo (1997)
19a	Lions Fountain at the Alhambra Palace, Granada (Spain).	Sarró et al. (2006)
20	Lungotevere walls, Rome (Italy)	Bellinzoni et al. (2003)
21	Lutheran church, Florence (Italy)	Tomaselli et al. (2000b)
22	Magistral church, Alcala de Henares (Spain)	Flores et al. (1997)
23	Michelangelo cloister, Natl. Roman Museum, Rome (Italy)	Pietrini et al. (1985)
24	Ordem de São Francisco Church, Oporto (Portugal)	Pereira de Oliveira (2008)
25	Orologio Tower, Martano (Italy)	Miller et al. (2009b)
26	Palace of Sts George and Michael, Corfu (Greece)	Pantazidou and Theoulakis (1997)
27	Paleolithic sculptures in Angles-sur-l'Anglin (France)	Dupuy et al. (1976)
28	Parthenon and Propylaea acropolis, Athens (Greece)	Anagnostidis et al. (1991)
29	Parthenon, Athens (Greece)	Anagnostidis et al. (1983)
30	Roman monuments in Appia road, Rome (Italy)	Bartolini et al. (2004)
31	Roman Statue, Volterra (Italy)	Tomaselli et al. (2000b)
32	Romanic portal of the Sant Quirze de Pedret church, Berga (Spain)	Alvarez et al. (1994)
33	Salamanca Cathedral, Salamanca (Spain)	Ortega-Calvo et al. (1993b)
34	San Francisco church, Betanzos, La Coruña (Spain)	Noguerol-Seoane and Rifón-Lastra (1996)
35	San Miniato Basilica, Florence (Italy)	Tomaselli et al. (2000b)
36	Santa Clara-a-Velha Monastery, Coimbra (Portugal)	Miller et al. (2008, 2009b)
37	Santiago church, Betanzos, La Coruña (Spain)	Noguerol-Seoane and Rifón-Lastra (1996)
38	Sculptures in Ostia Antica (Italy)	Giaccone et al. (1976)
39	St. Maria church, Alcala de Henares (Spain)	Flores et al. (1997)
40	Tacca's Fountains, Florence (Italy)	Tomaselli et al. (2000a)
41	Temples of Athena, Neptune and Basilica, archaeological area of Paestum, Salerno (Italy)	Altieri et al. (2000)
42	The Pyramid, Florence (Italy)	Tomaselli et al. (2000b)
43	Toledo Cathedral, Toledo (Spain)	Ortega-Calvo et al. (1993b)
44	Trajan's Forum, Rome (Italy)	Caneva et al. (1992)
45	Vilar de Frades church, Barcelos (Portugal)	Miller and Macedo (2006)

Table 2.2. Cyanobacteria reported on stone monuments, statues and historic buildings in European countries from the Mediterranean Basin, on different substrata.

Cyanobacterium	Substratum	Monument no. (Table 2.1)
Aphanocapsa sp.	Marble, limestone	26, 27, 28
Aphanocapsa grevillei (Berkeley) Rabenhorst	Travertine	13
Aphanocapsa roeseana De Bary	Marble	6, 44
Aphanothece sp.	Sandstone, limestone	27, 32
Aphanothece saxicola Nägeli	Marble, limestone	19
Borzia periklei Anagn.	Marble	28
Borzia trilocularis Cohn ex Gomont	Marble	29
Calothrix sp.	Sandstone, limestone	26, 32
Calothrix braunii Bornet and Flahault.	Limestone	38
Calothrix marchica Lemmermann	Marble	6, 44
Calothrix parietina (Nägeli) Thuret	Marble	38
Chamaesiphon sp.	Limestone	2
Chamaesiphon incrustans	Marble, limestone	19
Chlorogloea sp.	Limestone, travertine	2, 41
Chlorogloea microcystoides Geitler	Travertine, marble, limestone	19, 41
Chlorogloea purpúrea Geitler	Marble, limestone	19
Chroococcidiopsis sp.	Limestone, marble, granite, sandstone	1, 2, 3, 8, 9a, 14, 18, 21, 40, 42
Chroococcopsis sp.	Granite	24
Chroococcus sp.	Limestone, travertine, sandstone, dolomite	2, 16, 32, 38, 41
Chroococcus lithophilus Ercegović	Travertine, marble	20, 30
Chroococcus minor (Kützing) Nägeli	Marble, limestone	6, 26, 28, 29, 44
Chroococcus minutus (Kützing) Nägeli	Travertine, limestone	13, 26
Chroococcus tenax (Kirchner) Hieronymus	Limestone	38
Cyanosarcina sp.	Marble, limestone	26, 28
Cyanosarcina parthenonensis Anagnostidis	Marble	28
Cylindrospermopsis sp.	Limestone	1
Dermocarpa kerneri (Hansgirg) Bourr.	Marble	29
Geitlerinema sp.	Marble	3, 10, 31, 35, 40
Gloeocapsa sp.	Limestone, marble, travertine, sandstone, dolomite, granite	2, 3, 5, 11, 15, 16, 27, 32, 35, 41, 42, 45
Gloeocapsa alpina (Nägeli) Brand	Limestone	45
Gloeocapsa biformis Ercegovic	Travertine, marble	6, 20, 26, 27, 28, 30, 44
Gloeocapsa calcarea Tilden	Marble	6, 44
Gloeocapsa compacta Kützing	Marble, travertine	30
Gloeocapsa decorticans (A. Braun) Richter	Marble	29
Gloeocapsa kuetzingiana Nägeli	Limestone	11, 26
Gloeocapsa novacekii Komárek & Anagnostidis	Limestone	11
Gloeocapsa sanguinea (Agardh) Kützing	Limestone	26
Gloeothece sp.	Sandstone	32
Gomphosphaeria sp.	Sandstone	32
Hydrocoleus homoeotrichus Kützing ex Gomont	Marble	29
Hyella fontana Huber and Jadini	Marble, limestone	19, 38
Hyella fontana var. maxima Geitler	Limestone	38
Leptolyngbya sp.	Marble, limestone	3, 9a, 18, 26, 28, 35, 36
Leptolyngbya boryanum (Gomont) Anagnostidis & Komárek	Marble, limestone	26, 28
Lyngbya sp.	Travertine, limestone	27, 41
Lyngbya spiralis Geitler	Travertine	20
Merismopedia sp.	Sandstone	32
Microcoleus sp.	Limestone	1, 2
Microcoleus chthonoplastes Gomont	Limestone	26
Microcoleus lacustris (Rabenh.) Farlow ex Gomont	Marble	29

Table 2.2. cont.

Cyanobacterium	Substratum	Monument no. (Table 2.1)
Microcoleus vaginatus (Vaucher) Gomont	Marble, sandstone	7, 29, 33, 43
Microcystis sp.	Marble, sandstone	6, 32, 44
Myxosarcina sp.	Limestone, marble, travertine	5, 10, 11, 19, 26, 41
Myxosarcina chroococcoides Geitler	Limestone, marble	19, 38
Myxosarcina concinna Printz	Marble	6, 29, 44
Myxosarcina spectabilis Geitler	Travertine, marble	6, 20, 44
Nodularia harveyana (Thwaites) Thuret	Marble	29
Nostoc sp.	Limestone, marble, travertine	1, 3, 10, 11, 19, 26, 27, 28, 38, 41
Nostoc punctiforme Hariot	Travertine	30
Oscillatoria sp.	Limestone	27
Oscillatoria lacustris (Klebahn) Geitler	Travertine	13
Phormidium sp.	Limestone, granite	2, 9, 11, 24
Phormidium ambiguum Gomont	Limestone, marble	19
Phormidium autumnale Gomont	Marble, sandstone, travertine	7, 13, 33, 43
Phormidium favosum (Bory) Gomont	Limestone, marble	19
Phormidium foveolarum Gomont	Marble, travertine, limestone	6, 13, 26, 28, 29, 44
Phormidium fragile Gomont	Sandstone, granite	33, 34
Phormidium retzii Gomont	Travertine, limestone, marble	13, 19
Phormidium subfuscum Kützing	Marble, sandstone	33, 43
Phormidium tenue (Meneghini) Gomont	Marble, granite, sandstone, limestone	7, 26, 43
Plectonema sp.	Granite, marble, limestone, sandstone	3, 12, 14, 21, 24, 42, 43
Plectonema boryanum Gomont	Granite	34, 37, 43
Plectonema boryanum f. hollerbachianum Elenk	Marble	29
Plectonema radiosum (Schiedermann) Gomont	Marble	6, 44
Pleurocapsa sp.	Limestone, marble, granite	1, 2, 3, 8, 9a, 10, 14, 18, 25, 28, 35, 36
Pleurocapsa minor Hansgirg	Limestone, marble	19
Schizothrix sp.	Limestone, marble	19, 27
Schizothrix bosniaca (Hansgirg) Geitler emend. Claus	Marble	29
Schizothrix coriacea Gomont	Limestone	26
Schizothrix tenuis Woronichin	Limestone, marble	19
Scytonema sp.	Limestone, marble	3, 11, 12, 21, 35
Scytonema crustaceum (Agardh) Bornet & Flahault	Limestone	26
Scytonema hofmanni Agardh	Limestone	26
Scytonema javanicum Bornet	Limestone	11
Scytonema julianum Meneghini	Travertine	20
Scytonema myochrous (Dillwyn) Agardh ex Bornet & Flahault	Limestone, marble and travertine	26, 30
Stigonema sp.	Limestone	27
Symploca sp.	Limestone	2
Symploca elegans Kützing ex Gomont	Limestone, marble	19
Synechococcus sp.	Marble, granite	3, 6, 18, 24, 44
Synechococcus aeruginosus Nägeli	Travertine	20
Synechococcus elongatus (Nägeli) Nägeli	Marble	28, 29
Synechocystis sp.	Sandstone, limestone, granite	7, 15, 20, 24, 30, 37
Synechocystis pevalekii Ercegovic	Travertine	20
Tolypothrix sp.	Limestone, sandstone	11, 32
Tolypothrix byssoidea (Agardh) Kirchner	Marble, travertine	6, 20, 30

2.3. Green algae on monuments

A considerable number of green algae have adapted to life on land. The chlorophyta, or green algae, comprise the most common group of algae colonising stone cultural heritage (Ortega-Calvo et al., 1993a). In Table 2.3, 76 taxa of chlorophyta, found on monuments and works of art in the Mediterranean Basin, are reported together with the indication of the substratum. Most of these genera are soil algae. This is predicted since the main source of biological colonisation of stone is the surrounding soil, containing large numbers of many different types of bacteria, algae and fungi, which can contaminate the stone shortly after quarrying, or they may be within the stone before quarry extraction. Windblown detritus or rising groundwater infiltration may also be a source of stone inoculation (Koestler, 2000).

From Table 2.3 we can see that chlorophyta was not found on dolomite. The genus *Chlorella* was the most widespread, occurring in 20 of the monuments reported, represented by 4 species and occurring in 4 different substrata. *Stichococcus* was found in 17 monuments and was present also in 4 substrata. Members of the chlorophyta genus *Chlorococcum* were detected on all the stone substrata considered, with the exception of dolomite, and it occurred in 15 distinct monuments. Therefore, we can consider that *Chlorella*, *Stichococcus* and *Chlorococcum* are the green algal genera most abundant on the monuments of the Mediterranean Basin. This is in fair agreement with Ortega-Calvo et al. (1995) who stated that *Chlorella*, *Chlorococcum Klebsormidium* and *Trentepohlia*, can be readily observed in monuments located in Europe, America and Asia. However, it was not possible to establish a correlation between these genera and a specific substratum or climate.

Klebsormidium, *Trebouxia* and *Trentepohlia* also showed a significant representation among the chlorophyta genera colonising stone substratum in the Mediterranean Basin. The occurrence of *Trebouxia* and *Trentepohlia* indicates that these microalgae could be involved in the lichenisation process leading to the colonisation by lichens. In fact, the genus *Trebouxia* occurs in approximately 20% of all lichen and has rarely been found free-living. Regarding endolithic growth of green algae, *Trentepohlia*, *Chorella* and *Klebsormidium* were found growing under a black patina, likely a cryptoendolithic niche, in the Ordem de São Francisco Church, Portugal (Pereira de Oliveira, 2008; Pereira de Oliveira et al., 2008). Cryptoendolithic

growth of *Stichococcus bacillaris* was also observed in granite from the Cathedral of Toledo, Spain (Ortega-Calvo *et al.*, 1995).

Figure 2.7 shows the number of chlorophyta taxa present in each litothype. We can see that limestone was colonised by a higher number of taxa (34) followed by marble (27). Travertine and granite were colonised by about the same number of taxa (21 and 22, respectively), although the number of monuments built on travertine (7%) was considerable lower than the ones made of granite (18%). From Table 2.3 we can see that *Oocystis*, *Cosmarium* and *Staurastrum* species appear almost exclusively in travertine. Nevertheless, the majority of the results suggest that green algae can colonise a wide variety of substrata and this is primarily related to the physical characteristics of the stone surface (porosity, roughness and permeability) and secondarily to the nature of the substratum. This is in accordance with Tiano *et al.* (1995). These authors carried out a laboratory experiment using two photosynthetic strains: a green alga (*Pleurococcus*) and a cyanobacterium (*Lyngbya*), inoculated on 12 different lithotypes exposed at constant climatic conditions. They demonstrated that the preferential colonisation (percentage of stone surface coverage) was correlated mainly with stone physical characteristics (roughness and porosity) while the chemical composition had low influence (Tiano et al., 1995).

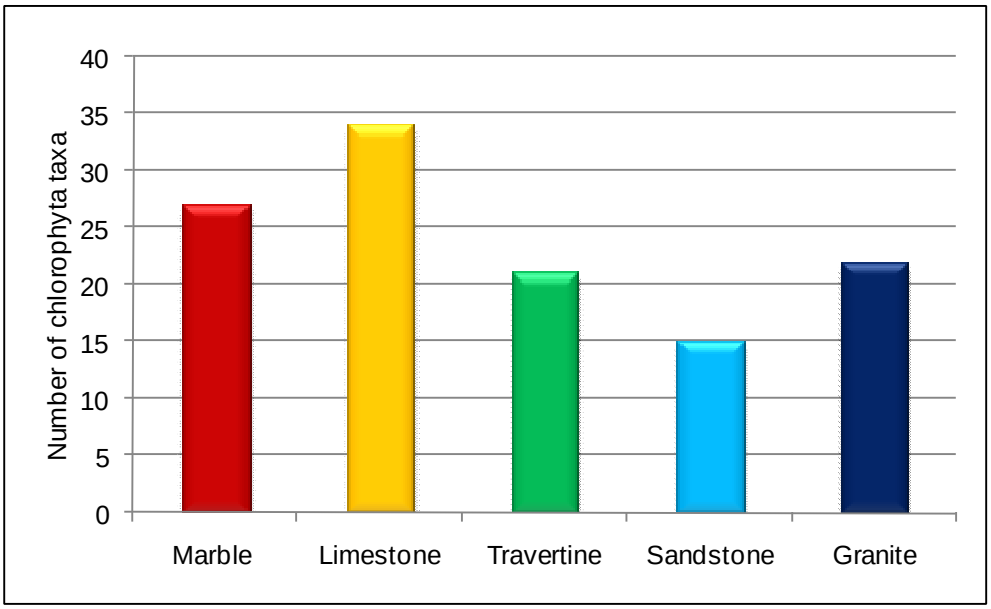

Fig. 2.7. Number of chlorophyte taxa found on each lithotype.

Table 2.3. Chlorophyta reported on stone monuments, statues and historic buildings in European countries from the Mediterranean Basin, on different substrata.

Chlorophyte	Substratum	Monument no.(Table 2.1)
Apatococcus sp.	Limestone, granite, marble	3, 10, 19, 21, 22, 35, 39, 40
Apatococcus lobatus (Chodat) Petersen	Marble, limestone	19, 30
Bracteacoccus sp.	Limestone, marble	11, 43
Chaetophorales sp.	Marble	19[a]
Chlamydocapsa sp.	Granite	45
Chlorella sp.	Granite, sandstone, marble, limestone	3, 4, 5, 7, 10, 14, 17, 19a, 24, 26, 21, 33, 35, 36, 40
Chlorella ellipsoidea Gerneck	Limestone, granite	11, 45
Chlorella homosphaera Skuja	Granite	34, 43
Chlorella reisiglii (Reisigl) Watanabe	Limestone	11
Chlorella vulgaris Beijerinck	Granite, limestone, sandstone	33, 34, 36, 37
Chlorococcum sp.	Granite, limestone, sandstone, marble, travertine	2, 3, 6, 17, 19a, 20, 26, 28, 32, 38, 40, 41, 42, 44, 45
Chlorococcum wimmery Rabenhorst	Marble	38
Chlorokybus atmophyticus Geitler	Sandstone, limestone	33, 11
Chlorosarcina sp.	Marble	28
Chlorosarcinopsis sp.	Limestone, marble	2, 19, 28
Chlorosarcinopsis minor (Gerneck) Herndon	Granite, marble, limestone	19, 34, 38
Choricystis chodatii (Jaag.) Fott	Granite	38
Cladophora sp.	Marble	19a
Coccomyxa sp.	Granite, marble	3, 14
Cosmarium sp.	Limestone	2, 11
Cosmarium depressum (Nägeli) Lundell	Travertine	13
Cosmarium granatum Brébisson	Travertine	13
Cosmarium reniforme (Ralfs) Archer	Travertine	13
Crucigenia quadrata Morren	Travertine	13
Cylindrocystis brebissonii (Meneghini) De Bary	Limestone	11
Desmococcus sp.	Sandstone, granite	32, 45
Desmococcus vulgaris Brand	Limestone, travertine	11, 20
Ecdysichlamys obliqua G.S. West.	Sandstone	33
Euastrum insulare (Wittrock) Roy	Travertine	13
Friedmannia israeliensis (Chantanachat & Bold) Friedl	Sandstone	7
Geminella terricola Petersen	Limestone	11
Gongrosira sp.	Marble, limestone	19, 38
Haematococcus pluvialis Flotow	Marble	23, 44
Klebsormidium sp.	Granite, limestone	11, 17, 24
Klebsormidium flaccidum (Kützing) Silva, Mattox & Blackwell	Limestone, granite, marble, sandstone	7, 11, 26, 33, 34, 37, 43
Monoraphidium sp.	Granite	17
Muriella terrestris Boye-Peterson	Sandstone, travertine, granite	20, 33, 34, 37, 43
Myrmecia sp.	Limestone	11, 36
Nannochloris sp.	Sandstone	33
Oocystis crassa Wittrock	Travertine	13
Oocystis lacustris Chodat	Travertine	13

Table 2.3. cont.

Chlorophyte	Substratum	Monument no.(Table 2.1)
Oocystis solitaria Wittrock	Travertine	13
Pediastrum boryanum (Turpin) Meneghini	Travertine	13
Pleurastrum sp.	Limestone	2
Pleurastrum terrestre Fritsch & John	Limestone	11
Podohedra bicaudata Geitler	Limestone	11
Poloidion didymos Pascher	Limestone, marble	19
Protococcus sp.	Limestone	15
Pseudococcomyxa simplex (Mainx) Fott	Limestone	11
Pseudodendoclonium basiliense Vischer	Marble	38
Pseudopleurococcus sp.	Limestone, marble	2, 19
Pseudopleurococcus printzii Vischer	Marble	38
Pseudosphaerocystis lacustris (Lemmermann) Novàkovà	Travertine	13
Rhizothallus sp.	Marble	3
Scenedesmus sp.	Travertine	41
	Granite	17
Scenedesmus ecornis (Ehrenberg) Chodat	Marble, limestone	19
Scenedesmus obliquus (Turp.) Kütz.	Marble, limestone	19
Scenedesmus quadricauda (Turpin) Brébisson	Sandstone	33
Scenedesmus smithii S.S. Wang	Marble, limestone	19
Scotiellopsis terrestris (Reisigl) Hanagata	Limestone, marble	11, 19
Staurastrum boreale West	Travertine	13
Staurastrum lunatum Ralfs	Travertine	13
Staurastrum lunatum var. planctonicum West & West	Travertine	13
Staurastrum manfeldtii Delponte	Travertine	13
Staurastrum pingue Teiling	Travertine	13
Stichococcus sp.	Granite, limestone, marble	2, 3, 10, 15, 17, 18, 21, 31, 36
Stichococcus bacillaris Nägeli	Limestone, granite, marble, sandstone	7, 11, 26, 33, 43, 44
Stichococcus minutus Grintzesco & Pterfi	Granite	34, 37
Trebouxia sp.	Limestone	11, 30, 34, 36, 37, 38, 45
Trebouxia decolorans Ahmadjian	Sandstone	33
Trentepohlia sp.	Marble, sandstone, granite	10, 24, 31, 32, 45
Trentepohlia aurea (Linnaeus) Martius	Granite	34, 37
Tetracystis sp.	Granite, marble, limestone	19, 45
Tetraedron muticum (Braun) Hansgirg	Travertine	13
Tetraspora gelatinosa (Vaucher) Desvaux	Travertine	13
Ulothrix sp.	Limestone, marble, sandstone	2, 3, 6, 21, 30, 42

2.4. Conclusions

The data reported in the literature showed that a wide range of stone monuments from the Mediterranean Basin are colonised by cyanobacteria and green algae, presenting a noticeable biodiversity. A total of 96 taxa of cyanobacteria and 76 taxa of chlorophyta were found. The most widespread taxa, occurring in the stone cultural heritage in the Mediterranean Basin, were among cyanobacteria *Gloeocapsa*, *Phormidium* and *Chroococcus*, and among chlorophyta *Chlorella*, *Stichococcus* and *Chlorococcum*. These genera were found associated with all lithotypes. Although an extensive literature survey was performed, the preference of the cyanobacteria and chlorophyta for a specific stone substratum was more complicated to correlate than expected. The majority of the results suggest that green algae and cyanobacteria can colonise a wide variety of substrata and this is primarily related to the physical characteristics of the stone surface (porosity, roughness and permeability) and secondarily to the substratum nature. Most cyanobacteria and chlorophyta did not show a clear relationship with the substratum nature, suggesting that environmental variables and site-specific characteristics (e.g. exposure to light, special architectural features) together with secondary, tertiary and/or extrinsic stone bioreceptivity have a stronger influence on community development than the substratum itself. In this complex amalgam of factors, it is often difficult to determine the influence of each factor alone; the evaluation of their combined effects, their synergy and dynamics is not linear and, probably, all factors are relevant. In order to attain a correlation between stone and organisms, we need more detail data about lithotype properties, microclimactic and environmental conditions of the monuments studied.

Cyanobacteria and green algae have an important role in deterioration of monuments and other stone works of art, since they are responsible for aesthetic, biogeophysical and biogeochemical damages. Future work should focus on ecological and physiological studies of specific species of cyanobacteria and green algae in order to understand their role in stone colonisation and biodeterioration processes. Moreover, a interdisciplinary team working in the same “case study” is necessary in order to contemporarily investigate all the factors involved in the biodeterioration process such as mineralogical-petrographic, physicochemical and climatic (and microclimatic) parameters.

CHAPTER THREE

Identification and growth of phototrophic biofilms from limestone monuments under laboratory conditions

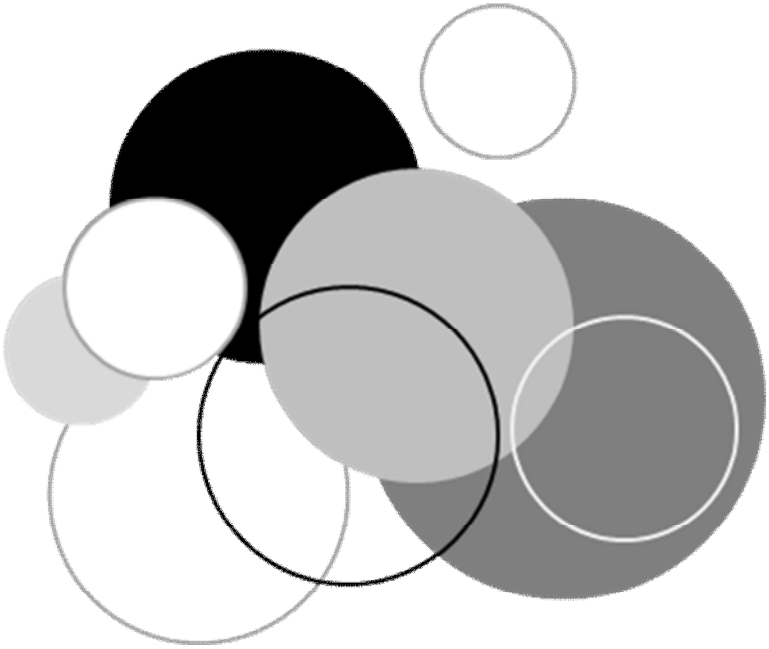

The main results presented in this chapter have been published in:

Miller, A.Z., Laiz, L., Dionísio, A., Macedo, M.F., Saiz-Jimenez, C. 2009a. Growth of phototrophic biofilms from limestone monuments under laboratory conditions. International Biodeterioration and Biodegradation 63, 860-867

CHAPTER THREE

Identification and growth of phototrophic biofilms from limestone monuments under laboratory conditions

3.1. Introduction

Sedimentary rocks, especially limestones, have been extensively used in the construction of monuments and historic buildings. This cultural heritage is at risk of biodeterioration caused by diverse communities of microorganisms, being extremely susceptible to cyanobacteria and algae. As showed in chapter two, a large number of studies have already assessed the occurrence of cyanobacteria and algae on sedimentary stone materials from cultural heritage (Dupuy et al., 1976; Ortega-Calvo et al., 1993a; Altieri et al., 2000; Bellinzoni et al., 2003; Ascaso et al., 2004; Zurita et al., 2005). Currently the complex interactions between lithobionts and the mineral substrata are of interest due to their implications in the biodeterioration of stone monuments. Since the natural biofilm communities are often difficult to investigate *in situ*, the study of artificial phototrophic biofilms under laboratory conditions may increase our understanding of the relative effects of physical and chemical changes in the substratum. Several investigators have developed laboratory-based stone colonisations (Ortega-Calvo et al., 1991a; Guillitte and Dreesen, 1995; Prieto and Silva, 2005; Miller et al., 2006). In most of these experiments the individual community members were studied separately avoiding the understanding of the complex stone biodeterioration processes caused by phototrophic biofilms. Laboratory studies using multiple-species and stable communities will enhance the understanding of the microbial processes involved in stone cultural heritage assets.

In this study, five phototrophic biofilms were collected from five different Southern Europe limestone monuments and compared using denaturing gradient gel

electrophoresis (DGGE) of PCR-amplified 16S rRNA gene fragments in conjunction with DNA sequencing and phylogenetic analysis. The samples were obtained from Orologio Tower in Martano (Italy), Santa Clara-a-Velha Monastery (Coimbra) and Ajuda National Palace (Lisbon), both in Portugal, and Seville and Granada Cathedrals from Spain. The microbial communities were analysed by molecular biology and complemented through culture techniques. DNA extracts from stone monuments samples were used to amplify parts of the ribosomal DNA using universal bacteria and cyanobacteria primers. The resulting mixture of DNA fragments, all of the same length but with different base pair composition, originating from the different microorganisms in the samples were separated by DGGE. As a result, band patterns were obtained, in which each band represents a microbial taxon from the original samples. Selected PCR products were then cloned and sequenced. The corresponding microorganisms were phylogenetically identified by database comparison. These five biofilms were also cultivated under laboratory conditions during 90 days of incubation and periodically sampled in order to monitor their evolution and changes in community composition by DGGE. The aim of this cultivation and monitoring approach was to obtain a multiple-species phototrophic community stable under laboratory conditions to be used for further colonisation experiments on stone.

3.2. Materials and methods

3.2.1. Site description and biological sampling

Samples of microbial communities developing as green biofilms were collected from five Southern Europe monuments constructed with different types of limestone. The samples were obtained from the Orologio Tower in Martano (Italy), two Portuguese monuments, Santa Clara-a-Velha Monastery (Coimbra) and Ajuda National Palace (Lisbon), and two Southern Spanish monuments, the cathedrals of Seville and Granada (Fig. 3.1). The monuments were chosen in function of their cultural importance in Europe, stone type used in their construction, exposition to similar climatic conditions, as well as the presence of green patina appearance on their stone surfaces.

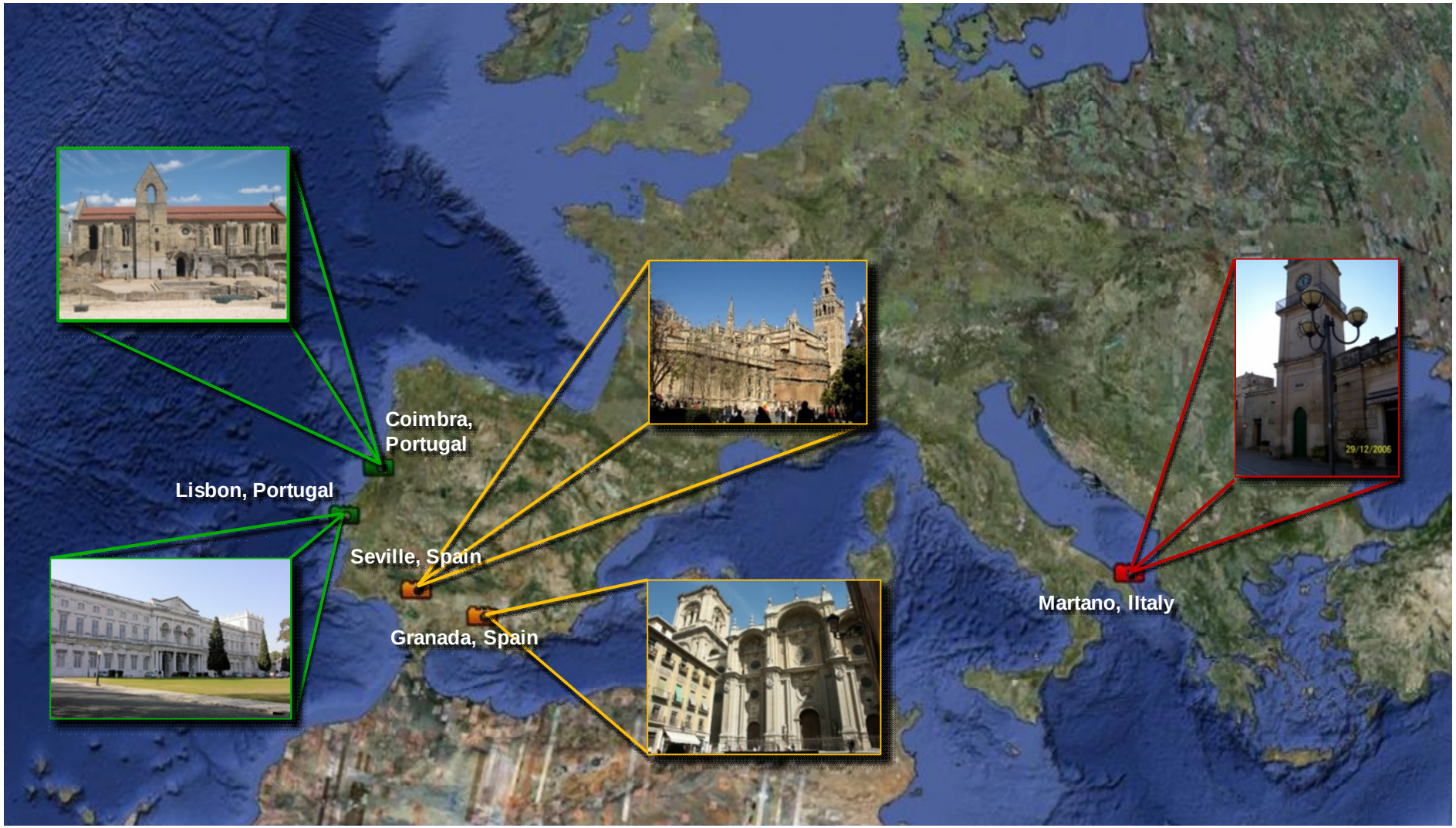

Fig. 3.1. View of the outside limestone monuments studied.

The **Orologio Tower**, built in 1892, is located in the city of Martano, province of Lecce, in the Salentine Peninsula (Italy). Like many historic buildings in Southern Italy, the Orologio Tower was built with *Lecce* stone, a very soft and malleable limestone dating from the Miocene period – Langhian age – widely used in the Late Baroque.

The **Santa Clara-a-Velha Monastery** is a National monument located in Coimbra (Central Portugal) and represents an emblematic monument from the Portuguese Gothic style, built in the 13th century on the left bank of Mondego River. Since the beginning of the 14th century, part of the monastery was buried by 5 to 7 meters of alluvial sediments due to several river flooding occurrences. The monastery was abandoned in the 17th century, triggering a progressive deterioration process leading to a state of ruin. An exhaustive restoration campaign of Santa Clara-a-Velha Monastery started in 1995, entailing the removal of accumulated sediments in the cloister and in the church. The Monastery was constructed with a yellowish dolomitic limestone of Sinemurian age (Aires-Barros et al., 2000), and a fine-grained compact and homogeneous limestone of Bathonian–Bajocian age, known locally as *Anç*ã limestone (Dionísio, 1997). The monastery is now under restoration works to rescue it from the swamp and its state of ruin.

The **Ajuda National Palace** is a National monument located in Lisbon (Portugal). Although the first stone was laid in 1795, only in 1802 did the construction of the Palace start. The original project showed clearly Baroque architectural trends, which was soon replaced by neoclassic style by the architects Francisco Xavier Fabri and José da Costa e Silva. Only in 1861, the Ajuda National Palace became the official residence of the Portuguese Monarchy and the centre of the Portuguese Court in the 19th century. The Palace was built with *Lioz* limestone, a light-coloured microcrystalline limestone from Middle Turonian (Middle Cretaceous) age.

The **Cathedral of Seville** (Andalusia, Spain), built on the site of a mosque in the 15th century, is the largest Gothic building in Europe and is considered one of the most important monuments of Christendom. Stones from the quarries of Cadiz and Seville provinces and Portugal were used in its construction. The most abundant

lithotype used was a yellowish fossiliferous calcarenitic limestone of Miocene age, extracted from El Puerto de Santa María quarry (Cadiz), since lack of stone was prominent in Seville. This limestone, locally known as *San Cristobal* stone, was transported through the Guadalquivir River and docked in Seville for the construction of the Cathedral (Fig. 3.2).

The **Cathedral of Granada** is located in Andalusia (Spain) and represents the country's finest Renaissance church. It was built in the 16th century, with a very soft and porous biocalcarenite from the Tortonian age, *Escúzar* stone, extracted from Santa Pudia quarries, in the Escúzar region (Granada).

Fig. 3.2. 17th century engraving depicting the landing in Seville of *San Cristobal* stone from El Puerto de Santa María (Cadiz) with the help of a crane (http://es.wikibooks.org/w/index.php?oldid=80480).

All cities, Martano, Coimbra, Lisbon, Seville and Granada, have limestone monuments of very high importance as cultural heritage buildings, triggering a progressive deterioration process, where phototrophic communities cause significant aesthetic damage. These monuments are exposed outdoors, being subjected to the Mediterranean climate, which was already described in chapter two.

The samples from each monument were collected from the vertical outer surfaces of the North facade between 20 and 50 cm above the ground. Biofilm biomass was scraped in triplicate from surface areas with approximately 5 cm^2 using sterilised material and gathering it in sterile tubes. The amount of sample material taken was around 1 g. The surveys were conducted on sunny days in 2006 and were restricted to surfaces with green patina appearance; lichens were not sampled (Table 3.1). Each sample was divided into subsamples for identification by molecular methods (stored at -80ºC), and for culturing procedures, preserved at 4ºC until being processed.

3.2.2. Characterisation of natural phototrophic biofilms

3.2.2.1. DNA extraction

The microbial components comprising the five green biofilms were analysed in triplicate by molecular biology techniques. DNA was extracted from small samples (1-5 mg) of green biofilms using the Nucleospin Food DNA Extraction Kit (Macherey-Nagel, Düren, Germany), following the manufacturer's protocol. This DNA Extraction Kit is used for small genomic DNA fragments from samples with very low DNA contents, such as in the case of food and environmental samples. The basic principle consists in the homogenisation of ~200 mg of material (which typically yields 0.1 – 10 µg DNA) with subsequent cell lysis, DNA binding, washing and eluting steps. Briefly, cell lysis consists in the disruption of cells using lysis buffers containing chaotropic salts, denaturing agents and detergents. Lysis mixtures are cleared by centrifugation in order to remove contaminants and cellular debris. The clear supernatant is then mixed with binding buffer and ethanol for DNA binding to a silica membrane. After washing with two different buffers, DNA is eluted in low salt buffer and stored at 4ºC for further analysis.

Table 3.1. Sampling areas and biofilm descriptions.

Monument	Sampling area	Substratum and description
Santa Clara-a-Velha Monastery, Coimbra (Portugal)		*Ançã* limestone Green biofilm with powdery growth covering the right side column of the North facade of the church
Ajuda National Palace, Lisbon (Portugal)		*Lioz* limestone Very well-attached green biofilm taken from the North wall of the Palace, with high moisture content of the substratum
Cathedral of Seville, Seville (Spain)		*San Cristobal* stone Widespread green biofilm from the North wall of the Cathedral with high moisture content of the substratum
Cathedral of Granada, Granada (Spain)		*Escúzar* stone Well-attached green biofilm from the North wall
Orologio Tower, Martano (Italy)		*Lecce* stone Well-attached green biofilm taken from the right side of the Tower

3.2.2.2. PCR amplification of 16S rDNA fragments

Amplification of 16S rRNA genes was carried out by PCR. Bacterial 16S rRNA gene fragments corresponding to nucleotide positions 27-907 of the *E*. *coli* 16S rRNA sequence were amplified with the forward primer 616F and the reverse primer 907R (Table 3.2). All PCR reactions were performed in 50 µL volumes, containing 2 µL of the extracted DNA used as template DNA, 5 µL of 10x PCR buffer Biotaq (Bioline, Randolph, Massachussets, USA), 1.5 µL of 50 mM $MgCl_2$ (Bioline), 1 µL of 10 mM deoxyribonucleoside triphosphate mixture (dNTPs) (Invitrogen, Carlsbad, California, USA), 0.5 µL of 50 µM of each primer and 0.25 µL of *Taq* DNA polymerase enzyme (Bioline), made up to 50 µL with nuclease-free water (Sigma-Aldrich, USA). PCR amplifications were performed with a thermal cycler iCycler BioRad (BioRad, California, USA) using the following thermocycling program: 2 min denaturing step at 95ºC, followed by 35 cycles of denaturing (95ºC for 15s), annealing (55ºC for 15s) and elongation (72ºC for 2 min). A final elongation step of 10 min at 72ºC was added at the end.

For cyanobacterial 16S rRNA genes amplification, fragments corresponding to nucleotide positions 106-781 in the *E*. *coli* 16S rRNA sequence were amplified using the primer pair Cya106F and Cya781R (Table 3.2). PCR cycling conditions comprised a denaturing step of 2 min at 95ºC, 35 cycles of denaturing (95ºC for 15s), annealing (55ºC for 15s) and elongation (72ºC for 30s), following a terminal elongation step of 30 min at 72ºC.

For DGGE analysis, a small 16S rDNA fragment (~180 bp) that covers the V3 region (Fig. 1.7, chapter one) was reamplified in the nested PCR reaction with the forward primer 341F-GC carrying a 40-base GC clamp at the 5' end, in order to generate fragments suitable for DGGE separation (Muyzer et al., 1993), and the reverse primer 518R (Table 3.2). PCR reactions were carried out in 25 µL volumes containing 1 µL of PCR product of the first amplification as template DNA. PCR conditions were as described for bacterial 16S rRNA gene amplification with the exception of an elongation step of only 30s. To detect possible cross contaminations, a negative control in which template DNA was replaced by sterile distilled water was included in each set of reactions.

Table 3.2. Primers used in this study.

	Primer[a]	Sequence (5' to 3')	Target site[b]	Reference
Bacteria	616F	AGAGTTTGATYMTGGCTCAG	27-46	Zimmermann et al. (2005)
	907R	AATTCCTTTGAGTTT	907-886	Weisburg et al. (1991)
Cyanobacteria	Cya 106F	CGGACGGGTGAGTAACGCGTGA	106-127	Nübel et al. (1998)
	Cya 781R	GACTACWGGGGTATCTAATCCCATT	781-757	Nübel et al. (1998)
Eukaryotes	Euk A	AACCTGGTTGATCCTGCCAGT	1-21[c]	Diez et al. (2001)
	Euk B	TGATCCTTCTGCAGGTTCACCTAC	1772-1795[c]	Diez et al. (2001)
Prokaryotes	341F-GC	GC clamb-CCTACGGGAGGCAGCAG	341-397	Muyzer et al. (1993)
	518R	ATTACCGCGGCTGCTGG	518-500	Muyzer et al. (1993)
Vector specific pCR4	T7p	TAATACGACTCACTATAGGG	-	Ausubel et al. (1992)
	M13rev	CAGGAAACAGCTATGAC	-	

[a] R (reverse) and F (forward) designations refer to primer orientation in relation to the rRNA.

[b] *E. coli* numbering of 16S rRNA nucleotides (Brosius et al., 1981).

[c] Eukaryotes numbering of 18S rRNA nucleotides.

In order to check positive DNA amplifications, 5 µL of PCR products, mixed with 1 µL of gel-loading buffer containing SYBR® Green II fluorescent dye (1/100.000 dilution, Molecular Probes, Eugene, USA), were inspected by electrophoresis in 1% (w/v) agarose gel (SeaKem®, Cambrex Bio Science Rockland, New York, USA). The agarose gel electrophoresis was carried out in a horizontal gel tank HU10 SCIE-PLAS (Southham, England) with 0.5x Tris-Acetate-EDTA (TAE) buffer. The gel was run at 90 V during approximately 30 min. After electrophoresis the gel was illuminated with a UV light transilluminator (Vilber Lourmat, France) to visualise the DNA bands. Photograph record was performed with a digital camera Kodak Edas® DC290 using the Kodak 1D Image Analysis Software® (Kodak, New Haven, USA).

3.2.2.3. Analysis of PCR products by Denaturing Gradient Gel Electrophoresis (DGGE)

For genetic fingerprinting of bacterial and cyanobacterial communities present in the samples, DGGE was performed as described by Muyzer et al. (1993). Nested PCR products with primers 341F-GC and 518R were loaded on 8% (w/v) polyacrylamide gels (40% Acrylamide/Bisacrylamide: 37.5:1; BioRad, Munich, Germany) with a denaturing gradient from 30 to 55% of urea and formamide (100% denaturant contains 7 M urea and 40% (v/v) formamide). Polyacrylamide gels were prepared using 0% and 80% denaturant stock solutions (see appendix two), and 10% (w/v) of ammonium persulfate (APS) and N'-tetramethylethylenediamine (TEMED) to catalyse the polymerisation of acrylamide solutions into gel matrices, with 0.75 mm thick. Denaturing gradient gel was prepared with a gradient former Gradient Delivery System® Model 475 (BioRad, Munich, Germany). After polymerisation, 10 µL of nested PCR products were mixed with 5 µL of loading buffer (see appendix two) and pipetted into the 25 gel slots along with one migration marker composed by four reference strains for determination of band positions and comparability of gels. The reference strains used were: *Pseudomonas* sp., *E. coli*, *Paenibacillus* sp. and *Streptomyces* sp. Gels were run at a constant temperature of 60ºC, with 200 V during 3.5 h. The electrophoresis took place in a vertically placed polyacrylamide gel in a gradient of denaturants, which was placed in a tank (DCode™ Universal Mutation Detection System, BioRad, Munich, Germany) containing 0.5x TAE buffer. After electrophoresis, gels were stained in an ethidium bromide solution (10 µL/mL) during 5 min and photographically documented with a digital camera Kodak Edas® DC290 with UV light illumination (Vilber Lourmat, France).

3.2.2.4. Construction of 16S rDNA clone libraries

In order to obtain 16S rDNA sequence information of the major members comprising the biofilm samples visualised by DGGE, clone libraries were constructed by cloning PCR products amplified with 616F-907R and Cya106F-Cya781R primers pairs. Before cloning, PCR products were purified using the JetQuick® PCR Purification Spin Kit (Genomed, Löhne, Germany) according to the manufacturer's protocol, in order to remove primers, dNTPs and enzyme that have not been used in

PCR. Cloning was performed with the TOPO TA Cloning Kit (Invitrogen, California, USA), following the manufacturer's protocol. The amplified DNA fragments were ligated into plasmid vector pCR®4-TOPO (Fig. 3.3). The ligation products were subsequently transformed into competent *E. coli* cells, which were then plated on Luria-Bertani (LB) medium containing ampicillin (100 µg/mL) and incubated overnight at 37ºC.

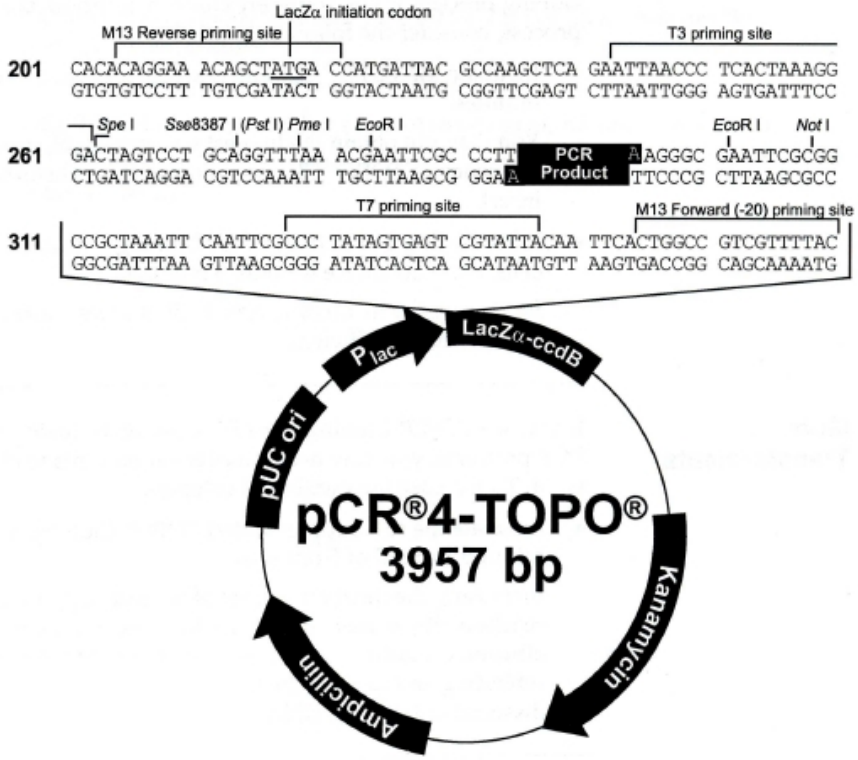

Fig. 3.3. Features of pCR®4-TOPO® and the sequence surrounding the TOPO® cloning site. The map shows the insertion site of PCR product (gene LacZα-ccdB) as well as the sequences for the vector-specific primers (M13 reverse, T3, T7 and M13 forward). LacZα-ccdB gene prevents the growth of untransformed bacterial cells on the nutrient agar medium containing antibiotic, which may be ampicillin or kanamycin, since the plasmid vector contain resistance genes for both antibiotics. The pCR®4-TOPO® vector has covalently bound topoisomerase I for fast cloning (5 min).

3.2.2.5. Screening of 16S rDNA clone libraries by PCR and DGGE

The presence of 16S rDNA inserts into the *E. coli* colonies was verified by picking *E. coli* colonies, resuspending in 50 µL of nuclease-free water (Sigma-

Aldrich) and subjecting to three freeze (-80ºC)/thawing (68ºC) cycles to lyse the cells. One microliter was subsequently used as template DNA for PCR in a volume of 25 µL using vector-specific T7p and M13rev primers. PCR cycling conditions comprised a denaturing step of 3 min at 95ºC, 35 cycles of denaturing (95ºC for 15s), annealing (55ºC for 15s) and elongation (72ºC for 30s), following a terminal elongation step of 10 min at 72ºC. The PCR products were checked by 1% (w/v) agarose gel electrophoresis as previously described.

In order to screen different 16S rDNA inserts for further sequencing, from each positive PCR product 1 µL was used as template DNA for a nested PCR with primers 341F-GC and 518R in a volume of 25 µL, as described in section 3.2.2.2. After nested PCR amplification, PCR products were analysed by DGGE for the selection of clones to be sequenced, as described by González et al. (2003), avoiding dereplication (sequence multiple times identical clones). 10 µL of PCR product mixed with 5 µL loading buffer were added into DGGE gel slots and run according to conditions described in section 3.2.2.3. All clones showing different positions in DGGE were compared with the band pattern of the original samples. Inserts of clones producing PCR products with an identical position in the DGGE fingerprints of the original samples were sequenced.

3.2.2.6. Sequencing and identification of microorganisms by comparative sequence analyses

For sequencing of clone inserts, *E. coli* colonies containing the select clones were grown overnight at 37ºC in LB medium plates containing ampicillin (100 µg/mL). Plasmids were extracted with the JetQuick® Plasmid Miniprep Spin Kit (Genomed, Löhne, Germany), following the manufacturer's protocol. Clone inserts were sequenced by Secugen Sequencing Services (CSIC, Madrid, Spain) with an ABI3730 sequencer (Applied Biosystems, California, USA).

The obtained sequences were visualised and edited using the software Chromas 2.01 (Technelysium, Tewantin, Australia). Edited sequences were compared with known sequences from the genetic sequence database Genbank® available on the NCBI (National Center for Biotechnology Information) site (http://www.ncbi.nlm.nih.gov/), using the Basic Local Alignment Search Tool (BLAST)

(Altschul et al., 1990). The BLAST finds regions of local similarity between sequences, comparing nucleotide sequences to sequence databases and calculating the statistical significance of matches.

3.2.3. Biofilms enrichment and monitoring

In parallel to the biofilms identification, each biofilm sample was inoculated in BG11 liquid medium for the enrichment of large volumes of the green biofilms collected on the five limestone monuments. These five cultures were monitored over a time span of 90 days in order to assess the temporal dynamics of the phototrophic communities. The aliquots for culturing procedures from the five monuments were suspended in 15 mL of sterile water and homogenised; the suspensions were inoculated into 500 mL flasks containing 400 mL of BG11 liquid medium. This culture medium was selected to promote the growth of the phototrophic components comprising the natural green biofilms (Normal 9/88). The cultures were incubated at room temperature (22ºC ± 2ºC), near a window and under artificial light. Air circulation inside the flasks was provided by an air pump (Fig. 3.4).

Fig. 3.4. Biofilms cultivation in BG11 liquid medium.

The growth and composition of the biofilms were monitored for 90 days by DGGE analysis in order to evaluate when the cultures reached a mature stage, representing an establishment of the microbial components comprising the natural biofilm communities. Every two weeks (days 15, 30, 45, 60, 75 and 90), 200 mL of each culture assemblage were aseptically sampled into sterile containers and three aliquots were stored into eppendorfs at -80ºC until further PCR-DGGE analysis. The sampled volume was replaced by fresh sterile BG11 medium. DNA extraction was performed by subjecting the eppendorfs to three freeze (-80ºC)/thawing (68ºC) cycles to lyse the cells. Subsequently, the suspensions were centrifuged during 10 min at 13000 rpm and the supernatant was transferred for sterile tubes. Amplification with primers cya106F and cya781R, and DGGE analysis were performed as described before (sections 3.2.2.2 and 3.2.2.3). This monitoring was achieved by comparing DGGE banding patterns of the phototrophic liquid cultures with the natural samples.

With this monitoring approach a multiple-species phototrophic culture stable under laboratory conditions was obtained for further colonisation experiments on stone. The selection criteria of the phototrophic culture as inoculum for stone inoculation were:

1. representative of the geographic regions, i.e. abundant phototrophic microorganisms on monuments from the Mediterranean Basin region (see chapter two);
2. stable and easy to culture under laboratory conditions;
3. multiple-species culture to simulate the existence of competition and/or synergy between colonising microorganisms.

3.3. Results

3.3.1. Microbial diversity of natural phototrophic biofilms as determined by molecular techniques

In this study, prokaryotic microorganisms, within the samples taken from five limestone monuments, have been approached by DNA-based molecular analysis. The molecular procedures employed to analyse these biofilms showed low variability in each replicate. The comparative analyses of the five different green biofilms revealed the presence of a variety of microorganisms belonging to different phyla and showed major differences among them. A total of twenty-three taxa have been identified, fifteen of which were Bacteria, six Cyanobacteria, one Chlorophyta and one Bacillariophyta.

The phyla Bacteria and Cyanobacteria detected in the analysed 16S rRNA gene library were found in the five locations. Chloroplasts from the phylum Chlorophyta were detected in two of the studied biofilms, Orologio Tower, in Martano, Italy (Fig. 3.5) and in Santa Clara-a-Velha Monastery, located in Coimbra, Portugal (Fig. 3.6).

Within the Cyanobacteria, only three genera were present in more than one monument. *Pleurocapsa* was the most widespread cyanobacterium, occurring in the five biofilms (Table 3.3). A high proportion of clones corresponding to microorganisms of the genus *Chroococcidiopsis* was detected in the biofilm from Ajuda National Palace (Fig. 3.7, bands 3, 4, 7 and 10). This cyanobacterium was also identified in the biofilms from Cathedral of Seville (Fig. 3.8, band 14) and Cathedral of Granada (Fig. 3.9, bands 3 and 8). *Leptolyngbya* sp. was present in the Cathedral of Seville (Fig. 3.8, band 12) and also in the Santa Clara-a-Velha Monastery (Fig. 3.6, bands 10 and 12). In the latter, bands affiliated to *Leptolyngbya* were only detected in the biofilm liquid culture. According to band migration during DGGE analysis, this cyanobacterium was also identified in the natural sample profiles. *Cylindrospermopsis*, *Nostoc* and *Microcoleus* were the genera represented just in one of the investigated monuments, namely in Ajuda National Palace (Fig. 3.7, bands 2, 9 and 11). This last biofilm comprised the largest genera diversity within Cyanobacteria and the lower within Bacteria. In contrast, the Cathedral of Seville showed the largest genera diversity within Bacteria (Fig. 3.8). This monument showed the presence of microorganisms belonging to Alpha- and

Gammaproteobacteria, Actinobacteria and Verrucomicrobia in a total of five bacterial phyla detected in this study. The major component of this bacterial community was Verrucomicrobia, with a high proportion of clones.

The bacterial composition of the five monuments showed only similarities in the phylum Proteobacteria, represented by members of the Alpha- Beta- and Gammaproteobacteria. Among the Alphaproteobacteria, members of the *Methylobacterium*, *Porphyrobacter*, *Sphingomonas* and *Nitrobacteria* genera were detected. *Saccharospirillum*, *Marinobacter*, *Stenotrophomonas* and *Lysobacter* were the most representative genera belonging to Gammaproteobacteria. *Variovorax* was the unique genus belonging to Betaproteobacteria detected in Orologio Tower, in Martano (Fig. 3.5). Phyla Bacteroidetes, Actinobacteria and Verrucomicrobia were detected in more than one biofilm and Acidobacteria were only found in the Lisbon biofilm (Fig. 3.7).

Chloroplasts of the phylum Chlorophyta were also detected in this study, which was represented by the genus *Chlorella*, detected in the Orologio Tower (Martano) and in the Santa Clara-a-Velha Monastery (Coimbra). Coimbra showed the highest proportion of clones affiliated to *Chlorella* (Fig. 3.6); the cyanobacterial 16S rRNA gene-DGGE profile from the natural sample consisted of two dominants bands and three faint bands, all affiliated to chloroplasts of *Chlorella* alga. Martano biofilm also revealed high proportion of *Chlorella*, as demonstrated by the DGGE pattern of 16S rRNA gene fragments obtained after amplification using cyanobacterial primers; the two dominant bands in this profile were affiliated to chloroplasts of this alga (Fig. 3.5, bands 8 and 9). Cathedral of Seville revealed chloroplasts of the Bacillariophyta *Gyrosigma* (Fig. 3.8, band 10).

Table 3.3 summarises the occurrence of the prokaryotic microorganisms detected in the green biofilms of the five monuments. It is clear that Cathedral of Seville showed the widest biodiversity, with six taxa of Bacteria and three of Cyanobacteria. Ajuda National Palace presented the highest biodiversity within Cyanobacteria, with five taxa identified. The microbial communities from Coimbra, Granada and Martano showed the lowest biodiversity.

Table 3.3. Occurrence of prokaryotic microorganisms in the green biofilms of the studied monuments, detected by amplification using bacterial and cyanobacterial primers.

	Orologio Tower (Italy)	Sta Clara-a-Velha Monastery (Portugal)	Ajuda National Palace (Portugal)	Cathedral of Seville (Spain)	Cathedral of Granada (Spain)
Bacteria					
Acidobacteria			•		
Actinobacteria		•		•	
Bacteroidetes		•			•
Lysobacter	•				
Luteolibacter				•	
Marinobacter				•	
Methylobacterium			•	•	
Nitrobacteria	•				
Porphyrobacter					•
Saccharospirillum				•	
Sphingomonas					•
Stenotrophomonas	•				•
Variovorax	•				
Verrucomicrobia		•		•	
Cyanobacteria					
Chroococcidiopsis			•	•	•
Cylindrospermopsis			•		
Leptolyngbya		•		•	
Microcoleus			•		
Nostoc			•		
Pleurocapsa	•	•	•	•	•

3.3.2. Monitoring of photosynthetic cultures

The biofilms growth was macroscopically monitored by the increase of green colour and photosynthetic cells distribution. Visible growth of the phototrophic biofilms started one week after inoculation, presenting a brightly green colour, with the exception of the Orologio Tower biofilm culture. After one month, notable dense green colour and homogeneously distributed photosynthetic cells were observed for Coimbra and Granada biofilm cultures, which remained constant until the end of the incubation period. Liquid cultures of Lisbon and Seville biofilms showed heterogeneous distribution of cells; as the cultures biomass increased, there was an increased tendency for algal aggregates precipitate and for the cells to stick to the glass and steel surfaces. No visible photosynthetic growth was observed for the green biofilm from Orologio Tower (Martano, Italy) during the 90 days of cultivation.

The composition and development of the microbial communities assemblages were monitored during different incubation times of the photosynthetic cultures by DGGE. Differences in richness over all cultures were observed in the DGGE profiles of the biofilms (Figs. 3.5 to 3.9).

The culture of Coimbra seemed very stable in composition, even over a time span of 90 days. According to band migration, the bands affiliated to chloroplasts of *Chlorella*, present in the cyanobacteria-specific inoculum profile, were dominant in the culture community (Fig. 3.6, bands 5-7), being detected in all sampling days as well as the bands affiliated to the cyanobacterium *Pleurocapsa* (band 9). *Leptolyngbya* (Fig. 3.6, bands 10 and 12) was also detected over the course of batch incubation of Coimbra culture. However, *Leptolyngbya* was not detected in the inoculum profiles probably due to altered extractability of the DNA or due to the presence of other dominant microorganisms, such as the microalga *Chlorella*. Minor changes in the Coimbra liquid culture fingerprints consisted in the intensity of bands; the only variation concerned band 1 corresponding to *Chlorella vulgaris*, which was present in the inoculum fingerprint and absent in the liquid culture. In addition, two bands corresponding to Verrucomicrobia were detected in the cyanobacteria-specific DGGE (Fig. 3.6, bands 11 and 13). The DGGE patterns of the liquid culture revealed that after 45 days the culture reached a mature stage, remaining constant until 90 days of incubation. Moreover, after this incubation period, this culture showed a high similarity with the natural sample DGGE profile.

In all other biofilm cultures variations in the banding patterns occurred. A wide variability was observed in the cultures of Lisbon and Seville biofilms. The cyanobacterial 16S rRNA gene-DGGE profiles from the Lisbon biofilm cultivation revealed little similarity with the inoculum profiles (Fig. 3.7). The cyanobacteria-specific inoculum profile contained only three visible bands. These dominant bands, affiliated to cyanobacteria *Pleurocapsa*, *Nostoc* and *Chroococcidiopsis* (Fig. 3.7, bands 8–10), were not visible in the culture fingerprints. The DGGE profiles of the cultivated biofilm showed only two dominant bands and several faintly visible bands. The two top bands of the liquid culture were dominant over the course of batch incubation; according to band migration, the first band corresponded to *Pleurocapsa* sp. In the sample from day 90, the DGGE profile contained up to seven distinguishable bands, suggesting a higher biodiversity.

The widest variations in the DGGE profiles of the cultures were recorded in the case of the Seville biofilm culture. Their inoculum profiles showed greatest biodiversity between all the natural samples studied, which was revealed by the presence of several bands with different intensities (Fig. 3.8). This variability was also recorded for its liquid culture which DGGE profiles showed marked changes in the number and intensity of bands in the different sampling days. Bands faintly visible in samples taken during the incubation were identically positioned to bands 8 and 9 (Fig. 3.8), which corresponded to *Pleurocapsa* sp.

The cyanobacteria-specific inoculum DGGE profile from Granada biofilm (Fig. 3.9) also showed a very faintly visible band affiliated to the cyanobacterium *Pleurocapsa*. As occurred to the cultivation of Coimbra biofilm, Granada culture showed similarities with the initial inoculum. Only minor variations were seen in the sample from day 30 which last band, strongly visible in the other sampling days, was faintly visible in this profile. Bands that migrated in the same position as band 8 (Fig. 3.9) were present in the first two sampling days and almost disappeared after 45 days of incubation. This is probably due to senescence of the microorganism.

The cyanobacterium *Pleurocapsa* was present in all biofilms cultivation, with one exception, the Martano biofilm cultivation which no photosynthetic growth was obtained during the batch incubation. Consequently, it was not possible to monitor by DGGE the composition and development of the phototrophic community assemblage. Nevertheless, bands affiliated to *Pleurocapsa* were also detected in the inoculum profiles (Fig. 3.5, bands 1 and 7).

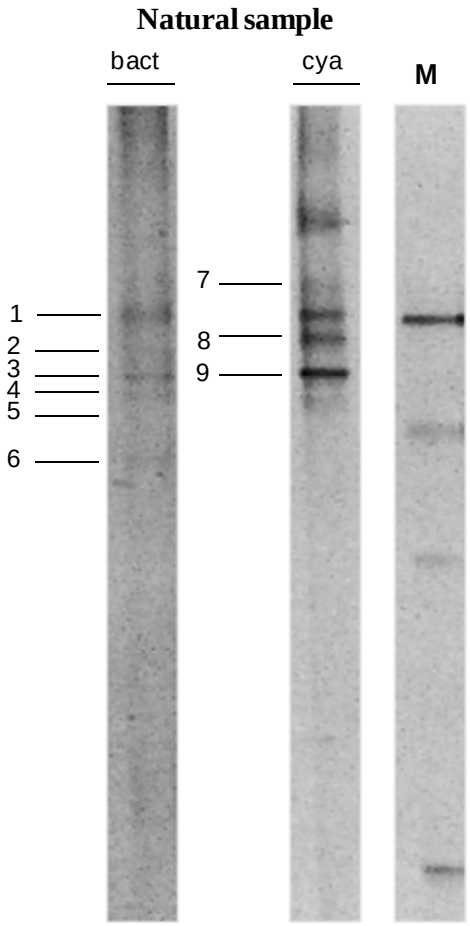

Fig. 3.5. DGGE profiles of 16S rRNA gene from the natural green biofilm collected from Orologio Tower, in Martano (natural sample), obtained after amplification using bacterial and cyanobacterial primers (Lanes "bact" and "cya", respectively). The band numbers refer to clones obtained from the natural sample. Lane "M" corresponds to DGGE markers, consisting of *Pseudomonas* sp., *E. coli*, *Paenibacillus* sp. and *Streptomyces* sp. Identification of bands based on comparison with closest relatives at NCBI databank (Acc. Number in parenthese): 1- *Pleurocapsa minor* (AJ344564), 2- *Variovorax* sp. (AB196432), 3- *Lysobacter* sp. (DQ191178), 4- Uncultured *Nitrobacteria* sp. (AM990004), 5- *Stenotrophomonas* sp. (DQ984206) 6- *Lysobacter* sp. (EF687714), 7- *Pleurocapsa minor* (AJ344564), 8- *Chlorella* sp. chloroplast (D11348), 9- *Chlorella* sp. chloroplast (X12742).

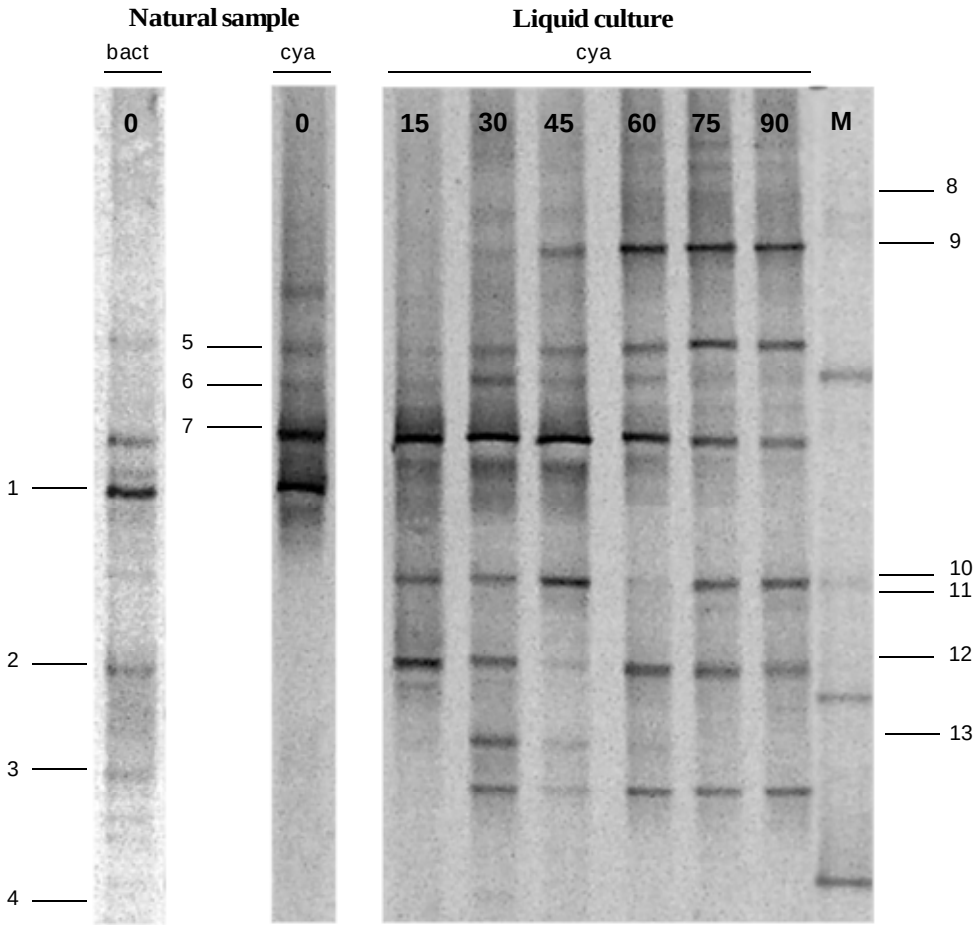

Fig.3.6. DGGE profiles of 16S rRNA gene from the natural green biofilm collected from Santa Clara-a-Velha Monastery (natural sample) and its liquid culture monitored during 90 days (Lanes 15, 30, 45, 60, 75 and 90, corresponding to the sampling days). Lanes "0 bact" and "0 cya" correspond to the DGGE profiles of the inoculum obtained after amplification using bacterial and cyanobacterial primers, respectively. DGGE profiles of the liquid culture were obtained using cyanobacterial primers. The band numbers refer to clones obtained from the natural sample (bands 1 to 7) and from the sample 75 of the liquid culture (bands 8 to 13). Lane "M" corresponds to DGGE markers, consisting of *Pseudomonas* sp., *E. coli*, *Paenibacillus* sp. and *Streptomyces* sp. Identification of bands based on comparison with closest relatives at NCBI databank (Acc. Number in parenthese): 1- *Chlorella vulgaris* chloroplast (EU333015), 2- Bacteroidetes (EU333004), 3- Alphaproteobacteria (EU333006), 4- Actinobacteria (EU333005), 5- *Chlorella vulgaris* chloroplast (EU333016), 6- *Chlorella vulgaris* chloroplast (EU333018), 7- *Chlorella* sp. chloroplast (EU333008), 8- *Chlorella* sp. chloroplast (EU333007), 9- *Pleurocapsa* sp. (EU333017), 10- *Leptolyngbya* sp. (EU333012), 11- Verrucomicrobia (EU333009), 12- *Leptolyngbya* sp. (EU333013), 13- Verrucomicrobia (EU333010).

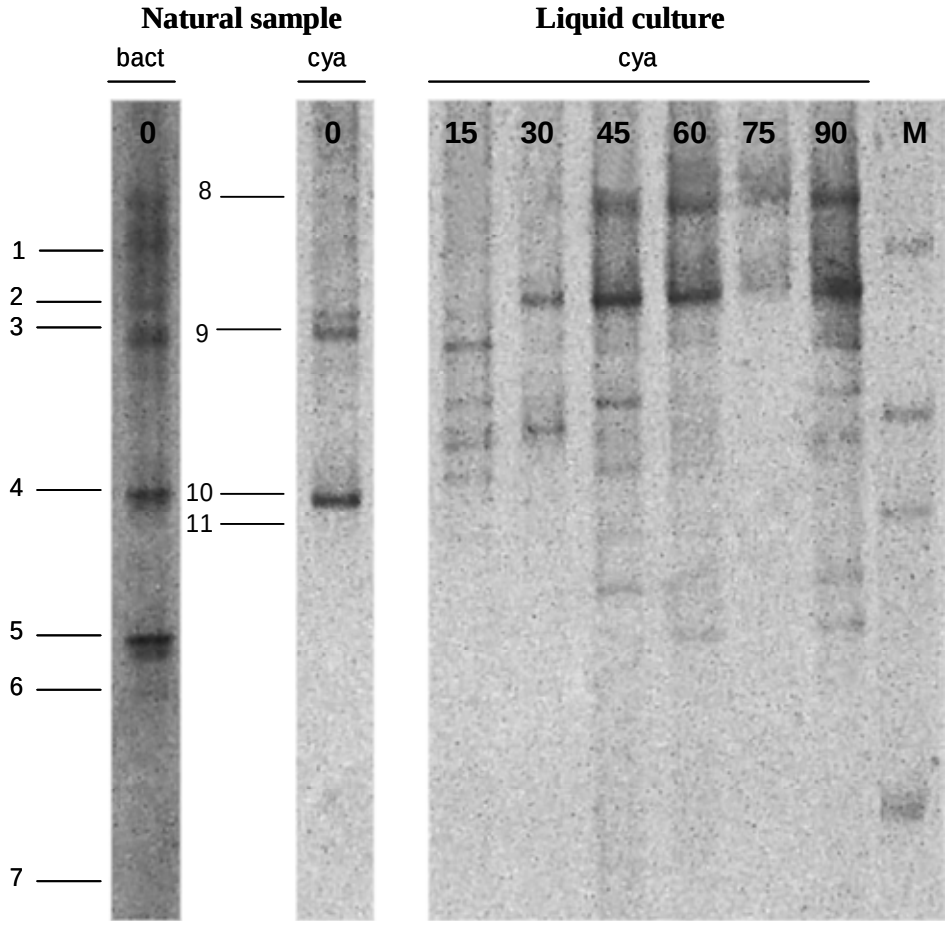

Fig. 3.7. DGGE profiles of 16S rRNA gene from the natural green biofilm collected from Ajuda National Palace (natural sample) and its liquid culture monitored during 90 days (Lanes 15, 30, 45, 60, 75 and 90, corresponding to the sampling days). Lanes "0 bact" and "0 cya" correspond to the DGGE profiles of the inoculum obtained after amplification using bacterial and cyanobacterial primers, respectively. DGGE profiles of the liquid culture were obtained using cyanobacterial primers. The band numbers refer to clones obtained from the natural sample. Lane "M" corresponds to DGGE markers, consisting of *Pseudomonas* sp., *E. coli*, *Paenibacillus* sp. and *Streptomyces* sp. Identification of bands based on comparison with closest relatives at NCBI databank (Acc. Number in parenthese): 1- Uncultured Acidobacteria (EU122726), 2- *Cylindrospermopsis* sp. (AF516732), 3- *Chroococcidiopsis* sp. (DQ914863), 4- *Chroococcidiopsis* sp. (EF150802), 5- *Methylobacterium* sp. (AY358007), 6- *Methylobacterium* sp. (AM237344), 7- *Chroococcidiopsis* sp. (DQ914865), 8- *Pleurocapsa* sp. (DQ293994), 9- *Nostoc* sp. (AY742448), 10- *Chroococcidiopsis* sp. (DQ914865), 11- *Microcoleus* sp. (AJ871987).

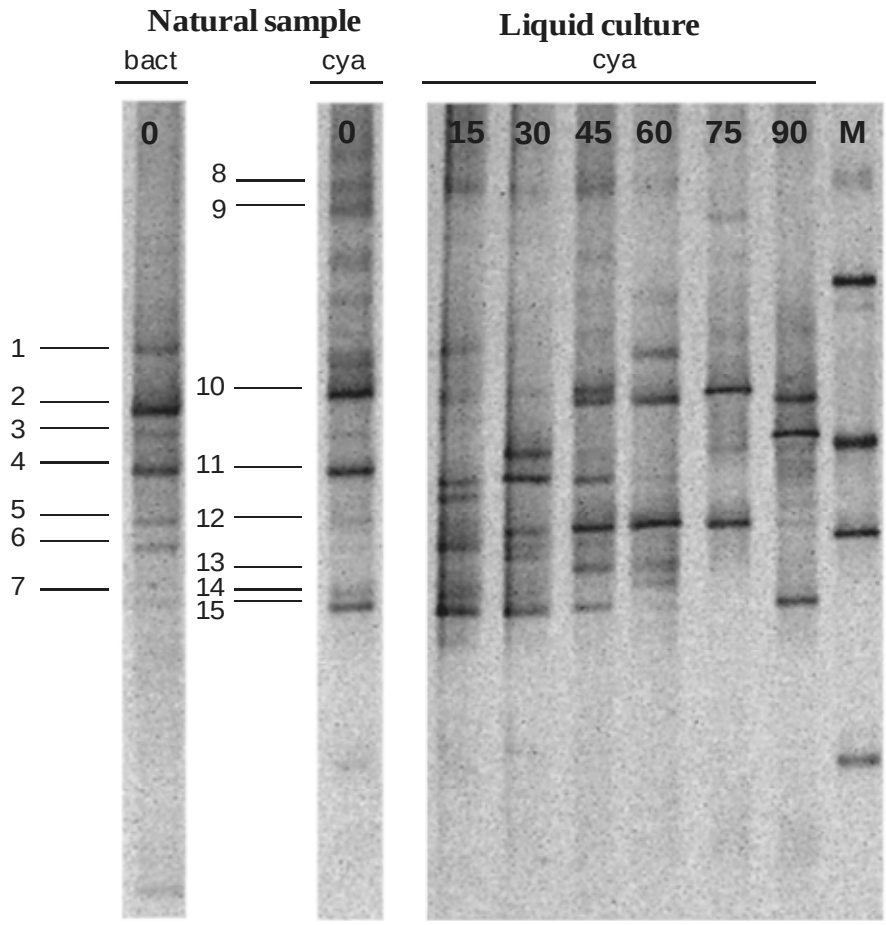

Fig. 3.8. DGGE profiles of 16S rRNA gene from the natural green biofilm collected from Cathedral of Seville (natural sample) and its liquid culture monitored during 90 days (Lanes 15, 30, 45, 60, 75 and 90, corresponding to the sampling days). Lanes "0 bact" and "0 cya" correspond to the DGGE profiles of the inoculum obtained after amplification using bacterial and cyanobacterial primers, respectively. DGGE profiles of the liquid culture were obtained using cyanobacterial primers. The band numbers refer to clones obtained from the natural sample. Lane "M" corresponds to DGGE markers, consisting of *Pseudomonas* sp., *E. coli*, *Paenibacillus* sp. and *Streptomyces* sp. Identification of bands based on comparison with closest relatives at NCBI databank (Acc. Number in parenthese): 1- *Methylobacterium* sp. (AB302928), 2- Uncultured bacterium (EU137447), 3- *Saccharospirillum* sp. (AJ315983), 4- *Marinobacter* sp. (DQ665805), 5- Uncultured actinobacterium (EU299252), 6- *Saccharospirillum* sp. (AJ315983), 7- *Marinobacter* sp. (CP000514), 8- *Pleurocapsa* sp. (DQ293994), 9- *Pleurocapsa* sp. (DQ293994), 10- *Gyrosigma fasciola* chloroplast (AF514847), 11- Uncultured Verrucomicrobia (AY770729), 12- *Leptolyngbya* sp. (X84809), 13- Uncultured Verrucomicrobia (AM690904), 14- *Chroococcidiopsis* sp. (DQ914863), 15- *Luteolibacter* sp. (AB331895).

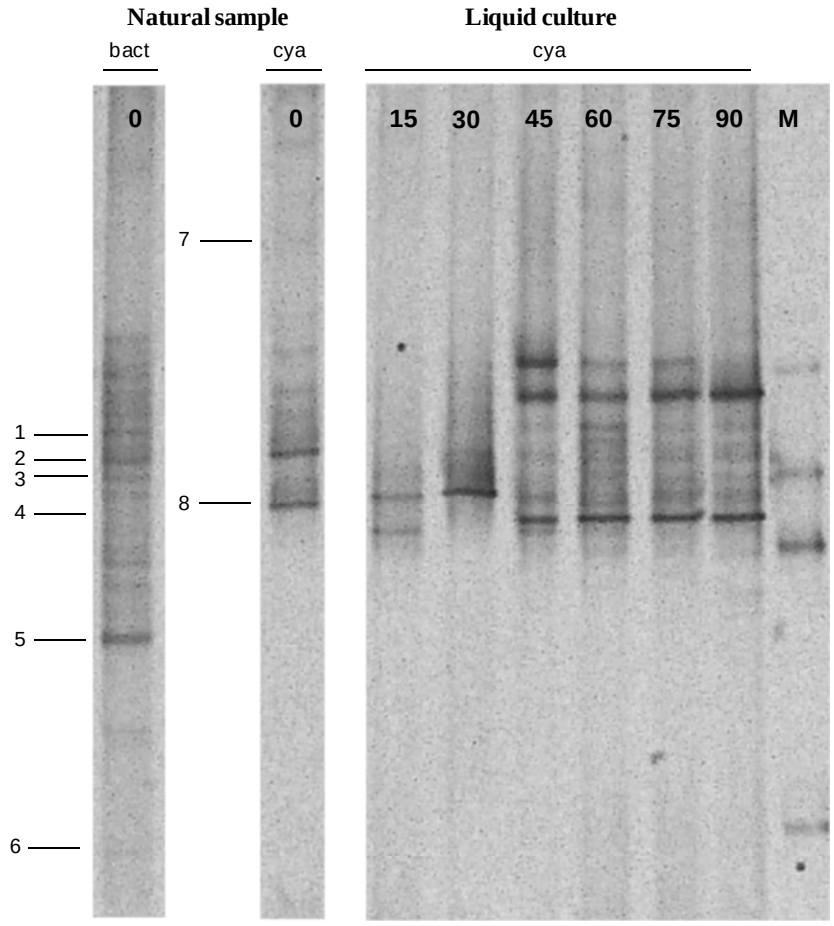

Fig. 3.9. DGGE profiles of 16S rRNA gene from the natural green biofilm collected from Cathedral of Granada (natural sample) and its liquid culture monitored during 90 days (Lanes 15, 30, 45, 60, 75 and 90, corresponding to the sampling days). Lanes "0 bact" and "0 cya" correspond to the DGGE profiles of the inoculum obtained after amplification using bacterial and cyanobacterial primers, respectively. DGGE profiles of the liquid culture were obtained using cyanobacterial primers. The band numbers refer to clones obtained from the natural sample. Lane "M" corresponds to DGGE markers, consisting of *Pseudomonas* sp., *E. coli*, *Paenibacillus* sp. and *Streptomyces* sp. Identification of bands based on comparison with closest relatives at NCBI databank (Acc. Number in parenthese): 1- Uncultured Bacteroidetes (AM168126), 2- *Porphyrobacter* sp. (AB033328), 3- *Chroococcidiopsis* sp. (DQ914863), 4- *Stenotrophomonas* sp. (DQ109037), 5- *Sphingomonas* sp. (EU814953), 6- Uncultured Bacteroidetes (EF522197), 7- *Pleurocapsa* sp. (DQ293994), 8- *Chroococcidiopsis* sp. (DQ914863).

3.4. Discussion

The analysed biofilms consisted of a phylogenetically diverse array of prokaryotes including cyanobacteria as well as bacteria belonging to Proteobacteria, Bacteroidetes, Actinobacteria, Verrucomicrobia and Acidobacteria. The biofilms also included green algae and Bacillariophyta, as indicated by the detection of chloroplasts through molecular techniques. The cyanobacterial and proteobacterial sequences were the most common and accounted for the largest fractions of each community.

The diversity of phototrophic species found in this study is similar to those observed in other studies carried out on historic buildings and monuments as reviewed in chapter two (e.g. Ortega-Calvo et al., 1991a; Lamenti et al., 2000; Tomaselli et al., 2000a; Bellinzoni et al., 2003). Comparative analyses of the sequences obtained in this work revealed clear differences between the microbial communities of the five green biofilms (Table 3.3). Differences in the bacterial and cyanobacterial diversity among the Martano, Coimbra and Granada samples were not as high as those between Lisbon and Seville samples. Lisbon biofilm presented the largest proportion of microorganisms belonging to Cyanobacteria, being dominated by the cyanobacterium *Chroococcidiopsis*, also present in Seville and Granada samples. As mentioned in the previous chapter, this cyanobacterium can survive extreme cold, heat and arid conditions and it may be the single autotrophic organism most tolerant to environmental extremes (Graham and Wilcox, 2000). It was detected in different lithic substrata, comprising limestone, marble, granite and sandstone surfaces, in a total of 10 monuments studied by several authors (see Table 2.2 from chapter two). Moreover, identification of *Chroococcidiopsis* indicates that endolithic growth may occur in the analysed monuments since its presence has been reported in studies concerning endolithic growth in rocks (Friedmann, 1982; Banerjee et al., 2000). The nitrogen-fixing cyanobacterium *Pleurocapsa* was detected in all analysed photosynthetic biofilms. As reported in chapter two, *Pleurocpasa* is a widespread cyanobacterium occurring in 13 different monuments from the Mediterranean Basin region, built in limestone, marble and granite. Tomaselli et al. (2000a) reported that the most widespread cyanobacteria occurring in photosynthetic communities dwelling on stone monuments were *Chroococcidiopsis*, *Pleurocapsa*, *Leptolyngbya* and *Plectonema*. Three nitrogen-fixing cyanobacteria,

Cylindrospermopsis, *Nostoc* and *Pleurocapsa*, were found in this work. The presence on buildings of nitrogen-fixing cyanobacteria has been considered as possibly relevant for the establishment and development of other organisms, such as heterotrophic bacteria (Grant, 1982).

Samples from the Cathedral of Seville presented the largest proportion of microorganisms belonging to Bacteria. Proteobacteria was the most representative phylum detected in these samples. Their presence have been previously reported and comprises common members of the bacterial community considering stone materials (Gurtner et al., 2000; Piñar et al., 2002; Akatova et al., 2007; Cappitelli et al., 2007). Stone monuments can represent extreme habitats, favouring the growth of a variety of specialized microorganisms. For instance, the detection of *Marinobacter*, belonging to Gammaproteobacteria, in samples from Cathedral of Seville could be an indicative of salt efflorescences since these organisms are capable of extremophilic lifestyles and are moderately halophilic and mesophilic (Gauthier et al., 1992). *Methylobacterium* is a facultative methylotroph, mostly found in soils and plants, which has the ability to grow by reducing carbon from methyl groups or short chain aliphatic compounds. Aliphatic hydrocarbons are examples of those sorts of organic compounds in building stones located in urban environments, which have been detected in samples from Seville Cathedral by Saiz-Jimenez (1993). The presence of this bacterium was reported in Lisbon and Seville samples, and also in samples derived from the wall paintings of Catherine Chapel in the Castle of Herberstein (Gurtner et al., 2000).

Since the bacteria detected in the analysed phototrophic biofilms are heterotrophic microorganisms, their growth must be dependent on the presence of organic matter. In fact, photoautotrophs, as major primary producers, are considered pioneer inhabitants of stone materials and heterotrophic microorganisms are known to inhabit these microbial communities (Ortega-Calvo et al., 1993a; Urzì and Krumbein, 1994). Organic matter provided by extracellular polymeric substances release by the phototrophs is the main source of organic carbon for the heterotrophic microorganisms. Furthermore, the phototrophic microorganisms, when dead, become a nutrient source for heterotrophic bacteria. Instead, stone monuments located in urban environments act as repositories of organic and inorganic pollutants which accumulate on their surfaces. Aliphatic hydrocarbons are examples of organic

compounds found on building stones located in urban environments, which were detected in samples from Seville Cathedral by Saiz-Jimenez (1993).

The results of this study showed that the photosynthetic biofilms can develop as a small ecosystem with many different functional groups of organisms. There is increasing evidence that there are specific bacterial taxa associated with photosynthetic microorganisms. Interactions of cyanobacteria and bacteria range from symbiotic, via commensal, to parasitic interactions. Most studies on bacterial-cyanobacterial interactions have focused in phytoplankton (González et al., 2000; Pinhassi et al., 2005). Bruno et al. (2006) analysed *Leptolyngbya* sp. strains isolated from biofilms developing inside Roman hypogea and their associated bacteria, identified as *Pseudomonas*, *Stenotrophomonas*, *Agrobacterium* and *Bacillus*. *Pseudomonas* and *Stenotrophomonas* genera might play a role in the exopolysaccharidic matrix formation and co-aggregation processes. Also *Stenotrophomonas* and *Bacillus* sp. have been associated to Mg-calcite precipitation processes occurring at the substratum/biofilm interface in Roman Catacombs and can contribute to biomineralisation of stone (Sànchez-Moral et al., 2003). According to Salomon et al. (2003), colonial and filamentous cyanobacteria frequently have bacteria associated with their extracellular mucus zone or more tightly attached to their cells surface. Paerly et al. (1989) indicated that cyanobacteria/bacteria association established in culture may be regarded as a mutual-beneficial association, where bacteria benefits from organic substances released from cyanobacteria returning remineralised inorganic nutrients and carbon dioxide that can be directly utilised by the host cyanobacteria. Therefore, experiments with microbial communities composed by different groups of organisms are essential for microbial ecology studies. In this respect, the culturing experiment with phototrophic biofilms performed in this work aimed to exhibit a high resemblance with the natural phototrophic communities. However, the results demonstrated that the phototrophic biofilms cultured in the laboratory do not easily generate stable and diverse microbial communities. Five different biofilm cultures were monitored and only one of them reached stable conditions with an acceptable natural-looking diversity. According to Roeselers et al. (2006), the end of exponential growth does not necessarily mean that a stable climax community has established. The biofilms may be still in a transient state, developing slowly towards a final convergence. The cases probably following this common evolution were Lisbon and Seville biofilm cultures, which

inocula showed the highest microbial diversity and the greatest variability during the incubation time, likely due to shortage or absence of special nutrient requirements. In the case of Seville biofilm, the culture variability indicates that a rather unstable community was cultivated or the biofilm culture was still in a transient state and a stable community has not established. The reason for this instability is probably due to the presence of bacteria degrading recalcitrant compounds (e.g. polycyclic aromatic hydrocarbons) (Saiz-Jimenez, 1995; Ortega-Calvo and Saiz-Jimenez, 1997). Obviously these bacteria were unable to growth under laboratory conditions, where no recalcitrant compounds were added.

In contrast, the cultured community obtained from Coimbra showed a stable and diverse community after 45 days of incubation. This community included algae, cyanobacteria and bacteria which were also the major components of the natural green biofilm causing deterioration on the Santa Clara-a-Velha Monastery. This similarity with the inoculum is a requirement for comparative monitoring and evaluation of biodeterioration studies under laboratory conditions. Biodeterioration studies, monitoring and control, require the development of standard procedures to quantify and approach these phenomena under reproducible conditions. One of the essentials of these procedures is the use of an acceptable microbial community able to simulate natural conditions of colonisation and in order to satisfy this requirement it is necessary to obtain a diverse microbial community composed by a stable set of components. In this study, a stable microbial community reflecting natural components and maintaining its diversity along the time was obtained for the Coimbra culture.

3.5. Conclusions

DNA–based molecular analysis of 16S rRNA gene fragments from the natural green biofilms revealed complex and different communities composition with respect to phototrophic microorganisms. The biofilms from Orologio Tower (Martano, Italy) and Santa Clara-a-Velha Monastery (Coimbra, Portugal) were dominated by the microalga *Chlorella*. The cyanobacterium *Chroococcidiopsis* was the dominating genus from Ajuda National Palace biofilm (Lisbon, Portugal). The biofilms from

Seville and Granada Cathedrals (Spain) were both dominated by the cyanobacterium *Pleurocapsa*.

The molecular biology approach used in this study was very useful for the characterisation and monitoring of the major microbial components of the five phototrophic biofilms studied, demonstrating that DGGE analysis is a useful and elegant method for profiling and monitoring microbial communities (Schabereiter-Gurtner et al., 2001).

This cultivation and monitoring approach showed that the five cultivated communities developed differently in terms of species establishment and community composition during the 90 days of incubation. The biofilm culture from Coimbra (Portugal) showed a remarkable stability of the microbial components of the natural community in laboratory conditions. With this work, the multiple-species community culture from Coimbra biofilm was selected for further stone colonisation experiments, comprising the inoculation of stone samples with this culture. These artificial colonisation experiments will allow studying the stone bioreceptivity and the biodeterioration processes caused by phototrophic microorganisms, as well as, the interaction between microorganisms and the mineral substratum.

CHAPTER FOUR

Reproducing stone monument photosynthetic-based colonisation under laboratory conditions

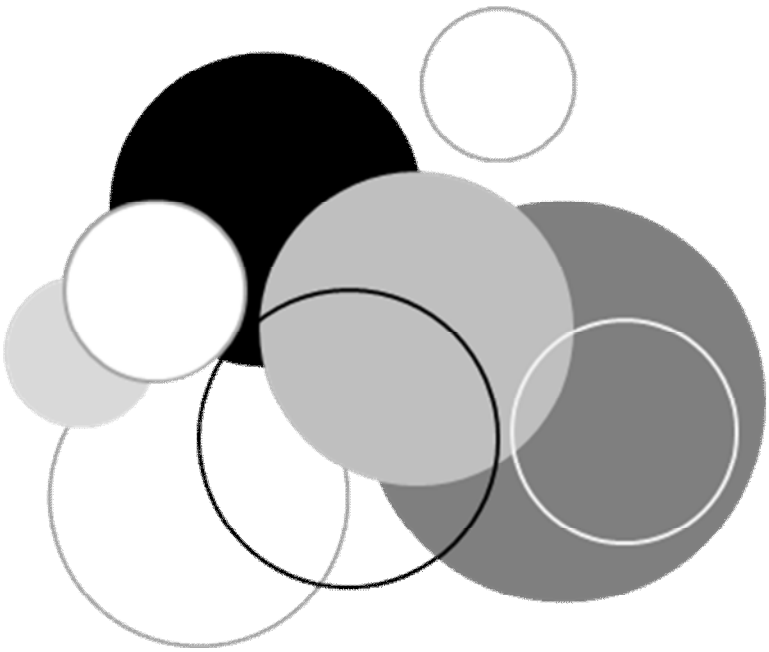

The main results presented in this chapter have been published in:

Miller, A.Z., Laiz, L., Gonzalez, J.M., Dionisio, A., Macedo, M.F., Saiz-Jimenez, C., 2008. Reproducing stone monument photosynthetic-based colonization under laboratory conditions. Science of the Total Environmental 405, 278-285.

CHAPTER FOUR

Reproducing stone monument photosynthetic-based colonisation under laboratory conditions

4.1. Introduction

One of the most complex problems in monument conservation is the biological deterioration or biodeterioration (Ortega-Calvo et al., 1995; Herrera et al., 2004; Miller et al., 2006). The interactions between environmental factors affecting stone monuments (e.g. light intensity, air pollution and humidity) and microorganisms are not well understood. As mentioned before, phototrophic organisms are, among the components of the microbial communities, the primary producers and play an important role in the colonisation and deterioration of stone monuments, causing extensive aesthetic, physical and chemical damages (Tomaselli et al., 2000b; Ciferri, 2002, Crispim and Gaylarde, 2005). In order to understand the biodeterioration process, laboratory experiments present the advantage of controlling environmental variables which simplifies the answering of important questions. A number of different laboratory-based experimental biofilm model systems have been developed (Guillitte and Desreen, 1995; Tiano et al., 1995; Tomaselli et al., 2000b; Monte, 2003; Prieto and Silva, 2005; Miller et al., 2006). In most cases, these systems were used to study single-species or a predefined mixed community, which cannot give a complete idea of the complex process involved in stone deterioration. Therefore, laboratory-based colonisation studies using a natural multiple-species consortium cultivated under laboratory conditions are important to understand the biodeterioration process.

In order to study the bioreceptivity and biodeterioration process occurring on stone monuments, a preliminary laboratory-based stone colonisation experiment was performed. The previously selected multiple-species community culture (Coimbra culture), described in the previous chapter, was used as inoculum of the *Ançã*

limestone samples to reproduce the phototrophic colonisation dwelling on the *Ançã* limestone surfaces of Santa Clara-a-Velha Monastery (Coimbra, Portugal). This phototrophic culture showed remarkable stability under laboratory conditions of the microbial components within the natural biofilm sample. The major components of the inoculum were *Chlorella*, *Stichococcus*, *Trebouxia* and *Myrmecia*, among the Chlorophyta, and *Leptolyngbya* and *Pleurocapsa* among the Cyanobacteria. Phototrophic microorganisms were selected because photoautotrophs are primary producers and, thus, pioneer inhabitants of stone materials being the most abundant organisms on monuments (see chapter two). In this work, the reliability of the Coimbra biofilm culture as inoculum for further accelerated stone colonisation experiments was also evaluated.

4.2. Materials and methods

4.2.1. Experimental setup

The previously cultivated and selected phototrophic community from Santa Clara-a-Velha Monastery (Coimbra, Portugal) was used as inoculum to assess its reliability for accelerated stone colonisation. Before inoculation, this biofilm was completely characterised by means of DGGE analyses and culture techniques for a better understanding of the major microorganisms present in the inoculum. In order to reproduce the natural biofilm dwelling on the Santa Clara-a-Velha Monastery, quarry *Ançã* limestone samples were selected since the biological samples were originally collected from this type of substratum.

The second experimental step was the inoculation of the lithic samples with the cultivated microbial community and incubation in a laboratory chamber for 90 days. In the last stage, the monitoring of the biofilm development on the stone samples was achieved. The methodology used to monitor the evolution and composition of the phototrophic community on the stone samples is a culture-independent technique described below.

4.2.2. Analysis of microbial community

4.2.2.1. Molecular biology techniques

The previously extracted DNA from Santa Clara-a-Velha Monastery biofilm and its culture, preserved at 4ºC, were used for the identification of eukaryotes (fungi and microalgae) within the biofilm and liquid culture samples (incubation days 0, 15 and 75). The eukaryotic 18S rRNA genes were amplified by PCR with the primer pair EukA and EukB, corresponding to nucleotide positions 21-1795 of the Eukaryotes 18S rRNA nucleotides (Table 3.2, chapter three). PCR reactions were performed in 50 µL volumes, containing 2 µL of the extracted DNA used as template DNA. This amplification was carried out with a denaturing step of 2 min at 95ºC, 35 cycles of denaturing (95ºC for 15s), annealing (50ºC for 12s) and elongation (72ºC for 2 min), following a terminal elongation step of 10 min at 72ºC.

In order to obtain 18S rDNA sequence information of the major members comprising the Coimbra samples, 18S rDNA clone libraries were constructed by cloning PCR products amplified with EukA-EukB primer pair. Before cloning, PCR products were purified using the JetQuick® PCR Purification Spin Kit (Genomed, Löhne, Germany) and cloned with the TOPO TA Cloning Kit (Invitrogen, California, USA). The presence of 18S rDNA inserts was verified by PCR using vector-specific T7p and M13rev primers. PCR cycling conditions comprised a denaturing step of 3 min at 95ºC, 35 cycles of denaturing (95ºC for 15s), annealing (55ºC for 15s) and elongation (72ºC for 30s), following a terminal elongation step of 10 min at 72ºC. The positive PCR products were inspected by electrophoresis in 1% (w/v) agarose gel as described in section 3.2.2.2 (chapter three).

For the screening of 18S rDNA inserts of Coimbra biofilm, a restriction digestion, using *Hin*6I and *Msp*I enzymes, combined with 2% (w/v) agarose gel electrophoresis was performed. The restriction digestion was carried out in 15 µL volumes, containing 10 µL of PCR product amplified T7p and M13rev primers, 1.5 µL of Y^+/Tango™ buffer, 0.3 µL of *Hin*6I enzyme (Fermentas, Burlington, ON Canada), 0.3 µL of *Msp*I enzyme (Fermentas) and 2.9 µL of nuclease-free water (Sigma-Aldrich). The digestion reaction was then incubated at 37ºC during 2 h in water bath. In order to visualise positive restriction digestion products, 2% (w/v) agarose gel electrophoresis was conducted with 60 V during 45 min. All products showing different positions in agarose gel were used for sequencing.

Plasmids were extracted using the JetQuick® Plasmid miniprep Spin Kit (Genomed, Löhne, Germany) and sequenced by Secugen Sequencing Services (CSIC, Madrid, Spain). Sequence data was edited using the software Chromas 2.01 (Technelysium, Tewantin, Australia). Homology searches with those sequences were performed using the Blast algorithm (Altschul et al., 1990) on the NCBI database (http://www.ncbi.nlm.nih.org/blast/). Nucleotide sequences obtained from the Santa Clara-a-Velha Monastery (Coimbra, Portugal) biofilm and from its cultivation have been deposited in the GenBank database under accession number from EU333004 to EU333026.

4.2.2.2. Culture techniques

For an enhanced assessment of the major phototrophic microorganisms comprising the natural green biofilm from the Santa Clara-a-Velha Monastery (Coimbra, Portugal), DNA-based molecular analyses were complemented with culture procedures as recommended by Elsas et al. (1998) and Gonzalez and Saiz-Jimenez (2006). For this objective solid culture medium on Petri dishes were prepared. Aliquots for culturing procedures of the natural biofilm samples were suspended in 1.5 mL of sterile water and homogenised for 1 min using a vortex mixer; 100 µL of the suspension was inoculated onto plates of BG11 medium supplemented with Vitamin B12 (Normal 9/88) and solidified with 2% Bacto-Agar. The plates were incubated under continuous light at 20ºC in an incubator chamber.

After 15-30 days incubation, all visible different green colonies grown on the agar medium were sampled by picking a single colony with a sterilised inoculation loop and spreading the inoculate back and forth over new solid BG11 plates, under a laminar flow cabinet. Features of individual strains were observed with a light microscope (Zeiss HAL 100) equipped with a photographic camera (AxioCam MRc5) for the characterisation and identification of the cyanobacterial and algal isolates. Taxonomic identification was carried out according to Bourrelly (1990) and Komárek and Anagnostidis (1999).

For storage, biomass of each isolated strain was collected from a fresh plate culture and suspended in triplicate in eppendorf tubes containing 15% (v/v) DMSO, an effective cryoprotective agent for cyanobacteria. Immediately, the tubes were shaken gently and stored at -80ºC. This storage at ultra-low temperature allows

further recovery of the stored organisms to the same living state as before it was stored. DMSO was used to minimise potentially lethal effects suffered by cyanobacteria during the freezing and thawing processes.

Additionally, the isolates from Santa Clara-a-Velha Monastery (Coimbra, Portugal) were also identified by 16S rDNA sequence analysis. DNA of the isolates was extracted by transferring cyanobacterial biomass with an inoculation loop into an eppendorf tube containing 100 µL TE buffer, and subjecting to three freeze (–80ºC)/thawing (68ºC) cycles to lyse the cells. Subsequently, the suspensions were centrifuged during 10 min at 13000 rpm and the supernatant was transferred for sterile tubes, which were conserved at -20ºC for further analysis. 16S rDNA was amplified with primers cya106F and cya781R (Table 3.2), cloned and sequenced as previously described (see section 3.2.2.4 - 3.2.2.6). For DGGE analysis, PCR products were used for nested PCR using 341F-GC and 518R primers as described in section 3.2.2.2 (chapter three). The fingerprints of the isolates were compared with the original fingerprint of the natural sample from Coimbra's monument.

4.2.3. Stone colonisation experiment

Quarry stone samples of *Ançã* limestone were used in the colonisation experiment. Petrophysical characteristics of *Ançã* limestone, open porosity and capillarity, were previously determined and described in Miller et al. (2006). Six replicate stone samples (parallelepipeds of 4 x 1 x 4 cm) were washed with sterile water and sterilised at 120ºC and 1 atm, for 20 min. After cooling, the samples were placed in a non-commercial incubator system (Fig. 4.1). This laboratory chamber allows the inoculation of materials with an active growing microbial culture using an automatic irrigation system with a pre-established periodicity.

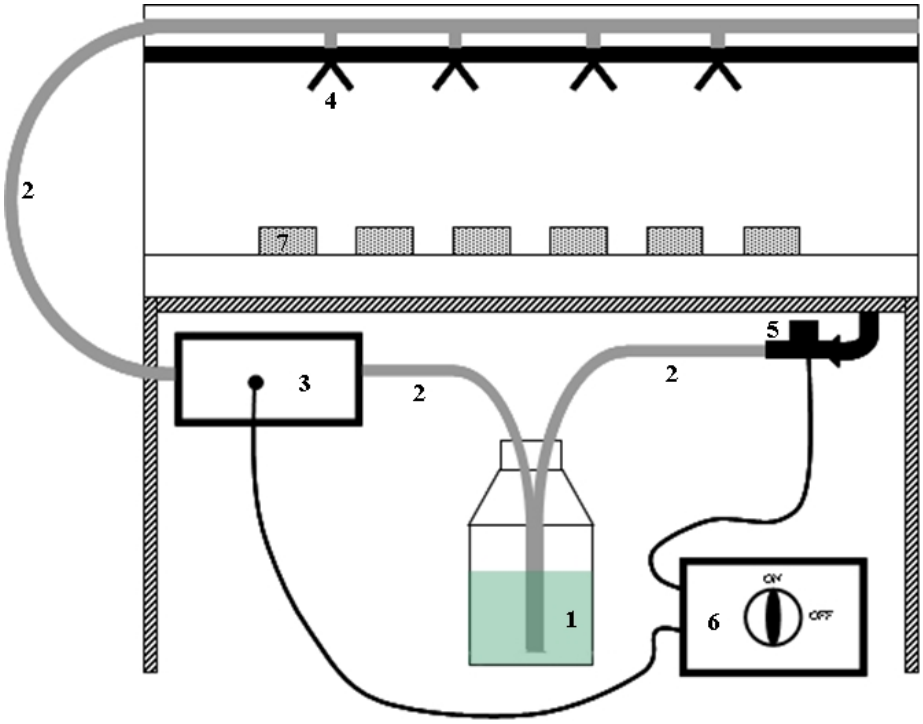

Fig. 4.1. Scheme of the laboratory chamber used to assess the ability of phototrophic communities to colonise stone samples: 1 – Phototrophic liquid culture; 2 – Silicon tubing; 3 – Automatic pumps; 4 – Sprinklers; 5 – Outlet valve device; 6 – Control unit; 7 – Stone samples.

During the first two weeks of this experiment, the stones samples within the chamber were inoculated with the cultivated phototrophic biofilm from Santa Clara-a-Velha Monastery, which passed through sprinkling rails and projected on the top of the stone samples for 5 min every 8 h. After each sprinkling, the liquid deposited in the chamber was collected, recycled by a pump and sent towards the sprinkling rails. During the following two weeks, the stone samples were sprinkled with 1000x diluted BG11 medium for 5 min every 8 h. After this period, the samples have been sprinkled for 5 min every 12 h, in order to simulate outdoor environmental conditions.

The development of photosynthetic biofilms on stone samples was monitored during 90 days by collecting, every two weeks, small samples of the biofilm covering the upper surface of two samples and analysed by DGGE. The samples were obtained by scraping the biofilm into sterile tubes and immediately stored at –80ºC until processing. DNA extraction, PCR amplification with cyanobacteria-specific primers Cya 106F and Cya 781R, and DGGE analysis were performed as described before (section 3.2.2, chapter three).

4.3. Results

4.3.1. Natural green biofilm composition as determined by DGGE analysis

As mentioned in the previous chapter, the DNA-based molecular analysis of the prokaryotic microorganisms present in the green biofilm collected from Santa Clara-a-Velha Monastery (Coimbra, Portugal) revealed the occurrence of cyanobacteria and heterotrophic bacteria. The major prokaryotic components of the biofilm were *Leptolyngbya* and *Pleurocapsa* among the Cyanobacteria, and Bacteroidetes, Actinobacteria, Alphaproteobacteria and Verrucomicrobia among the Bacteria. Chloroplasts of the phylum Chlorophyta were also detected using cyanobacteria-specific primers, which was represented by the genus *Chlorella*. Among the microorganisms detected from 16S rRNA genes using cyanobacteria-specific primers (39 clones), the most frequently found microbial group was the Verrucomicrobia with over a 43% of the processed sequences (Fig. 4.2). This group was represented by uncultured and unclassified microorganisms. The *Chlorella* genus represented the second microbial group in abundance of detected sequences (over 40%).

The 18S rRNA gene libraries, used to identify the eukaryotic components of the Coimbra's phototrophic community, revealed the presence of microorganisms belonging to Chlorophyta and Ascomycota phyla. *Chlorella*, *Stichococcus*, *Trebouxia* and *Myrmecia* were the genera identified within the Chlorophyta. The identified fungi belonging to the phylum Ascomycota were: *Cyphellophora* sp., *Phoma* sp., *Cladosporium* sp. and *Capnobotryella* sp. Using sequence analysis of 18S rRNA gene, high similarity (≥ 99%) was found with NCBI database entries of the algae *Chlorella vulgaris*, *Stichococcus bacillaris* and *Trebouxia asymmetrica*, and the fungi *Cladosporium cladosporioides*, *Cyphellophora laciniata* and *Phoma* sp. (Table 4.1).

Among the 22 sequenced clones for eukaryotes, the highest proportion was obtained for the phylum Ascomycota, besides the significant representation also showed for the Chlorophyta, with a 53% and 47%, respectively (Fig. 4.2). The most frequently found genera were the *Cyphellophora* among the detected Ascomycota, and the *Chlorella* among the analysed Chlorophyta sequences, showing the same proportion of clones (Fig. 4.3). The fungi *Phoma* sp. and *Cladosporium cladosporioides*, and the green algae *Stichococcus* sp. and *Trebouxia asymmetrica*

also showed significant representation among the analysed eukaryotic sequences (Fig. 4.3).

Table 4.1. Phylogenetic affiliations of eukaryotic microorganisms derived from the natural green biofilm of Santa Clara-a-Velha Monastery (Coimbra, Portugal).

Accession no.[a]	Phylogenetic affiliation[b]	Percent similarity (%)
Algae		
EU333011	*Chlorella vulgaris* (X13688)	99
EU333019	*Myrmecia bisecta* (Z47209)	97
EU333021	*Stichococcus* sp. (AF513370)	97
EU333025	*Stichococcus bacillaris* (AY380557)	99
EU333026	*Trebouxia asymmetrica* (Z21553)	99
Fungi		
EU333022	*Capnobotryella* sp. (AJ972854)	97
EU333023	*Cladosporium cladosporioides* (DQ678004)	99
EU333020	*Cyphellophora laciniata* (AY342010)	99
EU333024	*Phoma* sp. (AB252869)	100

[a] Accession numbers of the sequences obtained in this study by cloning, available at the NCBI database. Screening of clones was performed by restriction enzymatic digestion.

[b] Closest relatives obtained by comparison with the NCBI database. Accession numbers of the closest related database entries are given between brackets.

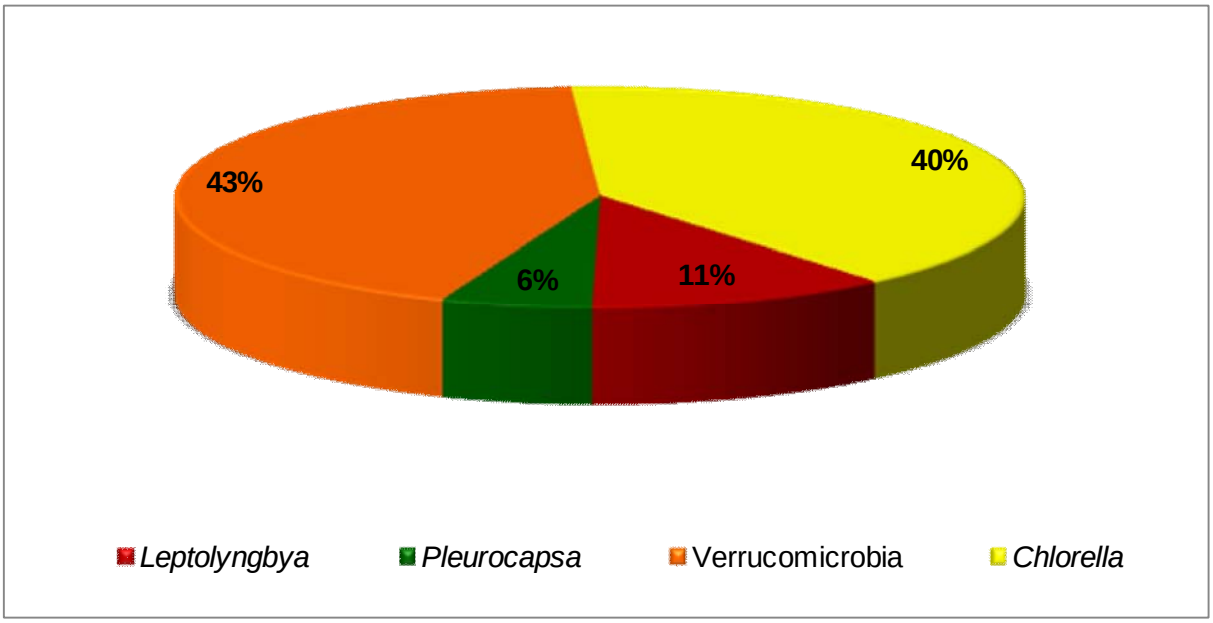

Fig. 4.2. Abundance graphical representation of the different microbial groups detected in the 16S rDNA clone libraries from Santa Clara-a-Velha Monastery (Coimbra, Portugal) green biofilm.

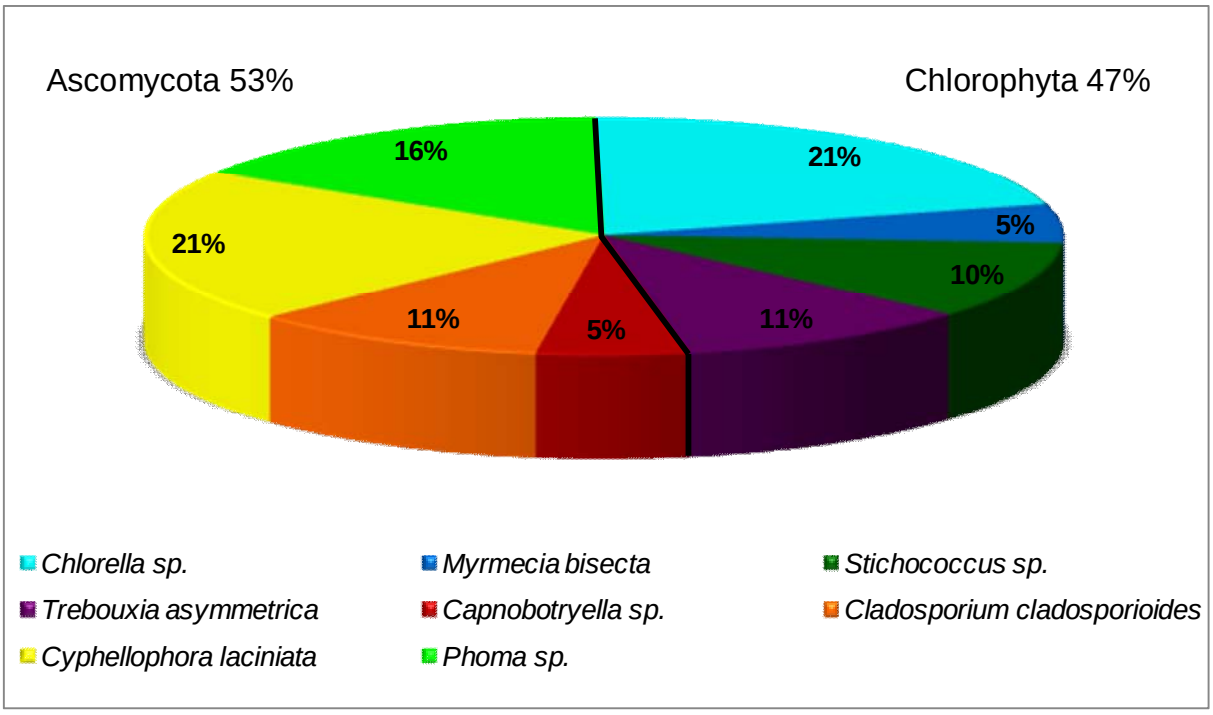

Fig. 4.3. Abundance graphical representation of the green algae and fungi types detected in the 18S rDNA clone libraries from Santa Clara-a-Velha Monastery (Coimbra, Portugal) green biofilm.

4.3.2. Biofilm composition as determined by culture techniques

The culture approach allowed the assessment of the major phototrophic microorganisms present in the natural green biofilm samples. Enrichments in BG11 of these samples revealed the microalga *Chlorella* (Fig. 4.4a,b), the filamentous cyanobacterium *Leptolyngbya* sp. (Fig. 4.4c,d) and the unicellular and nitrogen-fixing cyanobacterium *Pleurocapsa* sp. (Fig. 4.4e,f). These results are in fair agreement with the data obtained by culture-independent techniques. All the three strains identified by microscopy were detected in the natural green biofilm corresponding to the strains analysed by molecular techniques (Fig. 4.5).

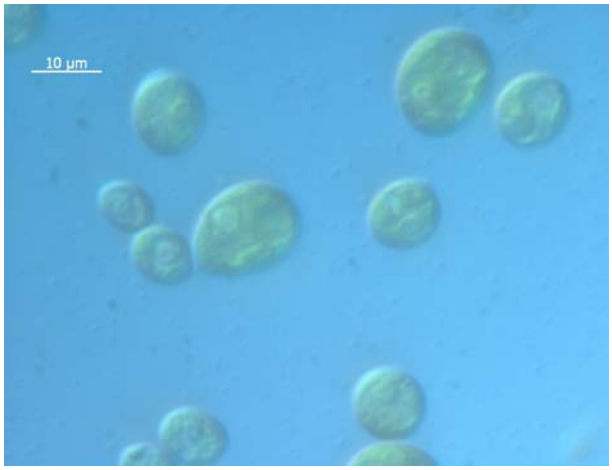

Fig. 4.4a. Light microscope micrograph of *Chlorella* sp.

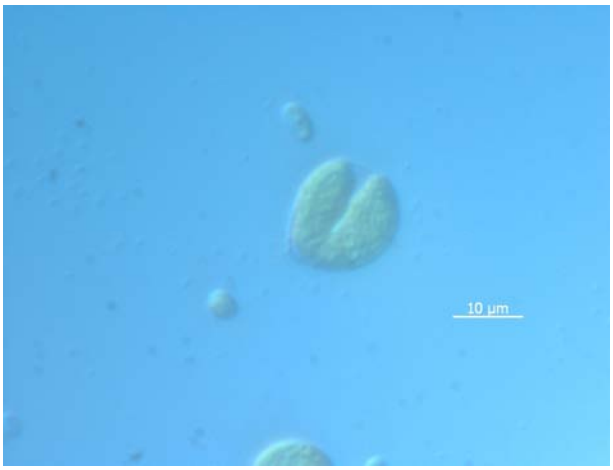

Fig. 4.4b. Light microscope micrograph of *Chlorella* sp.

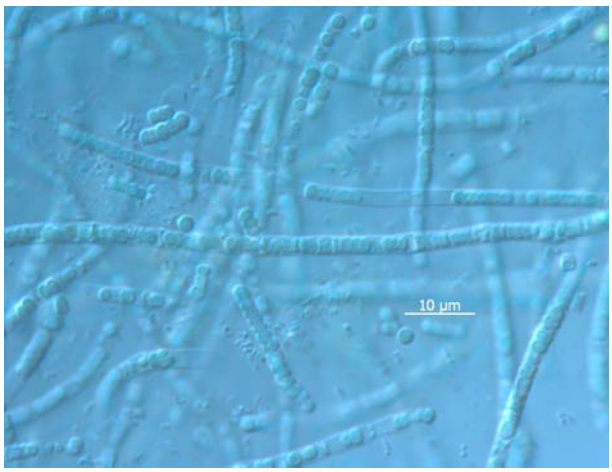

Fig. 4.4c. Light microscope micrograph of *Leptolyngbya* sp.

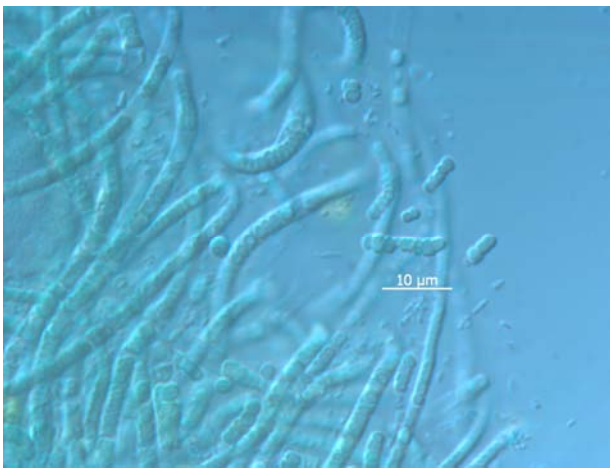

Fig. 4.4d. Light microscope micrograph of *Leptolyngbya* sp.

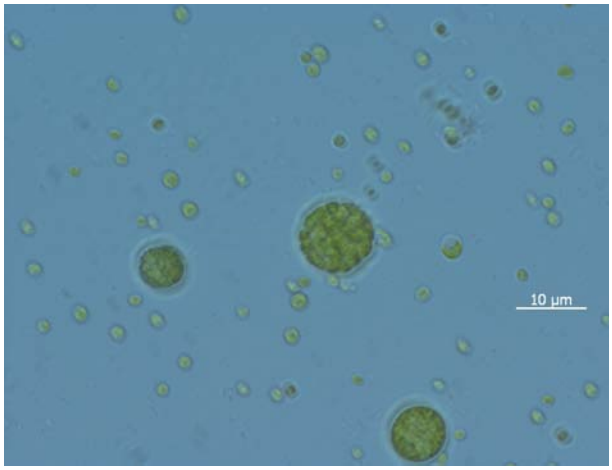

Fig. 4.4e. Light microscope micrograph of *Pleurocapsa* sp.

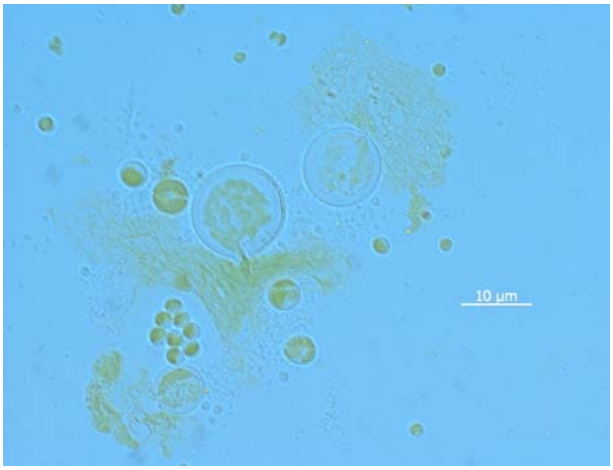

Fig. 4.4f. Light microscope micrograph of *Pleurocapsa* sp.

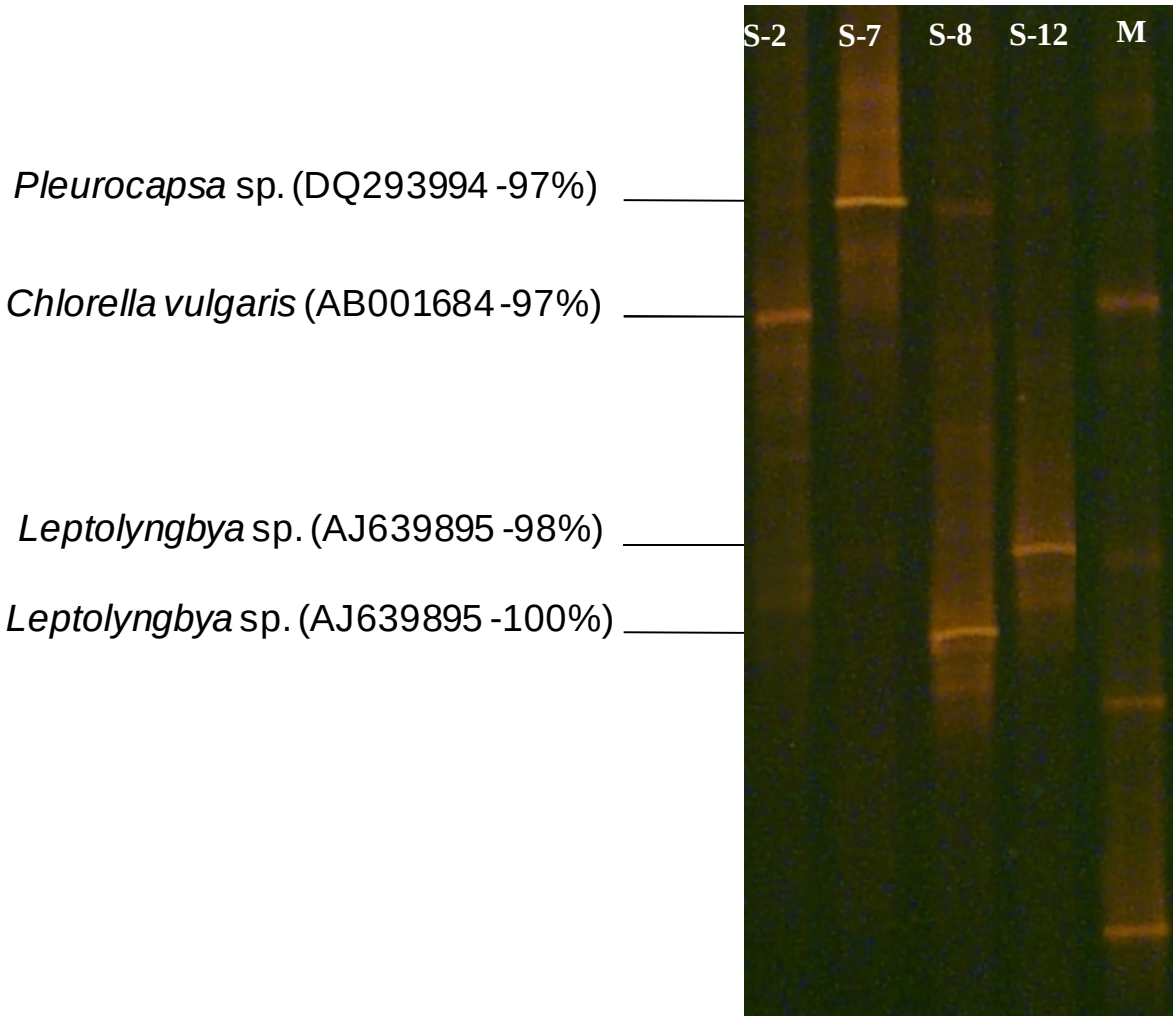

Fig. 4.5. DGGE fingerprints using cyanobacterial-specific primers of the isolated phototrophic strains identified by 16S rDNA amplification, DGGE, construction of clone libraries and sequence analyses. Accession numbers and similarity (%) of the closest related database entries are given between brackets.

4.3.3. Stone colonisation experiment

Judging by visual examination, the inoculated samples developed biofilms similar in appearance to those occurring on outdoor stone monuments. *Ançã* limestone samples were rapidly and highly colonised by phototrophic microorganisms. After 30 days of incubation, the stone samples presented a thick and homogeneously distributed green layer on the top face of the stones (Fig. 4.6). The colonisation process also led to increased photosynthetic biomass on the vertical sides of the samples, showing preferential growth on rough areas.

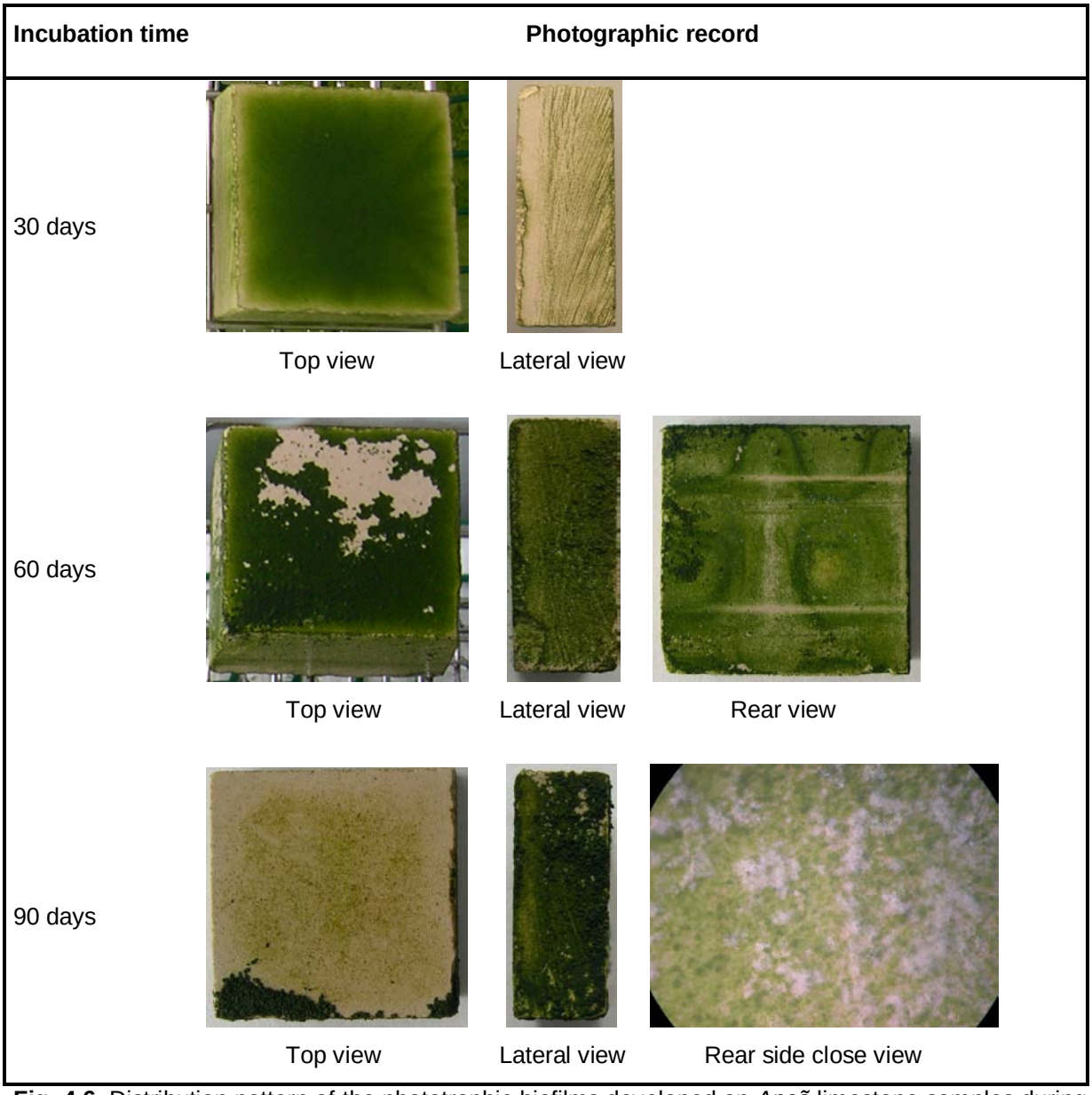

Fig. 4.6. Distribution pattern of the phototrophic biofilms developed on *Ançã* limestone samples during 90 days in a laboratory chamber.

At 30 days of exposure in the laboratory chamber, the setup had been exposed to more desiccating conditions (lower sprinkling frequency). One week later, the phototrophic layer covering the substrata started to detach from the top of the samples. However, new re-colonisation occurred on these stone surfaces, presenting a light green colour, which remained constant until the end of the experiment. In contrast, lateral and rear sides of the stone slabs were widespread covered by photosynthetic biomass, showing dark green and dense biofilms (Fig. 4.6).

After 90 days, it was observed that stone samples presented white colonies on the green biofilms covering the stone surfaces (Fig. 4.6). This colonisation was attributed to fungal growth as observed by binocular microscopy.

The development of photosynthetic biofilms on the stone samples was monitored during the 90 days of incubation and analysed by DGGE. The major colonisers of the stone samples during the laboratory experiment were represented by the unicellular microalga *Chlorella* and the filamentous cyanobacterium *Leptolyngbya* as revealed by DGGE analysis (Fig. 4.7). However, one of the *Chlorella* sp. showed less ability to adapt to the changes of exposing conditions than *Leptolyngbya* sp., as revealed by decreasing of intensity of the corresponding DGGE band (Fig. 4.7). The nitrogen-fixing cyanobacterium *Pleurocapsa* was a minor representative in the laboratory stone colonisation, suggesting that this microorganism was not a major coloniser of the stone surface. An unknown band was observed after 15 days of stone incubation which remained during all exposing period and likely corresponds to a microbial contamination.

The photosynthetic components of the natural green biofilm colonised the stone samples during the 90 days of incubation, and thereby demonstrated stability along time. Comparison of the microorganisms present in the natural biofilm samples, in the liquid culture (inoculums), and in the colonising community of the stone samples showed great similarities and the major phototrophic components were common in these three cases.

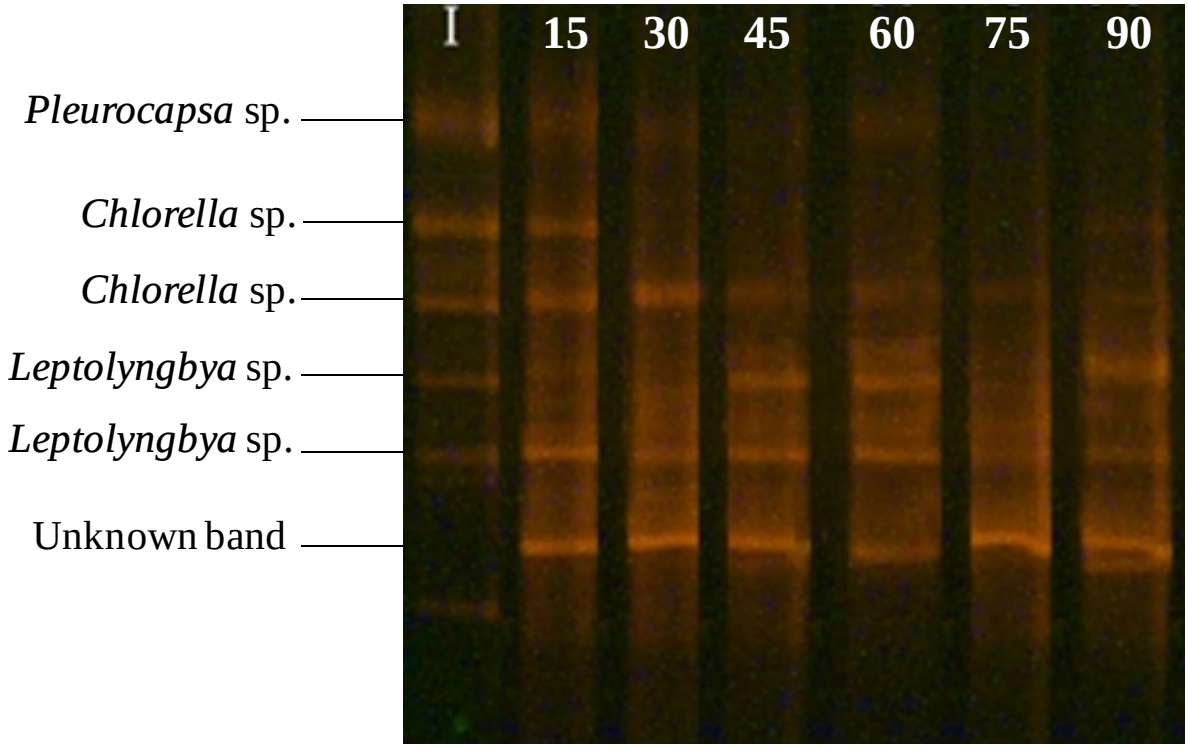

Fig. 4.7. DGGE fingerprints using cyanobacterial-specific primers from samples of artificially colonising biofilms on *Ançã* limestone incubated in a laboratory chamber over 90 days (15, 30, 45, 60, 75, and 90 days). Lane I corresponds to the inoculum used to start the colonisation process of these stone samples. Lanes 15 to 90 represents the microbial communities' profiles of this stone colonisation experiment at the indicated sampling time.

4.4. Discussion

The preliminary laboratory-based stone colonisation experiment performed in this work allowed to reproduce a colonisation equivalent to natural biodeteriorating process. Before inoculation, the previously selected multiple-species community culture used as inoculum was characterised by DNA-based molecular analysis targeting the 16S and 18S ribosomal RNA genes. The natural green biofilm from Santa Clara-a-Velha Monastery was mainly composed by the Chlorophyta *Chlorella*, *Stichococcus*, and *Trebouxia*, and by Cyanobacteria belonging to the genera *Leptolyngbya* and *Pleurocapsa*. As mentioned in the previous chapters, most of the microorganisms detected in this study are very widespread on stone monuments and historic building located in Europe according to several studies carried out by other

authors and revised in chapter two (Ortega-Calvo et al., 1993b; Tomaselli et al., 2000b; Bellinzoni et al., 2003; Ascaso et al., 2004; Miller and Macedo, 2006).

A number of bacteria belonging to Alphaproteobacteria, Bacteroidetes and Verrucomicrobia were identified, as well as fungi from the Ascomycota phylum: *Cyphellophora* sp., *Phoma* sp., *Cladosporium* sp. and *Capnobotryella* sp. The presence of fungi on stone monuments has been demonstrated by several authors (Wollenzien et al., 1995; Zagari et al., 2000; Urzì et al., 2001; Pitzurra et al., 2002; De Leo and Urzì, 2003). According to Wollenzien et al. (1995), the most abundant fungal genera on calcareous stone from monuments are *Cladosporium*, *Penicillium, Trichoderma, Fusarium* and *Phoma*. In this study, *Phoma* and *Cladosporium* genera showed significant representation among the analysed sequences. These species are colonisers of rock and monuments, as is the case of the taxa detected in this study. *Capnobotryella* sp. and *Cyphellophora* sp. were also encountered in samples from marble and limestone monuments, respectively (Sert et al., 2007; Berdoulay, 2008). As reported by Burford et al. (2003), fungi play an important role in rock weathering and also in the biodeterioration of stone monuments as suggested by their presence in the studied samples. Ascomycota includes most of the fungi that combine with algae to form lichens. The identification of *Cyphellophora*, *Phoma*, *Cladosporium* and *Capnobotryella* indicates that some of these fungi could be involved in the lichenization process conducting to the colonisation by lichens on the *Ançã* surfaces from Santa Clara-a-Velha Monastery.

The biphasic approach used for the characterisation of the natural green biofilm colonising the *Ançã* limestone from Santa Clara-a-Velha Monastery revealed a good agreement between the phototrophic microorganisms identified by molecular and culture techniques. However, DGGE analyses of PCR products produced by amplification of extracted DNA using either eukaryotic or prokaryotic primers demonstrated the presence of a larger number of species. By applying molecular methods we attempted to understand both the microorganisms growing easily on culture media and the uncultured microbial majority in the natural green biofilms. Molecular methods were very useful for this purpose, although microscopy techniques allowed visualising their spatial distribution. One of the drawbacks of molecular methods is that no morphological and physiological information is extracted. Therefore, it can be conjectured that microscopy and molecular techniques are complementary for a complete assessment of the microbial communities.

The laboratory colonisation experiment on stone samples showed a colonisation pattern similar to that occurring on stone monuments. The biofilm detachments observed after the 30 days of incubation on the top of the samples seemed to be determined by the relative humidity fluctuation in the chamber, which can also be an important factor under natural conditions. Monuments experience large fluctuations in water circulation, including repeated desiccation and wetting, which was reproduced in the laboratory chamber. This showed a similar pattern with that occurring in monuments where a great biomass growth is observed in humid areas protected from the rain. Guillitte and Dreesen (1995) in laboratory chamber studies also noticed that very rapidly the phototrophic biofilm covering the materials had cracked, forming partially curled-up scales, after decreasing sprinkling frequency. Detailed observations in different monuments suggest that the formation of a photosynthetic biofilm developed on the stone surface depends strongly on the length of the period of wetness and the spatial orientation of the substratum. If conditions favour water evaporation, the algal layers may shrink as a result of desiccation, and remove stone grains which detach from the surface (Ortega-Calvo et al., 1991b). If the stone remains wet long enough, the growth of the biofilm, production of organic matter and humification processes may produce protosoils, which may favour the settlement of mosses and higher plants (Ortega-Calvo et al., 1995).

At 90 days of incubation the green biofilms developing on the stone samples displayed white colonies, which seemed to be related to fungal growth. The phototrophic communities contributed through photosynthetic activity to a significant increase in the organic carbon content of the stone, favouring the growth of heterotrophic microorganisms, such as bacteria and fungi. These white colonies confirmed interactions between phototrophic and heterotrophic microorganisms. For instance, Saiz-Jimenez et al. (1995) observed that heterotrophic microorganisms, within samples from Belgian monuments, can live either at the expense of the extracellular organic matter synthesised by living algae.

Additionally, the bioreceptivity (Guillitte, 1995) of *Ançã* limestone to phototrophic microorganisms was also studied. The stone colonisation experiment showed that this lithotype is highly bioreceptive to phototrophic colonisation. According to Albertano et al. (2000), carbonate rocks have a high risk of colonisation by microorganisms and are extremely susceptible to cyanobacteria and algae. Previous

reports proposed that a high porosity, linked to important open capillarity, allows the rapid development of colonising organisms (Guillitte and Dreesen, 1995). The petrophysical characteristics of the lithotype used in this study, high porosity and capillary absorption, might be the keys to the establishment and development of the microbial biofilms. According to Miller et al. (2006), *Ançã* limestone showed the greatest bioreceptivity among the four studied Portuguese lihtotypes due to its high porosity and capillary absorption. The high bioreceptivity presented by this limestone may induce severe biodeterioration on the substratum, which should be assessed by using environmental scanning electron microscopy and confocal scanning laser microscopy (Roldán et al., 2006).

This preliminary stone colonisation experiment also allowed evaluating the reliability of the Coimbra biofilm culture as inoculum for further accelerated stone colonisation experiments. The great similarity between the phototrophic microorganisms present in the inoculum and in the colonising community of the artificial colonised stone samples suggested that the selected microbial assemblage dominated by phototrophs is a good inoculum for stone colonisation experiments to be performed under laboratory conditions.

4.5. Conclusions

The microbial community obtained during this study represents a complexity comparable to natural communities and the procedure using a laboratory chamber was able to reproduce colonisation of stone in the laboratory. This incubation system, which exposes stone samples to intermittently sprinkling water, allowed the development of photosynthetic biofilms similar to those occurring on stone monuments. This study shows that reproducible colonisation experiments under accelerated laboratory conditions can be performed using complex microbial communities, presenting the advantage of simulating the existence of competition and/or synergy between colonising microorganisms.

Further work using the multiple-species phototrophic culture from Santa Clara-a-Velha Monastery will allow the study of bioreceptivity of different stone types. Moreover, complementing molecular and microscopy will contribute to decipher the

actual role and effects of specific microbial cells on building stone materials. Since microbial ecology involves the study of the relationships between microorganisms and their environment, microscopy techniques are necessary to study the interaction between the microbial communities and the mineral substratum, including both taxonomical and morphological characterisations. Also, the substratum properties should be characterised since they seemed to be important in determining the composition and development of these phototrophic biofilms.

CHAPTER FIVE

Primary bioreceptivity of limestones: the influence of their intrinsic properties on phototrophic colonisation

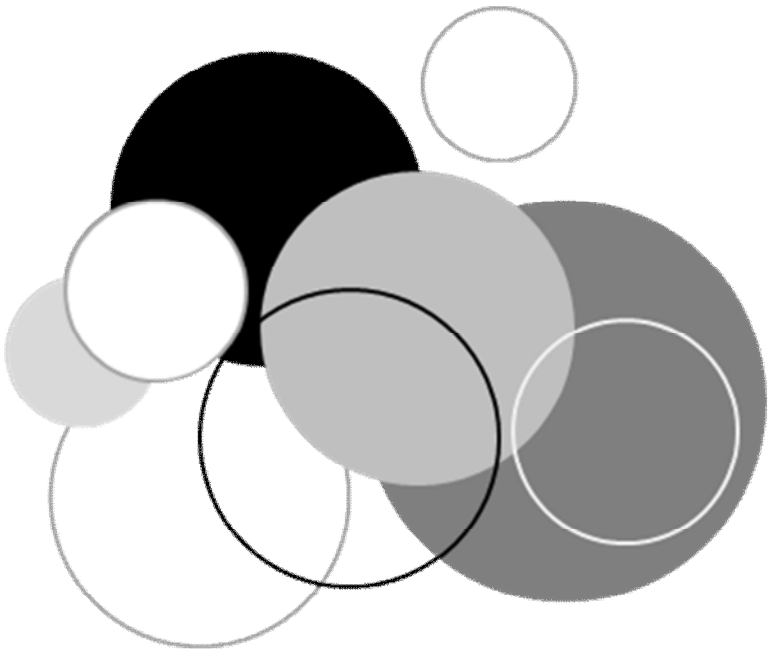

The main results presented in this chapter have been published in:

Miller, A.Z., Leal, N., Laiz, L., Rogerio-Candelera, M.A., Silva, R.J.C., Dionisio, A., Macedo, M.F., Saiz-Jimenez, C. 2010. Primary bioreceptivity of limestones used in Southern Europe monuments. In: Smith, B.J., Gomez-Heras, M., Viles, H.A., Cassar, J. (Eds), *Limestone in the Built Environment: Present Day Challenges for the Preservation of the Past*. Geological Society of London, Special Publications 331, 79-92.

Miller, A.Z., Dionísio, A., Laiz, L., Macedo, M.F., Saiz-Jimenez, C. 2009b. The influence of inherent properties of building limestones on their bioreceptivity to phototrophic microorganisms. Annals of Microbiology 59, 1-9.

CHAPTER FIVE

Primary bioreceptivity of limestones: the influence of their intrinsic properties on phototrophic colonisation

5.1. Introduction

Linking the bioreceptivity of building materials to their petrophysical and petrochemical properties has recently generated great interest in various fields of conservation sciences, biodeterioration, biology, architecture and earth sciences. At this point it is important to remind that bioreceptivity is the totality of material properties that contribute to biological colonisation by one or several groups of organisms (Guillitte, 1995). Reports on laboratory experiments focused on stone primary bioreceptivity, i.e. the initial potential of unaltered stone material for microbial colonisation (Guillitte, 1995), revealed that stone types with high values of petrophysical properties related with water movement through the rock matrix (e.g. open porosity, water vapour permeability, water absorption by capillarity) and surface roughness show higher bioreceptivity to phototrophic microorganisms than other lithotypes (Guillitte and Dreesen, 1995; Tiano et al., 1995; Tomaselli et al., 2000b; Prieto and Silva, 2005; Miller et al., 2006). The stone characteristics, and in particular the properties related with water movement through the rock matrix, are very important on the primary bioreceptivity of a rock since water is the main limiting factor for the settlement and development of colonising organisms. Prieto and Silva (2005) showed that capillary water is the best parameter to predict the bioreceptivity of granitic rocks. Abrasion pH, open porosity and bulk density (volume of empty space) were also good parameters for estimating the bioreceptivity of granites, according to those authors.

The importance of surface roughness in the bioreceptivity of stones to microbial colonisation was demonstrated by Guillitte and Dreesen (1995), Silva et al. (1997), Tomaselli et al. (2000b) and Prieto and Silva (2005). As reported, differences in surface roughness, gave by different surface finishings, have a significant effect on the extent or intensity of colonisation; rougher stone surfaces are more bioreceptive than polished surfaces (Prieto and Silva, 2005). Stones with large surface cavities may offer larger surface areas for the anchoring of microbial cells and deep penetration of moisture into the material, providing appropriate microenvironmental conditions for the development of the microorganisms.

This study aimed to assess the primary bioreceptivity of different limestone types largely used in the Mediterranean Basin region, and to study the relationship between their intrinsic properties and the susceptibility to be colonised by phototrophic microorganisms. The research relied on the inoculation of stone samples with the previous cultivated Santa Clara-a-Velha biofilm and incubation under laboratory conditions during 90 days. As mentioned before, this natural community culture composed mainly by cyanobacteria and microalgae was selected because they are pioneer inhabitants of stone substrata, which is emphasised by their photoautotrophic nature. Phototrophic growth was monitored during the time span of incubation by digital image analysis and by comparing the amount of photosynthetic biomass through *in vitro* and *in vivo* chlorophyll *a* (chl*a*) quantification methods.

As the colonisation of stone by phototrophic microorganisms is, to a great extent, associated with the availability of water at the stone surface, petrophysical characterisation was focused on hydric and hygric properties, such as open porosity, water absorption by capillarity and water vapour permeability. Other characteristics such as surface roughness, stone suspension pH and chemical composition of the five lithotypes were also determined. To achieve the aim of this study a multidisciplinary team operated to accomplish the bioreceptivity parameters measurements either for the quantification of photosynthetic biomass or the characterisation of the stone materials.

5.2. Materials and methods

5.2.1. Studied lithotypes

Five types of limestone with different petrographic, petrochemical and petrophysical characteristics were studied to investigate their primary bioreceptivity: *Ançã* limestone (Portugal), *Lioz* limestone (Portugal), *San Cristobal* stone (Spain), *Escúzar* stone (Spain) and *Lecce* stone (Italy) (Fig. 5.1). These lithotypes were selected according to their importance as building materials in the monumental architecture of Mediterranean Basin countries. They were widely used in Romanesque, Gothic, Renaissance, Baroque and Neoclassical monuments, and are still being used in the construction of modern buildings and sculptures.

The stone samples used in the experimental procedure were collected from outcrops located in the vicinities of the sites where, according to archaeological and historical evidence, the original stone blocks were extracted to the construction of the monuments described in chapter three (Table 5.1). The stone blocks were sampled from areas that exhibited similarly weathering patterns (sound material) and able to provide samples of the required dimensions (minimum 50 x 16 x 20 cm). Each stone block was later cut into cylinders with 4.4 cm diameter and 3 cm height using a circular diamond swan. Their surfaces were finished using carborundum 180 (silicium carbide) for finer graining stones, without any other surface finish.

Fig. 5.1. One representative sample of each studied lithotype: CA (*Ançã* limestone), CL (*Lioz* limestone), SC (*San Cristobal* stone), PF (*Escúzar* stone) and PL (*Lecce* stone).

Table 5.1. Quarry, location and monument of the five studied lithotypes.

Quarry	Location	Studied monument	Lithotype
D'El Rei quarry	Portunhos – Catanhede, Coimbra, Portugal	Santa Clara-a-Velha Monastery (Coimbra)	*Ançã* limestone (CA)
Freiplana quarry	Pêro Pinheiro – Armês, Portugal	Ajuda National Palace (Lisbon)	*Lioz* limestone (CL)
El Puerto de Santa Maria quarry	El Puerto de Santa Maria, Cadiz, Spain	Cathedral of Seville	*San Cristobal* stone (SC)
Los Linos quarry	Escúzar, Granada, Spain	Cathedral of Granada	*Escúzar* stone (PF)
Cursi quarry	Lecce, Italy	Orologio Tower (Martano, Lecce)	*Lecce* stone (PL)

***Ançã* limestone** (CA) is a fine-grained compact, homogeneous limestone, with colours ranging from white to grey, with some yellowish variations. Low compressive strength (45.8 MPa) and hardness are significant features of this rock (Dionísio, 1997). This limestone has been extensively used in monuments, buildings and sculptures in the central region of Portugal, such as Santa Cruz Church and Porta Especiosa from Coimbra Old Cathedral, as well as in many parts of Spain, reaching other places in Europe. Since the 14th century, this lithotype has been a natural choice for sculptures, mainly because it is a very soft light-coloured rock, without any veins (Dionísio, 1997). It occurs in a large outcrop area, located in the Beira Litoral region, in Coimbra (central Portugal), and is part of a thick carbonate formation of the Middle Jurassic (Bajocian-Bathonian) period.

***Lioz* limestone** is a beige-rosy microcrystalline limestone (with several varieties) present in many Portuguese emblematic monuments, such as the Jerónimos Monastery and the Tower of Belém, both in Lisbon, as well as in many other monuments and buildings in other parts of Portugal. This ornamental limestone is mainly quarried in the North region of Lisbon (Pêro Pinheiro region), where it widely occurs and where many quarries labour. It is the predominant local stone building material and during the 17th, 18th and 19th centuries, this rock was taken to Brazil for structural and decorative stonework, mainly in Bahia region (Silva, 2007).

From a geological point of view, it is a Middle Turonian (Middle Cretaceous) limestone.

***San Cristobal* stone** (SC) is a yellowish coarse-grained calcarenite of the Upper Miocene widely used in monuments from Seville (Andalusia, Spain), such as the Salvador's Church and Cathedral of Seville, and from Cadiz province (Andalusia, Spain), such as the Cathedral of Jerez. This lithotype is quarried in El Puerto de Santa María (Cadiz), from where a high amount of material was extracted for the construction of the Cathedral of Seville, since its beginning in 1403 and during the following construction phases (16^{th} and 18^{th} centuries). These quarries are still active and, nowadays, represent one of the most important industrial stone factories.

***Escúzar* stone** (PF), also known as *Piedra Franca*, is a light-coloured heterogeneous and coarse-grained biocalcarenite from the Tortonian age. This rock owns its name to the original quarries located in the Escúzar village (Granada, Spain), specifically, in Santa Pudia area. It has been widely used in historic buildings and monuments of Granada (Southern Spain), such as the Cathedral, the Royal Hospital and the Alhambra walls. The historic quarries are inactive but layers dating from the Tortonian age are still quarried in this region.

***Lecce* stone** (PL) is a Miocene (Langhian age) limestone of biological origin, quarried in the Lecce province (Salentine Peninsula, Italy). This dark yellow homogeneous and fine grained limestone was widely used in the Italian Late Baroque. It is present in the Basilica di Santa Croce, the most important baroque monument in the Salento region, as well as in many other temples.

5.2.2. Characterisation of the lithotypes

In order to understand the influence of the selected lithotypes on the growth of phototrophic microorganisms, petrographic, petrophysical and petrochemical properties of each substratum were studied.

5.2.2.1. Petrographic examination

Each stone lithotype was described by naked-eye visualisation and by petrographic microscopy of thin sections (30 µm thick), which allow the identification of their individual mineral constituents, as well as the study of their mutual interrelations (fabric), their morphology and their amounts. Four thin sections of each lithotype were examined under the microscope. This study was performed at Departamento de Ciências da Terra, Faculdade de Ciências e Tecnologia – Universidade Nova de Lisboa (Portugal).

5.2.2.2. Petrophysical characterisation

As the colonisation of a substratum by phototrophic microorganisms and other growths is, to a great extent, associated with the availability of water at the stone surface, particular attention was paid to those properties related to the absorption and movement of water through the stone pore structure. These properties included water absorption by capillarity, open porosity and water vapour permeability. Stone surface roughness was also determined since it has an important role in the attachment and settlement of microbial communities on its surfaces (Scardino et al., 2008), and it is also a major factor controlling the degree of surface wetness, with certain features encouraging entrapment of water.

The procedure of the European Standard EN 1925:1999 (1999) was followed to determine the kinetics and coefficient of water absorption by capillarity. Hence, 27 stone samples of each lithotype were dried to constant mass at 70ºC, desiccated and weighted (m_d). The samples were put on a 1 cm thick filter paper pad soaked in distilled water to a depth of 3±1 mm, maintaining a constant water level throughout the test. In succession, their mass (m_i) were weighted at increasing time intervals of 1 min, 5 min, 10 min, 15 min, 30 min, hourly and daily until reaching a constant weight. A graph, representing the mass of water absorbed (g) divided by the area (m^2) of the contact surface of the stone sample as a function of time (s) was plotted, according to the equation:

$$Q = \frac{m_i - m_d}{A \times \sqrt{t_i}} \quad (1)$$

where: m_d is the dry sample mass (g),

m_i is the sample mass (g) at the time t_i (s),

A is the contact surface area (m^2).

The coefficient of water absorption by capillarity Q ($g.m^{-2}.s^{-1/2}$) was calculated from the slope of the first linear part of the curve corresponding to the water capillary kinetics.

Open porosity (n_0) was quantified following the standard procedure EN 1936:1999 (1999). This parameter was also measured on 27 dried, desiccated and weighted samples of each lithotype. The samples were placed under vacuum (2.0 $\pm$0.7 kPa) for 24 h in order to eliminate air; distilled water was then slowly introduced into the vacuum vessel until the samples were covered. The vacuum was maintained for another 24 h and, after releasing the vacuum, the samples remained submerged in water at atmospheric pressure for 24 h; immediately, their hydrostatic mass were weighted using an hydrostatic balance and the saturated weight was determined after light wiping with a buckskin of the liquid water from the surface of the sample. The open porosity (n_0 %) was calculated according to the following equation:

$$n_0 = \left(\frac{m_s - m_d}{m_s - m_h} \right) \times 100(\%) \quad (2)$$

where: m_d is the dry sample mass (g),

m_s is the saturated sample mass (g),

m_h is the hydrostatic sample mass (g).

The open porosity is therefore the relationship (in percentage) among the volume of the open pores and the apparent volume of the sample.

Water vapour permeability measurements were carried out on three samples of each lithotype with 4.4 cm diameter x 1 cm height according to the wet cup ASTM E96/E96M – 05 (2005) standard method and Normal 21/85. Containers, with a known volume of water, closed by a sample of 1 cm in thickness were used. The containers were subjected to a controlled temperature of 20±2°C in an environment of 40±5% relative humidity inside a climatic chamber (Fitoclima®, Aralab). The containers were weighed at suitable time intervals until the weight stabilised and mass differences were less than 5%. The coefficient of water vapour permeability (k) is determined by the change in mass at the steady state of the system, according to the equation:

$$k = \frac{GT}{A\Delta p 36\times 10^{5}} \quad (3)$$

where: k is the coefficient of water vapour permeability (kg $m^{-1}.s^{-1}.Pa^{-1}$),

G is the flow-rate of water vapour per unit of time ($kg.s^{-1}$),

T is the thickness of the sample (m),

A is the cross-sectional area of the sample perpendicular to the flow direction (m^2),

Δp is the pressure gradient (Pa).

Permeability is used for describing the ability of rocks for transmitting fluids (air or water) through their porous space when they are subjected to a pressure gradient. It is directly related to the porous medium morphology, especially with its tortuosity and connection between pores (Aires-Barros, 2001).

The surface roughness, defined as the measure of the irregularities of a surface, was also measured. Rough surfaces usually wear more quickly and have higher friction coefficients than smooth surfaces. Roughness is often a good predictor of the bioreceptivity, since irregularities in the surface may form anchoring sites and microrefuges for the settlement of biological colonisation. It is quantified by the vertical deviations of a surface from its ideal regular form. If these deviations are large, the surface is rough; if they are small the surface is smooth. In general, surface roughness measurements are made by a stylus profilometry, which consists in an

instrument with a metal stylus (needle) that transverses a line. Although this instrument is developed and widely used for measuring surface roughness of metals, the technique has also been employed on stone (Grissom et al., 2000). However, the morphology of stone is quite different from metal surfaces and thus the stylus cannot measure deep stone pores and pits, which are generally absent from such metal surfaces. For macro-roughness stones the measurements cannot be achieved because the gauge range of the instrument is insufficient. Therefore, surface roughness features of the five lithotypes were measured using an optical surface roughness instrument (TRACEiT®), which was chosen for its great gauge range, simple execution and interesting data obtained. Roughness parameters like R_a (roughness average, µm), the arithmetic mean of the absolute values of the roughness profile ordinates, and R_z (mean roughness depth, µm), the arithmetic mean value of the single roughness depths (the vertical distance between the highest peak and the deepest valley within a sampling length) of five consecutive sampling lengths were evaluated. A standard area of 5 x 5 mm was surveyed for each measurement and four sampling areas of each stone sample were measured. Four stone samples of each lithotype were measured and the results were averaged. This instrument also allowed the establishment of 3D micro-topography of the stone samples, which was calculated with the highest resolution (1528 pixels in x and y direction). The measuring system consists of a sensing head connected to a special, modified notebook, in which storage, evaluation and analysis occur. The measured data are analysed by the TRACEiT® software, which shows the visual impression and the computed 3D topography together with the derived parameters. The 3D topography is documented by the roughness parameters and their standard deviations. The visual impression documents the appearance of the measured surface in gray tones.

5.2.2.3. Petrochemical characterisation

The chemical composition was determined in three replicates of each lithotype at Laboratório de Mineralogia e Petrologia, Instituto Superior Técnico (Portugal), using the following chemical analytical methods: atomic absorption spectrometry for Ca, Mg and Mn; emission spectrometry for Na and K; colorimetric methods for Al, Fe (total) and SiO_2. The loss on ignition (LOI), which includes CO_2, H_2O and OH, was

determined by weighing the powdered samples (1 g) both before and after being heated at 1000ºC for 5 h.

As a parameter influencing biological colonisation, stone suspension pH values were measured using a Eutech Instruments digital pH meter in a suspension (1:5, w/v) of 20 g of sieved powdered stone (grain-size < 2mm) in 100 mL of distilled water, after shaking and allowed to settle (Póvoas and Barral, 1992).

5.2.3. Stone bioreceptivity experiment

Stone primary bioreceptivity of the five selected limestone types was assessed by laboratory-based colonisation experiment as proposed by Guillitte (1995), which relied on the inoculation of stone types with previously isolated and enriched phototrophic microorganisms, incubation under optimal conditions for microbial growth and quantification of photosynthetic biomass.

5.2.3.1. Inoculation and incubation of the stone samples

The stone samples were inoculated with the standardised multiple-species phototrophic culture (Coimbra culture), described and tested in chapter four, which revealed to be an adequate inoculum for the laboratory-based colonisation of lithic substrata. Previously to inoculation, twenty seven replicate stone samples of each lithotype were washed with distilled water and sterilised at 120ºC and 1 atm, for 20 min. After cooling, the upper surface of the stone samples were inoculated with 0.75 mL of the Coimbra culture (chl*a* concentration: 2902 $\mu g.L^{-1}$) and placed in a non-commercial incubation system (with overall dimensions of 100 x 60 x 60 cm) containing 0.5 cm height of sterile water in the bottom of the chamber. Photosynthesis-inducing fluorescent lamp (Fluora, Osram) was installed in the upper part of the chamber to provide 12h dark/light (1200 lux) cycles for the growth of cyanobacteria and algae (Fig. 5.2). The incubation was conducted under constant conditions at 20 ± 2ºC (laboratory temperature) during 90 days. Moisture inside the chamber was kept by water circulation in the chamber bottom, fed by a water pump, favouring condensation. Sterile distilled water was also periodically added to the bottom of the chamber in order to maintain samples soaked with 0.5 cm water height.

The concentration of chl*a* of the inoculum (Coimbra culture) at the inoculation time was measured by extracting chlorophyll in dimethyl-sulfoxide (DMSO) (Shoaf and Lium, 1976) with subsequent determination by spectrophotometry, as described by Burnison (1980). Six samples were filtered in 0.45 µm membrane filters (Supelco, Bellefonte, Pennsylvania, USA) under vacuum (600 mbar) and the filtered volumes were 10 and 20 mL. The filters were placed in centrifuge tubes containing 4 mL DMSO and incubated at 65ºC during 15 min. After cooling, 6 mL of 90% acetone was added, mixed and centrifuged for 10 min at about 5000 rpm. The absorbance of the supernatant was determined at 750 and 664 nm, before and after acidification with 1N HCl. For spectrophotometric analysis the Perkin Elmer Lambda 35 UV/VIS spectrophotometer and a cuvette of 1 cm path length were used. The concentrations of chl*a* and pheophytin (chlorophyll molecule lacking a central Mg^{2+} ion, which is not active in photosynthesis – see appendix one) were determined based on the equations of Lorenzen (1967), using the extinction coefficient of Jeffrey and Humphrey (1975). The extinction coefficient of chl*a* in 90% acetone can be used for the solvent DMSO/acetone 90% (4:6) (Burnison, 1980).

$$\textit{Chla}\ (\mu g.L^{-1}) = \frac{A \times K \times [(664-750)_b - (664-750)_a] \times v}{V \times L} \quad (5)$$

$$\textit{Pheophytin}\ (\mu g.L^{-1}) = \frac{A \times K \times [R(664-750)_a - (664-750)_b] \times v}{V \times L} \quad (6)$$

where: A is the extinction coefficient for chl*a* in 90% acetone at 664 nm (11.0)

K is the factor to equate the reduction in absorbancy to initial chlorophyll concentration (2.43),

$(664-750)_b$ is the difference between the two absorbance values before acidification,

$(664-750)_a$ is the difference between the two absorbance values after acidification,

v is the volume of the solvent used for extraction (mL)

V is the volume of sample filtered (L)

L is the path length of cuvette (cm)

R maximum ratio of 664_b : 664_a in the absence of pheophytin (1.7)

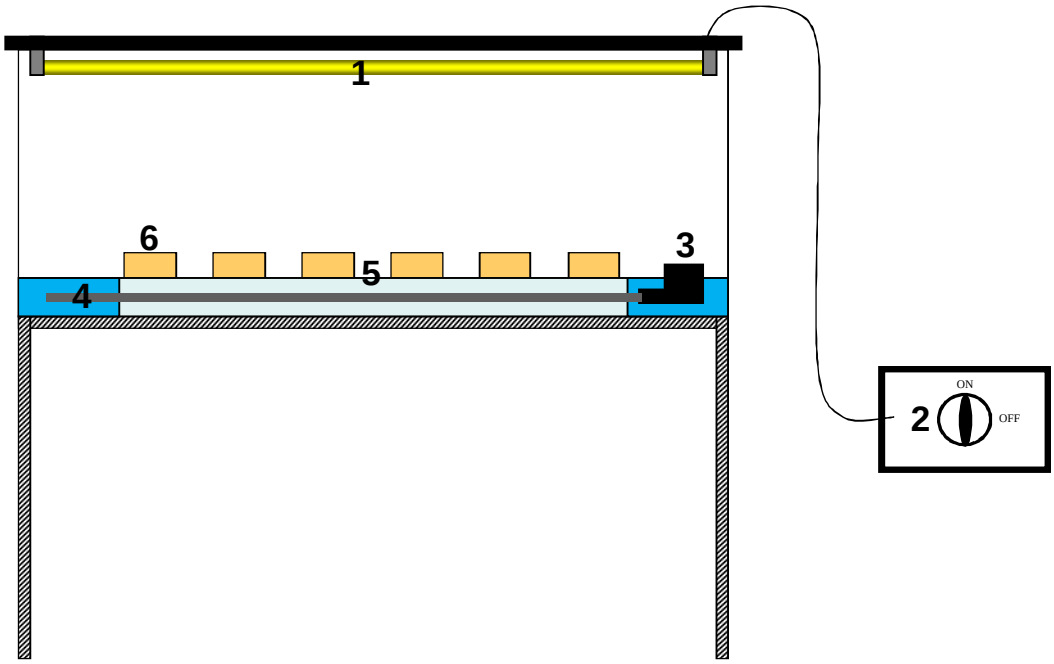

Fig. 5.2. Scheme of the non-commercial incubation system: 1 – fluorescent lamp; 2 – Control unit; 3 – water pump; 4 – Silicon tubing for water circulation; 5 – Plastic grid; 6 – Stone samples.

5.2.3.2. Monitoring of photosynthetic biomass during the incubation period

For the quantification of photosynthetic biomass on the inoculated limestone samples during 90 days of incubation, *in vitro* and *in vivo* chl*a* quantification methods were applied and compared. Chl*a* is a photosynthetic pigment present in all photoautotrophic microorganisms, including cyanobacteria and microalgae, used to estimate the amount of photosynthetic biomass present in liquid media, in soil and also on rock substrata. Moreover, the concentration of chl*a* is one of the most used forms for the determination of photosynthetic biomass, since it permits faster quantifications of biomass than microscopy methods. Therefore it is a useful tool in scientific studies and monitoring programs.

In vitro chlorophyll a quantification technique

Stone samples of each lithotype were taken out of the incubator system in triplicate after 30, 60 and 90 days of incubation in order to determine the amount of chlorophyll *a* by the *in vitro* technique, which is based on its extraction from

disintegrated cells and subsequent spectrophotometric measurements. The extraction of chl*a* from each stone sample was performed according to the pigment extraction protocol for periphyton from Vollenweider et al. (1974). Each stone sample was crushed into fragments (0.20-0.50 cm^3), which were added to 50 mL of DMSO and heated at 65ºC for 1 h. The samples were filtered to remove stone particles and absorbances of the extracts were measured at 664 and 750 nm before and after acidification with 1N HCl, in a Perkin Elmer Lambda 35 UV/Vis spectrophotometer. The Lorenzen (1967) equations were used to calculate chl*a* and pheophytin concentrations, using the extinction coefficient from Talling and Driver (1963), as follows:

$$Chla\ (\mu g.cm^{-3}) = \frac{A \times K \times [(664-750)_b - (664-750)_a] \times v}{a \times L} \quad (7)$$

$$Pheophytin\ (\mu g.cm^{-3}) = \frac{A \times K \times [R(664-750)_a - (664-750)_b] \times v}{a \times L} \quad (8)$$

where: A is the extinction coefficient for chl*a* in 90% acetone at 664 nm (11.9)

K is the factor to equate the reduction in absorbancy to initial chl*a* concentration (2.43),

$(664-750)_b$ is the difference between the two absorbance values before acidification,

$(664-750)_a$ is the difference between the two absorbance values after acidification,

v is the volume of the solvent used for extraction (mL)

a is the stone sample volume (cylinder volume = 30.4 cm^3)

L is the path length of cuvette (cm)

R maximum ratio of 664_b : 664_a in the absence of pheophytin (1.7)

In vivo chlorophyll a fluorescence technique

The growth of phototrophic microorganisms on the stone samples was also assessed by the *in vivo* chl*a* fluorescence method. This is a non-destructive, very fast, safe and easy method to apply for the estimation of phototrophic biofilms dwelling on solid substrata, without the extraction of chl*a* from disintegrated cells. Fluorescence properties of some compounds, such as the natural fluorescence of chl*a*, are detected with a spectrofluorometer, providing their intensity of fluorescence in counts per second (cps) which give information of their concentration in a sample. A certain excitation wavelength is selected, and a scan is performed to record the intensity versus wavelength, called an emission spectra. Stone samples of each lithotype were taken out of the chamber in triplicate at the inoculation time and after each 30 days of incubation (0, 30, 60 and 90 days). Emission spectra were determined using a spectrofluorometer SPEX Fluorolog-3 FL3-22 fitted with a fibre-optic platform (Horiba Jobin Yvon F-3000) (Fig. 5.3). For each stone sample five spectrofluorometric measurements were randomly carried out on the surface of the stone samples covered by the biofilm. The fibre-optic end-piece was held steady facing the sample surface at a distance of 2 mm. Measurements were performed with an excitation wavelength of 430 nm (optimum for chl*a* molecules, APHA/AWWA/WEF, 1992), slits of 4.5 nm, an integration time of 0.3 s and an increment of 1.0 nm.

Fig. 5.3. Spectrofluorometer (SPEX Fluorolog-3 FL3-22) fitted with a fibre-optic platform (Horiba Jobin Yvon F-3000) from Departamento de Química, Faculdade de Ciências e Tecnologia, Universidade Nova de Lisboa (Portugal).

Digital image analysis

Digital image analysis was also applied to quantify the photosynthetic biomass present on the stone samples during the incubation time by determining the stone surface areas covered by the biofilms. Three replicates of each lithotype were taken out of the incubator chamber after 0, 45 and 90 days of incubation and placed on paper towels to allow excess water to drain out. Subsequently, the samples were placed on millimetric paper under controlled light to ensure fixed conditions for all photographic records. The photographic recording was performed with a digital camera (Kodak EasyShare P850); the generated RGB digital images were transferred and processed on a PC in order to digitally rectify the geometry of the photographs with Adobe Photoshop© software. The results of these geometric corrections is a multi-layer file in .psd format, in which each layer correspond to one of the incubation stage recorded (Fig. 5.4).

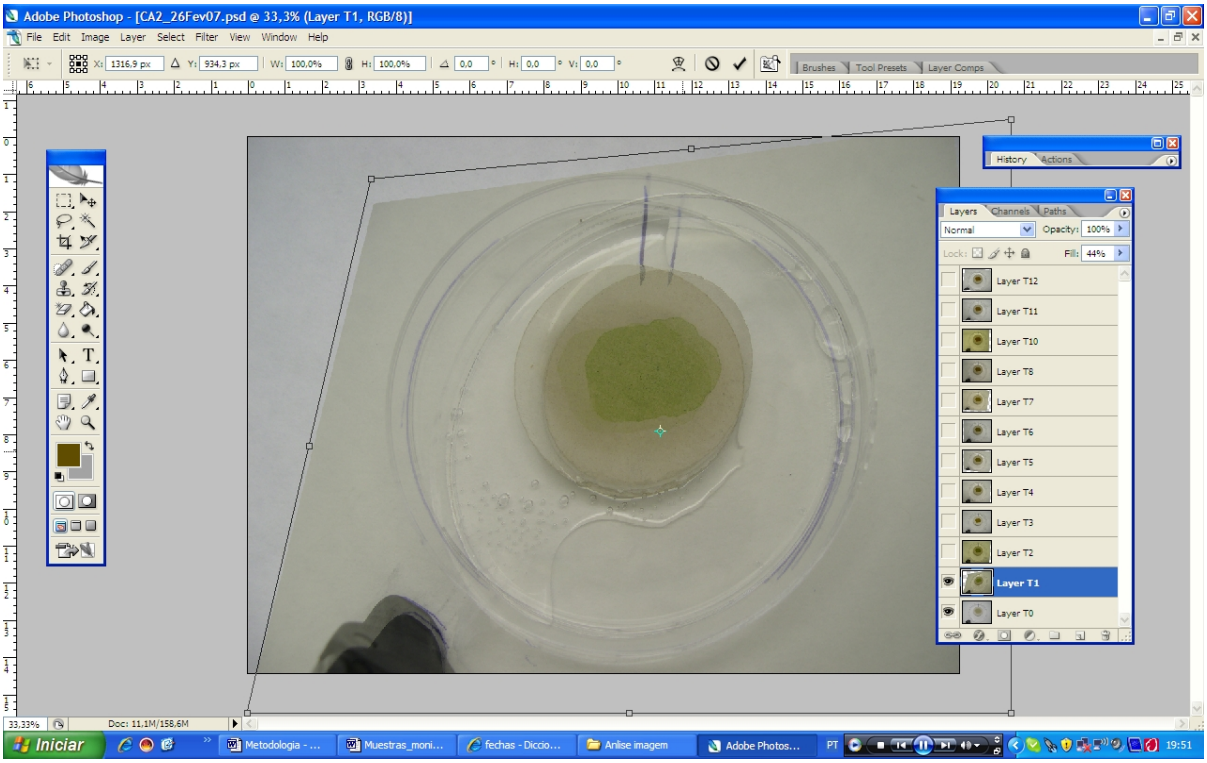

Fig. 5.4. Multi-layer file of Ançã limestone samples (CA), elaborated by Adobe Photoshop© software. Adapted from Gomes (2008).

Since the colour and texture of some lithotypes masked the possible biofilm growth, geometry rectified RGB images were decorrelated by Principal Component Analysis (PCA), using the HyperCube v. 9.5 software (*US Army Topographic Engineering Centre*, Alexandria, Virginia, USA). This approach allows the detection of minority elements (of different nature and composition) apparently absent in the RGB digital image but masked by the redundant data registered in the Red, Green and Blue bands of the image (PC1, PC2 and PC3 bands, respectively). This decorrelation allowed choosing the most appropriate PCA band (PC1, PC2 or PC3) which improved the visualisation of the photosynthetic biomass present on the stone surfaces. A thresholding algorithm was then applied in order to select the colonised areas, afterwards scaled and converted into binary. The detected particles within the selected area were measured using ImageJ software (*National Institutes of Health*, Bethesda, Maryland, USA) following the protocol developed in Rogerio-Candelera et al. (2008b). The obtained photographic series, geometrically coherent and comparable, allowed obtaining a series of numerical values related to biofilm extent.

5.2.4. Post-experiment observations of phototrophic colonisation

In order to characterise the development and distribution of phototrophic colonisation on and within the stone samples after the 90 days of experiment, two different examinations methods were used.

5.2.4.1. Digital image analysis

Sections perpendicular to the inoculated stone surfaces were examined under a binocular stereo microscope (Zeiss Discover V8 with phototube) and photographically recorded with a digital camera (Canon Powershot A630). The generated RGB digital images were transferred and processed on a PC in order to understand the distribution and penetration of photosynthetic biomass in the stone substrata. PCA approach was also applied to simplify the RGB images avoiding redundant data present in the different bands of the image (Red, Green and Blue bands). This approach was performed using HyperCube v.9.5 software (*US Army Topographic Engineering Centre*, Alexandria, Virginia, USA). PC1 (Red band), plotting more than 95% of the total information included in the three bands of each

image, was used as background in order to appreciate the microtopography of the sample. Green and Blue bands (PC2 and PC3) were used when appropriate to distinguish the lesser amounts of information included in the images, but relevant for the objectives of the work. Thus, compositions were elaborated following the scheme PC1, PC2, PC3, but also PC1, PC3, PC3.

For a better visualisation, false-colour images were composed from the PCA bands, based on those reflecting minority information (PC2 and PC3), as human eye can distinguish better colour differences than grey tones. These false-colour images were also elaborated using the HyperCube 9.5 software.

5.2.4.2. Scanning Electron microscopy analyses

Scanning electron microscopy analyses were also applied in order to assess penetration depth of photosynthetic microorganisms inside the stone samples and to estimate potential physical damage in the stones after 90 days of incubation. Fragments of each lithotype were cut perpendicularly to the colonised surfaces and coated with a high conductance thin layer (gold film). Subsequently, the samples were studied under a Scanning Electron Microscope (SEM), Zeiss DSM 962, with a Secondary Electrons detector (SE) and a Back Scattered Electrons detector (BSE), at Centro de Investigação dos Materiais (CENIMAT), Universidade Nova de Lisboa (Portugal).

5.2.5. Statistical analysis

In order to correlate the intrinsic stone properties that influence their bioreceptivity to phototrophic microorganisms, and to estimate the efficacy of both chl*a* quantification methods, the experimental data were subject to analysis of variance (ANOVA) using Statistica 7.0 software for Windows, and the averages were compared by the Tukey HDS Test at the 5% level of significance.

A principal component analysis (PCA) was also performed in order to establish the structure of the variable dependence. This involves identifying relationships between variables and in assigning a petrophysical/photosynthetic biomass meaning to each factor.

5.3. Results

5.3.1. Limestone characteristics

5.3.1.1. Petrographic characteristics

From an aesthetic point of view, all the studied lithotypes are light-coloured rocks varying from white to yellowish with homogeneous appearance, with exception of *Lioz* limestone that exhibits a heterogeneous texture mainly conditioned by the presence of fossil debris (Fig. 5.5). The most prominent macroscopic characteristic of the studied lithotypes is their particle size distribution, particularly heterogeneous for *San Cristobal* and *Escúzar* stones which present large-scale grains and pores visible to the naked-eye. Furthermore, the *San Cristobal* stone grains appear to be less cemented than those of the *Escúzar* stone (Fig. 5.5).

The petrographic study of thin sections of the five lithotypes revealed that they are almost exclusively composed by carbonate material, except *San Cristobal* stone, which has significant contributions of other materials, mainly quartz grains. The petrographic characteristics of the studied lithotypes are presented below:

***Ançã* limestone** (CA) is a white-light yellow, homogeneous, fine-grained and oolitic tendency limestone. It is composed by a micrite matrix, in which abundant bioclasts (formed by fibrous calcite) are present in less than 100 µm long, and containing very little spathised micritic cement (Fig. 5.6). The mineralogical composition is predominately calcitic with small quantities of quartz. The porosity visible under the petrographic microscope is scarce and the dimension of the pores is lower than 40 µm.

***Lioz* limestone** (CL) is a microcrystalline very fine-grained carbonate rock almost exclusively composed by sparite carbonate. The colour is generally whitish, although a pinkish hue is not uncommon. Its microstructure is very compact and no porosity can be detected under the petrographic microscope (Fig. 5.7). It has a heterogeneous texture, mainly conditioned by the presence of fossil debris, most of them of rudists. In some areas, strongly recrystallised bioclasts are observed (Fig. 5.7).

***San Cristobal* stone** (SC), in hand-specimen, can be described as a yellowish quartz-bearing fossiliferous limestone, with a bioclastic character. This lithotype exhibits an inequigranular heterogeneous texture, with very scarce matrix and low cementation level, causing a fair development of intergranular porosity. Pitting is observed on the stone surface, which can, in turn, enhance granular disaggregation processes. As thin sections examined under petrographic microscope, SC is a medium-grained (about 1 mm, attaining 2 mm) rock, mainly composed by micrite carbonate clasts, and less than 50% quartz clasts, involved by a micritic carbonate matrix (Fig. 5.8). Most of the carbonate clasts are of biological origin, featuring as microfossils. The quartz grains exhibit subeuedral (sometimes rounded) forms. In many places, the micrite carbonate matrix has turned into sparite, sometimes with white mica development associated with the micrite to sparite transformation process. Also the micrite carbonate clasts have been recrystalised to sparite, mainly in the inner parts of the fossilised organisms, thus revealing their internal structure. According to its grain size, this rock is recognised as a biogenic calcarenite (Grabau, 1904, 1913).

***Escúzar* stone** (PF) can be described as a whitish colour fine-to-medium grained biocalcarenite, in which only carbonate materials seem to be present. It is a biomicritic carbonate rock, almost completely composed by bioclasts up to 500 µm long. Some of the bioclasts micrite have been transformed into sparite, apparently because they probably have a different geological origin. Although the rock has almost no matrix, which is a well crystallised sparite, there are plenty of open spaces between the bioclasts, apparently reflecting the existence of a former matrix that probably has been dissolved. Sometimes empty spaces can be observed inside the bioclasts (Fig. 5.9).

***Lecce* stone** (PL) is a “honey” coloured, homogeneous, highly porous, fine grained limestone. It is almost exclusively composed by sparite bioclasts, in general less than 100 µm long, included in a very fine micrite matrix (Fig. 5.10). The scarce cementation allows a high porosity to exist, mainly present as 1 to 10 µm long cavities. It is soft and easy to cut and that can be carved with a “penknife”.

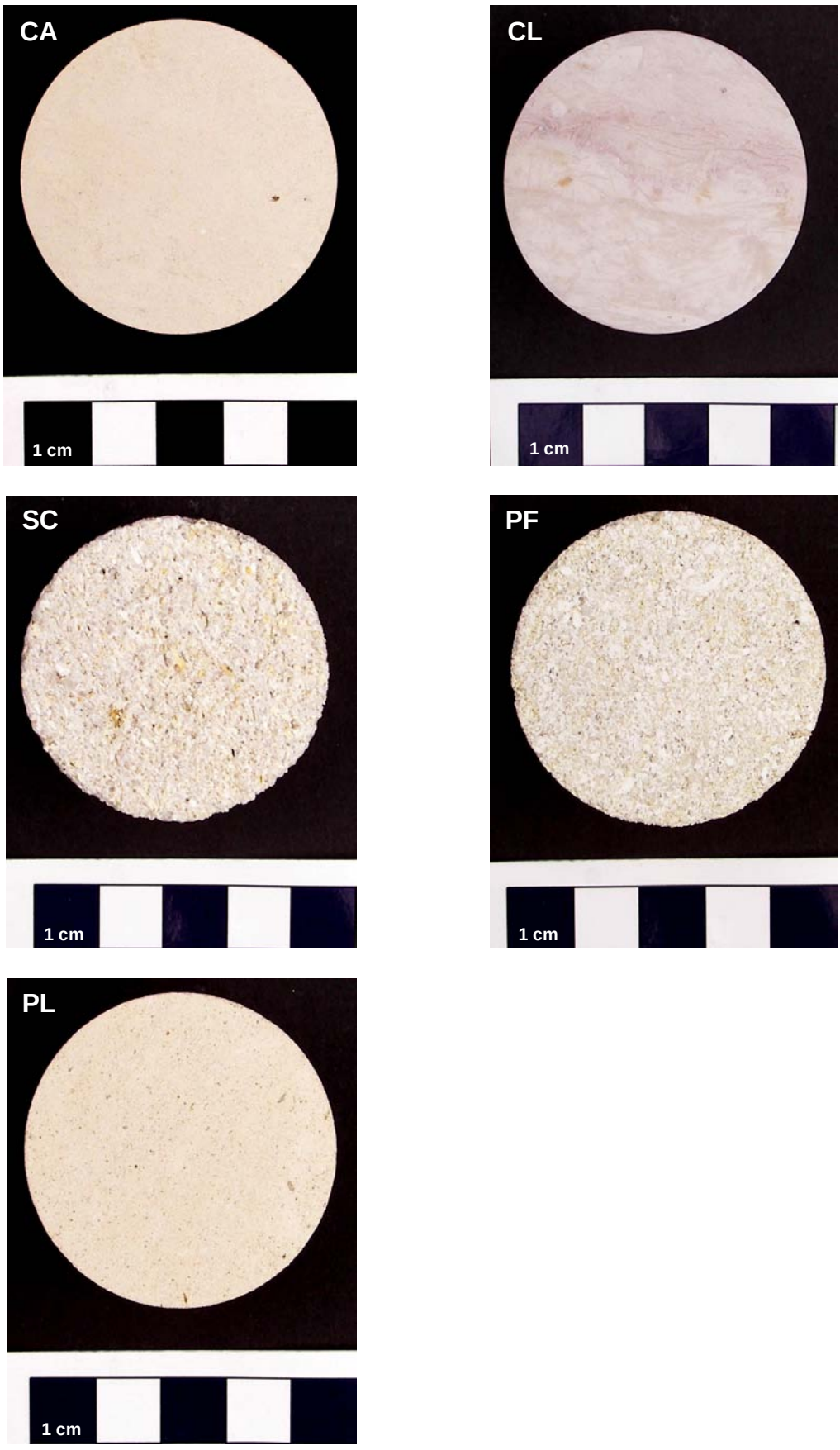

Fig. 5.5. One representative sample of each lithotype (CA – *Ançã* limestone, CL – *Lioz* limestone, SC – *San Cristobal* stone, PF – *Escúzar* stone, and PL – *Lecce* stone) selected for the stone bioreceptivity experiment.

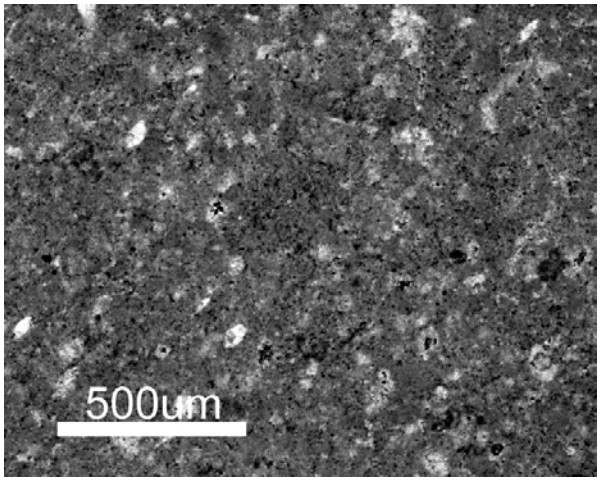

Fig. 5.6. Photomicrograph of a thin section of CA lithotype (crossed polars).

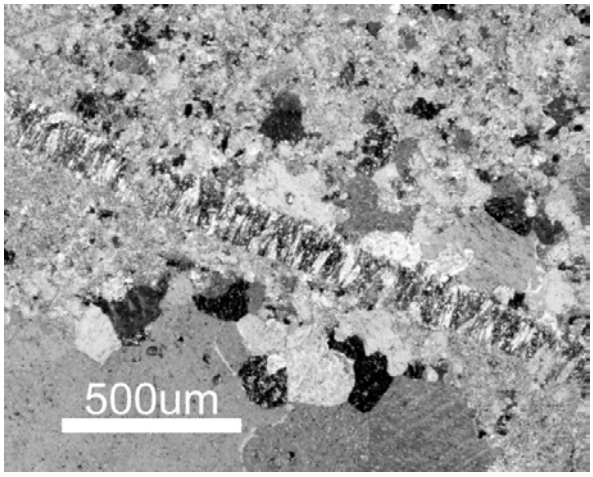

Fig. 5.7. Photomicrograph of a thin section of CL lithotype (crossed polars).

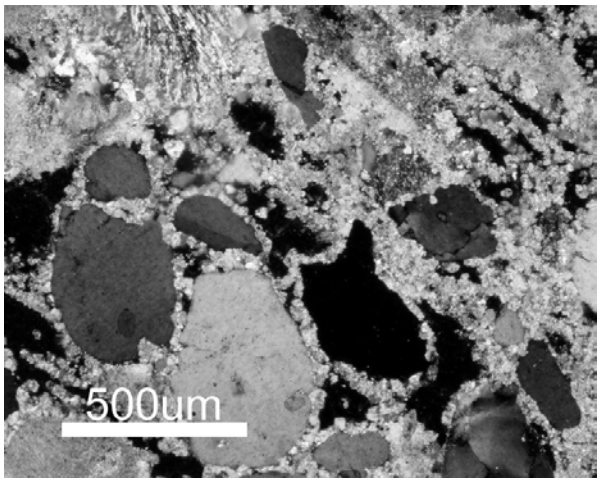

Fig. 5.8. Photomicrograph of a thin section of SC lithotype (crossed polars).

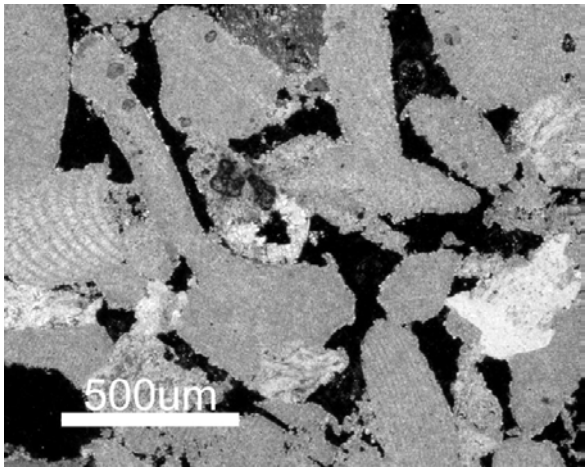

Fig. 5.9. Photomicrograph of a thin section of PF lithotype (crossed polars).

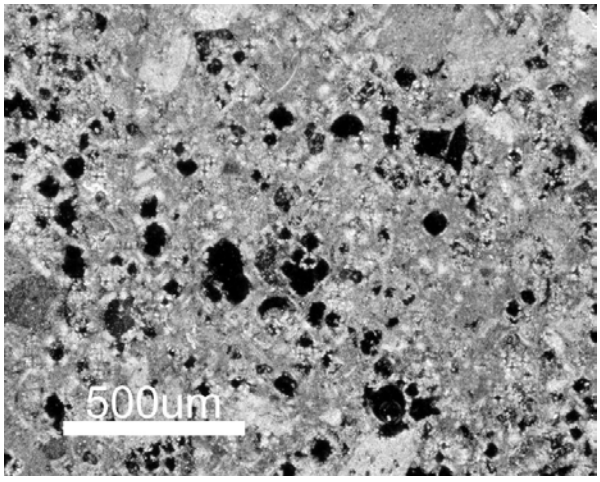

Fig. 5.10. Photomicrograph of a thin section of PL lithotype (crossed polars).

5.3.1.2. Petrophysical characteristics

The porosity accessible to water (open porosity) attained for the five assayed lithotypes showed a great array of values, ranging from about 0.5% to 43% (Fig. 5.11). PL is the most prominent lithotype, with 43% of open porosity, followed by PF, SC and CA, with 33%, 28% and 19%, respectively. The lowest open porosity value is observed for CL lithotype, with only 0.5%.

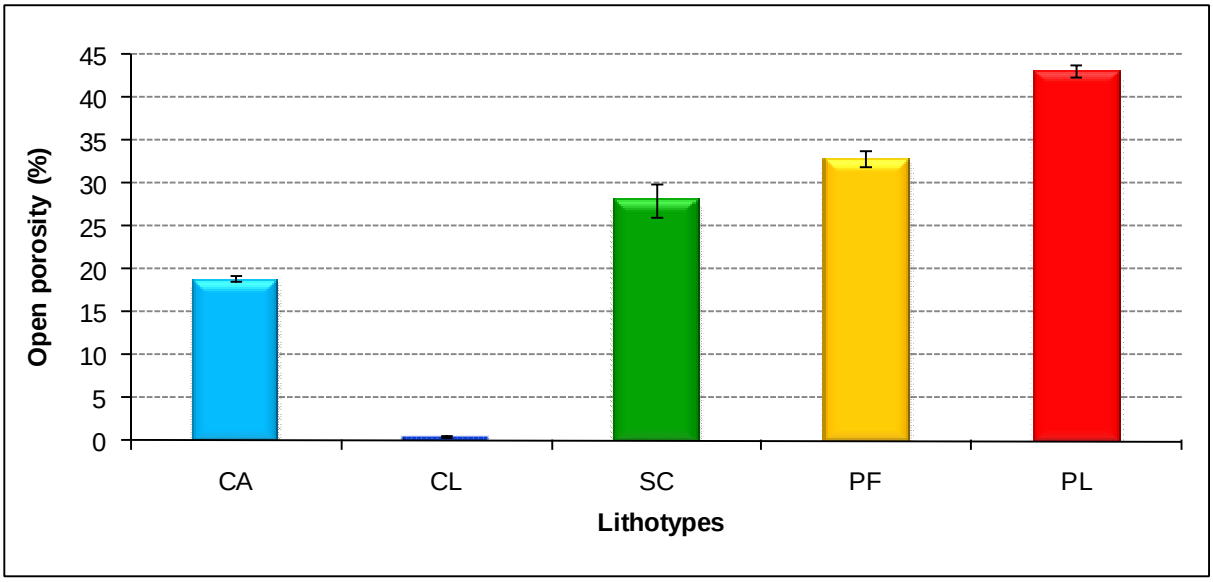

Fig. 5.11. Open porosity of the studied lithotypes: CA (*Ançã* limestone), CL (*Lioz* limestone), SC (*San Cristobal* stone), PF (*Escúzar* stone) and PL (*Lecce* stone). The values correspond to average ± SD for 27 samples of each lithotype.

Concerning the absorption of water by capillarity, a similar pattern was obtained. All lithotypes absorbed large quantities of water by capillarity suction and took up water more rapidly than CL (Fig. 5.12). The latter was found to absorb very low quantity of water, a characteristic typical of highly compact crystalline rocks. The kinetics of capillary water uptake present regular curves, obtained from capillary penetration that correspond to the filling of a unimodal and regular porous network. When the capillary suction phenomenon starts, the water suction rate is in general constant for all lithotypes. This lineal behaviour ends with a sharp change in suction rate. This evolution is clearly shown in Figure 5.12 for all lithotypes. However, their different hydric behaviour is clearly illustrated for their capillarity rates and in Table

5.2 for their capillarity water absorption coefficients. CL depicted the lowest uptake of water, showing that almost no water was absorbed by capillarity (Fig. 5.12, inset). CA and SC showed similar maximum water uptake by capillarity, but different kinetics: SC absorbed water by capillarity more rapidly than CA. The highest capillarity coefficient was observed for PF (269 $g.m^{-2}.s^{-1/2}$), closely followed by SC (199 $g.m^{-2}.s^{-1/2}$) and PL (129 $g.m^{-2}.s^{-1/2}$). CA showed a lower value of 57 $g.m^{-2}.s^{-1/2}$ (Table 5.2).

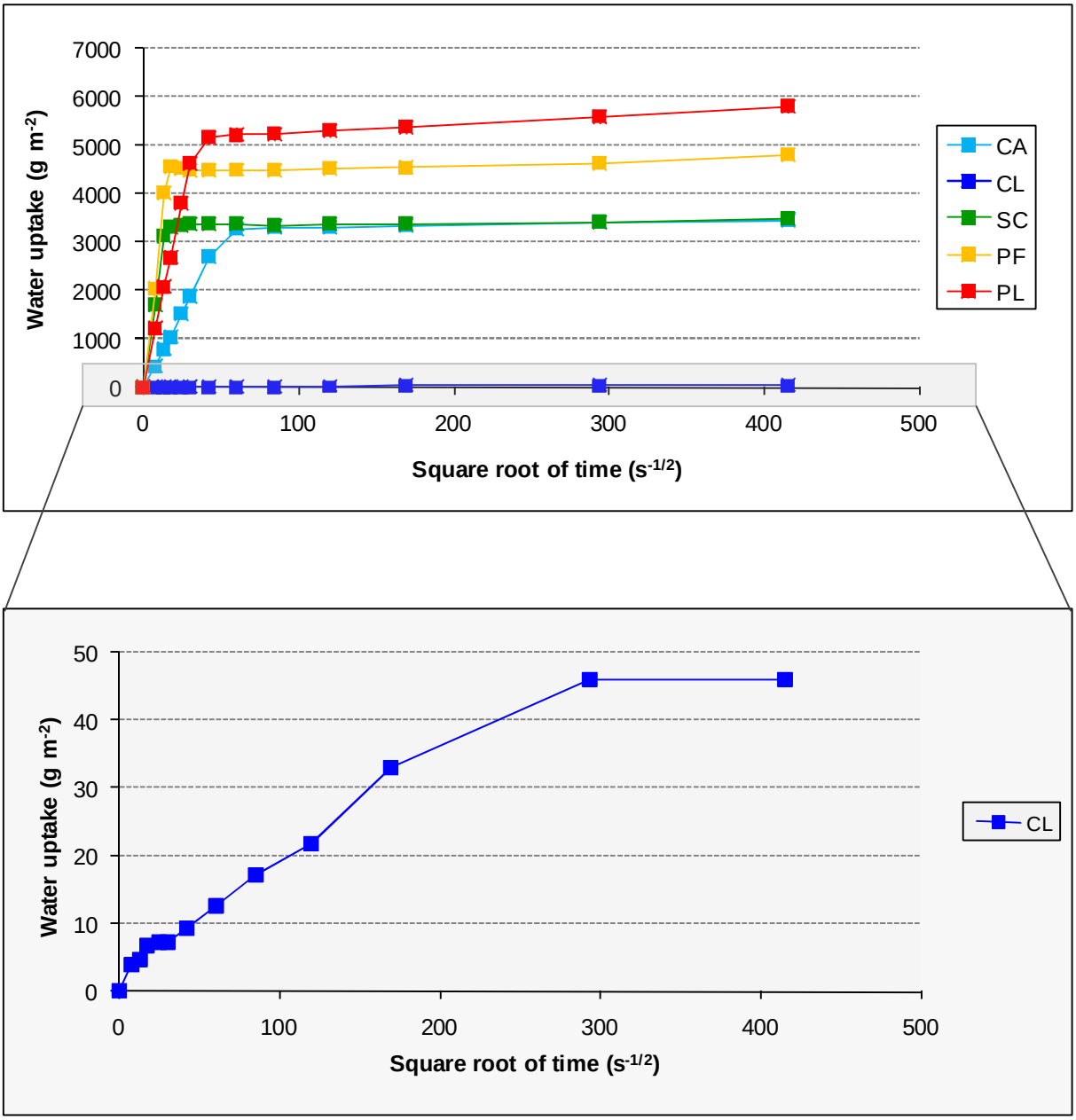

Fig. 5.12. Representative kinetics of water absorption by capillarity of the studied lithotypes: CA (*Ançã* limestone), CL (*Lioz* limestone) with enlarged inset, SC (*San Cristobal* stone), PF (*Escúzar* stone) and PL (*Lecce* stone).

In what concerns water vapour permeability, the values varied for the five limestone types. PL and PF exhibited the highest permeability values, followed by CA and SC, contrasting with the very low value of CL (Table 5.2). These values are indicative of a relative high ability of these lithotypes to fluids circulation on its porous media. It is important to denote that lowest mean values for water vapour permeability, open porosity and capillarity coefficient were recorded for CL (Table 5.2). Furthermore, the lowest stone surface roughness was also obtained for this limestone. The stone surface roughness measurements revealed that the studied lithotypes included either stones with very low surface roughness, namely CL and CA, or with considerable roughness values, i.e. SC and PF lithotypes. The roughness parameters resulting from the evaluation of the surface topographies are presented in Table 5.2. R_z values were approximately 3.7 – 5.30 times higher than R_a values. The relatively high standard deviations of SC and PF are not surprising for very heterogeneous materials like these stone types. The visual impression and 3D representation of the stone surfaces allowed the visualisation of its irregularities, as shown in Figures 5.13-5.17. It was clear that the roughest limestone was SC (Fig. 5.15), depicting macro-roughness. Widely spaced irregularities of texture were also observed on the samples of PF (Fig. 5.16). Both lithotypes presented very grany surfaces and consequently very high roughness values. CL and CA showed small-scale heterogeneity of the surface, and thus can be defined as smooth limestones. The small particle size in PL renders it smooth to the touch, but the porosity of this lithotype samples produced an elevated roughness (both R_a and R_z values).

Petrophysical characteristics of the various lithotypes are summarised in Table 5.2 together with the analysis of variance (ANOVA, $p<0.05$). ANOVA revealed that the studied lithotypes are significantly different ($p<0.05$) in terms of open porosity and capillarity coefficient, differentiating five homogeneous groups. In what concerns water vapour permeability, significant differences were obtained among samples of the Portuguese lithotypes (CA and CL) and among samples of the Spanish lithotypes (SC and PF), obtaining two homogeneous groups. CL is significantly different between all lithotypes, forming the third group. ANOVA results obtained for the surface roughness parameter were the same for R_a and R_z, showing internal variance among replicates of CA and CL ($p>0.05$), among SC and PF and between these and PL. Therefore, only two homogeneous groups were obtained for the surface roughness (Table 5.2).

Table 5.2. Major physical and chemical characteristics of the five lithotypes, together with the ANOVA results of open porosity (n = 27), capillarity water absorption coefficient (n = 27), water vapour permeability (n = 3), surface roughness (R_a and R_z) (n = 3 for each parameter) and stone suspension pH (n = 3).

Lithotype	Open porosity (%)	Capillarity coefficient ($g.m^{-2}.s^{-1/2}$)	Water vapour permeability ($kg.m^{-1}.s^{-1}.Pa$)	R_a (µm)	R_z (µm)	Stone suspension pH
CA	18.95 ± 0.27 a	57.25 ± 1.17 a	$7.04x10^{-12}$ ± 3.53 $x10^{-13}$ a	1.61 ± 0.40 a	8.52 ± 1.90 a	8.52± 0.04 a
CL	0.53 ± 0.06 b	0.20 ± 0.06 b	8.18 $x10^{-13}$± 1.95 $x10^{-13}$ b	1.59 ± 0.42 a	7.99 ± 1.92 a	8.61± 0.02 bc
SC	28.07 ± 1.88 c	199.30 ± 31.05 c	4.54 $x10^{-12}$ ± 2.12 $x10^{-12}$ a	8.16± 2.16 b	30.56 ± 10.56 b	8.67± 0.03 b
PF	32.92 ± 0.97 d	268.79 ± 77.54 d	1.08 $x10^{-11}$ ± 9.51 $x10^{-13}$ c	5.98± 1.28 b	24.99 ± 5.07 b	8.57± 0.02 ac
PL	43.24 ± 0.68 e	128.76 ± 3.04 e	1.09 $x10^{-11}$ ± 5.19 $x10^{-13}$ c	6.14± 0.63 b	27.67 ± 2.64 b	8.41± 0.03 d

The values correspond to average ± SD. Values followed by the same letters in a column are not significantly different by the Tukey HDS test at $p<0.05$.

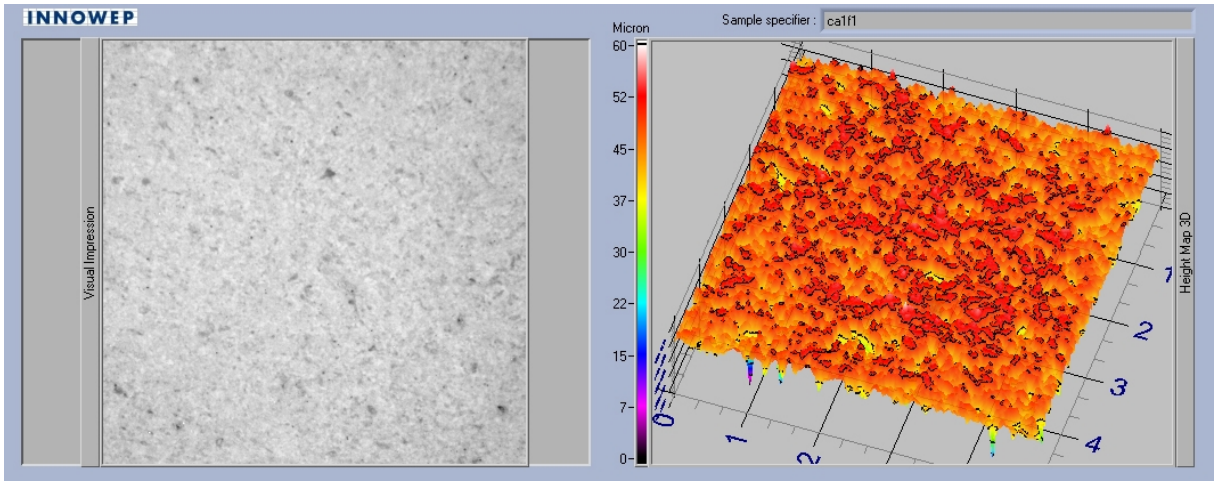

Fig. 5.13. Visual impression (left image) and computed 3D surface topography (right image) of one representative measured area of *Ançã* limestone (CA).

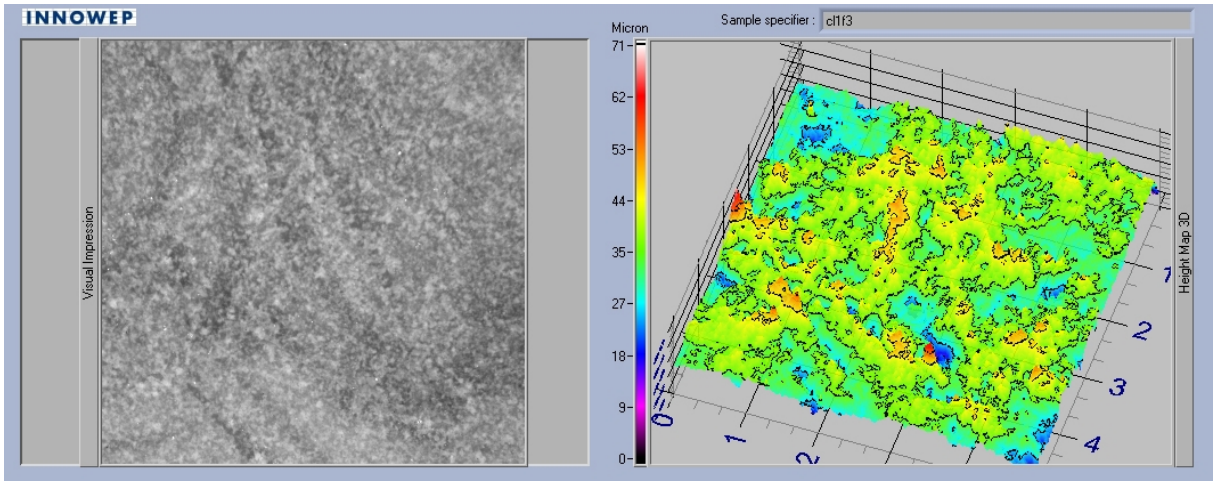

Fig. 5.14. Visual impression (left image) and computed 3D surface topography (right image) of one representative measured area of *Lioz* limestone (CL).

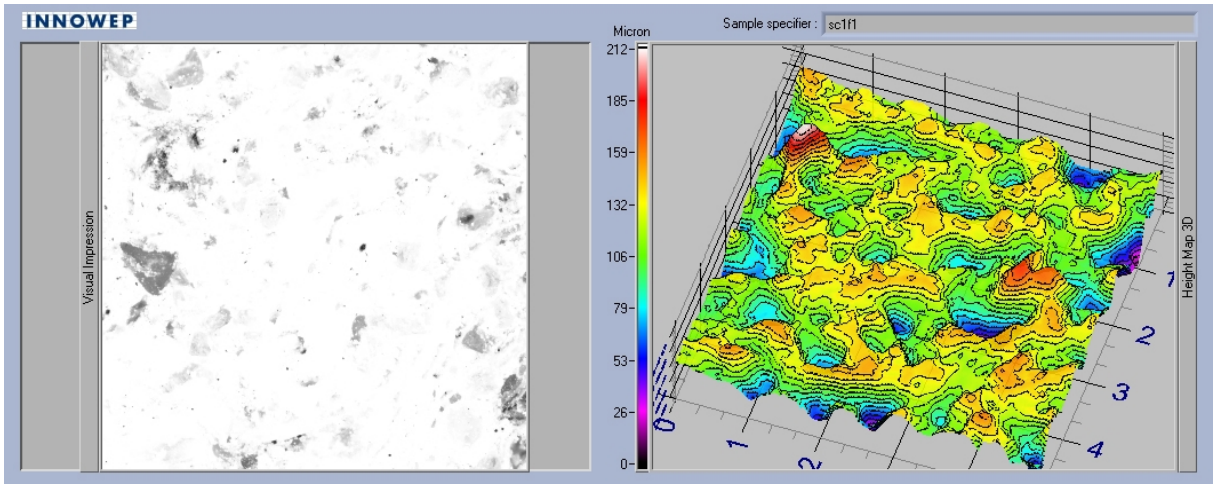

Fig. 5.15. Visual impression (left image) and computed 3D surface topography (right image) of one representative measured area of *San Cristobal* stone (SC).

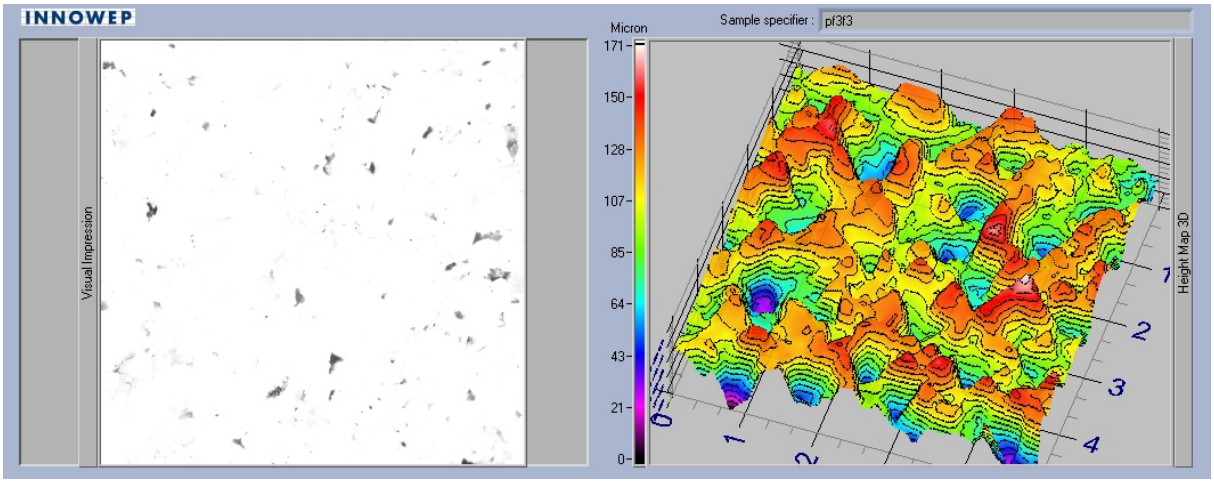

Fig. 5.16. Visual impression (left image) and computed 3D surface topography (right image) of one representative measured area of *Escúzar* stone (PF).

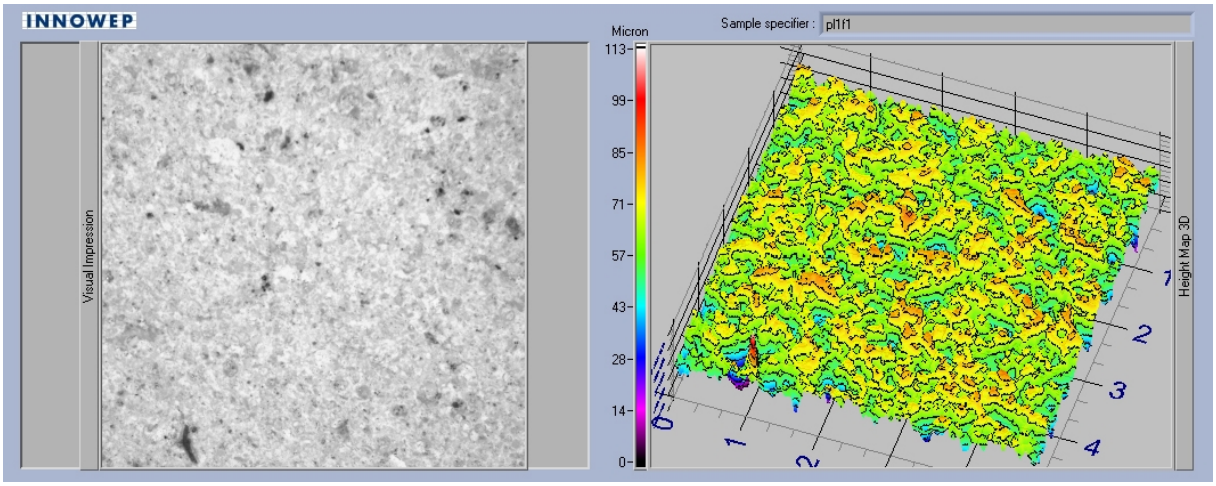

Fig. 5.17. Visual impression (left image) and computed 3D surface topography (right image) of one representative measured area of *Lecce* stone (PL).

5.3.1.3. Petrochemical characteristics

The chemical composition of the five lithotypes is strictly related to the mineralogical composition of each type of stone. The data of the main chemical composition of the studied stone materials are presented in Table 5.3. They are calcitic carbonates with CaO and CO_2 concentrations varying between 95.5% and 96.8% for CA, CL, SC and PF, and 58.3% for SC. The latter presented the highest concentration of SiO_2 (38.45%), confirming the presence of quartz clasts as observed under petrographic microscope. The lowest concentrations of Na_2O (0.12%) and K_2O (0.05%) were also displayed by this lithotype. In PF and PL lithotypes very low

contents of SiO_2 were obtained (1.19% and 0.33%, respectively). PL exhibited the highest content of Al_2O_3, which is related with the presence of clay minerals. On the basis of Ca/Mg (weight) ratios suggested by Chilingar et al. (1967), the studied lithotypes are classified as calcitic limestones since the Ca/Mg ratio is higher than 105 (Table 5.3).

Table 5.3. Chemical analysis in weight percent of the five lithotypes. Values are average ± SD (n = 3).

Constituent	Lithotypes				
	CA	**CL**	**SC**	**PF**	**PL**
SiO_2	3.11 ± 0.21	2.15 ± 0.11	38.45 ± 1.08	1.19 ± 0.08	0.33 ± 0.08
Al_2O_3	0.41 ± 0.01	0.12 ± 0.00	0.20 ± 0.00	0.252 ± 0.00	0.79 ± 0.01
Fe_2O_3	0.13 ± 0.03	0.11 ± 0.02	0.41 ± 0.02	0.16 ± 0.00	0.28 ± 0.01
MgO	0.40 ± 0.00	0.25 ± 0.00	0.10 ± 0.00	0.32 ± 0.00	0.45 ± 0.01
CaO	53.47 ± 0.57	53.67 ± 1.02	33.72 ± 0.66	53.39 ± 1.89	55.23 ± 1.07
Na_2O	0.15 ± 0.04	0.15 ± 0.05	0.12 ± 0.05	0.29 ± 0.08	0.29 ± 0.03
K_2O	0.13 ± 0.13	0.22 ± 0.13	0.05 ± 0.00	0.08 ± 0.05	0.13 ± 0.05
MnO	0.00 ± 0.00	0.00 ± 0.00	0.01 ± 0.00	0.02 ± 0.00	0.00 ± 0.00
LOI*	42.06 ± 0.14	42.90 ± 0.31	24.59 ± 0.93	42.89 ± 0.08	41.55 ± 0.20
Ca/Mg	158.35 ± 1.70	251.78 ± 3.22	412.23 ± 33.85	201.96 ± 10.74	146.51 ± 4.75

*LOI, loss on ignition

Concerning the stone suspension pH, the measured values did not vary greatly among the assayed stones, revealing that all lithotypes are alkaline. The analysis of variance (ANOVA) showed a significant difference ($p<0.05$) for PL lithotype (Table 5.2), forming one homogeneous group; the samples of CA, PF, CL and SC were not significantly different, allowing the differentiation of only two homogeneous groups for the stone suspension pH parameter (Table 5.2).

5.3.2. Stone bioreceptivity experiment

The laboratory-based colonisation of the five limestone types led to the increasing of photosynthetic biomass with different behaviours, distributions and degree of extension over the surface of the stone samples. During inoculation with the multiple-species phototrophic culture, the absorption of the inoculum occurred by distinct ways in the five lithotypes, accordingly to their petrophysical properties. On CL, the liquid culture absorption and penetration was almost inexistent due to its very low open porosity, capillarity water absorption coefficient and water vapour permeability values. When the liquid culture was inoculated on the CA and PL surfaces, a rapid absorption took place, which was enhanced by their high open porosities, combined with high capillarity water absorption coefficient and water vapour permeability. Due to the presence of larger pores, a faster process occurred for SC and PF lithotypes. This inoculum absorption behaviour observed for each lithotype influenced the distribution pattern of the biofilms on the stone surfaces. Figure 5.18 depicts one representative sample of each lithotype at the inoculation time, 30, 60 and 90 days of incubation under the laboratory chamber. After 30 days of exposure, the colonisation process led to the increase of green biofilms on the sample surfaces, clearly visible on the CA and PL lithotypes. In the case of CL, a greenish-brownish colour was observed, suggesting an apparent cessation of colonisation. For SC and PF a very slight green colour was barely observed due to the texture of these lithotypes. After 60 days of incubation, all lithotype surfaces were covered by brownish-greenish biofilms, remaining until the end of the experiment. However, despite of the biofilms brownish colour the surface covered area of PF samples seemed to increase. Furthermore, it was noticed that the lateral surfaces of SC and PF samples showed light green colour appearance, particularly evidenced on the samples of PF lithotype (Fig. 5.19).

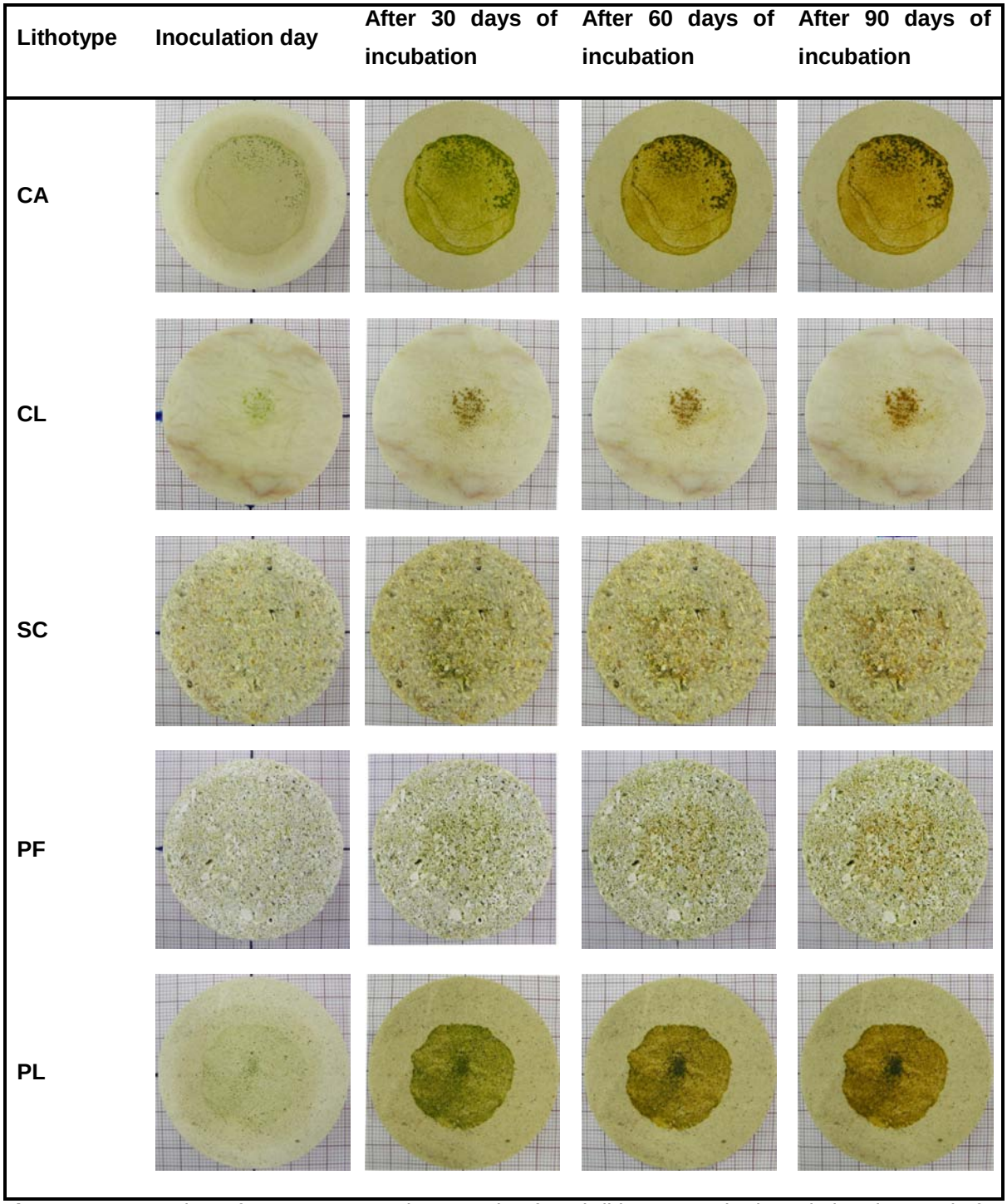

Fig. 5.18. Upper view of one representative sample of each lithotype at the inoculation time and after 30, 60 and 90 days of incubation.

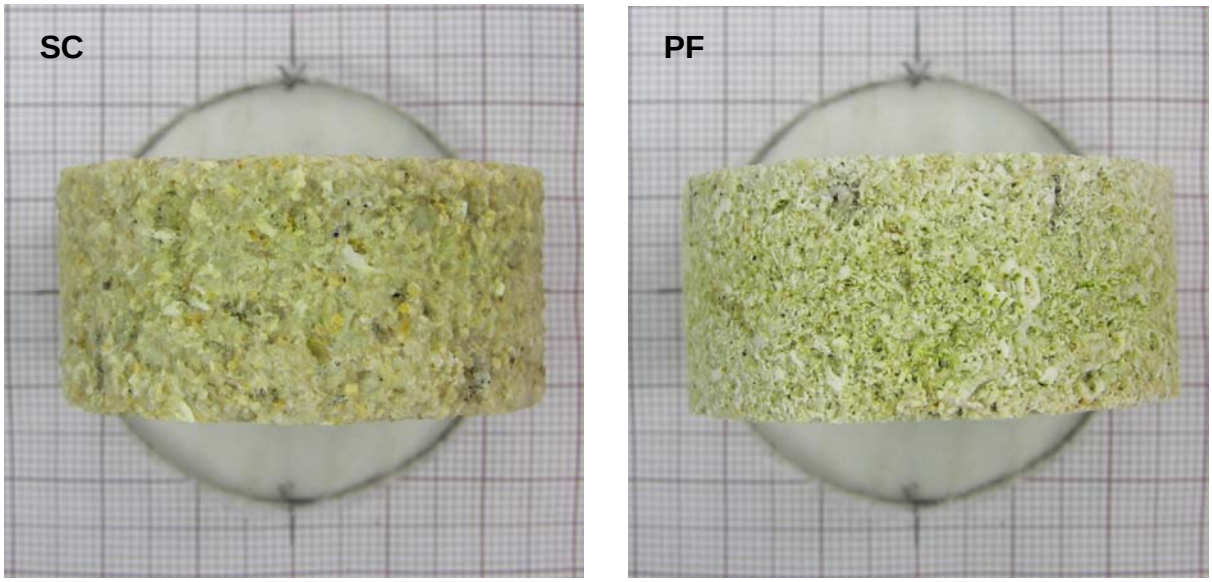

Fig. 5.19. Lateral views of the SC and PF samples depicting green colour appearance.

5.3.2.1. Photosynthetic biomass quantified during 90 days of incubation

For the evaluation of the colonisation process during the incubation time span, three different strategies were used: (i) the quantification of photosynthetic biomass by *in vitro* chl*a* method, by (ii) *in vivo* chl*a* fluorescence technique; and (iii) the measurement of areas covered by the biofilm by means of image analysis. Two methods of chl*a* estimation were applied and compared since the amount of chl*a* is indicative of the amount of phototrophic microorganisms present on the lithic substrata. Image analysis was used as a complementary and non-destructive method to measure the surface areas covered by the biofilms since the chl*a* with extraction procedure is not suitable for taking successive measurements of photosynthetic biomass on a single sample. Comparison of results was made and discussed to evaluate the accuracy of the techniques used.

In vitro chlorophyll a quantification technique

The monthly progress of photosynthetic biomass estimated by the *in vitro* chl*a* technique, expressed as µg chl*a* cm^{-3} (equation #7), revealed a great and steady increase of photosynthetic biomass during the incubation time for PF samples, followed by SC (Fig. 5.20). For the less porous lithotype (CL), the amount of chl*a* inoculated on the stone surface remained relatively constant during 60 days of

experimentation. After this incubation-period, a very slight increase was observed. ANOVA results revealed that the average amount of chl*a* was significantly different for CL, which showed very low values (Table 5.4). After 60 days of incubation, PF also showed significantly different values of chl*a*, but with very high values. CA and PL stones exhibited an abrupt increase of photosynthetic biomass during the first 30 days of incubation, which tended to progressively decrease after this incubation-period. These results are in accordance with macroscopic inspection, as the surfaces of CA and PL have become brown. SC photosynthetic biomass showed an oscillating behaviour, decreasing very slightly after 60 days-incubation, followed by an important increase at the last 30 days of incubation. Pheophytin concentrations, calculated according to the equation #8 (see section 5.2.3.2), resulted in negative values for all the studied samples, which indicate the absence of chl*a* degradation products (see appendix three). Consequently, the ratio of chlorophyll to pheophytin was null. This ratio has been reported as a good indicator of the physiological condition of photosynthetic microorganisms especially for phytoplankton (Vollenweider et al., 1974).

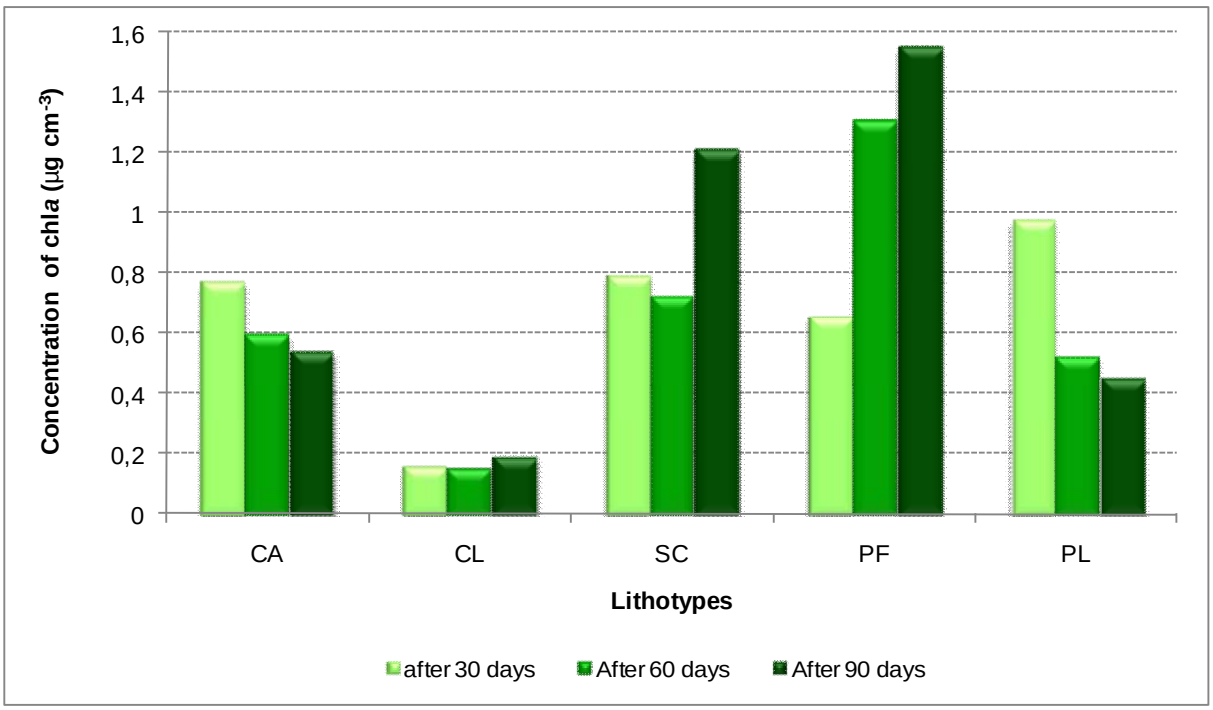

Fig. 5.20. Maximum concentration values of chl*a* (µg.cm^{-3}) present on the stone samples of CA, CL, SC, PF and PL lithotypes, measured by the *in vitro* chl*a* quantification technique after 30, 60 and 90 days of incubation.

Table 5.4. ANOVA results obtained for the concentration of chl*a* present on the studied lithotypes after 30, 60 and 90 days of incubation.

Lithotype	Concentration of chl*a* ($\mu g.cm^{-3}$)		
	After 30 days	After 60 days	After 90 days
a. **CA**	0.56 ± 0.19 a	0.39 ± 0.27 a	0.51 ± 0.05 ab
b. **CL**	0.14 ± 0.02 b	0.13 ± 0.04 a	0.11 ± 0.07 a
c. **SC**	0.70 ± 0.15 a	0.56 ± 0.16 a	0.94 ± 0.28 bcd
d. **PF**	0.51 ± 0.14 a	1.10 ± 0.18 b	1.20 ± 0.38 c
e. **PL**	0.87 ± 0.10 a	0.50 ± 0.03 a	0.38 ± 0.08 ad

The values correspond to average ± SD (n = 3). Average followed by the same letters in a column are not significantly different by the Tukey HDS test at $p<0.05$.

In vivo chlorophyll a fluorescence technique

Regarding the *in vivo* chl*a* fluorescence measured on the surface stone samples immediately after inoculation and after 30, 60 and 90 days of incubation, the initial fluorescence intensities obtained for CA and PL abruptly increased during the first 30 days of incubation (Fig. 5.21A). The *in vivo* chl*a* fluorescence values for SC and PF were also about three times higher than those immediately after inoculation. In contrast, for CL a great decrease was observed until 60 days of incubation, after which an increase was observed. In general, the chl*a* fluorescence intensities increased during the first 30 days of incubation in all cases, and decreased after 60 days of experimentation, with the exception of SC stone (Fig. 5.21A). The intensity of chl*a* fluorescence recorded for this medium-grained lithotype decreased after 60 days of incubation until the end of the experiment (Fig. 5.21A). PF was the only lithotype where the mean values of chl*a* fluorescence remained approximately the same during the 90 days of experimentation. The data values of *in vivo* chl*a* fluorescence obtained after 30, 60 and 90 days are shown in Table 5.5. For CA, CL and SC the mean fluorescence intensity values of chl*a* were significantly different ($p<0.05$) between the 30 and 60 days of incubation as demonstrated by the ANOVA analysis (Table 5.5).

The emission spectra obtained after 90 days showed the typical chlorophyll *a* fluorescence peak at 684 nm (Fig. 5.21B). After 90 days, high fluorescence

intensities were obtained for the lithotypes which presented visible biofilms formed on the surface of the stone samples. High fluorescence intensities represent a high quantity of photosynthetic biomass on the surface of the stone samples. These results were obtained for the lithotypes with fine grained textures, CA and PL (Fig. 5.21B).

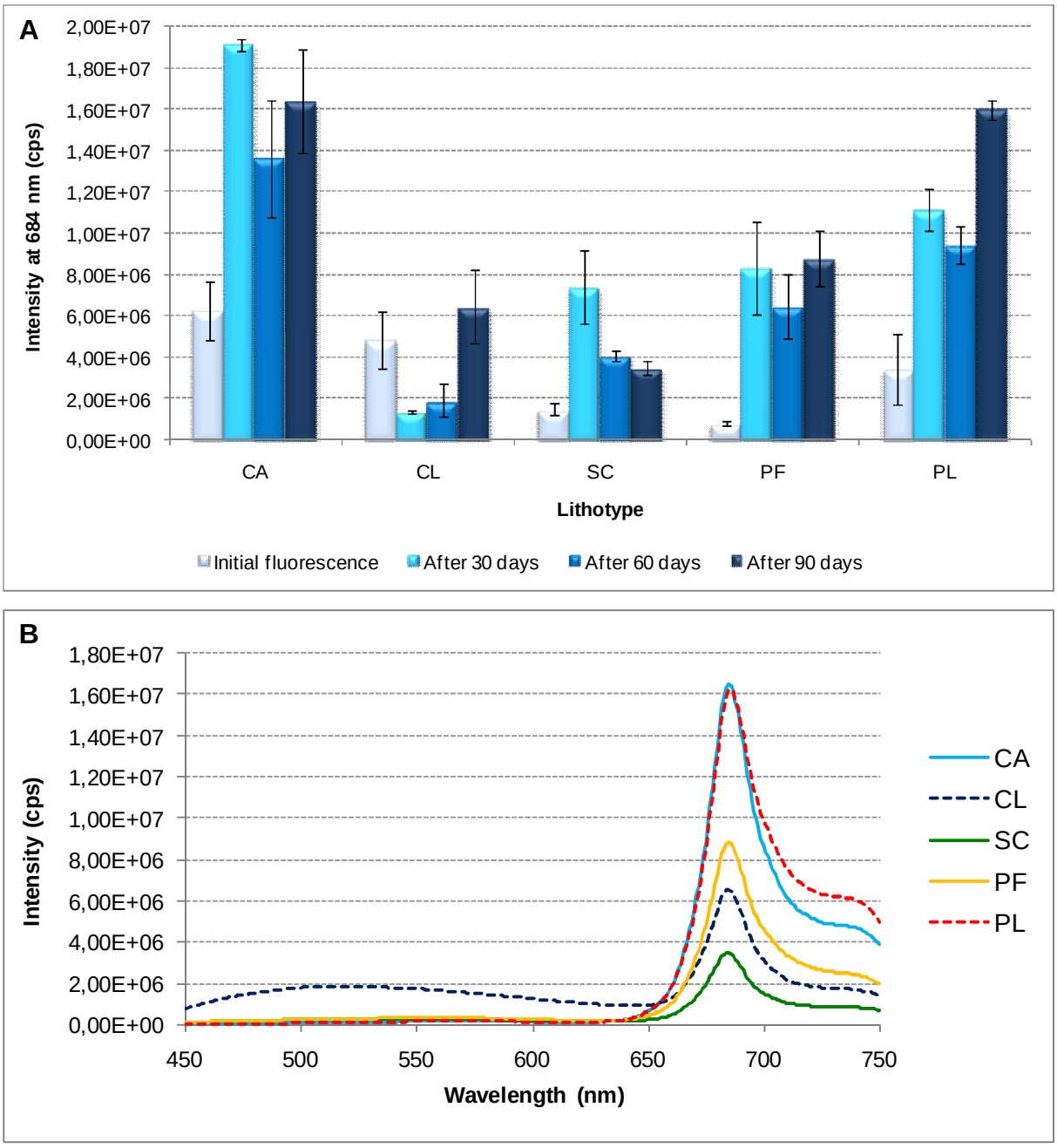

Fig. 5.21. Intensities of chl*a* fluorescence obtained for each lithotype (excitation wavelength: 430 nm): A) Fluorescence intensity values of chl*a* at 684 nm measured immediately after inoculation (initial fluorescence), and after 30, 60 and 90 days of incubation. Each column corresponds to the mean value of an average of 15 measurements ± SD. B) Chl*a* fluorescence spectra measured after 90 days of incubation. Each lithotype spectrum is an average of 15 spectra.

Table 5.5. Intensity of chl*a* fluorescence values measured at 684 nm together with ANOVA results obtained for the five studied lithotypes after 30, 60 and 90 days of incubation.

Lithotype	Intensity of chl*a* fluorescence (cps) at 684 nm		
	After 30 days	After 60 days	After 90 days
a. **CA**	$1.93x10^7 \pm 2.93x10^5$ a	$1.36x10^7 \pm 2.80x10^6$ a	$1.64x10^7 \pm 2.49x10^6$ a
b. **CL**	$1.37x10^7 \pm 9.39x10^4$ b	$1.92x10^6 \pm 7.97x10^5$ b	$6.49x10^6 \pm 1.78x10^6$ bc
c. **SC**	$7.43x10^6 \pm 1.76x10^6$ c	$4.11x10^6 \pm 2.59x10^5$ bc	$3.49x10^6 \pm 3.39x10^5$ b
d. **PF**	$8.33x10^6 \pm 2.24x10^6$ cd	$6.47x10^6 \pm 1.54x10^6$ cd	$8.79x10^6 \pm 1.32x10^6$ c
e. **PL**	$1.11x10^7 \pm 1.01x10^6$ d	$9.41x10^6 \pm 9.00x10^5$ d	$1.60x10^7 \pm 4.67x10^5$ a

The values correspond to average ± SD (n = 15). Average followed by the same letters in a column are not significantly different by the Tukey HDS test at $p<0.05$.

Comparing both techniques, different trends of *in vivo* chl*a* fluorescence and chl*a* concentration, calculated by the *in vitro* technique, was observed. For SC and PF there was a significant decrease of chl*a* fluorescence intensities, whereas the concentration of chl*a* determined by the *in vitro* chl*a* technique significantly increased for these lithotypes (Figs. 5.20 and 5.21A). Moreover, CA and PL were the lithotypes depicting the highest intensities of *in vivo* chl*a* fluorescence. However, these lithotypes were the ones showing a decrease of chl*a* amount during the incubation course as determined by the *in vitro* technique. By both techniques, CL was the limestone depicting the lowest quantity of chl*a*, which tended to increase during the last 30 days of incubation.

Digital image analysis

The image analysis approach allowed the monitoring of biofilm development on the stone samples throughout the quantification of stone surface areas covered by the biofilms. By means of the thresholding algorithms applied to bands obtained by PCA (Fig. 5.22), it was possible to isolate the areas covered by the biofilm and quantify the phototrophic cover through the time as represented in Figure 5.23.

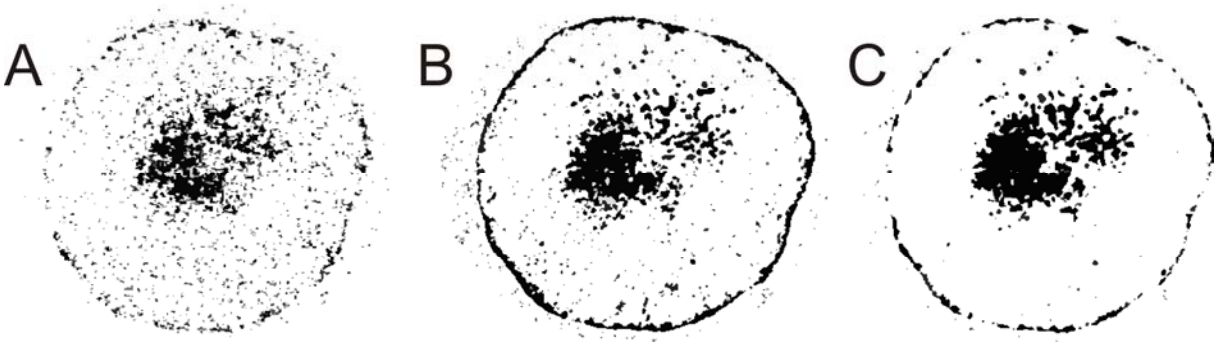

Fig. 5.22. Thresholded areas obtained by ImageJ software for CA: A) After inoculation; B) After 45 days incubation; C) After 90 days incubation. The detected particles are then measured using ImageJ software.

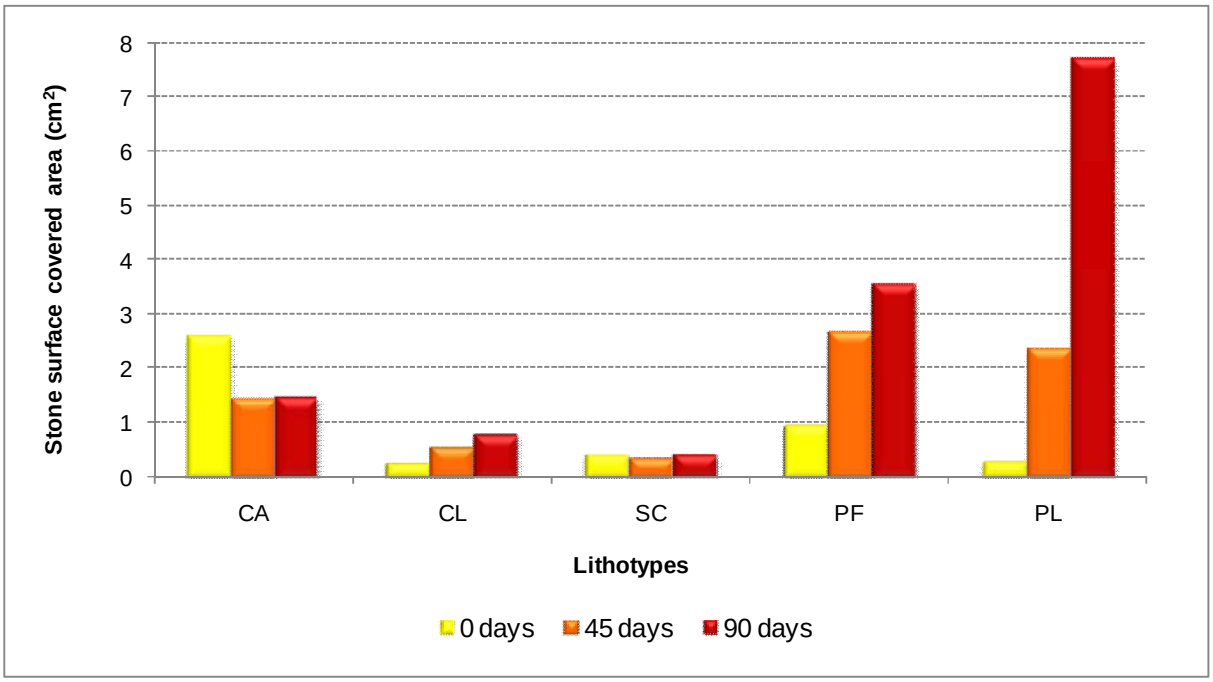

Fig. 5.23. Sum of the stone surface areas covered by the biofilms, quantified by digital image analysis.

According to this complementary visual monitoring technique, PL samples were the most extensively colonised surfaces, revealing significant epilithic growth. The phototrophic culture aggregates, randomly distributed on the lithic surfaces during the inoculation day, have grown during the incubation course leading to an increase of surface covered areas. CL showed a very slight increase of surface area covered by growth, also observed by the *in vivo* chl*a* fluorescence technique. In spite of the difficulties for measuring the extent of the epilithic phototrophic biofilms on the PF and SC samples, strongly masked by the high macroporosity of the lithotypes, the image analysis approach employed was successful since it allowed the quantification of the stone surface coverage. The total surface area covered by the phototrophic

biofilm showed no increase for SC lithotype over the course of batch incubation, being the lowest colonised surface samples among the studied lithotypes. Distinctively, it is noticeable the epilithic growth registered for PF, which showed a significant increase of phototrophic colonisation on its surfaces; the stone surface covered area was greater than after inoculation, showing a progressive increase during the experiment. As in the case of *in vivo* chl*a* fluorescence, CA showed a great increase after the inoculation time, followed by a great decrease. After 90 days-incubation a very slight increase of biomass returned to occur.

5.3.2.2. Post-experiment observations of phototrophic colonisation

Digital image analysis

Light microscopy examination with subsequent digital image analysis of transversally cut samples by means of pixel value decorrelation was applied for the detection and visual enhancement of endolithic microorganisms, allowing the estimation of penetration depth, and the assessment of the endolithic biomass distribution into the substrata (Figs. 5.24 to 5.28). When the stone samples were transversally cut, several green stains were macroscopically visible inside SC and PF samples. PCA of RGB images enhanced stains into the SC and PF samples, particularly in SC. A thin horizontal band with characteristic reflectance differences was observed parallel to the stone surface (Fig. 5.26). These bands and stains, coinciding with the green stains of the original digital images, revealed phototrophic endolithic colonisation. False colour images composed of the minority PCA bands helped to distinguish the extent of the assumed endolithic growth. PC1 plotted around 95% of the total information included in the three bands of each image; it was used as Red band, in order to create a homogeneous reddish background. The minority PC3, which plotted around 0.5% of the total information of the images, was used twice for representing the spatial dimension of the endolithic biofilm (Green and Blue bands). The resulting false-colour images showed in light blue the phototrophic biofilm inside the lithic substrata, which were plotted in red (Fig. 5.26). The detected band comprising the endolithic biofilm ranged from 1 to 3 mm in thickness, with a maximum penetration depth of 3 mm. The distribution of the subsurface biofilm was fairly tabular and strongly parallel to the surface. Considering PF samples (Fig. 5.27),

the stains were more discontinuous, in what seemed to follow the porous system of the stone, with penetration depths up to 3 mm. The appearance of this biofilm was more branched and connected to the outer epilithic biofilm through the porous system. Concerning the resulting false-colour images of CA and CL, these analyses revealed the presence of a thin green band only over the surface of the samples consisting of epilithic development of the phototrophic biofilm (Figs. 5.24 and 5.25). For PL, the biofilm marked as dark red colour was principally observed on the top of the sample, but also within the stone sample. PC3 was the most suitable PCA band to highlight the biofilm, reason for being used twice. Pixel values introduced by PC2 band of uncolonised areas were very close to pixel values of colonised areas and thus was not used (Fig. 5.29).

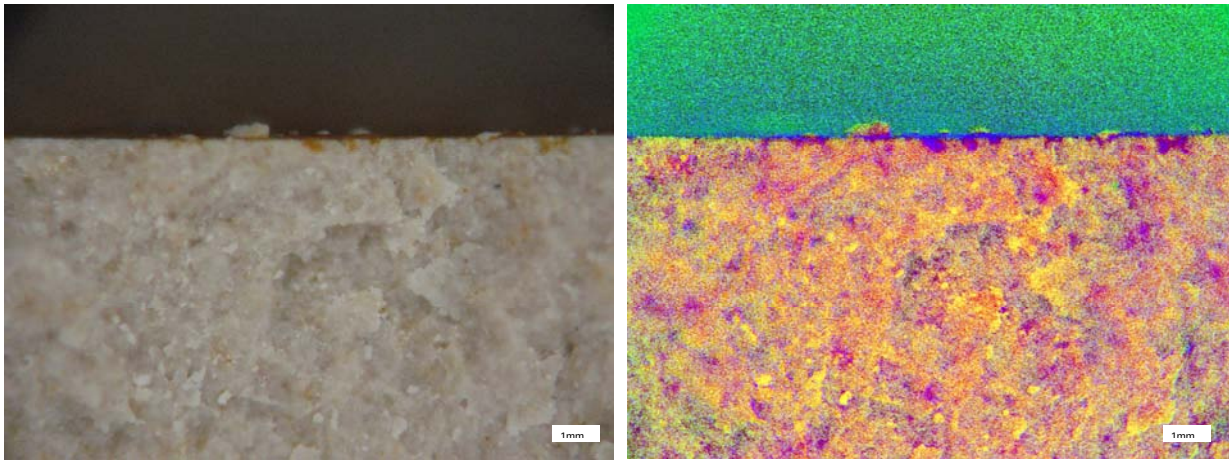

Fig. 5.24. CA sample micrograph (left) and false-colour image obtained by Principal Component Analysis (PC1, PC2, PC3) (right). The thin blue band with occasional occupations in the empty spaces is the photosynthetic biofilm.

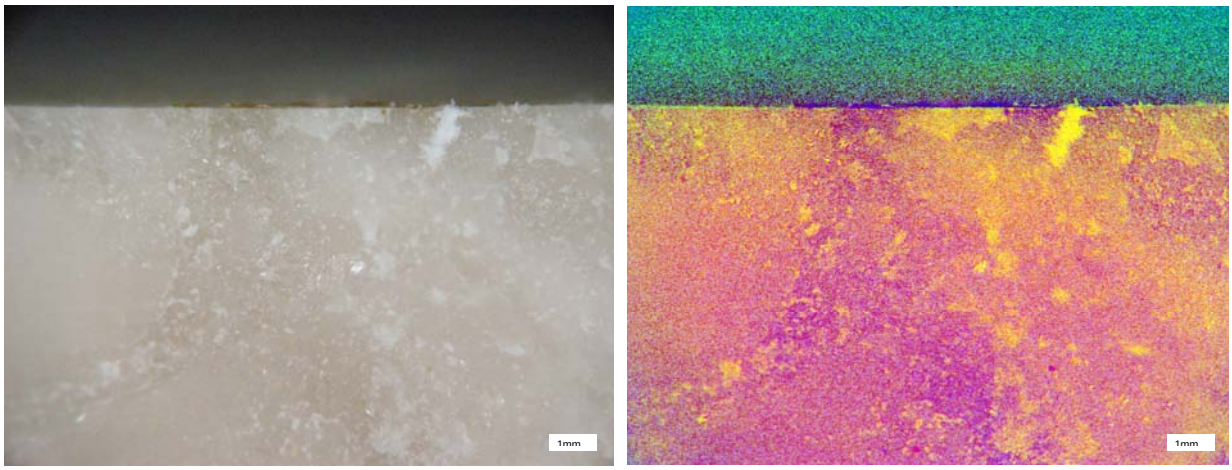

Fig. 5.25. CL sample micrograph (left) and false-colour image obtained by Principal Component Analysis (PC1, PC2, PC3) (right), showing the biofilm as a thin blue band at the top of the image.

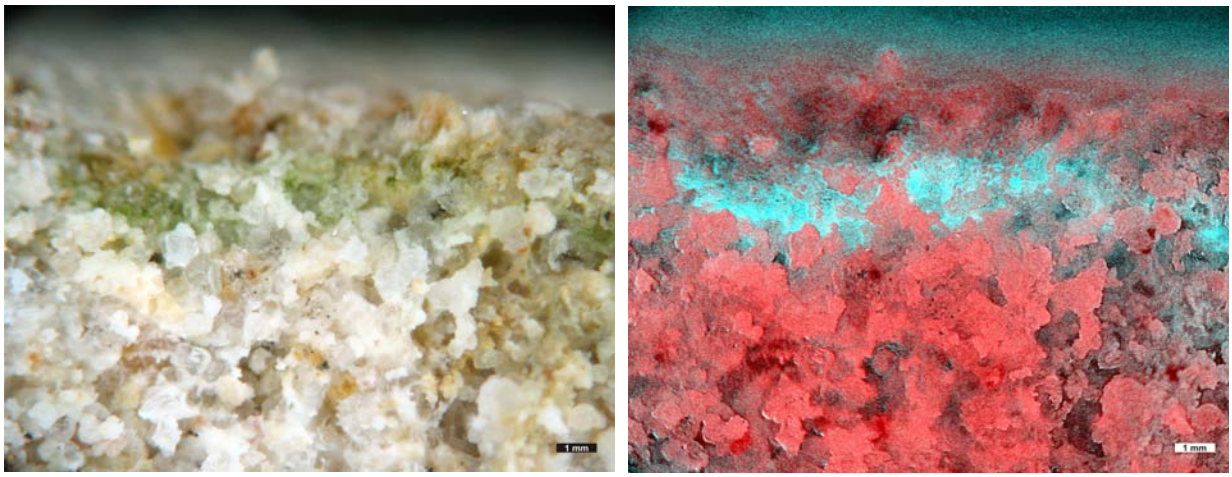

Fig. 5.26. SC sample micrograph (left) and false-colour image obtained by Principal Component Analysis (PC1, PC3, PC3) (right). The biofilm is presented as a blue band inside the stone sample.

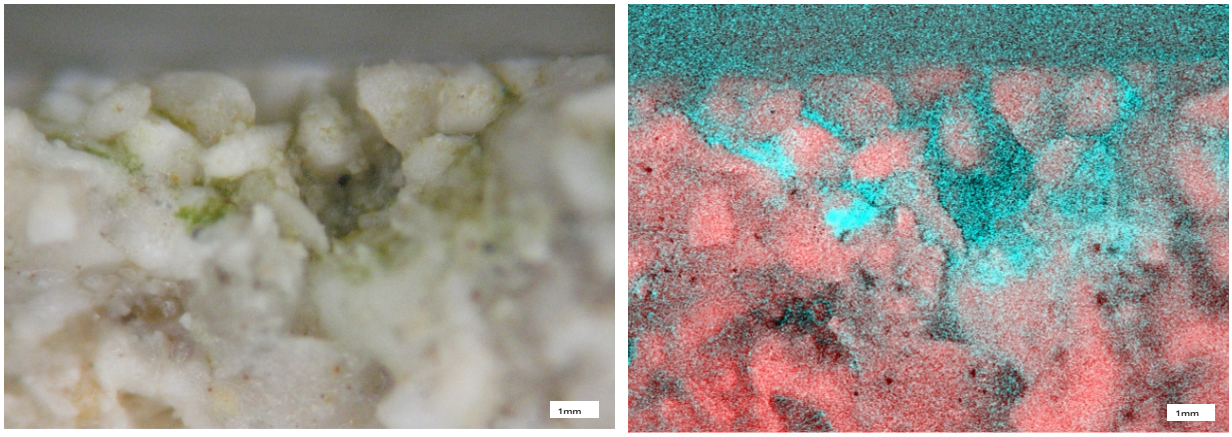

Fig. 5.27. PF sample micrograph (left) and false-colour image obtained by Principal Component Analysis (PC1, PC3, PC3) (right), enhancing the extent of the endolithic biofilm (blue band).

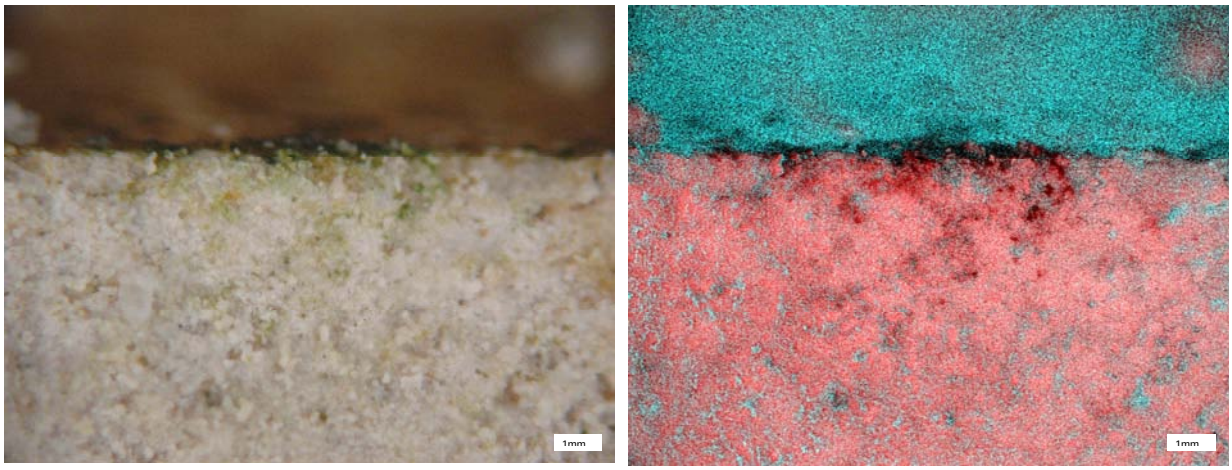

Fig. 5.28. PL sample micrograph (left) and false-colour image obtained by Principal Component Analysis (PC1, PC3, PC3) (right). The biofilm is represented in dark red to black.

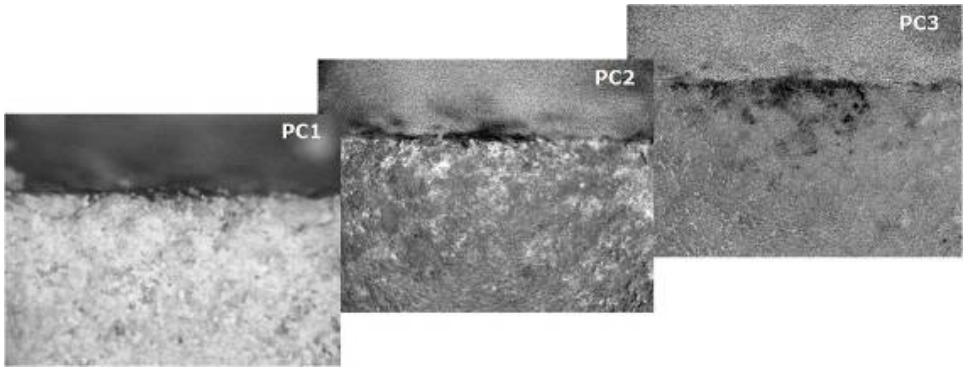

Fig. 5.29. Bands corresponding to the PC1, PC2 and PC3 of the original image of PL used in this work.

Scanning electron microscopy analysis

The visual examination performed in the present work was also complemented with scanning electron microscopy (SEM) observations of the colonised stone samples. SEM analysis on fresh fragments transversally cut to the colonised surface of each lithotype, allowed us to observe the presence of microorganisms on the stones. In all samples, it was observed microorganisms adhered to the stone surfaces embedded in matrix of extracellular polymeric substances (EPS), with the exception of CL, in which microbial cells were not observed (Figs. 5.30 to 5.33). In CA samples, this EPS matrix and its diffusion into the stone is particularly evident. The cells are involved in a glue-like substance, allowing the adhesion of the microbial cells on this stone substratum (Fig. 5.30). This analysis also permitted to observe some details of cellular penetration into the substrata. In SC and PF samples phototrophic cells could easily penetrate into the large pores of these lithotypes, using structural irregularities of the stones for their endolithic growth (Figs. 5.31 and 5.32). EPS are also clearly evidenced on the SC samples (Fig. 5.31). Moreover, the penetration of the organism cells into the stone samples, and the diffusion of their excreted products into the pores and intergranular fissures enhanced physical damages and decreased cohesion between grains, as observed on CA and PL samples (Figs. 5.30 and 5.33).

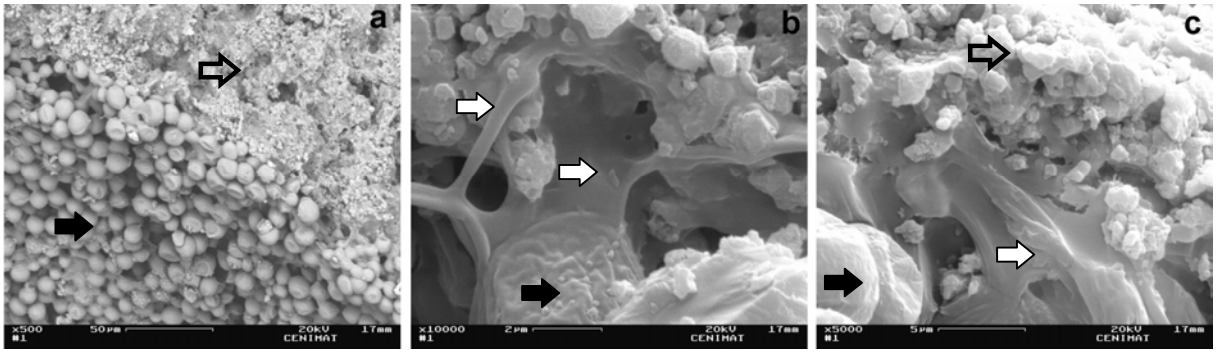

Fig. 5.30. SEM images of transversally cut fresh samples of CA lithotype after 90 days-incubation: a) phototrophic biofilm in external view; b) and c) details of image 5.30a. White arrows indicate EPS; empty arrows show mineral substratum; black arrows indicate microbial cells.

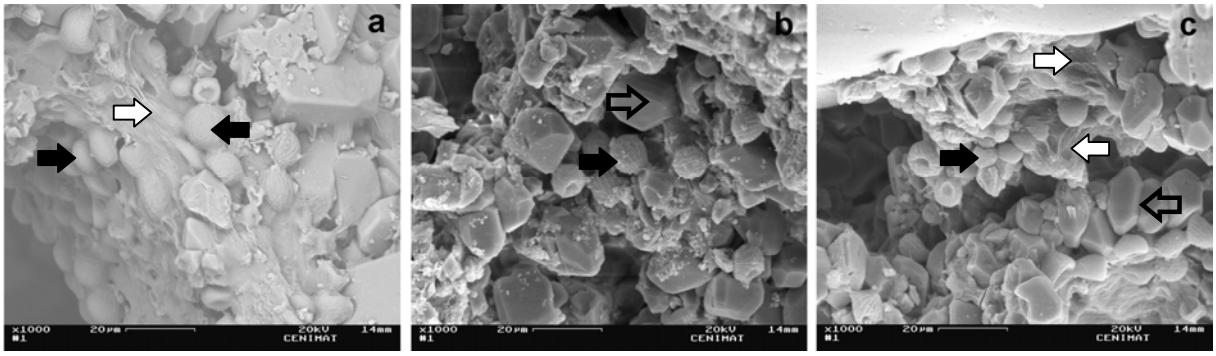

Fig. 5.31. SEM images of transversally cut samples of SC lithotype after 90 days-incubation: a) phototrophic biofilm in external view; b) and c) details of image 5.31a. White arrows indicate EPS; empty arrows show mineral substratum; black arrows indicate microbial cells.

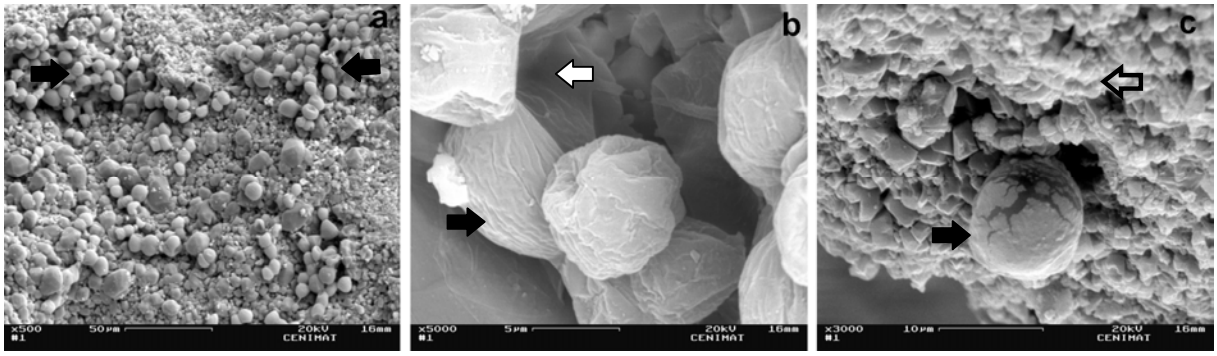

Fig. 5.32. SEM images of transversally cut samples of PF lithotype after 90 days-incubation: a) phototrophic biofilm in external view; b) and c) details of image 5.32a. White arrows indicate EPS; empty arrows show mineral substratum; black arrows indicate microbial cells.

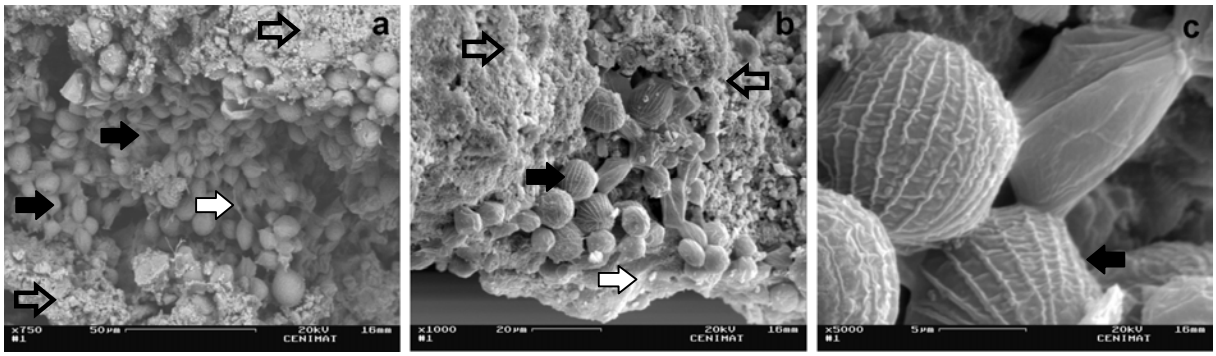

Fig. 5.33. SEM images of transversally cut samples of PL lithotype after 90 days-incubation: a) phototrophic biofilm in external view; b) and c) details of image 5.33a. White arrows indicate EPS; empty arrows show mineral substratum; black arrows indicate microbial cells.

5.3.2.3. Statistical Analysis

A principal component analysis (PCA) was performed in order to establish the structure of the variable dependence. This involves the identification of relationships between variables and in assigning a petrophysical/photosynthetic biomass meaning of each factor. Based on PCA results (Fig. 5.34), two principal components (PC) were extracted which account for 91.47% of the total variance. PC1 accounts for 65.32% of total variance and is mostly linked to open porosity, water vapour permeability, capillarity coefficient, surface roughness parameters and the concentration of chl*a* obtained by the *in vitro* technique after 90 days of incubation. The amount of chl*a* is substantially and linearly associated to the capillarity coefficient and roughness parameters, and less associated to the open porosity and water vapour permeability variables. PC2 accounts for 26.15 % of total variance and is associated with the intensity of *in vivo* chl*a* fluorescence obtained after 90 days. PC1 variables were not linearly related to the intensity of *in vivo* chl*a* fluorescence obtained after 90 days since they were positioned perpendicularly.

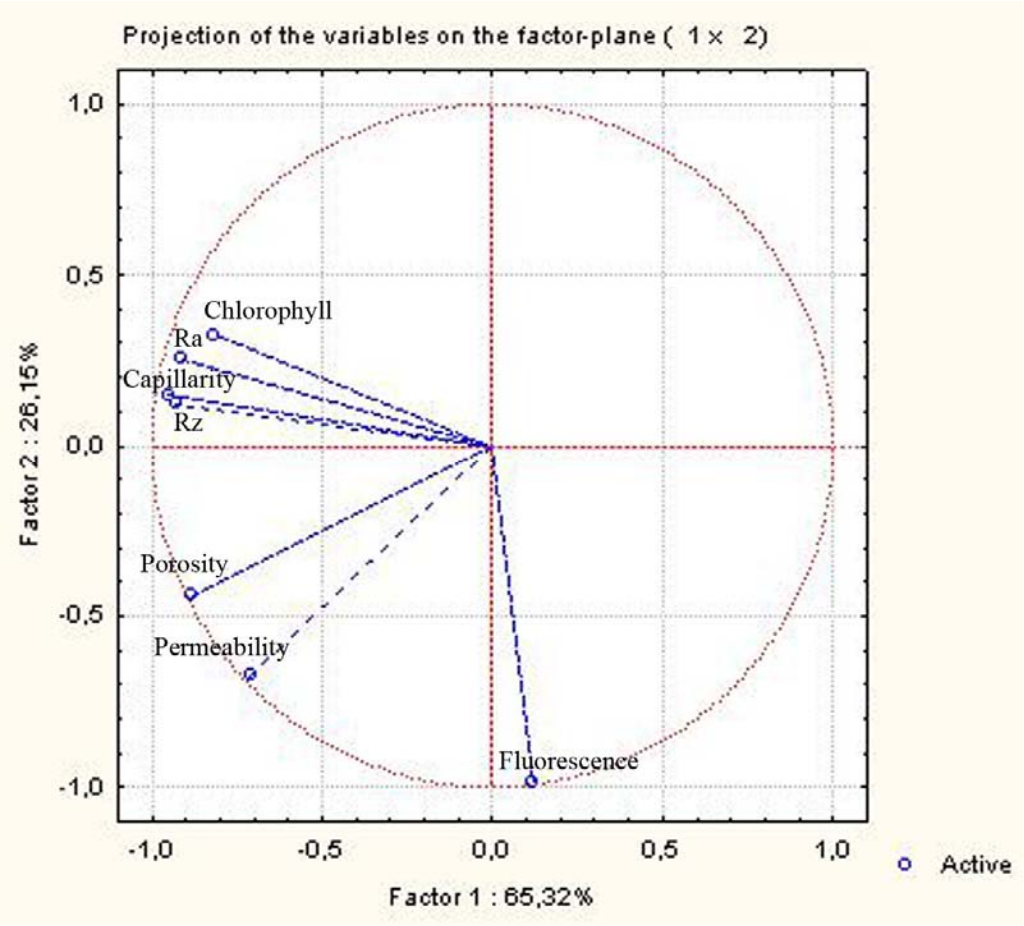

Fig. 5.34. Correlation among the variables capillarity coefficient (Capillarity), surface roughness (R_a and R_z), open porosity (Porosity), water vapour permeability (Permeability), concentration of chl*a* (Chlorophyll) and chl*a* fluorescence (Fluorescence), and the factors (components).

The results of the statistical analysis, derived from the correlation matrix, revealed a positive experimental correlation between the concentration of chl*a* and the capillarity coefficient (correlation > 0.94) and roughness (correlation > 0.68) of the five lithotypes. This shows that the establishment and development of phototrophic colonisation were mostly influenced by the capillarity coefficient and surface roughness (R_a and R_z), than by open porosity and water vapour permeability.

5.4. Discussion

5.4.1. Lithotypes characteristics

The bioreceptivity of stone materials applied on monuments is determined by the appropriate combination of environmental factors, stone intrinsic properties and architectural conditions, conferring the ecological and physiological requirements for microbial settlement. In an effort to assess the influence of intrinsic characteristics of the limestones on their primary bioreceptivity, some petrographic, petrophysical and petrochemical assays were included in this study.

Concerning the petrochemical characteristics of the five studied limestones, the results of chemical analysis reflected, as expected, their mineral composition. Because limestones are primarily calcite, the content of both CaO and CO_2 were extremely high, forming more than 95% of the whole, with the exception of SC. This limestone showed significant amount of silica indicating the presence of noncarbonated detritus such as quartz grains, which is in fair agreement with its petrography; the relatively low amount of alumina pointed out the scarce content of argillaceous materials (Table 5.3). On the other hand, CA, CL, PF and PL are pure, with more than 95% of calcium carbonate and less than 3% of silica. Similar results were obtained by Dionísio (1997) and Ferreira Pinto and Delgado Rodrigues (2008) for *Ançã* limestone, which reported that it is a very pure calcitic limestone almost wholly formed of calcite, with a $CaCO_3$ relative weight proportion higher than 96%. Figueiredo et al. (2007) also reported that the beige-white limestone (*Lioz* limestone) is pure with more than 95% of calcium carbonate.

Regarding petrophysical properties (Table 5.2), the studied limestones with the exception of CL, showed a high degree of porosity, a characteristic that is frequently found in this type of rocks. CL showed very low porosity since strong diagenetic processes may have caused a marked decrease in the volume of its pores. Despite of the fine-grained and homogeneous texture of PL contrasting with the very grainy and porous textural features of SC and PF, PL showed the highest open porosity probably due to the large amount of very small pores and interconnection between them. Its high capillarity water absorption coefficient corroborates the presence of high percentage of interconnected small capillaries. CA showed a similar pattern: large amount of very small pores associated with high open porosity and water

absorption by capillarity. The highest water absorption by capillarity was obtained for PF and SC, in which abundant macropores were observed under petrographic microscope and naked-eye. Absorption kinetic crucially depends on the porous space structure, particularly on the pore size and connection between pores. Pore size has two antagonistic effects: the water flow is facilitated in larger pores, but the driving force is inversely proportional to the radius (Aires-Barros, 2001). In other words, great amount of larger pores accounts for most of the rock porosity, whilst high percentage of interconnected capillaries significantly contributes to propel the fluid through the capillary network (Benavente et al., 2007). In fact, capillary rise kinetic is reported as the most usual mechanism of water penetration into building materials (Karoglou et al., 2005). Thus, it must be considered when stone conservation is taken under consideration because it permits the movement of water into the stone, favouring biological life and biodeterioration; this negative phenomenon becomes greater when the duration or frequency of the time of wetness increases. Therefore, the high values of water absorption by capillarity and open porosity obtained for PF, SC and PL indicate great susceptibility to biodeterioration. In addition, high values of water vapour permeability seem to render them unsuitable for outdoor environments in humid areas if preventive treatments, such as the application of hydro-repellents are not taking into account. Water vapour permeability is also influenced by the shape and size of pores and their interconnection, as well as by the cement and matrix content of the sedimentary rock (Chilingar, 1964; Bloch, 1991; Rezaee et al., 2006). Parameters related with the porous system and movement of water, such as porosity and permeability, have been investigated to assess the durability and susceptibility of stone to weathering during exposure trials and laboratory simulations (Ordóñez et al., 1997; Beck et al., 2003; Sousa et al., 2005; Benavente et al., 2007; Cultrone et al., 2007; Figueiredo et al., 2007; McKinley and Warke, 2007). Sousa et al. (2005) recommended precaution when using granites with open porosity greater than 3% as dimension stone outdoors in polluted continental and marine areas. Beck et al. (2003) described that tuffeau limestone is very sensitive to changes in relative humidity and suggested that the high porosity and high water retention capacity induce physicochemical deterioration. The high porosity and water vapour permeability of PL, PF and SC imply that water moves and transfers easily throughout the porous media, inducing a suitable habitat for colonising organisms. The very low water vapour permeability of CL, linked to a very

low open porosity, renders this lithotype less bioreceptive for microbial colonisation. According to Gerrard (1988), sound crystalline limestone usually exhibits low permeability, precluding water transfer and, thus disfavouring microbial settlement. Figueiredo et al. (2007) pointed out that *Lioz* limestone has the best durability of all the varieties of limestones studied.

As already exposed and discussed, open porosity, water absorption by capillarity and water vapour permeability strongly influence the bioreceptivity of stones to be colonised by living organisms. However, surface roughness also plays an important role among the petrophysical properties influencing stone bioreceptivity. It has a huge impact on a number of surface properties which determine microbial anchoring, such as adhesion, possibility of attachment points and microrefuges which protect microorganisms from hydrodynamic forces and reduce cell removal. These microrefuges occur when the cell is smaller than the size of the pore (Scardino et al., 2008). The attachment of organism cells and spores to surfaces with different microtextures was studied by Scardino et al. (2006, 2008). For several diatom species, attachment was reduced on surfaces with irregularities below the size of the cell, while attachment increased on smooth surfaces and when textures provided multiple numbers of attachment points. It is clear that surface roughness is an important parameter to predict stone bioreceptivity. Average roughness (R_a) and mean roughness depth (R_z) were obtained for the five lithotypes, which included great macro-roughness stones. The great R_a and R_z values obtained for SC and PF lithotypes may be correlated with visibly deep pits around grains apparently produced by removal of the soft matrix which binds grains together. It must be mentioned that all stone samples were prepared using a diamond swan, and thus the measured roughness is the result of combined action of stone factors that occurred during the swan process. However, roughness values were consistent with the textural features and porosities of the five lithotypes. CL and CA are smooth limestone, whereas PL, PF and SC are rough stones and thus may provide multiple attachment points to settling microorganisms. Moreover, they may encourage entrapment of water increasing surface wetness and consequently microbial growth and development.

According to the intrinsic properties determined for the five limestones, it can be concluded that the high capacity of water flow in PL, PF and SC, as well as their great surface roughness render them prone to microbial attack. Thus, precaution is recommended when using these lithotypes as ornamental stone in outdoor

applications without preventive treatments. In contrast, the physicochemical properties of CL can render it suitable for use in outdoor buildings and statuary. Stones with high values of water absorption by capillarity, water vapour permeability and surface roughness will be more susceptible to physical, chemical and biological deterioration.

5.4.2. Stone bioreceptivity experiment

Experimental simulations investigating stone colonisation are commonly used in ecological studies since they provide a valuable alternative for natural ecological niches by allowing experimental manipulation of the microbial ecosystem. These laboratory-based studies are of great interest for the particular case of cultural heritage materials. In this study, the laboratory-induced colonisation on initially uninhabited limestones was achieved by inoculating stone samples with a natural community culture composed mainly by phototrophic microorganisms. In nature microorganisms involved in stone biodeterioration develop in more or less complex communities because of the diversity of rock ecosystems. Consequently, the choice for the stone inoculation comprised a community of phototrophic microorganisms that are potential deteriorating agents of the selected stone materials. Furthermore, the use of a complex microbial community presents the advantage to simulate the existence of competition and/or synergy between colonising microorganisms, which act singly or in association with other microorganisms, or with physicochemical factors, to deteriorate stones (Koestler et al., 1996). In addition, the stone samples were not re-inoculated and no extra nutrients were added during the experiment. These procedures allowed the comparison of the primary bioreceptivity of five different limestones.

According to the results obtained in the laboratory-based bioreceptivity experiment it was possibly to indicate that the distribution pattern of the phototrophic biofilms on the stone samples was clearly influenced by the petrophysical properties of each lithotype. From a macroscopic point of view, surface roughness, texture and pore size controlled the absorption of the inoculum during inoculation (time 0), which had repercussions on the development of photosynthetic biofilms on the stone samples (Fig.5.18). The relatively high development of green biofilms observed after 30 days of incubation for all lithotypes, except for CL, were conceivably due to

residual BG11 medium elements present in the inoculum, providing nutrients for microbial growth. In contrast, on CL surfaces this development was not observed probably due to the very compact nature of this limestone, hindering the inoculum absorption into the samples.

It was also macroscopically observed that after 60 days-incubation, colour change from green to brown was observed for all lithotype surfaces (Fig. 5.18). This chromatic change could be attributed to the lack of nutrients provided by total consumption of the elements present in the inoculum and to a negative adaptation to the new type of nutrients supplied by the lithic substrata. However, if growth were only determined by the culture medium elements, similar results would be obtained in all lithotypes. The exposure conditions of the experiment, particularly light intensity, seemed to be important in determining the chromatic changes observed on the studied limestone surfaces. Indeed, if the values of a certain environmental parameter are not optimal for species, the limits of tolerance for other parameters also become narrower. Light represents the primary energy source for the growth of all photosynthetic organisms. From the ecological point of view, the parameters describing light are quality (colour), quantity (intensity) and duration (in time). The quality of the light used was not probably a limiting factor for photosynthetic growth due to the absent of green radiations, which obstruct the growth of photosynthetic microorganisms (Roldán et al., 2006). However, excessive light intensity inside the incubator chamber possibly inhibited the biological growth over the surface, favouring cryptoendolithic or euendolithic behaviour as a refuge from excessive light (Golubic et al., 1981). When an organism is growing under unfavourable conditions, its morphological appearance changes in colour and form. Colour changes arise in response to situations of physiological stress. The quantity of radiation received by the phototrophic microflora on the stone surfaces led them to protect from the direct and excessive light intensity by becoming darkly pigmented. At this point, it is important to remember that cyanobacteria and microalgae contain several pigments for the photosynthetic activity; they are mainly chlorophylls and carotenoids that in the cyanobacteria are also associated with secondary pigments such as phycobilins (phycocyanin and phycoerythrin). For example, cyanobacteria can take a yellow-brown colour when the nitrogen is scarce, leading to a dramatic reduction of chl*a* and phycocyanin, and an increase in carotenoids. Also green patinas of algae become red when the algae enter into a quiescent state forming cysts where carotenoids are

accumulated (Caneva et al., 1991). It is also important to remember that biological patinas of phototrophic microorganisms are not always green even if the organism are in a good physiological state, because chlorophylls may be obscured by carotenoids and phycobilins. The green alga *Trentepohlia* may appear orange or red-brown under normal conditions. In other cases, it has been shown that pigmentation changes can be an expression of environmental adaptation to optimise the photosynthetic process as a consequence of new exposure conditions, such as light intensity, temperature and cells age (Alakomi et al., 2004; Bartolini et al., 2004). Thus, light intensity together with stone intrinsic properties (surface roughness, open porosity, water absorption by capillarity and water vapour permeability) had an important contribution on the development of photosynthetic biofilms. The high surface roughness and pore size of SC and PF allowed photosynthetic growth into the substrata and on their lateral surfaces giving protection from intense light (Fig. 5.19). In contrast, the homogeneous texture, low surface roughness and pore size of CL, CA and PL almost certainly hindered a successful colonisation because these stone characteristics did not provide an endolithic habitat as refuge from high light intensity. Nevertheless, a chromatic adaptation seemed to occur as a survive strategy from excessive light intensity inside the incubator chamber.

Concerning the photosynthetic biomass developed on the stone samples, two chl*a* quantification methods, complemented with digital image analysis were used in order to determine the bioreceptivity of the five studied limestones (Figs. 5.20, 5.21 and 5.23). PF and SC, the biocalcarenites of medium coarse-grain, displayed an increase of photosynthetic biomass and the highest values of chl*a* concentration calculated by the *in vitro* chl*a* technique after 90 days of incubation. This result suggested a successful colonisation and an active growth. However, according to the *in vivo* chl*a* fluorescence and digital image analysis of the surface areas covered by the biofilms, SC samples showed very low values. A significant decrease was noticed by *in vivo* chl*a* fluorescence, indicating apparent cessation of epilithic colonisation. Similar results were obtained by digital image analysis, in which the surface area covered by the biofilm on SC samples did not show a significant increase over the course of batch incubation. These contradictory results led to corroborate that endolithic phototrophic colonisation occurred for SC samples. In contrast, the photosynthetic biomass determined on the very-fine grained limestone samples (CL) showed similar results for the three monitoring techniques (Figs. 5.20, 5.21 and

5.23). A slight increase of photosynthetic biomass after 90 days of incubation was noticed, suggesting that the phototrophic colonisation would progressively increase if the incubation period were extended. According to Roeselers et al. (2006), the end of exponential growth does not necessarily mean that a stable climax community has established or cessed. The biofilm may be still in an adaptation state, developing slowly towards a final convergence.

The progressive decrease of chl*a* concentration obtained for CA and PL by the *in vitro* technique (Fig. 5.20), in combination with the biofilms brownish colour, pointed out to relatively high concentrations of pheophytin degradation products and thus a low viability of the population considered after 60 days of incubation. However, the determination of pheophytin performed in this study revealed the absence of these products. Moreover, either *in vivo* chl*a* fluorescence or digital image analysis of biofilm covered areas on CA and especially on PL samples revealed a noteworthy increase of phototrophic biomass after 90 days of incubation (Fig. 5.21 and 5.23). This suggests the previously mentioned chromatic change, which might be associated with an adaptation to the lithic substrata and exposure conditions through the increase of carotenoids and reduction of chl*a*, rather than to the cessation of the phototrophic colonisation. According to Caneva et al. (1991), cyanobacteria and green algae may induce reddish to blackish patinas even if the organism is in good physiological state, explaining the increase of photosynthetic biomass. Wakefiled and Jones (1998) also suggested that nutrient stress can originate colour change of the cells from green to orange through the accumulation of carotenoids. Thus, PL and CA biofilms might be still in an adaptation state to the lithic substrata and exposure conditions, as in the case of CL samples, suggesting that the incubation time should be extended.

From the principal component analysis (PCA) used to correlate the influence of intrinsic properties in stone bioreceptivity (Fig. 5.34), two main components were obtained and assigned a petrophysical/photosynthetic biomass meaning. The first component was linked to the concentration of chl*a* and was highly associated to the coefficient of water absorption by capillarity and surface roughness parameters, and less associated with open porosity and water vapour permeability. The second component, linked to the *in vivo* chl*a* fluorescence measured on the stone surfaces, was not linearly associated with the petrophysical properties, suggesting the fallibility of *in vivo* chl*a* fluorescence technique on the estimation of endolithic photosynthetic

biomass present in lithic substrata. This apparent contradiction of data obtained for the *in vitro* chl*a* quantification technique and the *in vivo* chl*a* fluorescence, as well as digital image analysis looks likes a drawback in the experimental scenario. This discrepancy is related to the inherent feature of these techniques: the chl*a* concentration calculated by the *in vitro* technique allowed estimating the total amount of chl*a* present on and within the stone samples, while *in vivo* chl*a* fluorescence and digital image analysis only detected the photosynthetic biomass growing on the surfaces, being both non-destructive techniques.

Gathering all the data together it can be corroborated that the stone samples that displayed phototrophic biofilms on their surfaces were detected by macroscopic observation and by the non-destructive techniques, whereas endolithic growth was only detected by the *in vitro* chl*a* technique. The combination of digital image analysis approach and chl*a* quantification techniques gave a rather good presentation of photosynthetic biomass variation and provided qualitative and quantitative evaluations of phototrophic growth on the limestones studied. Digital image analysis, even though it produces rapid measurements and quantified observation in less time than conventional methods, is nevertheless insufficient to detect and evaluate endolithic growth without destroying of the sample. Thus, it can be corroborated that phototrophic colonisation arose mainly inside the SC and PF samples, but also epilithically on the PF samples. For the samples which only depicted epilithic colonisation (CA, PL and CL), the intensity of light (exposure conditions) together with the petrophysical properties of the lithic substrata may explain the limited phototrophic growth.

Digital image analysis was also applied in a destructive context to detect and measure penetration depth of endolithic microorganisms growing under the stone (Figs. 5.24 to 5.28). By conventional RGB images endolithic growth may be difficult to distinguish as the rock colour and texture may mask the real extent due to high visual correlation between biofilm and rock. PCA of digital images allowed discriminating between these two elements by means of decorrelation of pixel values in the different bands of the images. The endolithic biofilms detected on PF and SC showed a horizontal zonation parallel to the surface. Their thickness (from 100 µm to 3000 µm) was likely linked to laboratory-induced ecological factors such as light intensity and other non-controlled stresses. Pohl and Schneider (2002) applied computerised image analysis to detect and quantify the biomass and penetration

depth of endolithic microorganisms into carbonate rock. The authors examined that endolithic biofilms from protected sites (humid and shaded) showed a residual substratum thickness of only a few micrometres, whereas from intensely insolated dry sites retreated to depths of 150-250 µm below the rock surfaces. Therefore, it can be concluded that light intensity inside the chamber was a limiting factor influencing the behaviour and distribution pattern of the microbial communities. Great surface roughness and macroporosity observed for PF and SC allowed development of microbial cells inside the lithic substrata which conceivably provided protection from the high light intensity. The presence of translucent minerals, such as quartz, which filter surface light from lethal to suitable intensities for photosynthesis might also favoured the endolithic development according to Warren-Rhodes et al. (2006).

The penetration of the phototrophic microorganisms into the stones and the diffusion of EPS were also observed by SEM. The presence of EPS in all biofilms might increase the limestones biodeteriorating potential, contributing to weathering reactions and disaggregation of rock grains (Alakomi et al., 2004; Koestler, 2000; Pohl and Schneider, 2002). Kaplan et al. (1987) described the chelating properties of *Chlorella* exopolysaccharides, which are very important in the way these organisms deteriorate stone. The stone surface can lose cohesion due to contraction and expansion of these biofilms because EPS incorporate large amounts of water into its structure ensuring the maintenance of moisture by balancing changes in humidity and temperature. Moreover, polysaccharides promote adhesion of stone fragments and film, eventually detaching from the original material (Saiz-Jimenez, 1999). This aggressive action, mainly of cyanobacteria and microalgae on building stones is more relevant because of their penetration into the substrata.

In what concerns the primary bioreceptivity of the five limestone types, this study demonstrated its dependence on the petrophysical properties and exposure conditions, especially on the capillarity water absorption coefficient and surface roughness. The extent of microbial colonisation appeared to increase as the surface roughness increased. This is because shear forces are diminished, and total surface area is higher on rougher surfaces (Morton et al., 1998). The irregularities of the stone surfaces provided attachments points and microrefuges for the settlement of the microbial cells. The stone surface partially determines the availability of water, nutrients, niche possibilities, and thus the survivability of the microbes (Koestler et al., 1996). These results are in accordance with those reported by Guillitte and

Dreesen (1995), Tiano et al. (1995) and Tomaselli et al. (2000b). Therefore, the high amount of photosynthetic biomass detected for PF and SC limestones, linked to their intrinsic properties, especially high values of capillarity coefficient and surface roughness, but also open porosity, water vapour permeability, degree of cementation and carbonate composition, render them prone to phototrophic colonisation, showing the highest primary bioreceptivity. CL showed the lowest primary bioreceptivity, being weakly colonised due to both stone intrinsic properties and exposure conditions, which inhibited phototrophic development over the surface of these microcrystalline limestone samples. The very compact nature of this lithotype and its extremely low porosity constituted an impediment to microbial growth, as it has been demonstrated in low porous rocks such as marbles and granites (Tiano et al., 1995; Guillitte and Dreesen, 1995; Prieto and Silva, 2005; Miller et al., 2006). Thus, the low bioreceptivity of CL can render it suitable for use in outdoor applications, as previously anticipated. CA and PL showed a moderate bioreceptivity, which appeared to be mainly controlled by their high water absorption by capillarity and water vapour permeability linked to their fine-grained texture, which retain water and moisture into the substrata for long periods of time. According to Warscheid et al. (1991) and Tomaselli et al. (2002), high water-permeability of coarse-grained stones favours a rapid and temporary biological colonisation, while permanent microbial establishment occurs in fine-grained stones due to longer water retention time, as might be the case of CA and PL. Yet clearly, microbial colonisation of stone is dependent on the availability of water allowing microorganisms to form biofilms on the stone surfaces. Regarding the stone suspension pH, it was not possible to assess its influence on the stone primary bioreceptivity due to the similar values obtained for the five lithotypes. However, the values ranging from 8.4 to 8.7 seem not be a limiting factor for the growth of the phototrophic microorganisms. According to the study of Tiano et al. (1995), in which different pH values were tested for the growth of two phototrophic strains inoculated in different lithotypes suspensions (powdered and suspended in water), the maximum growth was observed in the suspension containing *Lecce* limestone with pH 8.8.

5.5. Conclusions

The stone bioreceptivity experiment addressed the primary bioreceptivity of the five limestone types and demonstrated its dependence on the petrophysical properties and exposure conditions. The bioreceptivity was evaluated through chl*a* quantification techniques and digital image analysis. The chl*a* concentration can be used as a parameter for the detection of phototrophic organisms on stone materials. However, the method of *in vitro* quantification of photosynthetic biomass is disruptive in nature, due to the extraction procedures. Therefore, it is not applicable for the monitoring of photosynthetic growth on stone monuments since it requires successive sampling procedures. This problem is overcome by the *in vivo* chl*a* technique and digital image analysis, which revealed to be important tools for the detection of epilithic photosynthetic colonisation. Moreover, these methods showed high sensitivity for the detection of very low concentrations of chl*a* allowing the detection of photosynthetic microorganisms at an early growth stage on the stone surfaces. Unfortunately, endolithic growth is not detected by these techniques, which represents a major obstacle when an integral study of the stone phototrophic ecosystem is needed.

The combined analytical approach performed in this study allowed the assessment of the photosynthetic colonisation induced on the limestone samples and to corroborate their primary bioreceptivity. PF, followed by SC, were considered the most bioreceptive lithotypes, in which preferential colonisation occurred endolithically. Microscopic and digital image analyses of transversely cut samples were essential to examine the endolithic growth of microorganisms and the diffusion of their excreted products into the porous system, which might enhanced their biodeteriorating potential, promoting the decreasing of grain cohesion. In contrast, CL showed the lowest bioreceptivity. The petrophysical characteristics, primarily water absorption by capillarity and surface roughness, and secondarily open porosity and water vapour permeability, were the keys for the development of the microbial community assayed, together with the exposure conditions, especially light intensity, which might have limited epilithic development on the stone samples, particularly on CA and PL. Endolithic growth was not observed on these lithotypes due to their intrinsic properties, especially microporosity and low surface roughness, which difficult microbial penetration. Therefore, especial attention must be taken in the

diagnosis of monuments built with high porous and rough stone materials since endolithic activity may be present. Furthermore, if endolithic behaviour is not examined, the commonly used biocidal treatments may not penetrate deep enough to eliminate completely the endolithic growth, widening the biodeteriorating process. The next chapter focus the appraisal of the endolithic growth detected in the SC and PF lithotypes since little if any attempt appears to have been made to the study of endolithic growth induced under laboratory conditions.

CHAPTER SIX

Appraisal of endolithic growth and its biodeteriorating potential on limestones

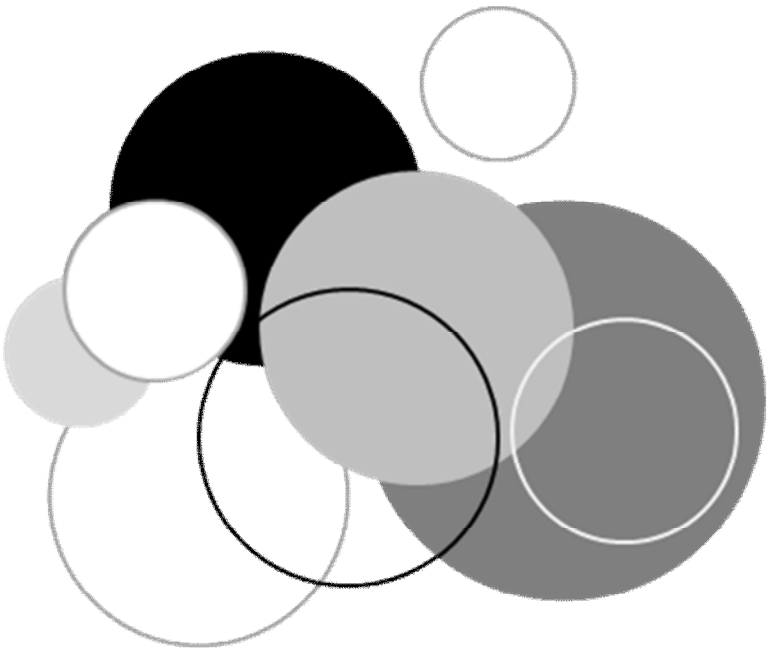

The main results presented in this chapter have been accepted for publication in:

Miller, A.Z., Rogerio-Candelera, M.A., Laiz, L., Wierzchos, J., Ascaso, C., Sequeira Braga, M.A., Hernández-Mariné, M., Maurício, A., Dionísio, A., Macedo, M.F., Saiz-Jimenez, C., 2010. Laboratory-induced endolithic growth in calcarenites: biodeteriorating potential assessment. Microbial Ecology (accepted).

CHAPTER SIX

Appraisal of endolithic growth and its biodeteriorating potential on limestones

6.1. Introduction

The presence of endolithic microorganisms (living inside rocks) such as cyanobacteria, algae and fungi on monuments has been rarely recognised. Only few authors reported the presence of endolithic phototrophic microorganisms on monuments, as mentioned in chapter two (Giaccone et al., 1976; Bolivar and Sanchez-Castillo, 1997; Saiz-Jimenez et al., 1991). On the contrary, several studies were performed on endolithic microflora in aquatic environments and in extreme environments like deserts and Antarctica given their role as carbon reservoirs across large areas (Friedmann, 1982; Pentecost, 1992; De los Ríos et al., 2006; Warren-Rhodes et al., 2006; Wierzchos et al., 2006).

The proliferation of microorganisms under stone surfaces can increase the potential biodeterioration of the lithic substrata, contributing to the decreasing of cohesion between grains (Saiz-Jimenez, 1999; Alakomi et al., 2004). Different studies have shown that penetration of growing organisms into stone porous system and the diffusion of their excreted products may arise to depths of several millimetres (Saiz-Jimenez, 1999; Koestler, 2000; Salvadori, 2000; Pohl and Schneider, 2002). Field observations and experiments in the laboratory have demonstrated the significant potential for damage by endolithic phototrophic organisms (Salvadori, 2000; Büdel et al., 2004; De los Ríos et al., 2004). The exudation of corrosive organic or inorganic acids is able to dissolve the carbonate substratum, which either cause leaching of stone materials or in many cases formation of new mineral deposits on the stone surface (Krumbien, 1988; Ariño et al., 1997; Sand, 1997; Gorbushina, 2007); the excretion of EPS cause water retention leading to changes in the porosity

and permeability of rocks (Krumbein and Urzì, 1991; Warscheid et al., 1991; Dornieden et al., 2000).

Considering that little if any attempt appears to have been made to the study of endolithic growth under laboratory conditions, this study is aimed to accurately assess the formation of endolithic photosynthetic biofilms within the *San Cristobal*, and *Escúzar* stones. *Lecce* stone was also analysed in order to assess its biogeophysical and biogeochemical deterioration through a multidisciplinary approach.

6.2. Materials and methods

6.2.1. Investigated stone materials

Post bioreceptivity experiment analyses of endolithic growth and its biodeteriorating potential were appraised for *Escúzar* (PF), *San Cristobal* (SC), and *Lecce* (PL) stones samples. Subsequently to the 90 days-incubation, thin green biofilms were observed mainly within PF and SC limestone samples by digital image analysis of transversally cut samples (see section 5.3.2.2, from chapter five). These preliminary observations conducted to an accurate assessment of the laboratory-induced endolithic growth.

PF and SC lithotypes are biocalcarenites widely used in the construction of Southern Spain monuments. As already described in chapter five, they are medium-grained limestones, with inequigranular heterogeneous textures, high open porosity (33% and 28%, respectively), high capillary water absorption coefficient and high surface roughness.

PL lithotype is a fine-grained limestone quarried in *Lecce* (Italy), depicting very high open porosity (43%) and capillary water absorption coefficient. The differences in the petrographic, petrophysic and petrochemical characteristics of these lithotypes are detailed described in the previous chapter.

6.2.2. Analysis of endolithic growth by microscopy techniques

6.2.2.1. Scanning electron microscopy

Three replicate stone samples of each lithotype were examined by Scanning Electron Microscopy with Back-Scattered Electron imaging (SEM-BSE) and an Energy Dispersive X-ray Spectroscopy (EDS), at Centro de Ciencias Medioambientales (CSIC – Spain), according to a method developed by Wierzchos and Ascaso (1994). The inoculated samples were investigated as fresh stone fragments coated with gold and as resin-casts. The later consisted of stone fragments perpendicularly cut to the colonised surfaces and fixed with 3.25% glutaraldehyde followed by 1% OsO_4. After fixing, the samples were dehydrated in series of ethanol solutions, embedded in epoxy resin and fine-polished after polymerisation. The resin-impregnated cross-sections of colonised stone samples, previously carbon coated, were examined using a DMS 940A Zeiss scanning electron microscope in BSE mode. Chemical analyses by EDS were simultaneously conducted. The microscope operating conditions were: 0 degree tilt angle, 35 degree X-ray take-off angle, 15 kV acceleration potential, 25 mm of working distance and 1–5 nA specimen current range.

6.2.2.2. Confocal laser scanning microscopy

Fresh fragmented samples of PF, SC and PL were also studied by means of Confocal Laser Scanning Microscopy (CLSM) in order to detect the presence, penetration depth and spatial organisation of the phototrophic microorganisms into the samples. They were examined at Universidad Autónoma de Barcelona (Spain) using a Leica TCS-SP2 equipped with four laser beams and three detection channels; wavelengths of the excitation lasers were in the UV Ar (351 nm and 364 nm), blue Ar (458,476, 488 nm), green Ar (514 nm); green HeNe (543 nm) and red HeNe (633 nm). Images were acquired in the three channels simultaneously as described by Roldán et al. (2004). Phototrophic microorganisms were visualised by their *in vivo* pigment fluorescence, without any preparation procedure. Reflection image (grey channel, excitation at 488 nm and emission at 480-490 nm) was employed to visualise the external surfaces, mineral particles and other compounds, which had a different refractive index from organic matter. A single compound image

was obtained by means of different algorithms from the TCS-SP2 confocal microscope software (Leica) and Imaris software package (*Bitplane AG*, Zurich, Switzerland), as described by Roldán et al. (2004).

Combined information supplied by both microscopic techniques was used to characterise the distribution pattern of the photosynthetic microorganisms on and/or inside stones, and to evaluate their interrelations and interactions with the substrata.

6.2.3. Biocalcarenite mineralogical and micromorphological characterisation

6.2.3.1. X-ray diffraction

X-ray Diffraction (XRD) was carried out on the PF samples (inoculated and non-inoculated samples) in order to identify the mineralogical composition, in particular, iron oxides-oxyhydroxides previously detected by SEM-EDS. These analyses were performed at Centro de Investigação Geológica, Ordenamento e Valorização de Recursos (CIG-R), Universidade do Minho (Portugal).

The mineralogy was determined by a Philips PW1710 (APD-version 3.6 j) diffractometer using CuKα radiation at 40kV and 30mA. The step size was 0.02 º2θ and the counting time was 1.25 s. Analytical software, “X’Pert Graphics” and “Identify” by Philips, were used. The bulk mineralogy was determined in random powders of non-inoculated and inoculated PF samples. Regarding the estimations of mineral phases in the bulk rock, the peak-height intensities for diagnostic reflections were used: calcite-3.03 Å; quartz-3.34 Å; mica-10 Å; clay minerals-4.43-4.48 Å; siderite-2.79 Å; goethite-4.18 Å; maghemite-2.51 Å; pyrolusite-3.11-3.16 Å; hausmannite-2.49 Å.

6.2.3.2. SEM-EDS analysis

Scanning electron microscopy analyses of colonised PF stone fragments were also carried out at CIG-R, Universidade do Minho (Portugal). Light microscopy and SEM-EDS were performed using secondary X-rays and standard ZAF corrections that allow semi-quantitative microanalyses and characterisation of mineralogical phases. These analyses were carried out with a LEICA Cambridge S360 microscope, and the samples were coated with a high conductance thin film (gold film).

6.3. Results

6.3.1. Lithotypes colonisation by endolithic biofilms

SEM examination of sections perpendicular to the stone surface enabled studying the distribution of microorganisms, their development on the subsurface of the samples, and their relationship with the substrata. SEM analyses of SC and PF samples confirmed they were colonised endolithically by phototrophic microorganisms, whereas PL samples only depicted epilithic colonisation. The colonisation density, penetration depth and biomass per unit area, varied for both lithotypes.

Considering PF samples, interaction between phototrophic microorganisms and the substrata was observed. It was particularly notable that endolithic microorganisms actively create small cavities easily penetrating the calcite crystals (Fig. 6.1).

Figure 6.2 confirmed the existence of endolithic microorganisms in the PF samples, as well as epilithic microorganisms on the stone surface (Fig. 6.2A). The likely depths endolithic cells penetrated the stone through the accessible void spaces. The cells were mainly concentrated in the bottle neck shaped parts of it (200 µm). Beyond that part, only a few of them reached approximately 200 µm more (Fig. 6.2A). The cells within the epilithic biofilm were randomly scattered on the surface. However, the structure of the endolithic colonisation seems to be very compact forming dense cell aggregates fulfilling almost completely the available pore space (Fig. 6.2B). In many stone-cell contact zones, the cells appear to exert an endolithic action, since they appear to be actively dissolving the substratum. This is clear in Figure 6.2B, where cells were tightly grouped together, as well as in other zones where there was contact between the cells and the minerals. Dissolutions features of the calcite in this endolithic microhabitat were corroborated by the corresponding distribution map of Ca (Fig. 6.2C). The calcium occupied the intercellular spaces perfectly delimiting the occupied space by cell walls, as well as some calcium carbonate grains, which revealed characteristic dissolving patterns produced by the phototrophic cells. The disaggregated carbonate grain zones revealed less relative calcium concentration and higher relative carbon concentration, as analysed by EDS microanalytical Line-Scan analysis.

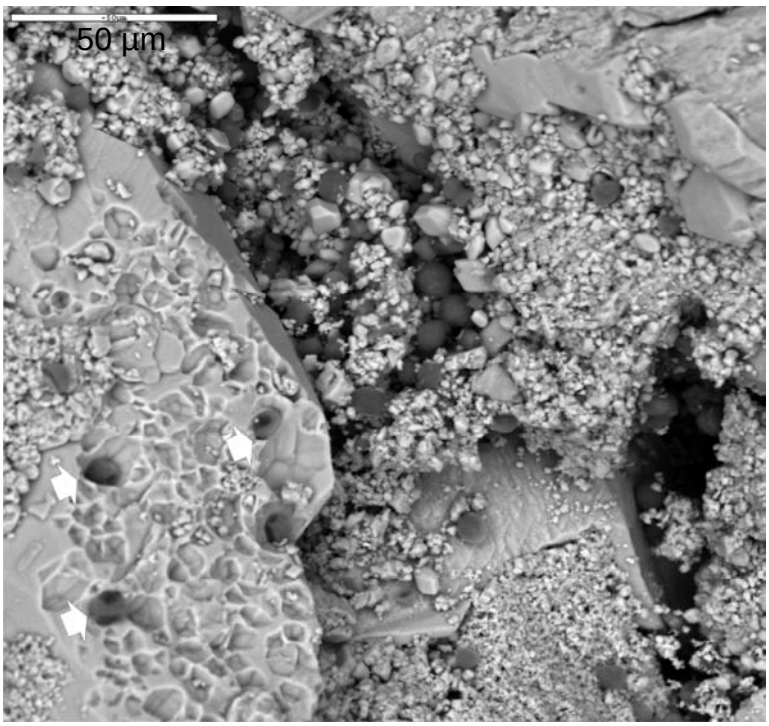

Fig. 6.1. SEM-BSE image from PF lithotype depicting an interaction result between the inoculated phototrophic microorganisms and the substratum. It is particularly noticeable the endolithic activity creating small cavities (white arrows) in the calcite crystals.

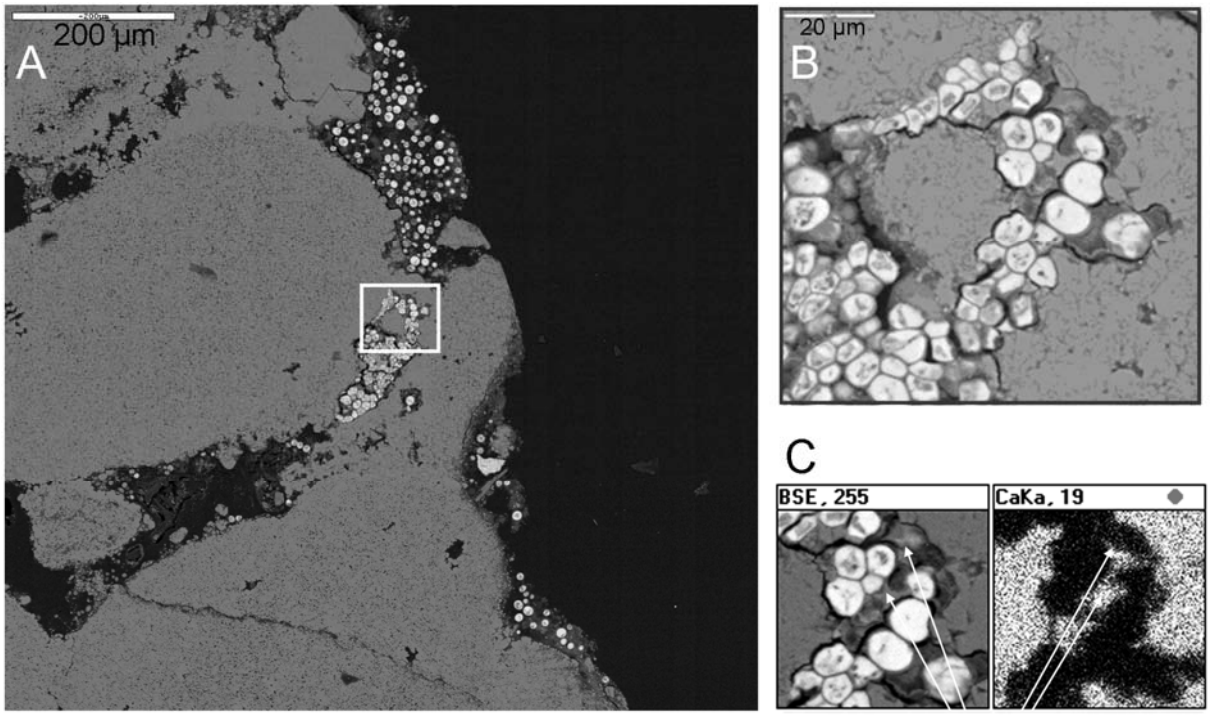

Fig. 6.2. SEM-BSE images of phototrophic microorganisms in PF samples illustrating: A) epilithic microorganisms randomly scattered on the stone surface and the likely depths endolithic cells penetrating the stone through the accessible void spaces; B) detail from 6.2A showing compact cell aggregates of the endolithic colonisation; C) distribution map of Ca showing the dissolutions features of the calcite in the endolithic microhabitat analysed by EDS microanalytical Line-Scan analysis.

Yet, considering PF samples, SEM-BSE observations showed grains with cubic crystalline habit forming concentric or dispersed aggregates (Fig. 6.3A). These grains were mainly observed on the surface of the stone but they were also found in the interior (at a depth of several mm), as shown in Figure 6.3B,C. The chemical composition of these grains, confirmed by EDS, was the same in each case, indicating they were deposits of iron oxides-oxyhydroxides. Further details on their characterisation are presented in section 6.3.2.

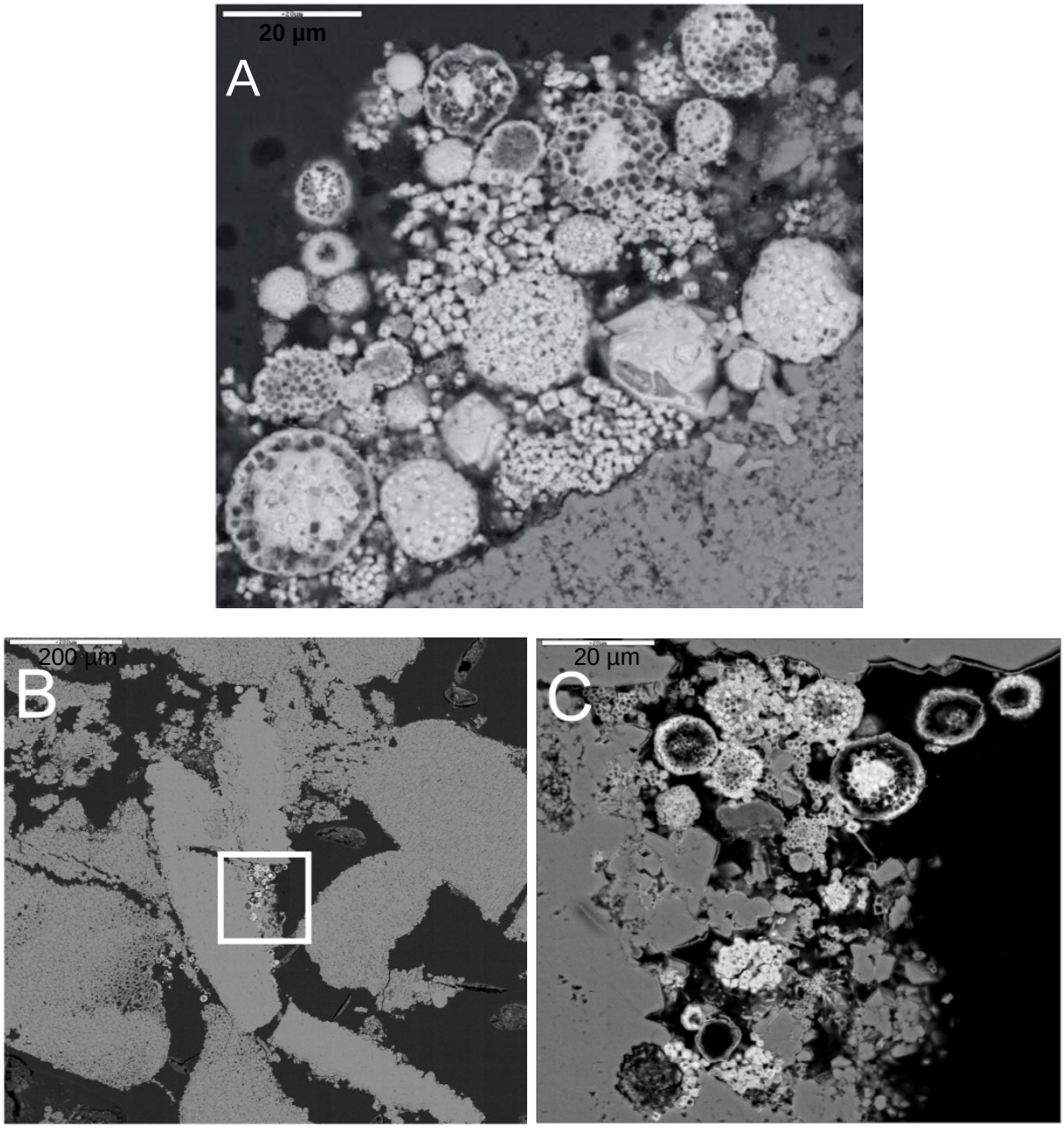

Fig. 6.3. SEM-BSE images from PF samples depicting: A) grains with cubic crystalline habit forming concentric or dispersed aggregates on the stone surface; and B) in the interior; C) enlarged view from image 6.3B.

Polished sections of SC samples examined by SEM-BSE showed randomly scattered cells on and within the pores (80 – 100 µm from the surface) of SC biocalcarenite together with calcite grains (Fig. 6.4). Figure 6.5 showed cubic crystalline aggregates, similar to those detected in the PF samples.

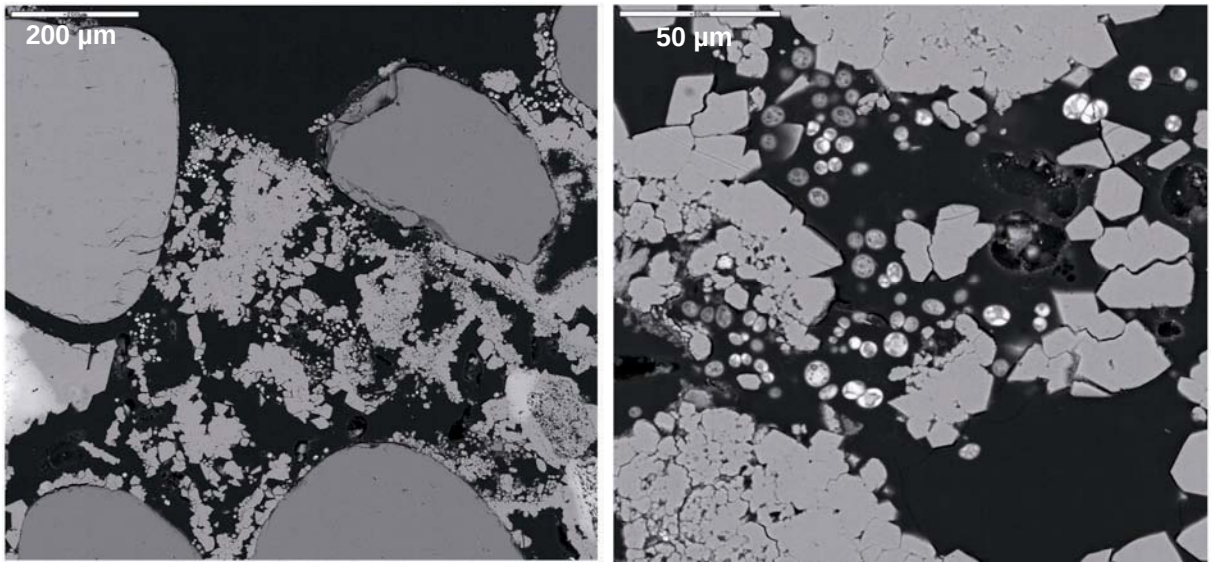

Fig. 6.4. SEM-BSE images from SC samples showing randomly scattered cells within the pores of the calcarenite together with calcite grains.

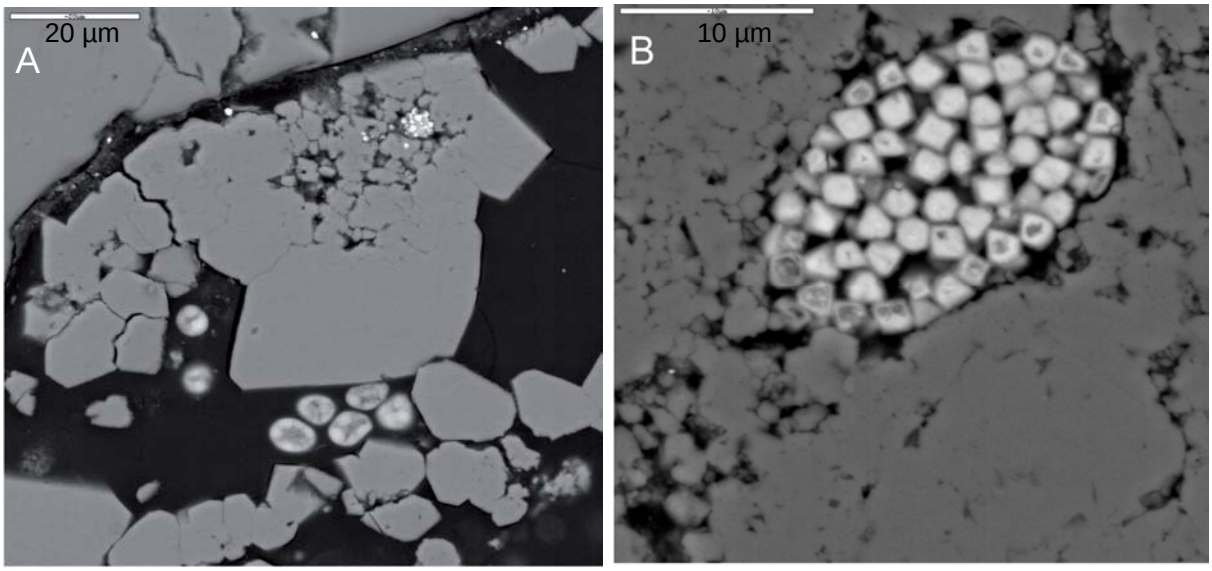

Fig. 6.5. SEM-BSE images from SC samples showing: A) cubic crystalline aggregates within the calcite grains; B) close view of the cubic crystalline aggregates.

SEM-BSE observations of vertically fractured samples of PL lithotype showed the development of microbial cells mainly on the surface of the samples (Fig. 6.6). It was also noticed the physical action of growing microorganisms on this samples, comprising the breaking of surface layers due to microbial adhesion and development between particles of the substratum (Fig. 6.6B). In contrast to PF and SC samples, cubic crystalline aggregates were not observed on this lithotype.

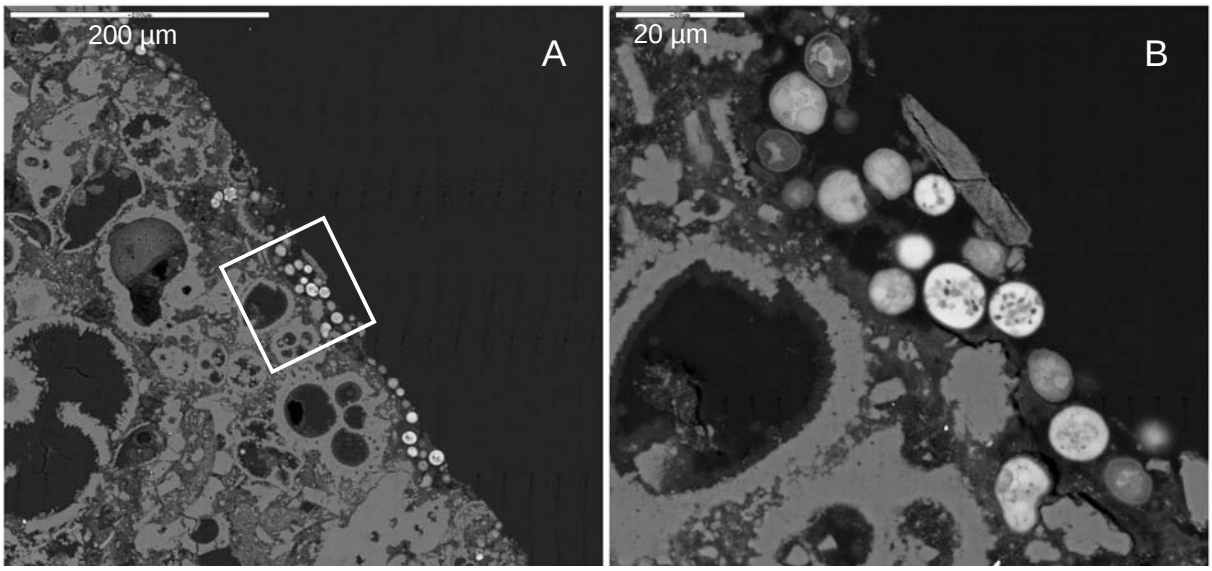

Fig. 6.6. SEM-BSE images from PL samples showing: A) the epilithic microbial colonisation, in which cells are distributed on the surface of the sample or very close to the surface; B) close view of the microbial cells showing disaggregation of the calcite grains.

Confocal laser scanning microscopy revealed irregular distribution of phototrophic microorganisms on the SC and PF samples. Photosynthetic pigments, chl*a* and phycobilins, have natural red autofluorescence emitted at 590-800 nm and excited at 543 nm and 633 nm. Maximum intensity projection of pigment fluorescence of unicellular phototrophic microorganisms is displayed as bluish colour and irregularly distributed in SC sample (Fig. 6.7). Cells with a high red fluorescence indicate active growth, which was clearly noticed in PF sample as an intense blue colour more than in SC (Fig. 6.8). Figure 6.8 is a three-dimensional image, which is divided into three frames that represent the maximum intensity projection for the x-y (main frame), x-z (lower frame) and y-z (right frame) planes. This CLSM image evidences the differential distribution in depth of the microorganisms in the sample, revealing that phototriphic cells penetrate several micrometers under the surface.

Moreover, in Figure 6.8 it is clearly evidenced the localisation of active growth (intense blue) into the stone rather than near the surface, where the cells showed yellowish-greenish colour, indicating higher concentrations of carotenoids on this surface. Inherent fluorescences other than pigment fluorescence such as $CaCO_3$ fluorescence of the carbonate substrata were also detected, which is depicted in Figures 6.7 and 6.8 as whitish-greyish colour.

Bluish colour cells were also observed in higher amount for PL samples by CLSM (Fig. 6.9). Three-dimensional projections revealed randomly distribution of the cells on the surface of the sample or very close to the surface, as also observed by SEM-BSE analysis.

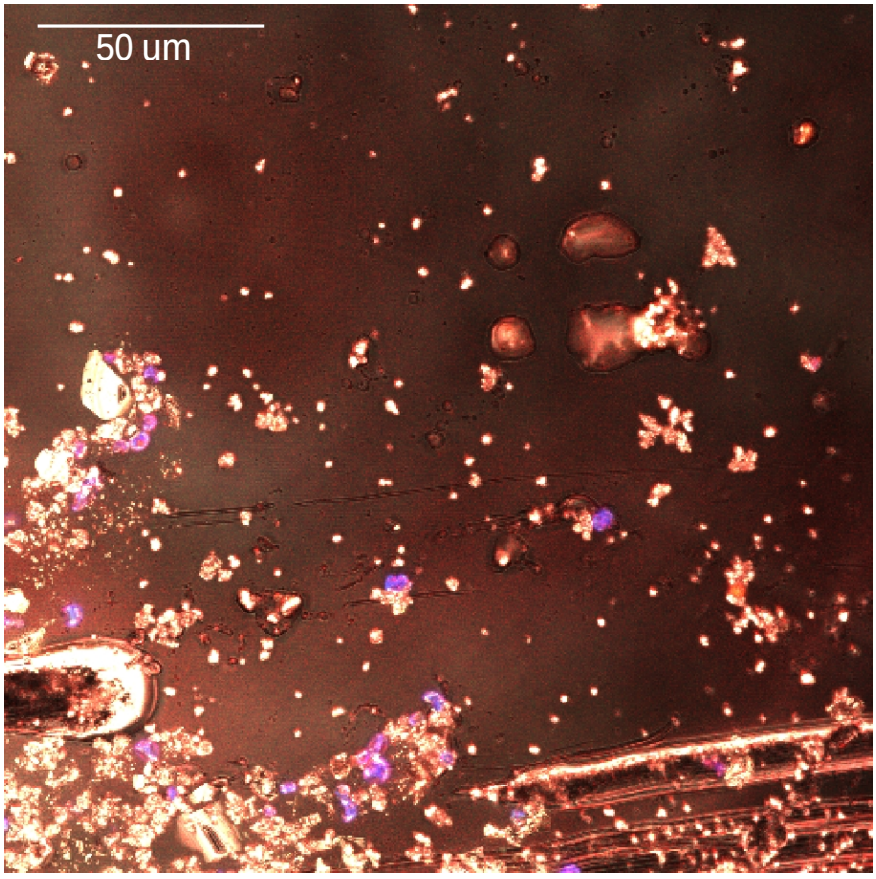

Fig. 6.7. Three-channel maximum intensity projection of pigment fluorescence of unicellular phototrophic microorganisms in SC sample. It consists of a two-dimensional compound image of x-y optical selected section of acquisition.

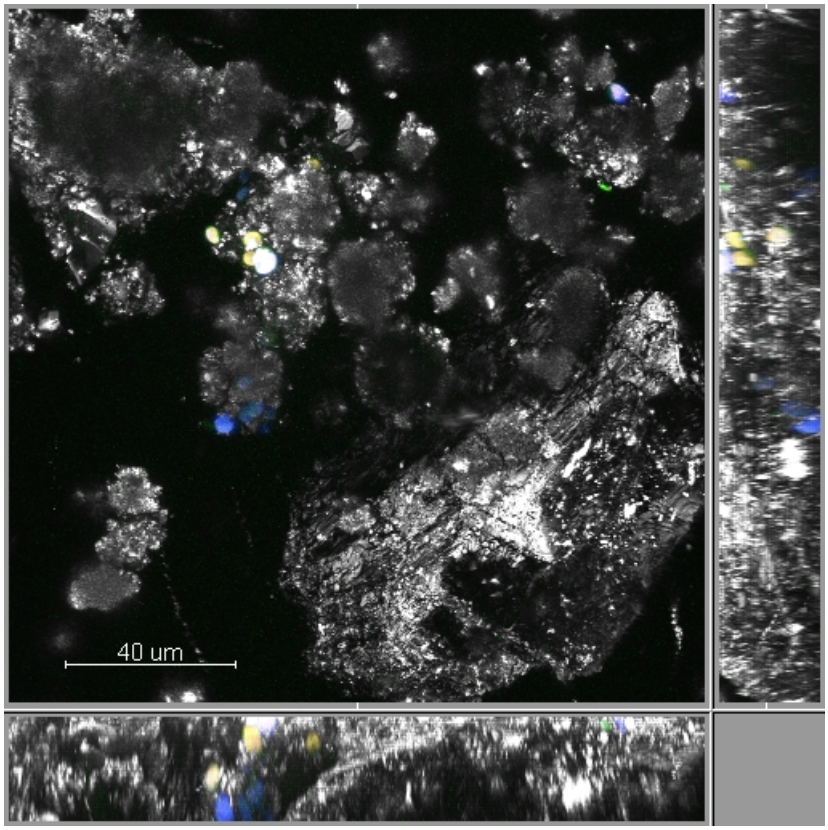

Fig. 6.8. Three-dimensional extended focus projections in x-y, x-z and y-z views of a selected fragment of the PF sample.

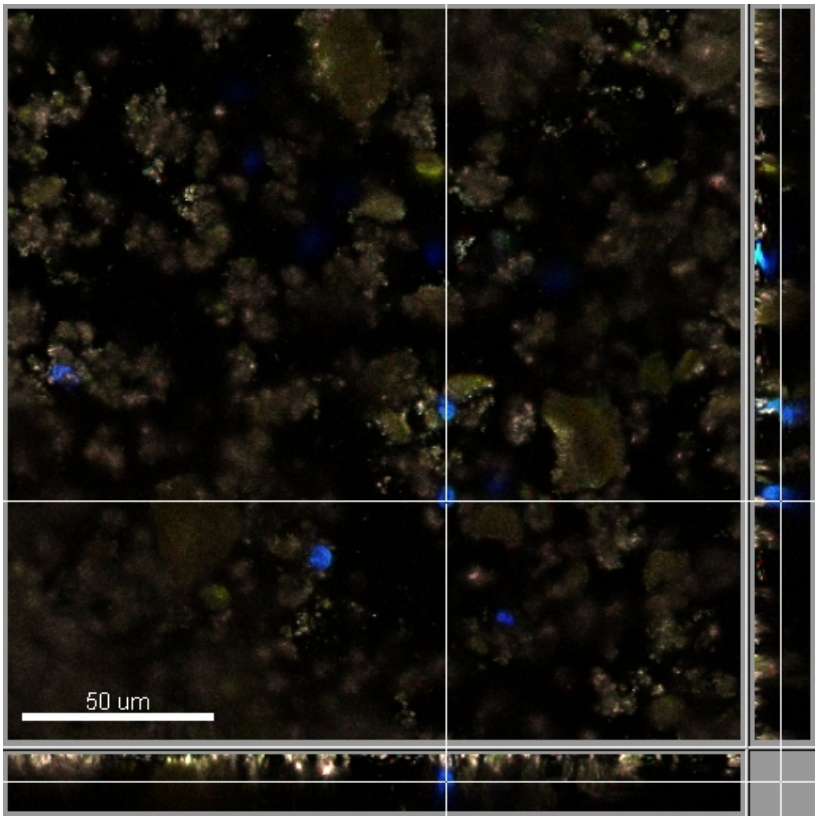

Fig. 6.9. Three-dimensional extended focus projections in x-y, x-z and y-z views of a selected fragment of the PL sample.

6.3.2. Biocalcarenite mineralogical and micromorphological characteristics

6.3.2.1. X-ray diffraction

The bulk mineralogy of the non-inoculated biocalcarenite sample PF comprised calcite (99%) and quartz (1%). K-feldspar, muscovite, biotite, granada, siderite, pyrolusite, clay minerals, goethite were the associated minerals that occur in vestigial amounts (< 1%). In the bulk colonised sample, calcite (99%), quartz (1%), and both goethite and pyrolusite (< 1%) were the identified minerals. This last sample was separated by hand-picking for some mineral phases which were brown-black in colour, with sub-metallic lustre and with very good cleavage. These mineral phases were analysed from the interior of a stone sample fissure showing yellow pigment zones, visible to the naked-eye and also reddish dots. The bulk mineralogical composition of this concentrated sample was: calcite (86%), quartz (3%), mica and clay minerals (< 1%), maghemite (1%) and hausmannite (10%).

Taking into account that poorly crystalline hydrous iron oxides (goethite), anhydrous oxides of iron (maghemite) and manganese minerals usually give even poorer diffraction patterns with fewer broader weaker reflections (Brown, 1980), the interpretation of the obtained XRD patterns leaded us to consider that pyrolusite (MnO_2) was identified by its diagnostic line at 3.16 Å, followed by the reflections at 2.42, 2.21, 2.13, 1.98 and 1.56 Å. Other reflections were coincident with those of calcite. The *d* values of about 4.93 Å, 2.77 Å, 2.49 Å, 2.46 Å, 1.576 Å and 1.544 Å resemble those of hausmannite ($Mn^{2+}Mn_2^{3+}O_4$). Goethite (α-FeOOH) was identified by its peaks at 4.17-4.18 Å and 2.69-2.70 Å. The behaviour of the reflections indicated the presence of one disordered goethite. Maghemite (γ-Fe_2O_3) was identified by its more intense reflections at 2.519 and 1.474 Å, as well as by smaller and broader reflections at 2.95, 2.086 and 1.604 Å.

6.3.2.2. SEM-EDS analysis

The biocalcarenite morphological characterisation was carried out on the PF colonised stone fragments. The selected fragments for XRD were the same for SEM-EDS analysis to enable comparing stone substratum mineralogy and the poorly crystalline mineral phases identified by XRD, in particular iron oxides-oxyhydroxides and manganese minerals. The difficulties rose in identifying Mn oxides from XRD could be exceeded by combining both visual identification (brown-black in colour mineral phases) and SEM-EDS analysis.

Figure 6.10A,B shows the biofilm deposition in an endolithic microenvironment of the biocalcarenite with Fe and Mn reniform coats associated with kaolin minerals. Figure 6.11A,B depicts clumps of Mn oxide and clay minerals (smectite) coating a massive calcareous fissure.

SEM-EDS study confirmed the goethite occurrence owing to the presence of needle-like shapes (Fig. 6.12). Goethite, identified by XRD as very poorly crystalline phase, was associated with ferrihydrite, which appeared as very small spherical particles coating faces and edges of calcite crystals (Fig. 6.13A). XRD patterns of ferrihydrite were not identified (since the presence of two broad bands with maxima at angles corresponding to d = 2.5 Å and d = 1.5 Å attributed to ferrihydrite were not observed), but the morphology of the iron-rich coatings most likely suggests its presence. Figure 6.13A illustrated one globular aggregate (particle size 6 μm diameter) of calcite grains surrounded by a likely biogenic irregular iron-film. Figure 6.13B showed other globular aggregate (particle size 15 μm diameter) of calcite grains, similar to the pyrite framboidal morphology. All the particles of this aggregate were Fe-richer than Ca-rich. Some Al and Si were also analysed in this aggregate. On the left side of the Figure 6.13B a biogenic porous round particle (10 μm diameter) was observed, like those referred by Krumbein (1992), Leite Magalhães et al. (1998) and Leite Magalhães (2000).

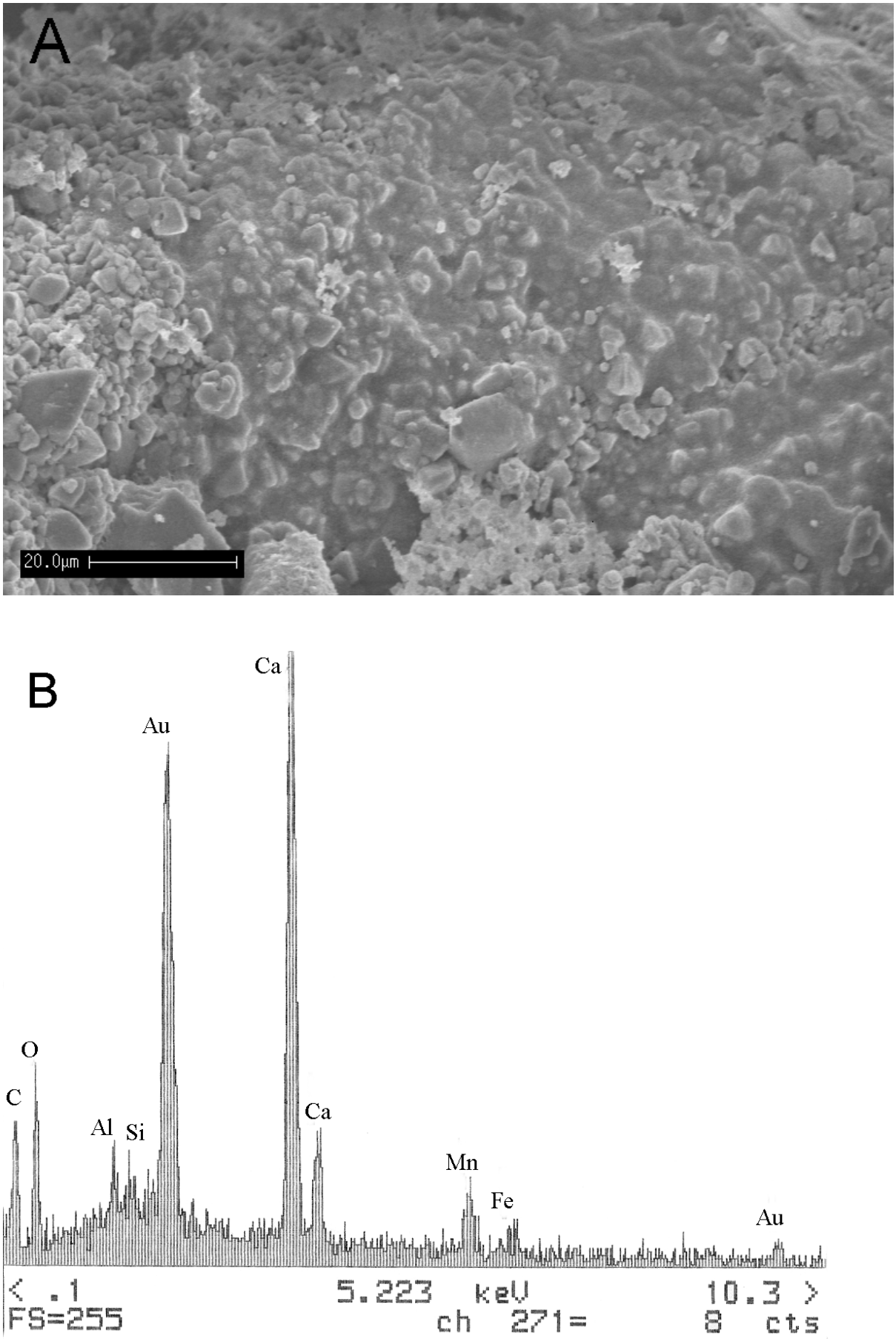

Fig. 6.10. A) SEM image of non resin-cast samples of PF lithotype showing a biofilm deposition with Fe and Mn in its composition; B) EDS spectrum performed for this sample area.

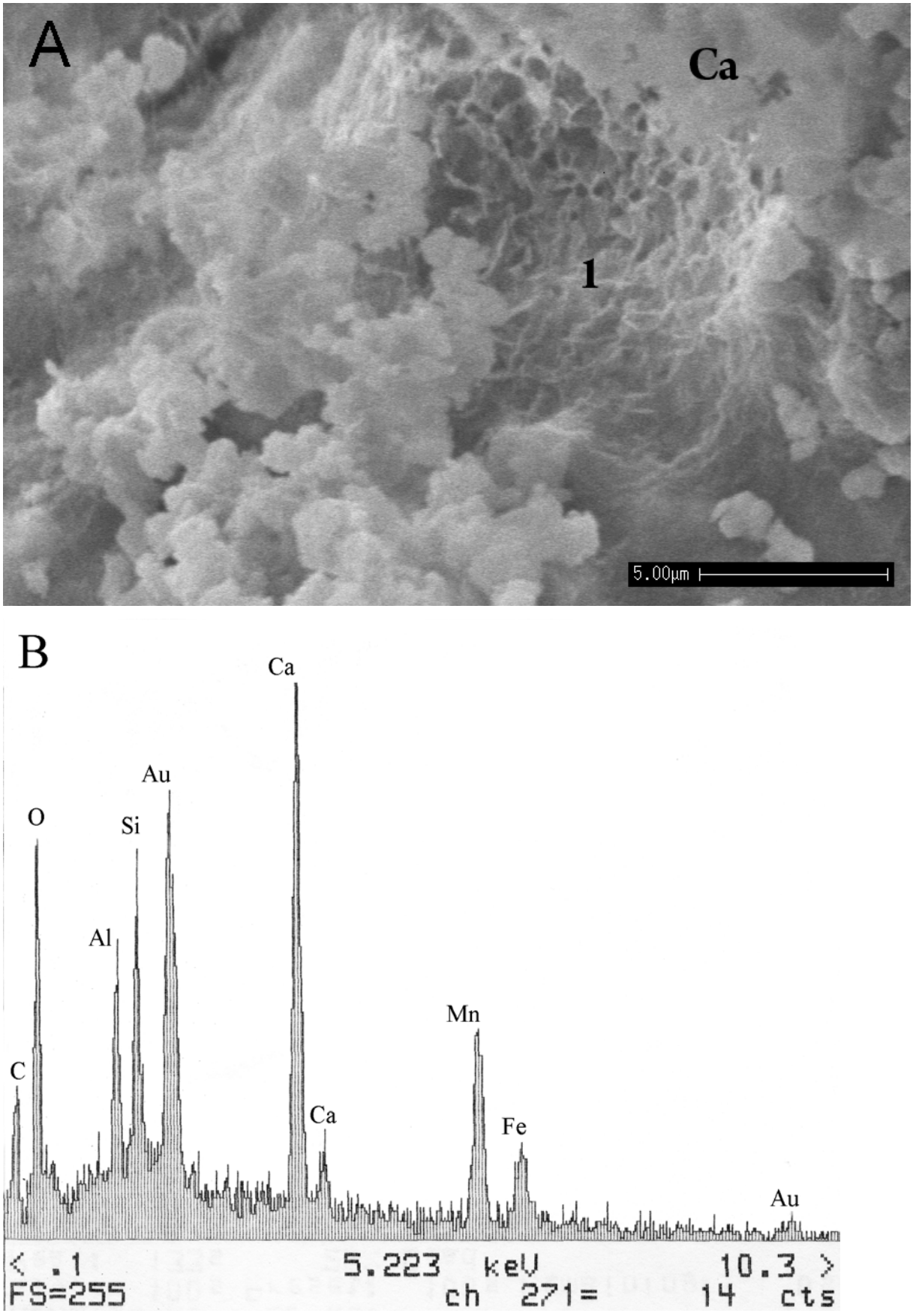

Fig. 6.11. A) SEM image of a Mn oxide and clay minerals coating a calcareous (Ca) fissure in the PF lithotype; b) EDS spectrum obtained in position 1 from image 6.11A.

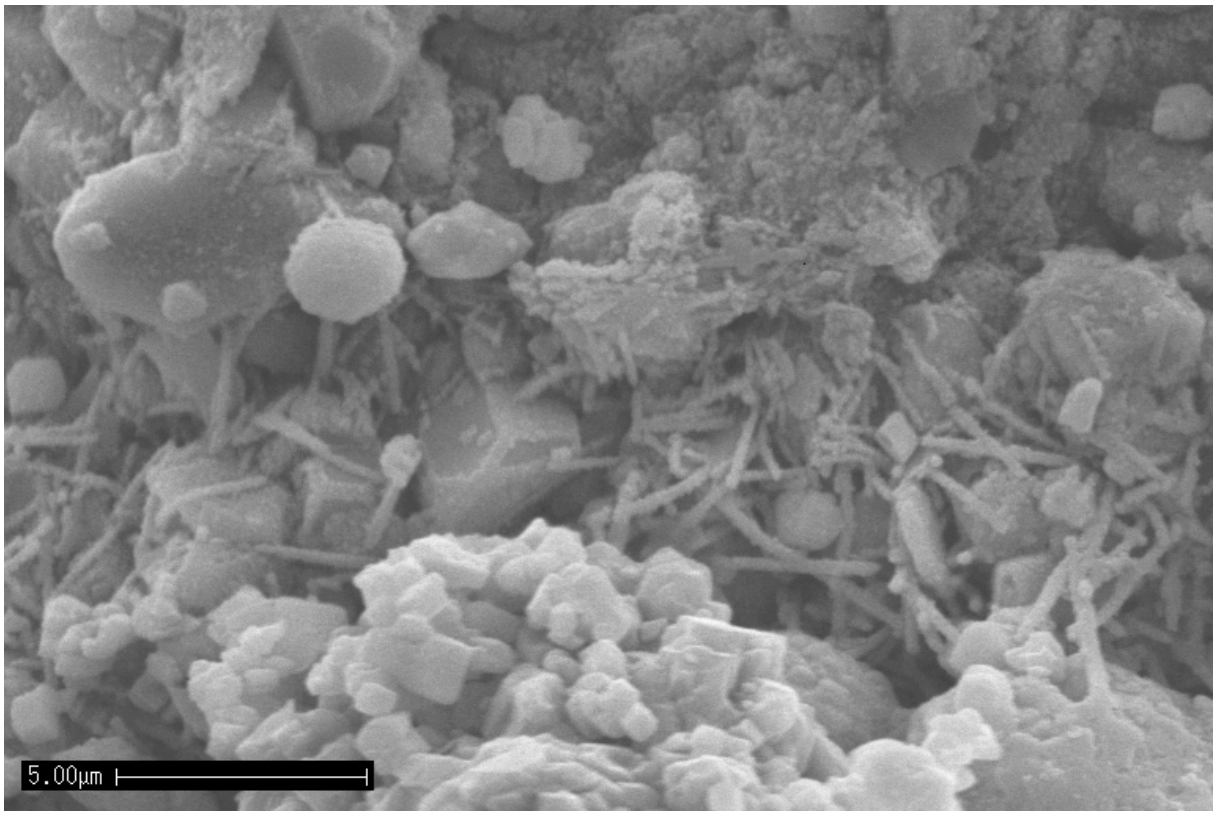

Fig. 6.12. SEM image of colonised PF lithotype presenting needle-like shaped goethite and very small iron-rich spherical particles, mostly likely ferrihydrite.

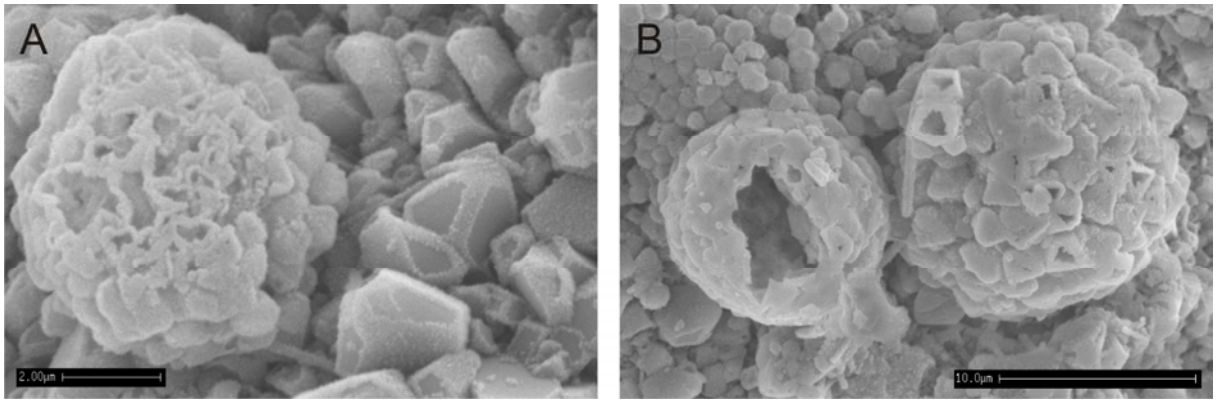

Fig. 6.13. SEM images of PF lithotype showing: A) calcite crystals coated by iron-oxyhydroxides and a globular aggregate of calcite grains surrounded by an iron-film; B) one globular aggregate of calcite grains with iron-rich coating and other porous round particle, likely biogeneous.

6.4. Discussion

The potential for damage of the stone substrata by phototrophic microorganisms was demonstrated in this experiment. The multidisciplinary approach that used different microscopic techniques, namely, SEM-BSE, SEM-EDS and CLSM, as well as XRD analyses revealed the close association between microorganisms and rock alteration processes clearly reflecting the biological contribution to these deterioration phenomena. Features for the characterisation of biofilm distribution were obtained from the various microscopic images, corroborating the formation of phototrophic biofilms within the stone substrata for PF and SC samples, and merely on the surface for PL. Such images clearly evidenced endolithic spatial distribution of microorganisms into the stone samples of PF and SC and the presence of EPS. Moreover, the development of the microorganisms within the samples indicates their strategy of response to the exposure conditions conducted during the bioreceptivity experiment. The observation of pigment autofluorescence *in vivo* by CLSM allowed the detection of phototrophic microorganisms on and within the samples. The use of the CLSM revealed to be of great interest to study the distribution of microorganisms on and within lithic substrata in which the microbial relationship, tri-dimensional structure and pattern of attachment should be preserved. The penetration of unicellular cyanobacteria and algae into the stones and the diffusion of EPS led to biogeomechanical and biogeochemical alterations. De los Ríos et al. (2004) referred biogeomechanical and biogeochemical processes associated with epilithic and endolithic microorganisms detected at the convent of Santa Cruz la Real (Segovia, Spain). Due to the inoculation procedure carried out for the stone bioreceptivity experiment, it was observed that the cells were dragged into the rock through their macroporosity (a purely physical process) and thus, they cannot be considered as endolithic active-colonisers but rather, they were passively installed there by the percolating inoculum. However, the observed small cavities actively created by endolithic microorganisms in the calcite crystals of PF samples revealed the interaction between the microorganisms and the substratum. As a result of biogeochemical activity the stone was probably dissolved due to the release of organic acids by the cells. These chemical effects were visible in places where the cavity harboured the microorganisms and took on the shape of the cell or colony. This substratum-altering capacity might suggest an euendolithic niche, even though

some components of the biofilm were cryptoendolithic since they seemed to be occupying pre-existing cavities in the stone.

Biogeophysical deterioration was clearly evidenced for the PL lithotype, instead of chemical actions which were not detected. SEM-BSE images revealed the potential mechanical impact of phototrophic biofilms which can be attributed to the increased mass of microorganisms as they grow. Furthermore, the detection of bluish colour cells by CLSM on the surfaces of PL samples indicated active growth, which is in fair agreement with the increase of photosynthetic biomass detected by *in vivo* chl*a* fluorescence technique and digital image analysis after 90 days-incubation time (see section 5.3.2.1 – chapter five).

In the context of the mineralogical and micromorphological characterisation of PF lithotype, the cubic aggregates observed in Figures 6.3 and 6.5 were considered to be maghemite (γ-Fe_2O_3) and hausmannite ($Mn^{2+}Mn_2^{3+}O_4$), which are usually of crystal cube-morphology and square-shaped, respectively. Since several manganese and iron minerals are essential for bacterial cell metabolism and are often associated with clays and iron oxides in soils and other environments (Dixon, 1977; Brown, 1980; Krumbein, 1983; Dorn, 1998), concomitant precipitation of Fe-Mn oxides must be considered in this biogenic microenvironment. However, manganese minerals, hydrous and anhydrous iron oxides are usually poorly crystalline and often show fewer reflections (Brown, 1980), as occurred in this study. According to Brown (1980), some difficulties arise in recognising these poorly crystalline hydrous iron oxides (goethite, ferrihydrite), anhydrous iron oxides (maghemite) and manganese minerals because they often show fewer reflections or they occur in small amounts in the samples. The XRD patterns of some Mn oxides and hydroxides obtained for PF samples were similar and suggested that the materials were structurally related. The scarcity of the manganese minerals and the absence of peaks could hide the presence of mineral mixtures. Nevertheless, the diffuse nature of the XRD patterns of Fe-Mn oxides-oxyhydroxides and the coincidence of the diagnostic reflections with those of other minerals could be performed in more detail, following some concentrate pre-treatment (Dixon, 1977).

Previous investigations have shown that in spite of the importance of Mn oxides in the environment, the molecular mechanisms, rates, intermediates, and products of Mn oxide biomineralisation are poorly understood. Even the relationship between biotic and abiotic Mn oxidation cycles is not well documented (Bargar et al., 2000).

However, in a recent work carried out by Fischer et al. (2008) about a biologically mediated mineral reaction, bioreduction and dissolution of birnessite, a layered $Mn^{3+,4+}$ oxide and the concomitant precipitation of rhodocrosite ($Mn^{2+}CO_3$) and hausmannite ($Mn^{2+}Mn_2{}^{3+}O_4$) was observed, using both synchrotron and conventional X-ray sources.

In this study, mineralogical data showed the presence of pyrolusite (MnO_2) in the non-inoculated stone, whereas hausmannite ($Mn^{2+}Mn_2{}^{3+}O_4$) was the Mn oxide identified by XRD in the colonised stone samples. The divalent manganese form is soluble and the more stable tetravalent form, usually represented by the dioxide MnO_2, is insoluble. Thus, the availability of Mn from MnO_2 and the microbial activity alter the Eh/pH of the microenvironment and indirectly modify the valence of manganese. This process is not necessarily cell associated and may occur at considerable distances from the cell (Krumbein, 1983). According to this author it is not surprising that manganese transformations occur as an indirect consequence of microbial growth and metabolism. Probably, the precipitation of hausmannite (Mn II, III) was conceivable in such particular endolithic environment. Figures 6.10 and 6.11 are one of the evidences of the biomineralisation due to: (i) presence of a biofilm deposition with Fe and Mn in its composition (Fig. 6.10A,B); (ii) cyanobacteria remains on a fissure, yellow-brown in colour, coated by Mn oxide and clay minerals (Fig. 6.11A,B).

XRD and SEM-EDS studies allowed the identification of goethite and maghemite. In addition to these oxides-oxyhydroxides, a poorly crystalline natural hydrated iron oxide, which is analogous to the so-called “colloidal ferric hydroxide”, named ferrihydrite (Brown, 1980), may be responsible to the observed coatings depicted in Figure 6.13. Brown (1980) referred that materials commonly formed by bacterial oxidation of ferrous solutions, give similar XRD patterns to ferrihydrite. According to Robert (1993), some bacteria use both oxidation-reduction reaction energy and carbon for the soluble Fe transportation. Successive fixation of Fe onto the exopolysaccharides excreted by the microbial community creates a capsule involving the cells and forming ferrihydrite, which can develop to iron oxide after cells death. Other relevant reactions governed by bacteria concern iron and manganese reduction or oxidation (Gonzalez et al., 1999).

These chemical transformations related with biomineralisation showed that the chemical composition of the lithic substrata, in particular, the presence of some

elements, are important for the development of biogeochemical deterioration. Differences in chemical composition were observed for the five limestone types, in which PF and SC were the only lithotypes exhibiting MnO (see Table 5.3 from chapter five). Moreover, they were both the most bioreceptive lithotypes, depicting the highest concentration of chl*a* mainly inside the samples. Thus, the manganese transformations detected on PF and also conceivably present on SC samples may suggest a preferential growth of phototrophic microorganisms within these lithotypes due to Mn availability. Nevertheless, from the results of this work the petrophysical properties seemed to play a major role particularly on the anchoring and settlement of phototrophic colonisation on the limestone substrata.

6.5. Conclusions

This study aimed to assess the formation of photosynthetic biofilms within different natural stone limestones, and to analyse their biogeophysical and biogeochemical deterioration potential. Microscopy investigations were carried out to study relationships between microorganisms and the mineral substrata. The methodology applied in this work corroborated a successful survival strategy of phototrophic microorganisms inside endolithic microhabitat, which increased intrinsic porosity by active mineral dissolution. These findings helped to explain: (i) the presence of mineral like iron derivatives (e.g. maghemite) around the cells and intracellular; (ii) locally enhanced moisture availability by the occurrence of clay minerals (kaolinite and smectite) stimulating microbial growth; (iii) the role of Mn oxides, in particular by the precipitation of hausmannite, manganese (II, III) suggesting manganese transformations related to biomineralisation.

In conclusion, this study shows for the first time a laboratory-induced biogenic deterioration of limestones caused by phototrophic microorganisms, and associated biomineralisation.

CHAPTER SEVEN

Concluding remarks

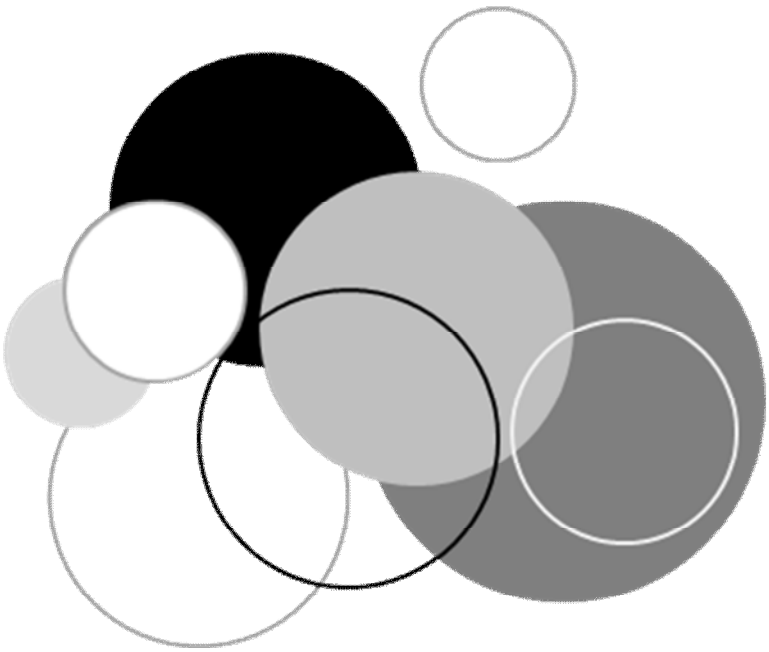

CHAPTER SEVEN

Concluding remarks

7.1. Conclusions

This thesis dealt with different aspects of biodeterioration of limestone substrata caused by the growth of phototrophic microorganisms. The experimental approaches displayed through the different chapters of this thesis were developed in accordance with the objectives proposed for this work. Initially, the identification of cyanobacteria and microalgae dwelling on limestone monuments from Portugal, Spain and Italy has been carried out through different analytical approaches. Subsequently, the primary bioreceptivity of five limestone types have been determined, evaluating the relationship between stone intrinsic properties and photosynthetic growth. Finally, the laboratory-induced endolithic growth has been appraised focusing particularly on the observed biomineralisation process.

In light of the results of this study, the following general conclusions can be reached:

- The literature review concerning cyanobacteria and green algae detected on stone monuments from the Mediterranean Basin revealed that a high biodiversity of species inhabit these monuments. The major diversity was determined within cyanobacteria, which revealed to be the most widespread group occurring on outdoor stone monuments due to their capacity to survive under extreme conditions. *Gloeocapsa*, *Phormidium* and *Chroococcus* were the most recurring genera among cyanobacteria. Nevertheless, chlorophyta was also very well represented, among which the genera *Chlorella, Stichococcus* and *Chlorococcum* were the most widespread green algae, being associated with all substratra considered. Limestone and marble were the lithotypes presenting the greatest diversity of cyanobacteria and chlorophyta.

- The use of molecular biology techniques was of great benefit for the study of phototrophic biofilms dwelling on the five stone monuments investigated in this work. The characterisation of the five biofilms allowed an accurate identification of the stone colonising microorganisms, as well as comparisons of their evolutionary growth under laboratory conditions. The biofilms from Orologio Tower (Martano, Italy) and Santa Clara-a-Velha Monastery (Coimbra, Portugal) were dominated by the microalga *Chlorella*, whereas the cyanobacterium *Chroococcidiopsis* was the dominating genus from Ajuda National Palace biofilm (Lisbon, Portugal). The biofilms from Seville and Granada Cathedrals (Spain) were both dominated by the cyanobacterium *Pleurocapsa*. The diversity of phototrophic species found in this study was similar to those observed in other studies carried out on historic buildings and monuments as reported in the literature review. DGGE was also a useful and elegant method for monitoring and profiling the changes in the community composition of the phototrophic cultures during 90 days of incubation. As a result, the selection of a multiple-species community culture was obtained due to the remarkable stability and development of the microbial components. The unicellular *Chlorella* alga was detected from PCR-derived 16S and 18S rDNA, revealing its abundance in the analysed samples, particularly, within the selected multiple-species community culture which was further used as inoculum for the laboratory-based colonisation experiments.

- The petrographic, petrophysical and petrochemical assays gave a good characterisation of the five studied limestone types (*Ançã* and *Lioz* limestones from Portugal, *San Cristobal* and *Escúzar* stones from Spain and *Lecce* stone from Italy) and it was possible to predict their susceptibility to biological deterioration. The high values of capillary water absorption coefficient, water vapour permeability, open porosity and surface roughness obtained for PL, PF and SC seem to affect notably their primary bioreceptivity, by providing high amount of water availability for microbial colonisation. In contrast, the physicochemical properties of CL seem to render it unsuitable as habitat for colonising organisms.

- During the experimental work, accelerated stone colonisations were conducted using the cultivated Coimbra biofilm. The use of this community

culture allowed the development of phototrophic biofilms similar to those obtained on stone monuments. During the laboratory-based bioreceptivity experiment, a significant increase of photosynthetic biomass was achieved for SC and PF lithotypes, which occurred mainly inside the stone samples. The phototrophic community culture assayed seemed to be very sensitive to the intensity of light inside the chamber, limiting the epilithic growth on PL, CA and CL over the course of batch incubation.

§ The combination of chl*a* quantification techniques and digital image analysis was useful for the monitoring of photosynthetic biomass, providing qualitative and quantitative evaluations of phototrophic growth on the limestone samples. Digital Image analysis and *in vivo* chl*a* fluorescence are reliable, non-destructive techniques suitable for taking successive surface measurements of epilithic colonisation in the time course study. However, they are not suitable to detect and evaluate endolithic growth without destroying of the sample. In turn, the amount of chl*a* estimated by the *in vitro* technique allowed the quantification of the complete amount of photosynthetic biomass growing on and within the stone samples. However, this method is destructive and thus not suitable to time course screening studies on cultural heritage assets due to the excessive sampling required. Moreover, this technique is only reliable for biofilms with greenish colour appearance, because if a reduction of chl*a* and an increase of carotenoids occur the *in vitro* technique suggests cessation of phototrophic growth even if the community is in a good physiological state. Thus, it can be concluded that only with the combined analytical approach performed in this study an integral study of the phototrophic colonisation could be assessed.

§ The experimental set-up performed in this work was very useful to determine the primary bioreceptivity of the five selected lithotypes. The coarse-grained limestones, PF and SC, showed the highest bioreceptivity to phototrophic microorganisms, being strongly colonised by phototrophic microorganisms, especially inside the stone samples. The fine-grained limestones PL and CA, showed moderate bioreceptivity, being merely colonised on their surfaces. In contrast, CL was almost devoid of any primary bioreceptivity. Within the parameters assessed during the experimental set-up, the five limestone types were classified into the following bioreceptivity groups:

- High bioreceptivity: *Escúzar* (PF) and *San Cristobal* (SC) stones
- Moderate bioreceptivity: *Lecce* stone (PL) and *Ançã* limestone (CA)
- Low bioreceptivity: *Lioz* limestone (CL)

Thus, a bioreceptivity index can be established, following the decreasing order of susceptibility to biodeterioration: PF > SC > PL > CA > CL.

§ As the exposure conditions of the laboratory-based colonisation experiment were the same, the variable involved in the differences observed in terms of bioreceptivity must be related to the different intrinsic properties of the stone materials. The previous characterisation of the five lithotypes and the principal component analysis (PCA) allowed the correlation between the intrinsic stone properties assayed and the photosynthetic biomass. There was a good correlation between the petrophysical properties of the substrata, particularly, surface roughness and capillarity water absorption coefficient, followed by open porosity and water vapour permeability, and the photosynthetic biomass expressed by the concentration of chl*a*. The macroporosity and consequent surface roughness favoured the anchoring and establishment of phototrophic microorganisms within PF and SC lithotypes, providing suitable habitat for endolithic colonisation. Their high values of water absorption by capillarity and water vapour permeability could cause water to easily wet and penetrate through these porous limestones leading them to biodeteriorate more quickly under the laboratory conditions. The fact that water cannot flow easily through the less porous stone (CL) could render it unsuitable to photosynthetic colonisation under the conditions of the experiment. The moderate bioreceptivity observed for PL and CA was assumed to be due to excessive light intensity within the incubator chamber linked to their petrophysical characteristics. Moreover, nutrient stress could also influence their bioreceptivity, extending the adaptation state to the lithic substrata and originating the colour change of the cells from green to orange.

§ The post-experiment microscopy analyses consisting of epoxy-impregnated thin sections revealed that the bioreceptivity experiment induced endolithic growth on PF and SC stones. Consequently, physicochemical changes were observed within both lithotypes. Mineral particles were detached from the

stone matrix by the physicochemical action of the microorganisms. Mineral like iron derivatives (e.g. maghemite) around the cells and intracellular and the precipitation of hausmannite were identified in the assayed stone samples by XRD, suggesting manganese transformations related to biomineralisation and thus biogeochemical deterioration. Organic acids exudated from the microorganisms could act as chelating agents, which sequestered metallic cations from stone, such as Fe^{3+} and $Mn^{2+,3+}$, and precipitate on polysaccharidic sheaths of the microorganisms in the form of salts of maghemite and hausmannite (Fe-Mn oxides-oxyhydroxides).

§ The experimental procedures developed in this work contributed to achieving the main goal of this PhD thesis, as well as, all the proposed specific objectives. The accelerated stone colonisation experiments, including cultivation of phototrophic biofilms from limestone monuments, inoculation of five limestone types with a multiple-species phototrophic culture, incubation within a growth chamber and monitoring through different analytical approaches, provided important input for bioreceptivity studies. This work was mainly developed over three laboratories, DCR-FCT-UNL (Portugal), IST (Portugal) and IRNAS (Spain), which made possible this multidisciplinary work, bringing together expertises in different areas such as microbiology, chemistry, geology, ecology, diagnostics and conservation and restoration. Moreover, it should be mentioned that molecular biology techniques was implemented for the first time in the study of microbial communities dwelling on Portuguese stone monuments.

With a view towards the future conservation of deteriorated stone monuments, it is necessary to perform precise comparisons between the microflora present on different sites showing biodeterioration. It is obvious that a reliable characterisation of the present microorganisms is a prerequisite for such comparisons, as well as the relationships between microorganisms, mineral substrata and environmental conditions. The laboratory-based study of bioreceptivity to primary producers presented in this study is an important contribution to understand and predict the susceptibility and behaviour of new constructions using limestone as building stone. Three main recommendations with respect to prevention and treatment of microbial colonisation can be pointed out:

1. Special attention should be taking when using PF and SC lithotypes, with high surface roughness and water absorption by capillarity, as well as stone materials showing previous advanced weathering, for the construction of new buildings without previous hydrophobic treatments.
2. In the case of materials already placed in a structure, the exact identification of the colonising microflora, as well as, the assessment of the biodeterioration damage are of great importance since it will allow the determination of the colonisation stage, the type of bioreceptivity and the design of integrated intervention with respect to a long-term prevention of respective stone monument. Therefore, the benefit of a multidisciplinary evaluation with the complementary cooperation of conservators and scientists in the diagnosis and handling of the biodeterioration effects are necessary to its conservation.
3. The control and eradication of phototrophic biofilms on the stone surfaces are strongly recommended. If biocidal treatments cannot be avoided, it should be applied preferably during the first stage of colonisation to prevent the development of ecological succession. Great care should be taken, when using biocides, to applying the minimum concentration which is less harmful for the construction environment and human health. As an alternative to biocides, hydrophobic treatments can be applied to prevent water from coming into the stone by the use of organic or silico-organic products. It must be said that such products should meet a specific list of chemical, physical and aesthetic requirements.

7.2. Further perspectives

It is well known that stone monuments and cultural assets in general can be deteriorated by microorganisms. However, our knowledge on the processes and microbial communities involved is still fragmentary and this is linked to the complexity of biodeterioration processes. First of all, research dealing with biodeterioration of stone monuments has to take many variables (chemical, physical, biological) into consideration, which makes it very difficult to reach general conclusions. Secondly, biodeterioration can occur very slowly, which makes it hard to reach conclusions in a limited time frame. Thirdly, the limitations imposed by the conservation of the cultural asset require the minimum amount and size of sampling.

In this perspective, the following research needs can be summed-up:

- There is a clear need for a precise knowledge on the microbial communities associated with stone biodeterioration, which will help to choose the appropriate treatments and conservation strategies. Moreover, such research will allow the comparison of different microbial communities associated with different damages. In this context, future research should focus the taxonomic identification of dominant microflora dwelling on different and representative stone materials through accurate and reliable methodologies, such as molecular biology techniques. Thus, the enhancement of the application, through a suitable dissemination, of molecular biology techniques in the field of conservation and restoration of monuments is of great importance. Detailed knowledge on the species colonising historic buildings and cultural assets are of great interest not only concerning conservation practice, but also health and safety (including working conditions). Precise identification of microorganisms has also socio-economic value when decisions are made on the methods of renovation and the suitability of the historic buildings for residential or professional uses.
- Laboratory-based experiments should be frequently developed since they allow not only the prediction of stone biodeterioration but also the management of preventive conservation strategies. Laboratory experiments present the advantage of controlling environmental variables which simplifies the answering of important questions, particularly in the field of

stone biodeterioration. These experiments are prerequisite in the diagnosis of monuments and in the design of effective treatments for eliminating active microbial communities, since they allow an affordable evaluation of the efficacy of biocides and cleaning treatments, as well as the validation of the methods for colonisation monitoring.

§ Bioreceptivity is an important concept in the conservation and restoration of stone monuments. Future research will focus on stone bioreceptivity experiments of different stone types in order to determine an index of bioreceptivity. For that, a standardised laboratory protocol for evaluating stone bioreceptivity will be compulsory, since it will allow the creation of a database concerning the primary bioreceptivity of lithotypes applied on building constructions. A growing database could offer a quick and powerful guide to end-users, such as, architects, engineers, conservators and restorers, for the selection of appropriate lithotypes to be used in future constructions, as well as, for the development of conservation strategies.

§ Taking into account the results of this PhD work, future laboratory-based stone colonisation experiments should comprise longer incubation periods and environmental parameters should be settled according to the optimal conditions for the microorganisms growth. Thus, previous physiological studies concerning different experimental conditions should be tested, such as different light intensities, temperatures and pHs. Moreover, representative organism(s) of the geographic region to which the stone material will be exposed should be used. The inventory of the microorganisms performed in this PhD will allow the selection of the microorganisms to be used as inoculum.

§ Finally, multidisciplinary research bringing together researchers in different scientific areas, not only will improve the knowledge in the field of stone biodeterioration, but will also assure the transfer of technology from the research community to the conservation/restoration community, providing strategies for minimising biodeterioration, and the development of new sustainable treatments and research initiatives based on nanotechnology.

Resumo

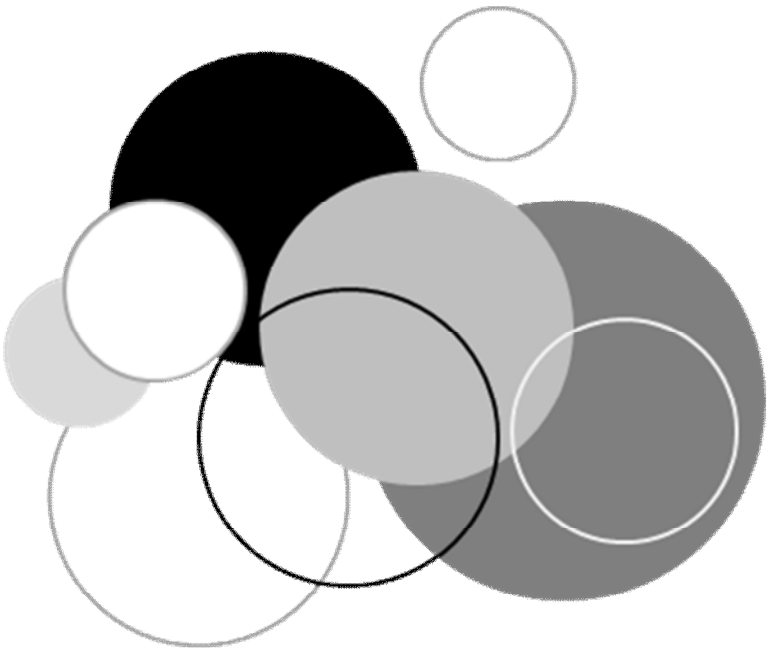

RESUMO

A conservação de monumentos e edifícios históricos que constituem a herança de um país é um desafio científico actual, tanto do ponto de vista económico como cultural. O presente trabalho surge do interesse e importância crescentes que os aspectos relacionados com a biodeterioração do património cultural construído em pedra apresentam, tanto a nível nacional como internacional, sendo um dos problemas mais complexos da área da conservação e restauro. Esta complexidade advém não só do facto de os factores ambientais externos (e.g. intensidade luminosa, humidade relativa, temperatura, contaminação atmosférica) não poderem ser controlados, mas também de as interacções entre os diferentes factores ambientais e os microrganismos serem bastante complexas.

Os microrganismos fotoautróficos (microalgas, cianobactérias e líquenes) são particularmente lesivos das superfícies expostas, devido à sua capacidade de sobreviver em ambientes inóspitos, possuindo provavelmente a maior importância ecológica como organismos pioneiros na colonização das superfícies pétreas (Ortega-Calvo et al., 1991a; Gómez-Alarcón et al., 1995; Lamenti et al., 2000; Tomaselli et al., 2000b; Bellinzoni et al., 2003). A facilidade de instalação destes microrganismos nos monumentos e edifícios históricos, esculturas em pedra e qualquer artefacto lítico deve-se à sua natureza fotoautotrófica: desenvolvem-se apenas com a presença de dióxido de carbono (CO_2), azoto (N_2) e vestígios de minerais, utilizando a luz como fonte de energia. Estes requisitos proporcionam o crescimento destes microrganismos em ambientes inóspitos, e promovem o enriquecimento do substrato com matéria orgânica, permitindo a instalação e desenvolvimento de organismos heterotróficos (Ortega-Calvo et al., 1992; Albertano et al., 2000; Lamenti et al., 2003, Crispim and Gaylarde, 2005).

A instalação e desenvolvimento das microalgas e cianobactérias nos materiais pétreos estão sobretudo condicionados pelas propriedades dos materiais, tais como rugosidade, porosidade e composição química das camadas superficiais (Guillitte, 1995; Tiano et al., 1995), condições arquitecturais (geometria da construção, sua orientação geográfica, lavrado das superfícies, etc.) e os factores ambientais do

local (Ariño et al., 2002; Bellinzoni et al., 2003). Estes parâmetros satisfazem as necessidades ecológicas e fisiológicas das espécies biológicas e determinam a intensidade e velocidade de desenvolvimento da colonização fotossintética, constituindo substrato adequado para o crescimento e acção corrosiva de algas e cianobactérias (Warscheid e Braams, 2000; Arino et al., 2002). A aptidão de um material para ser colonizado por um ou vários grupos de organismos foi definida por Guillitte (1995) como "bioreceptividade". Este conceito implica, como refere o autor, o estabelecimento de uma relação ecológica entre o material e o organismo colonizador. Assim, a bioreceptividade pode também ser definida como a totalidade das propriedades do material que contribuem para o estabelecimento, fixação e desenvolvimento da flora e/ou fauna. Nos materiais pétreos está sobretudo relacionada com as propriedades dos materiais, tais como, rugosidade, porosidade, capacidade de retenção de humidade e composição química das camadas superficiais (Guillitte, 1995; Tiano, 1998). O mesmo autor define ainda três termos de bioreceptividade: "bioreceptividade primária" referente à susceptibilidade do material para ser colonizado por organismos quando a pedra apresenta propriedades similares ou idênticas às do seu estado inicial (rocha sã). As características do material podem evoluir no tempo sob a acção dos organismos colonizadores ou outros factores, resultando num novo tipo de bioreceptividade, designada "bioreceptividade secundária". Qualquer actividade humana, como seja a aplicação de consolidantes, hidrófugos ou biocidas, também modificam as características iniciais ou secundárias do material, induzindo à "bioreceptividade terciária" (Guillitte, 1995).

A bioreceptividade de um material a um organismo pode ser avaliada através da inoculação artificial do substrato com a cultura desse organismo, incubando-o em condições óptimas para o seu crescimento. Desta forma pode ser determinado um índice de bioreceptividade que é expresso nas condições de máxima acessibilidade para o desenvolvimento desse organismo específico (Guillitte, 1995). Sob estas condições, é esperado obter-se uma manifestação máxima de bioreceptividade, a qual permitirá comparar os parâmetros de colonização biológica nos materiais (desenvolvimento e abundância das espécies) e relacioná-los com as características dos substratos pétreos que influenciam a bioreceptividade (e.g., porosidade, permeabilidade, rugosidade, composição mineralógica).

Este estudo procura contribuir para o aprofundamento do conhecimento da bioreceptividade diferentes tipos de calcário com presença importante no património cultural construído de países da Bacia do Mediterrâneo, em particular no que concerne à sua aptidão para serem colonizados por microrganismos fotossintéticos. O principal objectivo consistiu em estudar a bioreceptividade primária de calcários utilizados na Bacia do Mediterrâneo e avaliar a influência das suas propriedades no desenvolvimento de microrganismos fotossintéticos. Para atingir este objectivo foi necessário resolver algumas questões metodológicas/experimentais que nos levaram aos seguintes objectivos específicos:

1. Preparar um inventário das espécies de microrganismos fototróficos identificados em monumentos líticos de países da Bacia do Mediterrâneo, tendo em vista a comparação e tomada de conhecimento das espécies mais abundantes ocorrentes em calcários.

2. Recolher biofilmes fotossintéticos de monumentos em calcário localizados em países europeus da Bacia Mediterrânica, que apresentem condições climatéricas semelhantes, e identificar os seus principais componentes microbianos por técnicas de biologia molecular.

3. Cultivar os biofilmes fotossintéticos, compostos principalmente por cianobactérias e algas, acompanhando a sua evolução e progressão por DGGE, com o fim de seleccionar uma cultura fototrófica de várias espécies estável em condições de laboratório para posteriores ensaios de colonização de diferentes variedades calcárias.

4. Caracterizar do ponto de vista petrográfico, petrofisico e petroquimico diferentes tipos de calcário usados nos monumentos estudados numa tentativa de compreender a sua bioreceptividade primária e a relação entre os microrganismos fototróficos e as características intrínsecas dos substratos líticos.

5. Inocular as amostras calcárias dos cinco litótipos adquiridos em pedreiras com a cultura fototrófica seleccionada e incubar durante 90 dias numa câmara de incubação.

6. Monitorizar o desenvolvimento dos biofilmes fototróficos através da quantificação da biomassa fotossintética por meio de diferentes técnicas analíticas.

7. Avaliar a bioreceptividade primária dos litótipos testados e a influência das características petrofísicas e petroquímicas dos cinco litótipos na sua bioreceptividade.

8. Estudar os efeitos de biodeterioração induzidos pelos microrganismos fototróficos nas amostras calcárias e compreender as interacções entre estes microrganismos e os substratos.

9. Divulgar o estudo da bioreceptividade dos litótipos a utilizadores finais, tais como, conservadores/restauradores, arquitectos e engenheiros, bem como difundir as metodologias moleculares dentro do campo da conservação e restauro, especialmente no caso de Portugal. Isto envolve a contribuição a conferências cujo foco central é a conservação de monumentos e a publicação em revistas internacionais.

O trabalho experimental realizado para estudar a bioreceptividade primária de cinco calcários provenientes de países europeus da bacia do Mediterrâneo foi realizado em seis etapas diferentes:

i. Levantamento do estado actual do conhecimento relativo à biodeterioração dos materiais pétreos por microrganismos fotossintéticos:

   Uma profunda e exaustiva pesquisa bibliográfica na área de investigação do presente trabalho de doutoramento revelou-se de extrema importância para a obtenção de um domínio profundo, actual e detalhado de conhecimentos nesta área, bem como para a definição e aperfeiçoamento dos métodos e ensaios utilizados neste trabalho. No seguimento desta campanha bibliográfica foi elaborada uma revisão de literatura, na qual os dados qualitativos de uma grande variedade de cianobactérias e algas identificadas em monumentos da Bacia do Mediterrâneo foram sintetizados a fim de comparar de uma forma rápida e concisa as espécies que colonizam os diferentes monumentos pétreos. Cerca de 45 casos de estudos relativos a 32 artigos científicos publicados entre

1976 e 2009 foram analisados (Tabela 2.1). Seis distintos substratos líticos foram considerados nesta revisão: mármore, calcário, travertino, dolomia, arenito e granito. A maior diversidade foi detectada para a divisão das cianobactérias, sendo os géneros *Gloeocapsa*, *Phormidium* e *Chroococcus* os mais identificados (Tabela 2.2). A divisão das algas verdes (Chlorophyta) foi também bem representada, entre as quais os géneros *Chlorella*, *Stichococcus* e *Chlorococcum* foram os mais difundidos (Tabela 2.3).

ii. Identificação de microrganismos fotossintéticos colonizadores de monumentos em calcário, mediante técnicas de biologia molecular e técnicas microbiológicas:

O estudo de comunidades microbianas foi desenvolvido no Instituto de Recursos Naturales y Agrobiologia de Sevilla, Consejo Superior de Investigaciones Cientificas (IRNAS-CSIC). Este estudo consistiu na caracterização de comunidades fotossintéticas presentes em monumentos de Portugal, Espanha e Itália, construídos com diferentes tipos de calcário: pedra *Lecce*, calcário *Ançã*, calcário *Lioz*, pedra *San Cristobal* e pedra *Escúzar*. As comunidades de bactérias, cianobactérias e microalgas presentes nas amostras de biofilmes verdes foram recolhidas na Torre Orologio (Lecce, Itália), no Mosteiro de Santa Clara-a-Velha (Coimbra, Portugal), no Palácio Nacional de Ajuda (Lisboa, Portugal), na Catedral de Sevilha (Sevilha, Espanha), e na Catedral de Granada (Granada, Espanha) (Figura 3.1 e Tabela 3.1). A identificação dos microrganismos foi efectuada mediante extracção de ADN, amplificação dos genes de ARN ribossómico 16S(Fig. 1.6 and Tabela 3.2), electroforese em gel de gradiente desnaturante (DGGE) (Fig. 1.7), clonagem (Fig. 1.8) e sequenciação. A diversidade dos microrganismos fotoautotróficos encontrada neste estudo foi semelhante aquela observada em outros estudos realizados em monumentos e edifícios históricos, como relatado na revisão de literatura (Tabela 3.3). Os biofilmes da Torre Orologio (Martano, Itália) e Santa Clara-a-Velha (Coimbra, Portugal) foram dominados pela microalga *Chlorella*, enquanto que a cianobactéria *Chroococcidiopsis* sp. foi o género dominante no biofilme do Palácio Nacional da Ajuda (Lisboa, Portugal). Os biofilmes das catedrais de Sevilha e Granada (Espanha) foram dominados pela cianobactéria *Pleurocapsa* sp.

iii. Selecção dos microrganismos fotossintéticos para o estudo da bioreceptividade primária em laboratório:

Com o objectivo de seleccionar uma comunidade fotossintética estável em condições laboratoriais, os cinco biofilmes estudados na etapa anterior foram cultivados em meio de cultura líquido BG11 durante um período de 90 dias. A dinâmica do crescimento fotossintético ao longo do período de incubação foi monitorizada mediante DGGE (Figs. 3.5 – 3.9). A análise dos perfis de DGGE das cinco culturas permitiu verificar que a comunidade fotossintética mais estável e diversa ao longo do período de incubação foi a do biofilme do Mosteiro de Santa Clara-a-Velha (Coimbra, Portugal), acrescentando a sua facilidade e rapidez de crescimento em laboratório. Para uma completa identificação deste biofilme, as análises de biologia molecular foram complementadas com técnicas convencionais de microbiologia para o isolamento e caracterização morfológica das espécies do biofilme de Santa Clara-a-Velha (Fig. 4.4 e 4.5). Subsequentemente, a cultura fotossintética seleccionada foi inoculada em amostras de calcário *Ançã* e incubada numa câmara climática durante 90 dias (Fig. 4.1), com o objectivo de avaliar a sua proficiência como inóculo para posteriores ensaios de bioreceptividade primária. A colonização induzida em laboratório promoveu o desenvolvimento de biofilmes sobre as amostras pétreas semelhantes às patinas biológicas que ocorrem em monumentos pétreos (Fig. 4.6), demonstrando a eficiência da cultura fotossintética de Coimbra como inoculo de ensaios de colonização acelerada.

iv. Selecção e caracterização dos cinco tipos de calcário utilizados nos monumentos da Bacia do Mediterrâneo analisados na etapa ii:

Os litótipos seleccionados para o presente estudo corresponderam às cinco variedades calcárias usadas para a construção dos monumentos estudados na etapa ii. Estes materiais pétreos são representativos do património cultural imóvel específico da região onde afloram: calcário *Ançã* de Coimbra (Portugal), calcário *Lioz* de Pêro-Pinheiro (Portugal), pedra *San Cristobal* de El Puerto de Santa Maria (Cádiz, Espanha), pedra *Escúzar* de Granada (Espanha) e pedra *Lecce* da região de Lecce (Itália) (Fig. 5.1 e Tabela 5.1). Os blocos pétreos de cada litótipo foram adquiridos nas respectivas pedreiras, com as dimensões aproximadas de 50 (largura) x 16 (altura) x 20 cm (profundidade) e cortados em

provetes de 4.4 cm de diâmetro e 3 cm de altura. Em seguida foram efectuados os ensaios petrográficos, petrofísicos e petroquímicos; a caracterização petrográfica consistiu no estudo ao microscópio petrográfico de lâminas delgadas (30 µm de espessura) de cada um dos litótipos. Os ensaios petrofísicos com interesse para o presente trabalho foram o da porosidade aberta acessível à água, absorção de água por capilaridade, permeabilidade ao vapor de água e rugosidade das superfícies pétreas. Na maior parte dos casos, os processos de alteração dos materiais pétreos em obra dependem da circulação de água no meio poroso, pelo que estes ensaios são importantes para conhecer o comportamento dos materiais pétreos seleccionados quanto à sua bioreceptividade, alterabilidade e durabilidade. A composição química foi determinada com base em diferentes métodos de análise química, os quais permitiram classificar os cinco litótipos como calcários calcíticos (Chilingar, 1967). A caracterização petrográfica, petrofísica e petroquímica dos cinco tipos de calcário estudados permitiu prever a susceptibilidade de cada litótipo face à biodeterioração. Os factos mais notórios ao analisar os resultados obtidos nestes ensaios foram os elevadíssimos valores de porosidade aberta, absorção de água por capilaridade, permeabilidade ao vapor de água e rugosidade superficial da pedra *San Cristobal* (SC) e pedra *Escúzar* (PF) face aos do calcário *Lioz* (CL) (Tabela 5.2). Desta forma pode-se inferir que os calcários SC e PF serão mais susceptíveis às acções nefastas da água, e por conseguinte à colonização microbiana, do que o CL, o qual apresentará mais resistência à deterioração por agentes bióticos.

v. Ensaio de bioreceptividade primária de cinco tipos de calcário:

Para estudar a bioreceptividade primária dos cinco tipos de calcário, 27 provetes de cada litótipo, previamente esterilizados, foram inoculados com 750 µl da cultura fotossintética de Coimbra e incubados numa câmara de incubação durante 90 dias (Fig. 5.2). O desenvolvimento dos biofilmes nas amostras pétreas foi monitorizado mediante: (a) quantificação *in vitro* de clorofila *a* (chl*a*), a qual consiste na extracção deste pigmento num solvente orgânico (DMSO) e posterior leitura das absorvâncias num espectrofotómetro; (b) determinação da fluorescência de chl*a* *in vivo*, efectuada com um espectrofluorímetro adaptado com um cabo de fibra óptica, o qual permite a medição da fluorescência da chl*a*

sem a destruição das amostras; e (c) quantificação das áreas de cobertura biológica através de técnicas de análise digital de imagem. Estas técnicas podem ser definidas como uma metodologia de estudo recente sustentada em conhecimentos matemáticos e computacionais, permitindo, a partir do tratamento de imagens digitais (macroscópicas e microscópicas), a obtenção de informação numérica e gráfica (quantitativa e qualitativa). As técnicas de quantificação de chl*a* foram realizadas no Departamento de Conservação e Restauro (FCT-UNL), enquanto que as técnicas de análise de imagem foram efectuadas no IRNAS-CSIC. A combinação das três técnicas de quantificação de biomassa fotossintética proporcionou avaliações qualitativas e quantitativas do crescimento fotoautrófico levado a cabo nas amostras dos diferentes litótipos. As técnicas não-destrutivas, nomeadamente fluorescência de chl*a in vivo* e análise digital de imagem, demonstraram grande utilidade para a detecção e quantificação de biomassa fotossintética presente em superfícies líticas (colonização epilítica). No entanto, mostraram ser ineficazes na detecção de biomassa fotossintética presente no interior das amostras (colonização endolítica), visto serem técnicas de medida a nível de superfície. Por sua vez, a técnica de quantificação de chl*a in vitro* permitiu analisar a quantidade total de chl*a* presente na superfície e no interior das amostras, mas apresenta a desvantagem de ser uma técnica não destrutiva e, como tal, não aconselhada para estudos de monitorização de amostras do património cultural devido ao excesso de amostragem exigido. Assim, de acordo com os resultados obtidos mediante as três distintas técnicas de análise (Fig. 5.20, 5.21 e 5.23), os cinco tipos de calcário foram classificados nos seguintes grupos:

- Bioreceptividade elevada: Pedra *Escúzar* (PF) e Pedra *San Cristobal* (SC)
- Bioreceptividade moderada: pedra *Lecce* (PL) e calcário *Ançã* (CA)
- Bioreceptividade baixa: calcário *Lioz* (CL)

Este ensaio permitiu ainda avaliar a influência dos parâmetros específicos dos materiais pétreos na bioreceptividade primária desses materiais para microrganismos fototróficos. Assim, a intensidade da colonização biológica encontrou-se determinada pelos parâmetros petrofísicos dos materiais pétreos, nomeadamente pela rugosidade da superfície pétrea e coeficiente de absorção de água por capilaridade, seguidos da porosidade aberta e permeabilidade ao

vapor de água. As condições de exposição do ensaio também mostraram ser determinantes no desenvolvimento da colonização fotossintética sobre as amostras pétreas, em particular a excessiva intensidade de luz, a qual limitou o crescimento epilítico. Após 30 dias de incubação os biofilmes presentes na superfície das amostras modificaram a sua pigmentação, exibindo patinas laranja-acastanhadas. Estas mudanças cromáticas sugeriram uma adaptação às condições de luz e aos substratos líticos e não a cessão da colonização, uma vez que as técnicas de análise superficial revelaram um aumento da colonização epilítica, em especial nas amostras de PL e CA (Fig. 5.21 e 5.23).

vi. Análise da biodeterioração biogeofísica e biogeoquímica induzida pelos microrganismos fotossintéticos nas amostras pétreas:

Por último, análises de microscopia electrónica de varrimento, microscopia confocal e difracção de raios-X permitiram avaliar a biodeterioração biogeoquímica e biogeofísica induzida pelos microrganismos fotossintéticos nas amostras pétreas, com especial enfoque para o crescimento endolítico. As análises de microscopia electrónica foram levadas a cabo para avaliar a profundidade de penetração dos microrganismos no interior das amostras e estimar os danos causados após os 90 dias de incubação. Estas análises foram efectuadas no CENIMAT (FCT-UNL) e no centro de Ciencias Medioambientales – CSIC, em Madrid (Espanha), onde se efectuou a preparação de amostras biológicas e respectiva observação ao microscópio electrónico de varrimento em modo de electrões retrodifundidos (SEM-BSE). Análises de SEM e difracção de raios-X foram também efectuadas no Centro de Investigação Geológica, Ordenamento e Valorização de Recursos (CIG-R) da Universidade do Minho (Portugal). Por sua vez, a microscopia confocal (Confocal Laser Scanning Microscopy – CLSM) foi efectuada na Faculdade de Farmácia da Universidade Autónoma de Barcelona (Espanha), demonstrando ser uma técnica exímia para o estudo da distribuição dos microrganismos fotossintéticos e do seu efeito biodeteriorante. Os resultados obtidos neste estudo mostraram que o ensaio de colonização em laboratório permitiu o desenvolvimento de colonização endolítica nas amostras de PF e SC, o que levou a um aumento da porosidade intrínseca por dissolução mineral devido à excreção de ácidos orgânicos (Fig. 6.1). Estes exames microscópicos permitiram ainda observar a presença de biominerais, os

quais foram à actividade metabólica dos microrganismos fotossintéticos inoculados nas amostras pétreas (Fig. 6.3 e 6.5). Merece ser referido que neste estudo observou-se pela primeira vez crescimento endolítico induzido em laboratório, dando lugar a processos de biomineralização. Os ácidos orgânicos exsudados pelos microrganismos actuaram provavelmente como agentes quelantes, sequestrando catiões metálicos da pedra calcária, tais como Fe^{3+} e $Mn^{2+,3+}$, e precipitando-os sobre as bainhas celulares na forma de sais de hausmannite e maghemite (óxidos-oxihidróxidos de Mn e Fe, respectivamente).

Os resultados deste estudo experimental permitiram inferir que os calcários de *Escúzar* e de *San Cristobal* são os mais bioreceptíveis, seguidos dos calcários de *Lecce* e de *Ançã*, os quais apresentaram bioreceptividade moderada. O calcário *Lioz* mostrou ser o litótipo menos bioreceptível, apresentando a mais baixa aptidão para ser colonizado pela comunidade fotossintética testada. Espera-se que estes resultados apoiem a compreensão da colonização do património cultural construído e que sejam um contributo para a tomada de decisão sobre os litótipos a utilizar em construções futuras ou sobre os tipos de tratamento a utilizar em intervenções de conservação e restauro.

Ao desenvolver este trabalho em diferentes laboratórios de Portugal e Espanha foi possível realizar um estudo multidisciplinar, reunindo competências em diferentes áreas científicas, tais como microbiologia, química, geologia, ecologia, diagnóstico e conservação e restauro, permitindo uma investigação mais precisa dos objectivos proposto para este doutoramento. Além disso, convém referir que, com este trabalho foi possível implementar, pela primeira vez, técnicas de biologia molecular ao estudo de comunidades microbianas presentes em monumentos do património cultural Português.

References

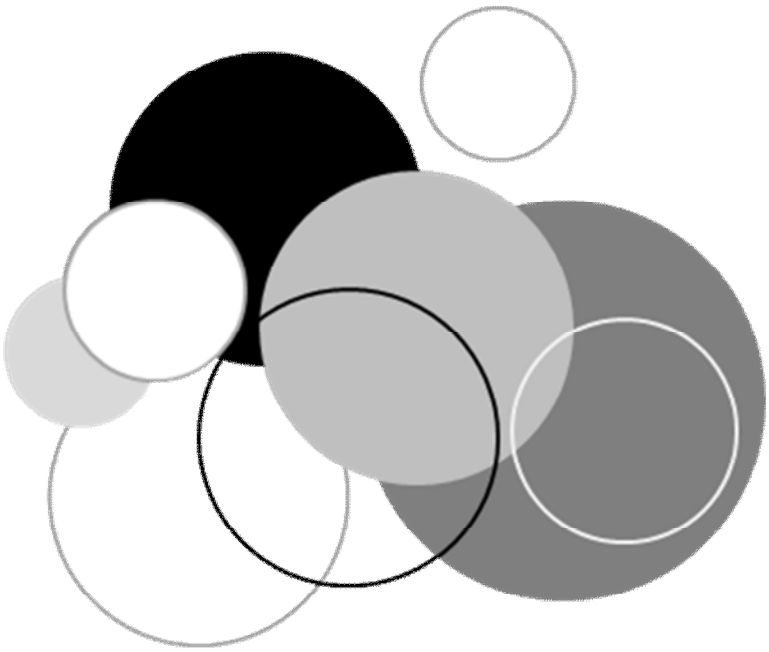

REFERENCES

Aires-Barros, L., Maurício, A.M., 1995. Contaminação liquénica no Claustro do Mosteiro dos Jerónimos e correlação com factores de alteração meteórica das suas rochas. Revista Semestral de Edifícios e Monumentos 3, 51-61.

Aires-Barros, L., Basto, M.J., Charola, A.E., 2000. Black Crusts: "Fossil" and Modern. A comparison from two case studies in Coimbra Monuments (Central Portugal). Internationale Zeitschrift für Bauinstandsetzen und Baudenkmalpflege 6, 63-72.

Aires-Barros, L., 2001. As rochas dos monumentos portugueses – tipologias e patologias. Volume 1, Cadernos Instituto Português do Património Arquitectónico, Lisboa, 335 p.

Akatova, E., Jurado, V., Laiz, L., Gonzalez, J.M., Saiz-Jimenez, C., 2007. Monitoring microbial community development on restored mural paintings. In: Zezza, F., Perthuisot, V., Plançon, A. (Eds), Proceedings of the 7th International Symposium on the Conservation of Monuments in the Mediterranean Basin, Orléans, France, pp. 16-21.

Alakomi, H.L., Arrien, N., Gorbushina, A.A., Krumbein, W.E., Maxwell, I., McCullagh, C., Robertson, P., Ross, N., Saarela, M., Valero, J., Vendrell, M. & Young, M.E. 2004. Inhibitors of biofilm damage on mineral materials (Biodam). In: Kwiatkowski, D., Löfvendahl, R., (Eds), Proceedings of the 10th International Congress on Deterioration and Conservation of Stone, ICOMOS, Stockholm, pp. 399-406.

Albertano, P., Bruno, L., Bellezza, S., Paradossi, G., 2000. Polysaccharides as a key step in stone bio-erosion. In: Fassina, V. (Ed), 9th International Congress on Deterioration and Conservation of Stone, Elsevier, Venice, pp. 425-432.

Almagro, A., 2002. Técnicas infográficas en el estudio del Patrimonio Cultural. In: Ruiz Conde, A., Sánchez Soto, P.J. (Eds), Técnicas instrumentales y su aplicación al estudio del Patrimonio Histórico y Cultural, CSIC, Sevilla, 19 p.

Altieri, A., Pietrini, A.M., Ricci, S., Roccardi, A., 2000. The temples of the archaeological area of Paestum (Italy): a case study on biodeterioration. In: Fassina, V., (Ed), Proceedings of the 9th International Congress on

Deterioration and Conservation of Stone, Elsevier, Venice, pp. 433-443.

Altschul, S.F., Gish, W., Miller, W., Myers, E.W., Lipman, D.J., 1990. Basic local alignment search tool. Journal of molecular biology 215, 403-410.

Alvarez, A., Argemí, M., Laorden, V., Doménech, X., Verbal, J., Navarro, A., Prada, J. L., Pugés, M., Rocabayera, R., Vilaseca, L. 1994. Physical, chemical and biological weathering detected in the romanic portal of the Sant Quirze de Pedret church (XIIc.). In: Fassina, V., Ott, H., Zezza, F. (Eds), Proceedings of the 3rd International Symposium on the conservation of monuments in the Mediterranean Basin, Venice, Soprintendenza ai Beni Artistici e Storici di Venezia, pp. 365-369.

Alves, C., Sequeira Braga, M.A., Hammecker, C., 1996. Water transfer and decay of granitic monuments. Comptes Rendues de l' Academie de Sciences 323, 397-402.

Amann, R.I., Ludwig, W., Schleifer, K.H., 1995. Phylogenetic identification and in situ detection of individual microbial cells without cultivation. Microbiological reviews 59, 143-169.

American Public Health Association (APHA), American Water Works Association (AWWA), Water Environmental Federation (WEF), 1992. Standard methods for the examination of water and wastewater, 18th edition, APHA/AWWA/WEF, Washington, D.C.

Anagnostidis, K., Economou-Amilli. A., Roussomoustakaki, M., 1983. Epilithic and chasmolithic microflora (Cyanophyta, Bacillariophyta) from marbles of the Parthenon (Acropolis-Athens, Greece). Nova Hedwigia 38, 227-287.

Anagnostidis, K., Komarek, J., 1988. Modern approach to the classification system of cyanophytes. 3. Oscillatoriales. Algological Studies 50-53, 327-472.

Anagnostidis, K., Gehrmann, C.K., Gross, M., Krumbein, W.E., Lisi, S., Pantazidou, A., Urzi, C., Zagari, M., 1991. Biodeterioration of marbles of the Parthenon and Propylaea, Acropolis, Athens – Associated organisms, decay and treatment suggestions. In: Decrouez, D., Chamay, J., Zezza, F. (Eds), Proceedings of the 2nd International Symposium on the conservation of monuments in the Mediterranean Basin, Geneve (Switzerland), Ville de Geneve-Museum d'Histoire Naturelle & Musee D'Art et d'Histoire, pp. 305-325.

Ariño, X., Hernandez-Marine, M., Saiz-Jimenez, C., 1997. Colonization of Roman tombs by calcifying cyanobacteria. Phycologia 36, 366-373.

Ariño, X., Saiz-Jimenez, C., Hernandez-Marine, M., 2002. Colonization of cryptoendolithic niches in mortars by phototrophic microorganisms. In: Galán, Zezza (Eds), Protection and Conservation of the Cultural Heritage of the Mediterranean Cities, 127-131.

Ascaso, C., Wierzchos, J., Castello, R., 1998a. Study of the biogenic weathering of calcareous litharenite stones caused by lichen and endolithic microorganisms. International Biodeterioration and Biodegradation 42, 29-38.

Ascaso, C., Wierzchos, J., Delgado Rodrigues, J., Aires-Barros, L., Henriques, F.M.A., Charola, A.E., 1998b. Endolithic Microorganisms in the biodeterioration of the Tower of Belem. Internationale Zeitschrift für Bauinstandsetzen 4, 627-640.

Ascaso, C., Wierzchos, J., Souza-Egipsy, V., De Los Ríos, A., Rodrigues, J.D., 2002. In situ evaluation of the biodeteriorating action of microorganisms and the effects of biocides on carbonate rock of the Jeronimos Monastery (Lisbon). International Biodeterioration and Biodegradation 49, 1-12.

Ascaso, C., Garciá del Cura, M.A., De Los Ríos, A., 2004. Microbial biofilms on carbonate rocks from a quarry and monuments in Novelda (Alicante, Spain). In: Clair, S., Seaward, M. (Eds), Biodeterioration of Stone Surfaces, Kluwer Academic Publishers, Netherlands, pp. 79-98.

ASTM E96/E96M – 05 (2005). Standard test methods for water vapour transmission of materials, ASTM.

Ausubel, F.M., Brent, R., Kingston, R.E., Moore, D.D., Seidman, J.G., Smith, J.A., Struhl, K., (Eds), 1992. Current Protocols in Molecular Biology. Wiley, New York.

Badalyan, A.G., Gorbushina, A.A., Krumbein, W.E., Kumzerov, Y.A., Panina, L.K., Vlasov, D.Y., 1996. Physical and microbiological investigations of rock weathering at Hellenic excavation sites on the Crimean Peninsula. In: Riederer, J. (Ed), Proceedings of the 8th International Congress of Deterioration and Conservation of stone, Berlin, pp. 671-679.

Banerjee, M., Whitton, B.A., Wynn-Williams, D.D., 2000. Phosphatase activities of endolithic communities in rocks of the Antarctic dry valleys. Microbial Ecology 39, 80-91.

Banse, K., 1977. Determining the carbon to chlorophyll ratio of natural phytoplankton. Marine Biology 41, 199-212.

Barberousse, H., Ruiz, G., Gloaguen, V., Lombardo, R.J., Djediat, C., Mascarell, G., Castaing, J.C., 2006. Capsular polysaccharides secreted by building façade colonisers: characterisation and adsorption to surfaces. Biofouling 22, 361-370.

Bargar, J.R., Tebo, B.M., Pecher, K.H., Chiu, V., Villinski, J.E., Tonner, B.P., 2000. Kinetics and products on Mn oxide biomineralization by spores of the marine *Bacillus* sp. strain-1. Symposia papers presented before the division of Environment Chemistry American Chemical Society, vol. 40, nº 2, pp. 491-493.

Bartolini, M., Ricci, S., Del Signore, G., 2004. Release of photosynthetic pigments from epilithic biocenosis after biocide treatments. In: Kwiatkowski, D., Löfvendahl, R. (eds), Proceedings of the 10th International Congress on Deterioration and Conservation of Stone, ICOMOS, Stockholm, pp. 519-526.

Beck, K., Al-Mukhtar, M., Rozenbaum, O., Rautureau, M., 2003. Characterization, water transfer properties and deterioration in tuffeau: building material in the Loire valley – France. Building and Environment 38, 1151-1162.

Bell, F.G., 1993a. Durability of carbonate rock as building stone with comments on its preservation. Environmental Geology 21, 187-200.

Bell, R.A., 1993b. Cryptoendolithic algae of hot semiarid lands and deserts. Journal of Phycology 29, 133-139.

Bellinzoni, A.M., Caneva, G., Ricci, S., 2003. Ecological trends in travertine colonisation by pioneer algae and plant communities. International Biodeterioration and Biodegradation 51, 203-210.

Benavente, D., Cueto, N., Martínez-Martínez, J., García del Cura, M.A., Cañaveras, J.C., 2007. The influence of petrophysical properties on the salt weathering of porous building rocks. Environmental Geology 52, 215-224.

Berdoulay, M., 2008. Analyses physico-chimiques et microbiologiques de façades en pierre exposées aux embruns marins du Golfe de Gascogne. PhD thesis, Université de Pau et des Pays de l'Adour, France.

Bloch, S., 1991. Empirical prediction of porosity and permeability in sandstones. AAPG Bulletin 75, 1145-1160.

Bock, E., Sand, W., 1993. The microbiology of mansonry biodeterioration. Journal of Applied Bacteriology 74, 503-514.

Bolívar, F.C., Sánchez-Castillo, P.M., 1997. Biomineralization processes in the Fountais of the Alambra, Ganada, Spain. International Biodeterioration and Biodegradation 40, 205-215.

Bourrelly, P., 1990. Les algues d'eau douce – Initiation à la systématique, I: Les Algues Vertes. N. Boubée, Paris, 572 p.

Brosius, J., Dull, T., Sleeter, D.D., Noller, H.F., 1981. Gene organization and primary structure of a ribosomal RNA operon from *Escherichia coli*. Journal of Molecular Biology 148, 107-127.

Brown, G., 1980. Associated minerals. In: Brindley, G.W., Brown, G. (Eds), Crystal Structures of Clay Minerals and their X-Ray Identification, vol. 5, Mineralogical Society, London, pp. 361-410.

Bruno, L., Billi, D., Albertano, P., Urzì, C., 2006. Genetic characterization of epilithic cyanobacteria and their associated bacteria. Geomicrobiology Journal 23, 293-299.

Burford, E.P., Kierans, M., Gadd, G.M., 2003. Geomycology: fungi in mineral substrata. Mycologist 17, 98-107.

Burnison, B.K., 1980. Modified Dimethyl Sulfoxide (DMSO) Extraction for Chlorophyll Analysis of Phytoplankton. Canadian Journal of Fisheries and Aquatic Sciences 37, 729-733.

Büdel, B.,Weber, B., Kühl, M., Pfanz, H., Sültemeyer, D., Wessels, D., 2004. Reshaping of sandstone surfaces by cryptoendolithic cyanobacteria: bioalkalization causes chemical weathering in arid landscapes. Geobiology 3, 261-268.

Camara, B., De los Rios, A., García-del-Cura, M.A., Galván, V., Ascaso, C., 2008. Dolostone bioreceptivity to fungal colonization. Materiales de Construcción 58, 113-124.

Camuffo, D., 1995. Physical weathering of stones. The Sience of the Total Environment 167, 1-14.

Caneva, G., Nugari, M.P., Salvadori, O., 1991. Biology in the conservation of work of art. ICCROM, Roma, 182 p.

Caneva, G., Nugari, M.P., Ricci, S., Salvadori, O., 1992. Pitting of marble roman monuments and the related microflora. In: Delgado, J., Henriques, F., Telmo, F. (Eds), Proceedings of the 7th International Congress on Deterioration and Conservation of Stone, Lisbon, Laboratório Nacional de Engenharia Civil, pp. 521-530.

Cañaveras, J.C., Cuezva, S., Sanchez-Moral, S., Lario, J., Laiz, L., Gonzalez, J.M., Saiz-Jimenez, C., 2006. On the origin of fiber calcite crystals in moonmilk

deposit. Naturwissenschaften 93, 27-32.

Cappitelli, F., Principi, P., Pedrazzani, R., Toniolo, L., Sorlini, C., 2007. Bacterial and fungal deterioration of the Milan Cathedral marble treated with protective synthetic resins. International Biodeterioration and Biodegradation 385, 172-181.

Castenholz, R.W., 2001. Phylum BX. Cyanobacteria, Oxygenic Photosynthetic Bacteria. In: Boone, D.R., Castenholz, R.W. (Eds), Bergey's Manual of Systematic Bacteriology, 2nd ed., Vol. 1. Springer-Verlag, New York, pp. 473-597.

Cecchi, G., Pantani, L., Raimondi, V., Tomaselli, L., Lamenti, G., Tiano, P., Chiari, R., 2000. Fluorescence lidar technique for the remote sensing of stone monuments. Journal of Cultural Heritage 1, 29-36.

Cetica, M., Marras, L., Materazzi, M., Poggi, P., 2002. Tecniche di imaging multispettrale. In: Castellano, A., Martini, M., Sibilia, E. (Eds), Elementi di Archeometria. Metodi fisici per i Beni Culturali, Egea, Milano, pp. 205-226.

Chilingar, G., 1964. Relationship between porosity, permeability and grain size distribution of sands and sandstones. In: van Straaten (Ed), Deltaic and Shallow Marine Deposits, Elsevier, New York, pp. 71-75.

Chilingar, G.V., Bissel, H.J., Fairbridge, R.W., 1967. Developments in sedimentology 9B. Carbonate rocks. Physical and chemical aspects, Elsevier, 471 p.

Christensen, B.E., 1989. The role of extracellular polysaccharides in biofilms. Journal of Biotechnology 10, 181-202.

Chuvieco Salinero, E., 2002. Teledetección espacial. La observación de la tierra desde el espacio. Ariel, Barcelona.

Ciferri, O., 2002. The role of microorganisms in the degradation of cultural heritage. Reviews in Conservation 3, 35-45.

Costerton, J.W., Lewandowski, Z., Debeer, Caldwell, D., Korber, D., James, G., 1994. Biofilms, the customized microniche. Journal of Bacteriology 176, 2137-2142.

Costerton, J.W., Lewandowski, Z., Caldwell, D.E., Korber, D.R., Lappin-Scott, H.M., 1995. Microbial biofilms. Annual Review of Microbiology 49, 711-745.

Crispim, C.A., Gaylarde, P.M., Gaylarde, C.C., 2003. Algal and cyanobacterial biofilms on calcareous historic buildings. Current Microbiology 46, 79-82.

Crispim, C.A., Gaylarde, C.C., 2005. Cyanobacteria and biodeterioration of cultural

heritage: A review. Microbial Ecology 49, 1-9.

Cultrone, G., Sebastián, E., Ortega Huertas, M., 2007. Durability of masonry systems: A laboratory study. Construction and Building Materials 21, 40-51.

Daffonchio, D., Borin, S., Zanardini, E., Abbruscato, P., Realini, M., Urzì, C., Sorlini, C., 2000. Molecular tools applied to the study of deteriorated artworks. In: Ciferri, O., Tiano, P., Mastromei, G. (Eds), Of Microbes and Art – The role of microbial communities in the degradation and protection of cultural heritage, Kluwer Academic, New York, pp. 21-38.

Danin, A., Caneva, G., 1990. Deterioration of limestone walls in Jerusalem and marble monuments in Rome caused by cyanobacteria and cyanophilous lichens. International Biodeterioration 26, 397-417.

De Leo, F., Urzì, C., 2003. Fungal colonization on treated and untreated stone surfaces. In: Saiz-Jimenez (ed.), Molecular biology and Cultural Heritage, Swets and Zeitlinger, Lisse, pp. 213-217.

De Los Ríos, A., Galván, V., Ascaso, C., 2004. In situ microscopical diagnosis of biodeterioration processes at the convent of Santa Cruz la Real, Segovia, Spain. International Biodeterioration and Biodegradation 54, 113-120.

De Los Ríos, A., Ascaso, C., 2005. Contributions of in situ microscopy to the current understanding of stone biodeterioration. International Microbiology 8, 181-188.

De Los Ríos, A., Grube, M., Sancho, L.G., Ascaso, C., 2006. Ultrastructural and genetic characteristics of endolithic cyanobacterial biofilms colonizing Antarctic granite rocks. FEMS Microbiology Ecology 59, 386-395.

Delgado Rodrigues, J., Valero, J., Wakefield, R.D., Brechet, E., Larranaga, I., 2002. Biocolonization and biocidal monitoring by means of a portable fluorescent instrument. Int. Symposium "Life and Rocs: Bio-inert Interactions", S. Petersburg.

Diez, B., Pedros-Alio, C., Marsh, T.L., Massana, R., 2001. Application of denaturing gradient gel electrophoresis (DGGE) to study the diversity of marine picoeukaryotic assemblages and comparison of DGGE with other molecular techniques. Applied and environmental microbiology 67, 2942-2951.

Dimes, F.G., 1998. Sedimentary rocks. In: Ashurst, J., Dimes, F.G. (Eds), Conservation of building and decorative stone. Elsevier, pp. 61-134.

Dionísio, A., 1997. A Pedra de Ançã: características minero-químicas e petrofísicas. MscE Thesis, Universidade Técnica de Lisboa, Instituto Superior Técnico,

Portugal.

Dionísio, A., 2007. Stone decay induced by fire on historical buildings: the case of the Cloister of Lisbon Cathedral (Portugal). In: Prikryl, R., Smith, B.J. (Eds), Building Stone decay: from diagnosis to conservation, Geological Society, London, Special Publication 271, 87-98.

Dixon, J., 1977. Minerals in soil environments. Soil Science Society of America, Wisconsin USA.

Donlan, R.M., 2002. Biofilms: microbial life on surfaces. Emerging Infectious Diseases 8, 881-890.

Dorn, R., 1998. Rock coatings. Developments in Earth Surface Processes 6, Elsevier, Amsterdam.

Dornieden, T., Gorbushina, A.A., Krumbein, W.E., 2000. Patina – physical and chemical interactions of sub-aerial biofilms with objects of art. In. Ciferri, O., Tiano, P., Mastromei, G. (Eds), Of microbes and Art – The role of microbial communities in the degradation and protection of cultural heritage. Kluwer Academic, New York, pp. 105-114.

Drever, J.I., Stillings, L.L., 1997. The role of organic acids in mineral weathering. Colloids and Surfaces A: Physicochemical and Engineering Aspects 120, 167-181.

Dunham, R.J., 1962. Classification of carbonate rocks according to depositional texture. In: Ham, W.E. (ed), Classification of carbonate rocks. American Association of Petroleum Geologists Memoir 1, pp. 108-121.

Dupuy, P., Trotet, G., Grossin, F., 1976. Protection des monuments contre les cyanophycees en milieu abrite et humide. In: The Conservation of Stone I., Rossi-Manaressi, R. (Ed), Centro per la Conservazione delle Sculture all' Aperto, Bologna, pp. 205-219.

Edwards, H.G., Garcia-Pichel, F., Newton, E.M., Wynn-Williams, D.D., 2000. Vibrational raman spectroscopic study of scytonemin, the UV-protective cyanobacterial pigment. Spectrochimica Acta Part A: Molecular and Biomolecular Spectroscopy 56A, 193-200.

Elsas, J.D., Duarte, G.F., Rosado, A.S., Smalla, K., 1998. Microbiological and molecular biological methods for monitoring microbial inoculants and their effects in the soil environmental. Journal of Microbiological Methods 32, 133-154.

Embry, A.F., Klovan, J.E., 1971. A Late Devonian reef tract on northeastern Banks Island, Northwest territories. Bulletin of Canadian Petroleum Geology 19, 730-781.

EN 1925:1999, 1999. Natural stone test methods – Determination of water absorption coefficient by capillarity. European Committee for Standardization (CEN), Belgian.

EN 1936:1999, 1999. Natural stone test method – Determination of real density and apparent density, and of total and open porosity. European Committee for Standardization (CEN), Belgian.

Fernandes, P., 2006. Applied microbiology and biotechnology in the conservation of stone cultural heritage materials. Applied Microbiology and Biotechnology 73, 291-296.

Ferreira Pinto, A.P., Delgado Rodrigues, J., 2008. Stone consolidation: the role of treatment procedures. Journal of Cultural Heritage 9, 38-53.

Figueiredo, C.A.M., Aires-Barros, L., Basto, M.J., Graça, R.C., Maurício, A., 2007. The weathering and weatherability of Basílica da Estrela stones, Lisbon, Portugal. In: Prikryl, R., Smith, B.J. (Eds), Building stone decay: from diagnosis to conservation, Geological Society, London, Special Publication 271, 99-107.

Flores, M., Lorenzo, J., Gómez-Alarcón, G., 1997. Algae and bacteria on historic monuments at Alcala de Henares, Spain. International Biodeterioration and Biodegradation 40, 241-246.

Folk, R.L., 1962. Spectral subdivision of limestone types. In: Ham, W.E. (ed), Classification of Carbonate Rocks. American Association of Petroleum Geologists Memoir 1, pp. 62-84.

Friedmann, E.I., 1982. Endolithic microorganisms in the Antarctic Cold Desert. Science 215, 1045-1053.

Fischer, T.B., Heaney, P.J., Jang, J.H., Ross, D.E., Brantley, S.L., Post, J.E., Tien, M., 2008. Continuous time-resolved X-ray diffraction of the biocatalysed reduction of Mn oxide. American Mineralogist, vol. 93, nº 11-12, pp. 1929-1932.

Gauthier, M.J., Lafay, B., Christen, R., Fernandez, L., Acquaviva, M., Bonin, P., Bertrand, J.C., 1992. *Marinobacter hydrocarbonoclasticus* gen. nov., sp. nov., a new, extremely halotolerant, hydrocarbon-degrading marine bacterium. International Journal of Systematic Bacteriology 42, 568-576.

Gaylarde, C., Gaylarde, P., Copp, J., Neilan, B., 2004. Polyphasic detection of

cyanobacteria in terrestrial biofilms. Biofouling 20, 71-79.

Gaylarde, C.C., Morton, L.H.G., 1999. Deteriogenic biofilms on buildings and their control: a review. Biofouling 14, 59-74.

Gaylarde, C., Gaylarde, P., 2005. A comparative study of the major microbial biomass of biofilms on exteriors of buildings in Europe and Latin America. International Biodeterioration and Biodegradation 55, 131-139.

Gerrard, A.J., 1988. Rocks and landforms. Unwin Hyman, London, 319 p.

Giaccone, G., Einaldi, M.L.V., Giacobini, C., 1976. Forme biologische delle alghe esistenti sulle sculture all'aperto. In: Rossi-Manaresi (Ed), The conservation of stone I. Proceedings of the International Symposium on the Conservation of Stone, Bologna (Italy), Centro per la conservazione delle sculture all'aperto, pp. 245-256.

Gillespie, A.R., Kahle, A.B., Walker, R.E., 1986. Color enhancement of highly correlated images. I. Decorrelation and HSI contrast stretches. Remote Sensing of Environment 20, 209-235.

Goeyens, L., Post, E., Dehairs, F., Vandenhoudt, A., Baeyens, W., 1982. The Use of High Pressure Liquid Chromatography with Fluorimetric Detection for Chlorophyll A Determination in Natural Extracts of Chloropigments and their Degradation Products. International Journal of Environmental Analytical Chemistry 12, 51-63.

Golubic, S., Friedmann, I., Schneider, J., 1981. The lithobiontic ecological niche, with special reference to microorganisms. Journal of Sedimentary Petrology 51, 475-478.

Gomes, M.I. Sardinha, 2008. Monitorização do crescimento de um biofilme fotossintético por análise de imagem. MscE Thesis, Faculdade de Ciências e Tecnologia, Universidade Nova de Lisboa, Portugal.

Gómez-Alarcón, G., Muñoz, M., Ariño, X., Ortega-Calvo, J.J., 1995. Microbial communities in weathered sandstones: the case of Carrascosa del Campo church, Spain. Science of the Total Environment 167, 249-254.

Gonzalez, I., Laiz, L., Hermosin, B., Caballero, B., Incerti, C., Saiz-Jimenez, C., 1999. Bacteria isolated from rock art paintings: The case of Atlanterra shelter (south Spain). Journal of Microbiology Methods 36, 123-127.

González, J.M., Simó, R., Massana, R., Covert, J.S., Casamayor, E.O.,Pedrós-Alió, C., Moran, M.A., 2000. Bacterial community structure associated with a

dimethylsulfoniopropionate-producing north Atlantic algal bloom. Applied and Environmental Microbiology 66, 4237-4246.

González, J.M., Ortiz-Martinez, A., Gonzalez-delValle, M.A., Laiz, L., Saiz-Jimenez, C., 2003. An efficient strategy for screening large cloned libraries of amplified 16S rDNA sequences from complex environmental communities. Journal of Microbiological Methods 55, 459-463.

Gonzalez, J.M., Saiz-Jimenez, C., 2004. Microbial diversity in biodeteriorated monuments as studied by denaturing gradient gel electrophoresis. Journal of Separation Science 27, 174-180.

Gonzalez, J.M., Saiz-Jimenez, C., 2006. Current advances in the molecular characterization of microbial communities on cultural heritage. In: Fort, R., Alvarez de Buergo, M., Gomez-Heras, M., Vazquez-Calvo, C., (Eds), 1st International Conference Heritage, Weathering and Conservation, Taylor and Francis, London, pp. 343-348.

Gorbushina, A.A., Krumbein, W.E., Hamman, C.H., Panina, L., Soukharjevski, S., Wollenzien, U., 1993. Role of black fungi in colour change and biodeterioration of antique marbles. Geomicrobiology Journal 11, 205-220.

Gorbushina, A.A., Krumbein, W.E., 2005. Role of microorganisms in wear down of rocks and minerals. In: Buscot, F., Varma, A. (Eds), Microorganisms in soils: roles in genesis and functions, Springer, pp. 59-84.

Gorbushina, A.A., 2007. Life on the rocks. Environmental Microbiology 9, 1613-1631.

Grabau, A.W., 1904. On the classification of sedimentary rocks. Am. Geologist 33, 228-247.

Grabau, A.W., 1913. Principles-of stratigraphy. Seiler, New York, 1185p.

Graham, L.E., Wilcox, L.W., 2000. Algae. Prentice-Hall, Upper Saddle River, 640p.

Grant, C., 1982. Fouling of terrestrial substrates by algae and implications for control – a review. International Biodeterioration Bulletin 18, 57-65.

Griffin, P.S., Indictor, N., Kloestler, R.J., 1991. The biodeterioration of stone: a review of deterioration mechanisms, conservation case histories, and treatment. International Biodeterioration 28, 187-207.

Grissom, C.A., Charola, A.E., Wachowiak, M.J., 2000. Measuring surface roughness on stone: back to basics. Studies in Conservation 45, 73-84.

Guillitte, O., 1995. Bioreceptivity: A new concept for building ecology studies.

Science of the Total Environment 167, 215-220.

Guillitte, O., Dreesen, R., 1995. Laboratory chamber studies and petrographical analysis as bioreceptivity assessment tools of building materials. Science of the Total Environment 167, 365-374.

Gurtner, C., Heyrman, J., Piñar, G., Lubitz, W., Swings, J., Rölleke, S., 2000. Comparative analyses of the bacterial diversity on two different biodeteriorated wall paintings by DGGE and 16S rDNA sequence analysis. International Biodeterioration and Biodegradation 46, 229-239.

Hernandez-Marine, M., Saiz-Jimenez, C., Ariño, X., 1997. *Borzia periklei* Anag. (Cyanoprokaryota): a taxonomical approach. Lagascalia 21, 457-462.

Hernandéz-Mariné, M., Roldán, M., Clavero, E., Canals, A., Ariño, X., 2001. Phototrophic biofilm morphology in dim light. The case of the Puigmoltó sinkhole. Nova Hedwigia 123, 237-253.

Hernández-Mariné M., Clavero, E., Roldán, M., 2003. Why there is such luxurious growth in the hypogean environments. Algological Studies 109, 229-239.

Hernandéz-Mariné, M., Clavero, E., Roldán, M., 2004. Microscopy methods applied to research on cyanobacteria. Limnetica 23, 179-186.

Herrera, L.K., Videla, H., 2004. The importance of atmospheric effects on biodeterioration of cultural heritage constructional materials. International Biodeterioration and Biodegradation 54, 125-134.

Herrera, L.K., Arroyave, C., Guiamet, P., De Saravia, S.G., Videla, H., 2004. Biodeterioration of peridotite and other constructional materials in a building of the Colombian cultural heritage. International Biodeterioration and Biodegradation 54, 135-141.

Holm-Hansen, O.C.J., Lorenzen, C.J., Holmes, R.W., Strickland, J.D.H., 1965. Fluorometric determination of chlorophyll. Journal du Conseil Permanent International pour l'Exploration de la Mer 30, 3-15.

Hougthon, D.R., Eggins, S. (Eds.), 1988. Biodeterioration 7, Elsevier Applied Science.

Hueck, H.J., 1965. The biodeterioration of materials as part of hylobiology. Material und Organismen 1, 5-34.

Hueck, H.J., 2001. The biodeterioration of materials – an appraisal. International Biodeterioration and Biodegradation 48, 5-11.

Hugenholtz, P., Goebel, B.M., Pace, N.R., 1998. Impact of culture-independent

studies on the emerging phylogenetic view of bacterial diversity. Journal of Bacteriology 180, 4765-4774.

Jeffrey, S.W., Humphrey, G.F., 1975. New spectrophotometric equations for determining chlorophylls *a*, *b*, c_1 and c_2 in higher plants, algae and natural phytoplankton. Biochemie und Physiologie der Pflanzen 167, 191-194.

Kaplan, D., Christiaen, D., Arad, S., 1987. Chelating Properties of Extracellular Polysaccharides from *Chlorella* spp. Applied and Environmental Microbiology, 53, 2953-2956.

Karoglou, M., Moropoulou, A., Giakoumaki, A., Krokida, M.K., 2005. Capillary rise kinetics of stone building materials. Journal of Colloid and Interface Science 284, 260-264.

Karras, G.E., Petsa, E., 1999. Metric information from uncalibrated single images. In: XVII CIPA International Sympsium. Olinda, Brasil, 3-6 October 1999. [On-line: http://cipa.icomos.org/fileadmin/papers/olinda/99c802.pdf visit: 10/10/2006]

Kawaguchi, T., Decho, A.W., 2002. In situ analysis of carboxyl (-COOH) and sulfhydral (-SH) groups of extracellular polymeric secretions (EPS) by confocal scanning laser microscopy. Analytical Biochemistry 304, 266-267.

Kemmling, A., Kämper, M., Flies, C.O, Schieweck, C., Hoppert, M., 2004. Biofilms and extracellular matrices on geomaterials. Environmental Geology 46, 429-435.

Koestler, R., Warscheid, T., Nieto, F., 1996. Biodeterioration: Risk factors and their management. In: Baer, N.S., Snethlage, R. (Eds) Saving Our Architectural Heritage – The Conservation of Historic Stone Structures, John Wiley & Sons, pp. 25-35.

Koestler, R., 2000. Polymers and resins as food for microbes. In: Ciferri, O., Tiano, P. Mastromei, G. (Eds), Of Microbes and Art – The Role of Microbial Communities in the Degradation and Protection of Cultural Heritage, Kluwer Academic, New York, pp. 153-167.

Komárek, J., Anagnostidis, K., 1999. Cyanoprocaryota I. In: Ettl, H., Gerloff, J., Heynig, H., Mollenhauer, D. (Eds), Süßwasserflora von Mitteleuropa, Band 19/1, Gustav Fischer Verlag, 548 p.

Krumbein, W.E., 1966. Zur Frage der Gesteinsverwitterung. Ph. D. Thesis, Würzburg 106 p.

Krumbein, W.E., 1983. Microbial Geochemistry. Blackwell Scientific Publications,

Oxford.

Krumbein, W.E., 1988. Microbial interactions with mineral materials. In: Hougthon, D.R., Eggins, S. (Eds.), Biodeterioration 7, Elsevier Applied Science, pp. 78-100.

Krumbein, W.E., Urzì, C., 1991. Biologically induced decay phenomena of antique marbles – some general considerations. In: Decrouez, D., Chamay, J., Zezza, F. (Eds), Proceedings of the 2nd International Symposium on the conservation of monuments in the Mediterranean Basin, Geneve (Switzerland), Ville de Geneve-Museum d'Histoire Naturelle & Musee D'Art et d'Histoire, pp. 219-235.

Krumbein, W.E., 1992. Colour changes of building stones and their direct and indirect biological causes. Proceedings of 7th International congress on Deterioration and Conservation of Stone, Lisboa, pp. 443-452.

Krumbein, W.E., Brehm, U., Gerdes, G., Gorbushina, A.A., Levit, G. Palinska, K., 2003. Biofilm, Biodictyon, and Biomat - Biolaminites, Oolites, Stromatolites - Geophysiology, Global mechanisms and Parahistology. In: Krumbein, W.E., Paterson, D.W., Zavarzin, G.A. (Eds), Fossil and recent Biofilms: A natural History of Life on Earth, Kluwer Academic Press Publishers, pp.1-28.

Krumbein, W.E., 2004. Life on and in stone – an endless story? In: Kwiatkowski, D., Löfvendahl, R. (Eds), Proceedings of the 10th International congress on deterioration and conservation of stone. ICOMOS, Stockholm, pp. 259-266.

Laiz, L., Piñar, G., Lubitz, W., Saiz-Jimenez, C., 2003. The colonisation of building materials by microorganisms as revealed by culturing and molecular methods. In: Saiz-Jimenez, C. (Ed) Molecular biology and cultural heritage, A.A. Balkema, Lisse, pp. 23-28.

Lamenti, G., Tiano, P., Tomaselli, L., 2000. Biodeterioration of ornamental marble statues in the Boboli Gardens (Florence, Italy). Journal of Applied Phycology 12, 427-433.

Leighton, M.W., Pendexter, C., 1962. Carbonate Rock Types. In: Ham, W.E., (ed), Classification of Carbonate Rocks. American Association of Petroleum Geologists Memoir 1, pp. 33-61.

Leite Magalhães, S., Sequeira Braga, M.A., Ascaso, C., 1998. Pátinas biogénicas numa fachada granítica do edifício do Largo do Paço (Braga). Actas do V Congresso Nacional de Geologia, Tomo 84, Fas. 2, Lisboa, pp. F-194-F-197.

Leite Magalhães, S., 2000. Biodeterioração de um monumento da cidade de Braga.

Estudo microbiológico da pedra granítica. MScE thesis, Universidade do Minho, Braga, Portugal.

Leite Magalhães, S., Sequeira Braga, M.A., 2000. Biological colonization features on a granite monument from Braga (NW, Portugal). In: Fassina, V. (Ed), Proceedings of the 9th International Congress on Deterioration and Conservation of Stone, Amsterdam, Elsevier, pp. 521–529.

Lorenzen, C.J., 1967. Determination of chlorophyll and pheo-pigments: spectrophotometric equations. Limnology Oceanography 12, 343-346.

Macedo, M.F., Duarte, P., Alves, M., Ferreira, J.G., Costa, V., 2000. Analysis of the deep chlorophyll maximum across the Azores Front. Hydrobiologia 441, 155-172.

Macedo, M.F., Duarte, P., Mendes, P., Ferreira, J.G., 2001. Annual variation of environmental variables, phytoplankton species composition and photosynthetic parameters in a Coastal Lagoon. Journal of Plankton Research 23, 719-732.

Mark, R., Billo, E., 2006. Computer-assisted photographic documentation of rock art. Coalition 11, 10-14.

Martinez-Alonso, M., Van Bleijswijk, J., Gaju, N., Muyzer, G., 2005. Diversity of anoxygenic phototrophic sulfur bacteria in the microbial mats of the Ebro Delta: a combined morphological and molecular approach. FEMS Microbiology Ecology 52, 339-350.

Martínez Arias, R., 1999. El análisis multivariante en la investigación científica. La Muralla/Hespérides, Madrid.

Maurício, A., Figueiredo, C., 2000. Texture analysis of grey-tone images by mathematical morphology: a nondestructive tool for the quantitative assessment of stone decay. Journal of Mathematical Geology 32, 619-642.

Maurício, A., Pacheco, A., Brito, P., Castro, B., Figueiredo, C., Aires-Barros, L., 2005. An ionic conductivity-based methodology for monitoring salt systems in monument stones. Journal of Cultural Heritage 6, 287-293.

May, E., Lewis F.J., Pereira, S., Tayler, S., Seaward, M.R.D., Allsopp D., 1993. Microbial deterioration of building stone – a review. Biodeterioration Abstracts 7, 109-123.

Mazor, G., Kidron, G.J., Vonshak, A., Abeliovich, A., 1996. The role of cyanobacterial exopolysaccharides in structuring desert microbial crusts. FEMS Microbiology Ecology 21, 121-130.

McKinley, J.M., Warke, P.A., 2007. Controls on permeability: implications for stone weathering. In: Prikryl, R., Smith, B.J. (Eds), Building stone decay: from diagnosis to conservation. Geological Society, London, Special Publications 271, 225-236.

McNamara, C.J., Mitchell, R., 2005. Microbial deterioration of historic stone. Frontiers in Ecology and the Environment 3, 445-451.

McNamara, C.J., Perry, IV T.D., Bearce, K.A., Hernandez-Duque, G., Mitchell, R., 2006. Epilithic and endolithic bacterial communities in limestone from a Maya archaeological site. Microbial Ecology 51, 51-64.

Miller, A., Macedo, M.F., 2006. Mapping and characterization of a green biofilm inside of Vilar de Frades Church (Portugal). In: Fort, R., Alvarez de Buergo, M., Gomez-Heras, M., Vazquez-Calvo, C., (Eds), 1st International Conference Heritage, Weathering and Conservation, Taylor and Francis, London, pp. 329-335.

Miller, A., Dionísio, A., Macedo, M.F., 2006. Primary bioreceptivity: A comparative study of different Portuguese lithotypes. International Biodeterioration and Biodegradation 57, 136-142.

Monte, M., Rattazzi, A., Romão, P., Rossi, P., 1996. The role of lichens in the weathering of granitic buildings. In: Degradation and Conservation of Granitic rocks in monuments, Proceedings of the EC workshop held in Santiago de Compostela (Spain), Directorate – General XII, Science, Research and Development, pp. 301-306.

Monte, M., 2003. Oxalate film formation on marble caused by fungus. Journal of Cultural Heritage 4, 255-258.

Morton, L.H.G., Greenway, D.L.A., Gaylarde, C.C., Surman, S.B., 1998. Consideration of some implications of the resistance of biofilms to biocides. International Biodeterioration and Biodegradation 41, 247-259.

Muyzer, G., de Waal, E.C., Uitterlinden, A.G., 1993. Profiling of complex microbial populations by denaturing gradient gel electrophoresis analysis of polymerase chain reaction-amplified genes coding for 16S rRNA. Applied and environmental microbiology 59, 695-700.

Neu, T.R., Lawrence, J.R., 1999. In situ characterization of extracellular polymeric substances (EPS) in biofilm systems. In: Wingender, J., Neu, T.R., Flemming, H. (Eds), Microbial Extracellular Polymeric Substances, Springer-Verlag, New

York, pp. 21-47.

Nelissen, B., van de Peer, Y., Wilmotte, A., De Wachter, R., 1995. An early origin of plastids within the cyanobacterial divergence is suggested by evolutionary trees based on complete 16S rRNA sequences. Molecular Biology and Evolution 12, 1166-1173.

Noguerol-Seoane, A., Rifón-Lastra, A., 1996. Epilithic ficoflora on two monuments of historic-artistic interest from Galicia (N.W. Spain). In: Degradation and conservation of granitic rocks in monument. Environmental protection and conservation of the European cultural heritage. Brussels, European Commission Directorate-General XII, Science, Research and Development, Research Report nº 5, pp. 417-421.

Normal 21/85, 1985. Permeabilità al vapor d'acqua. Commissione Normal, Instituto Centrale del Restauro-Commissione Normal, ICR-CNR, Rome, Italy.

Normal 9/88, 1988. Microflora autotrofa ed eterotrofa: tecniche di isolamento in coltura. Instituto Centrale del Restauro-Commissione Normal, ICR-CNR, Rome, Italy.

Nübel, U., Garcia-Pichel, F., Muyzer, G., 1997. PCR primers to amplify 16S rRNA genes from cyanobacteria. Applied and environmental microbiology 63, 3327-3332.

Ordóñez, S., Fort, R., Gracía del Cura, M.A., 1997, Pore size distribution and the durability of a porous limestone. Quarterly Journal of Engineering Geology 30, 221-230.

Ortega-Calvo, J.J., Hernandez-Marine, M., Saiz-Jimenez, C., 1991a. Biodeterioration of building materials by cyanobacteria and algae. International Biodeterioration 28, 165-185.

Ortega-Calvo, J.J., Hernandez-Marine, M., Saiz-Jimenez, C., 1991b. Mechanical deterioration of building stones by cyanobacteria and algae. In: Rossmoore, H.W., (Ed), Biodeterioration and Biodegradation 8, Elsevier, London, pp. 392-394.

Ortega-Calvo, J.J., Hernandez-Marine, M., Saiz-Jimenez, C., 1992. Experimental strategies for investigating algal deterioration of stone. In: Delgado, J., Henriques, F., Telmo, F. (Eds), Proceedings of the 7th International Congress on Deterioration and Conservation of Stone, Lisbon, Laboratório Nacional de Engenharia Civil, pp. 541-549.

Ortega-Calvo, J.J., Hernandez-Marine, M., Saiz-Jimenez, C., 1993a. Cyanobacteria and algae on historic buildings and monuments. In: Garg, K.L., Garg, N., Mukerji, K.G. (Eds), Recent Advances in Biodeterioration and Biodegradation, Volume I, Naya Prokash, India, pp.175-203.

Ortega-Calvo, J.J., Sanchez-Castillo, P.M., Hernandez-Marine, M., Saiz-Jimenez, C., 1993b. Isolation and characterization of epilithic chlorophyta and cyanobacteria from two Spanish cathedrals (Salamanca and Toledo). Nova Hedwigia 57, 239-253.

Ortega-Calvo, J.J., Ariño, X., Hernandez-Marine, M., Saiz-Jimenez, C., 1995. Factors affecting the weathering and colonization of monuments by phototrophic microorganisms. Science of the Total Environment 167, 329-341.

Ortega-Calvo, J.J., Saiz-Jimenez, C., 1997. Microbial degradation of phenanthrene in two European cathedrals. FEMS Microbiology Ecology 22, 95-101.

Paerly, H.W., Bebout, B.M., Prufert, L.E., 1989. Bacterial associations with marine *Oscillatoria* sp. (*Trichodesmiun* sp.) populations: ecophysiological implications. Journal of Phycology 25, 773-784.

Pantazidou, A., Theoulakis, P., 1997. Cyanophytes and associated flora at the neoclassical Palace of Sts George and Michael in Corfu (Greece). Aspects of cleanning procedures. In: Moropoulou, A., Zezza, F., Kollias, E., Papachistodoulou, I. (eds), Proceedings of the 4th International Symposium on the Conservation of Monuments in the Mediterranean Basin, Rhodes, Technical Chamber of Greece, pp. 355-368.

Papida, S., Murphy, W., May, E., 2000. Enhancement of physical weathering of building stones by microbial populations. International Biodeterioration and Biodegradation 46, 305-317.

Parsons, T.R., Strickland, J.D.H., 1963. Discussion of spectrophotometric determination of marine pigments with revised equations for ascertaining chlorophylls and carotenoids. Journal of Marine Research 21, 155-63.

Pearson, K., 1901. On lines and planes of closest fit to systems of points in space. Philosophical Magazine 2, 559-572.

Pentecost, A., 1992. Growth and distribution of endolithic algae in some North Yorkshire streams (UK). European Journal of Phycology 27, 145-151.

Pereira de Oliveira, B., 2008. Caracterização de filmes negros em pedras graníticas. O caso de estudo da Igreja da Venerável ordem Terceira de São Francisco.

MScE thesis, Universidade Nova de Lisboa, Portugal.

Pereira de Oliveira, B., Miller, A., Sequeira Braga, M.A., Macedo, M.F., Dionísio, A., Silveira, T., 2008. Characterization of dark films in granites. The case study of Igreja da Ordem de São Francisco in Oporto (Portugal). In: Urzì, C. (Ed), Proceedings of the 14th Interational Biodeterioration and Biodegradation Symposium, Messina (Italy), International Biodeterioration and Biodegradation Society, p. 72.

Pereira de Oliveira, B., Dionísio, A., Sequeira Braga, M.A., Miller, A., Macedo, M. F., Silveira, T., 2009. A contribuição da comunidade microbiológica nos processos de decaimento do granito. O caso de estudo da Igreja dos Terceiros da Ordem de São Francisco (Porto, Portugal). Cadernos do Laboratório Xeolóxico de Laxe 34, 75-88.

Pietrini, A.M., Ricci, S., Bartolini, M., Giuliani, M.R., 1985. A reddish colour alteration caused by algae on stoneworks. Preliminary studies. In: Felix, G. (Ed), Proceedings of the 5th International Congress on Deterioration and Conservation of Stone, Lausanne (Switzerland), Presses Polytechniques Romandes, pp. 653-662.

Piñar, G., Saiz-Jimenez, C., Schabereiter-Gurtner, C., Blanco-Varela, M.T., Lubitz, W., Rölleke, S., 2001. Archaeal communities in two disparate deteriorated ancient wall paintings: detection, identification and temporal monitoring by denaturing gradient gel electrophoresis. FEMS Microbiology Ecology 37, 45-54.

Piñar, G., Laiz, L., Lubitz, W., Saiz-Jimenez, C., 2002. Estudio comparativo de comunidades bacterianas en monumentos mediante tecnicas moleculares y microbiologicas. In: Saiz-Jimenez, C., Videla, H.A. (Eds), Biodeterioro de Monumentos de Iberoamérica, CYTED, Spain, pp. 57–79.

Pinhassi, J., Simó, R., González, J.M.,Vila, M., Alonso-Sáez, L., Kiene, R.P., Moran, M.A., Pedrós-Alió, C., 2005. Dimethylsulfoniopropionate turnover is linked to the composition and dynamics of the bacterioplankton assemblage during a microcosm phytoplankton bloom. Applied and Environmental Microbiology 71, 7650-7660.

Pitzurra, L., Moroni, B., Nocentini, A., Sbaraglia, G., Poli, G., Bistoni, F., 2002. Microbial growth amd air pollution in carbonate rock weathering. International Biodeterioration and Biodegradation 52, 63-68.

Pohl, W., Schneider, J., 2002. Impact of endolithic biofilms on carbonate rock

surfaces. In: Siegesmund, S., Weiss, T., Vollbrecht, A. (Eds), Natural Stone, Weathering Phenomena, Conservation Strategies and Case Studies. Geological Society, London, Special Publications 205, 177-194.

Póvoas, I., Barral, M.F., 1992. Métodos de análise de solos. Série de ciências agrárias nº 10. Instituto de Investigação Científica Tropical, Ministério de Planeamento e da Administração do Território, Lisboa, Portugal.

Powers, R.W., 1962. Arabian Upper Jurassic carbonate reservoir rocks. In: Ham, W.E., (ed), Classification of Carbonate Rocks. American Association of Petroleum Geologists Memoir 1, pp. 122-192.

Prakash, B., Veeregowda, B.M., Krishnappa, G., 2003. Biofilms: A survival strategy of bacteria. Current Science 85, 1299-1307.

Prieto, B., Silva, B., Rivas, T., Wierzchos, J., Ascaso, C., 1997. Mineralogical transformation and neoformation in granite caused by the Lichens *Tephromela atra* and *Ochrolechia parella*. International Biodeterioration and Biodegradation 40, 191-199.

Prieto, B., Silva, B., 2005. Estimation of the potential bioreceptivity of granitic rocks from their intrinsic properties. International Biodeterioration and Biodegradation 56, 206-215.

Prieto, B., Silva, B., Aira, N., Álvarez, L., 2006. Toward a definition of a bioreceptivity index for granitic rocks: Perception of the change in appearance of the rock. International Biodeterioration and Biodegradation 58, 150-154.

Rezaee, M.R., Jafari, A., Kazemzadeh, E., 2006. Relationships between permeability, porosity and pore throat size in carbonate rocks using regression analysis and neural networks. Journal of Geophysics and Engineering 3, 370-376.

Ricci, S., Pietrini, A.M., 1994. Caratterizzazione della microflora algale presente sulla Fontana dei Quattro Fiumi, Roma. In: Fassina, V., Ott, H., Zezza, F. (Eds), Proceedings of the 3rd International Symposium on the conservation of monuments in the Mediterranean Basin, Venice, Soprintendenza ai Beni Artistici e Storici di Venezia, pp. 353-357.

Robert, M., 1993. Rôle du facteur biologique dans la dégradation des roches et des monuments. In: Vincente Hernández, M.A., Molina Ballesteros, E., Rives Arnau, V. (Eds), Actas del workshop: Alteración de granitos y rocas afines, empleados como materiales de contrucción, CSIC, Madrid, pp. 103-115.

Rodriguez-Navarro, C., Sebastian, E., 1996. Role of particulate matter from vehicle exhaust on porous building stones (limestone) sulfation. Science of the Total Environment 187, 79-91.

Rodríguez-Navarro, C., Sebastián, E., Doehne, E., Ginell, W.S., 1998. The role of sepiolite-palygorskite in the decay of ancient egyptian limestone sculptures. Clays and Clay Minerals 46, 414-422.

Roeselers, G., Zippel, B., Staal, M., Van Loosdrecht, M., Muyzer, G., 2006. On the reproducibility of microcosm experiments - Different community composition in parallel phototrophic biofilm microcosms. FEMS Microbiology Ecology 58, 169-178.

Rogerio-Candelera, M.A., 2008. Una propuesta no invasiva para la documentación integral del arte rupestre. MScE thesis, Universidad de Sevilla, Spain.

Rogerio-Candelera, M.A., Laiz, L., Saiz-Jimenez, C., 2008a. Una experiencia de laboratorio para la separación de cubiertas en la documentación de pinturas rupestres y murales afectadas por biodeterioro. In: Saiz-Jimenez, C., Rogerio-Candelera, M.A. (Eds) Novena Reunión de la Red Temática del CSIC de Patrimonio Histórico y Cultural “Avances recientes en la investigación sobre Patrimonio”, Sevilla, pp. 71-72.

Rogerio-Candelera, M.A., Laiz, L., González, J.M., Saiz-Jimenez, C., 2008b. Monitorización del crecimiento microbiano en una tumba romana mediante técnicas de teledetección. Actas del VII Congreso Ibérico de Arqueometría, CSIC, Madrid.

Roldan, M., Clavero, E., Hernández-Marine, M., 2003. Aerophytic biofilms in dim habitats. In: Saiz-Jiménez, C. (Ed), Molecular biology and cultural heritage. A.A. Balkema, Lisse, pp. 163-169.

Roldán, M., Clavero, E., Castel, S., Hernández-Mariné, M., 2004. Biofilms fluorescence and image analysis in hypogean monuments research. Algological Studies 111, 127-143.

Roldán, M., Oliva, F., Gónzalez Del Valle, M.A., Saiz-Jimenez, C., Hernández-Mariné, M., 2006. Does green light influence the fluorescence properties and structure of phototrophic biofilms? Applied and Environmental Microbiology 72, 3026-3031.

Rölleke, S., Muyzer, G., Wawer, C., Wanner, G., Lubitz, W., 1996. Identification of bacteria in a biodegraded wall painting by denaturing gel electrophoresis of

PCR-amplified gene fragments coding 16S rRNA. Applied and Environmental Microbiology 62, 2059-2065.

Romão, P., Prudêncio, M.I., Trindade, M.J., Nasraoui, M., Gouveia, M.A., Figueiredo, M.O., Silva, T., 2000. The S. Sebastião Church of Terceira Island (Azores, Portugal) - Characterization of the stones and their biological colonization. 9th International Congress on Deterioration and Conservation of Stone, Elsevier, Venice, pp. 493-497.

Rossmoore, H.W. (Ed), 1991. Biodeterioration and Biodegradation 8, Elsevier, London.

Sabbioni, C., 2003. Mechanisms of Air Pollution Damage to Stone. In: Bimblecombe, P. (Ed), The effects of air pollution on the built environment, Air pollution reviews, Vol. 2, Imperial College Press, pp. 63-106.

Saiz-Jimenez, C., Garcia-Rowe, J., Garcia del Cura, M.A., Ortega-Calvo, J.J., Roekens, E., Van Grieten, R., 1990. Endolithic cyanobacteria in Maastricht limestone. Science of the Total Environment 94, 209-220.

Saiz-Jimenez, C., Hermosin, B., Ortega-Calvo, J.J., Gómez-Alarcón, G., 1991. Applications of analytical pyrolysis to the study of stony cultural properties. Journal of Analytical and Applied Pyrolysis 20, 239-521.

Saiz-Jimenez, C., 1993. Deposition of airborne organic pollutants on historic buildings. Atmospheric Environment - Part B Urban Atmosphere 27 B, 77-85.

Saiz-Jimenez, C., 1995. Deposition of anthropogenic compounds on monuments and their effect on airborne microorganisms. Aerobiologia 11, 161-175.

Saiz-Jimenez, C., Ariño, X., Ortega-Calvo, J.J. 1995. Mechanisms of stone biodeterioration by photosynthesis-based epilithic biofilms. In: De Cleene, M., (Ed). Interactive physical weathering and bioreceptivity study on building stones, monitored by Computerized X-Ray Tomography (CT) as a potential non-destructive research tool. Protection and Conservation of the European Cultural Heritage Research Report N° 2. European Commission, Directorate-General XII, Brussels, pp. 25-62.

Saiz-Jimenez, C., 1999. Biogeochemistry of weathering processes in monuments. Geomicrobiology Journal 16, 27-37.

Saiz-Jimenez, C. (ed.), 2003. Molecular biology and cultural heritage. A.A. Balkema, Lisse, 287p.

Salomon, P.S., Janson, S., Granéli, E., 2003. Molecular identification of bacteria

associated with filaments of *Nodularia spumigena* and their effect on the cyanobacterial growth. Harmful Algae 2, 261-272.

Salvadori, O., Sorlini, C., Zanardini, E., 1994. Microbiological and biochemical investigations on stone of the Ca' d'Oro facade (Venice). In: Fassina, F., Ott, V., Zezza, F. (Eds), Proceedings of the 3rd International Symposium on the conservation of monuments in the Mediterranean Basin, Venice, Soprintendenza ai Beni Artistici e Storici di Venezia, pp. 343-347.

Salvadori, O., 2000. Characterization of endolithic communities of stone monuments and natural outcrops. In: Ciferri, O., Tiano, P., Mastromei, G. (Eds), Of Microbes and Art – The role of microbial communities in the degradation and protection of cultural heritage, Kluwer Academic, New York, pp. 89-101.

Sànchez-Moral, S., Bedoya, J., Luque, L., Cañaveras, J.C., Jurado, V., Laiz, L., Saiz-Jimenez, C. 2003. Biomineralization of different crystalline phases by bactéria isolated from catacombs. In: Saiz-Jimenez, C. (Ed), Molecular biology and cultural heritage, Swets & Zeitlinger, Lisse, pp. 179-185.

Sanchez-Moral, S., Luque, L., Cuezva, S., Soler, V., Benavente, D., Laiz, L., Gonzalez, J.M., Saiz-Jimenez, C., 2005. Deterioration of building materials in Roman catacombs: The influence of visitors. Science of the Total Environment 349, 260-276.

Sand, W., 1997. Microbial mechanisms of deterioration of inorganic substrates - A general mechanistic overview. International Biodeterioration and Biodegradation 40, 183-190.

Santos, M.F.A., 2003. Optical microscopy of the microbial samples collected on the cloisters of church of Santa Cruz in Coimbra (Portugal). Internal Report, Coimbra, Universidade de Coimbra (Portugal).

Sarró, M.I., Garcia, A.M., Rivalta, V.M., Moreno, D.A., Arroyo, I., 2006. Biodeterioration of the Lions Fountain at the Alhambra Palace, Granada (Spain). Building and Environment 41, 1811-1820.

Scardino, A.J., Harvey, E., De Nys, R., 2006. Testing attachment point theory: diatom attachment on microtextured polyimide biomimics. Biofouling 22, 55-60.

Scardino, A.J., Guenther, J., De Nys, R., 2008. Attachment point theory revisited: the fouling response to a microtextured matrix. Biofouling 24, 45-53.

Schabereiter-Gurtner, C., Piñar, G., Lubitz, W., Rölleke, S., 2001. An advanced molecular strategy to identify bacterial communities on art objects. Journal of

Microbiological Methods 45, 77-87.

Schumann, R., Häubner, N., Klausch, S., Karsten, U., 2005. Chlorophyll extraction methods for the quantification of green microalgae colonizing building facades. International Biodeterioration and Biodegradation 55, 213-222.

Schuhr, W., Kanngieser, E., 1999. Single images in conservation. In: XVII CIPA International Sympsium. Olinda, Brasil, 3-6 October 1999. [On-line: http://cipa.icomos.org/fileadmin/papers/olinda/99c803.pdf visit: 10/10/2006].

Schuhr, W., Kanngieser, E., 2001. Modern methods for using single images in conservation. In: XVIII CIPA International Symposium. Potsdam, Germany. [On-line: http//cipa.icomos.org/fileadmin/papers/potsdam/2001-13-ws01.pdf visit: 30/10/2006].

Schuhr, W., Kanngieser, E., 2003. New perspectives for single images in conservation. In: XIX CIPA International Symposium "New perspectives to save Cultural Heritage", 30 Sep-04 Oct 2003. Antalya, Turkey. [On-line: http://cipa.icomos.org/fileadmin/papers/antalya/62.pdf visit: 28/10/2006].

Shirakawa, M.A., Beech, I.B., Tapper, R., Cincotto, M.A., Gambale, W., 2003. The development of a method to evaluate bioreceptivity of indoor mortar plastering to fungal growth. International Biodeterioration and Biodegradation 51, 83-92.

Shoaf, W.T., Lium, B.W., 1976. Improved extraction of chlorophyll *a* and *b* from algae using dimethyl sulfoxide. Limnology Oceanography 21, 926-928.

Silva, B., Prieto, B., Rivas, T., Sanchez-Biezma, M.J., Paz, G., Carhallal, R., 1997. Rapid biological colonization of a granitic building by lichens. International Biodeterioration and Biodegradation 40, 263-267.

Silva, Z.C., 2007. O Lioz Português. De lastro de navio a arte na Bahia. Edições Afrontamento, Porto.

Smith, B.J., 2003. Background controls on urban stone decay: lessons from natural rock weathering. In: Bimblecombe, P. (Ed), The effects of air pollution on the built environment, Air pollution reviews, Vol. 2, Imperial College Press, pp.31-61.

Sousa, L.M.O., Suárez del Río, L.M., Calleja, L., Ruiz de Argandoña, V.G., Rodríguez Rey, A., 2005. Influence of microfractures and porosity on the physico-mechanical properties and weathering of ornamental granites. Engineering Geology 77, 153-168.

Stal, L.J., Gemerden, H., Krumbein, W.E., 1984. The simultaneous assay of

chlorophyll and bacteriochlorophyll in natural microbial communities. Journal of Microbiological Methods 2, 295-306.

Sterflinger, K., Krumbein W.E., 1997. Dematiacous fungi as a major agent of biopitting for Mediterranean marbles and limestones. Geomicrobiology Journal 14, 219-231.

Sutherland, I.W., 2001. Biofilm exopolysaccharides: a strong and sticky framework. Microbiology 147, 3-9.

Talling, J.F., Driver, D., 1963. Some problems in the estimation of chlorophyll a in phytoplankton. In: Doty, M.S. (Ed), Conference of primary productivity measurement, marine and freshwater, Atomic Energy Comm, U.S., pp. 142-146.

Tiano, P., Accolla, P., Tomaselli, L., 1995. Phototrophic biodeteriogens on lithoid surfaces: An ecological study. Microbial Ecology 29, 299-309.

Tiano, P., 1998. Biodeterioration of Monumental rocks: decay mechanisms and control methods. Science and Technology for Cultural Heritage 7, 19-38.

Tomaselli, L., Tiano, P., Lamenti, G., 2000a. Occurrence and fluctuation in photosynthetic biocoenoses dwelling on stone monuments. In: Ciferri, O., Tiano, P., Mastromei, G. (Eds), Of Microbes and Art – The role of microbial communities in the degradation and protection of cultural heritage, Kluwer Academic, New York, pp. 63-76.

Tomaselli, L., Lamenti, G., Bosco, M., Tiano, P., 2000b. Biodiversity of photosynthetic micro-organisms dwelling on stone monuments. International Biodeterioration and Biodegradation 46, 251-258.

Tomaselli, L., Lamenti, G., Tiano, P., 2002. Chlorophyll fluorescence for evaluating biocide treatments against phototrophic biodeteriogens. Annals of Microbiology 52, 197-206.

Tomaselli, L., 2003. Biodeterioration processes on inorganic substrata. Coalition 6, 5-9.

Urzì, C., Krumbein, W.E., Warscheid, T., 1991. On the question of biogenic colour changes of mediterranean monuments. In: Decrouez, D., Chamay, J., Zezza, F. (Eds), The Conservation of Monuments in the Mediterranean Basin, pp. 397-420.

Urzì, C., Krumbein, W.E., 1994. Microbial impacts on the cultural heritage. In Krumbein, W.E., Brimblecombe, P., Cosgrove, D. E., Stainford, S. (Eds),

Durability and changes: The Science, Responsibility, and Cost of Sustaining Cultural Heritage. Wiley, New York, pp. 107-135.

Urzì, C., Realini, M., 1998. Colour changes of Noto's calcareous sandstone as related to its colonisation by microorganisms. International Biodeterioration and Biodegradation 42, 45-54.

Urzì, C., Albertano, P., 2001. Studying phototrophic and heterotrophic microbial communities on stone monuments. Methods in Enzymology 336, 340-355.

Urzì, C., De Leo, F., Salamonee, P., Criseo, G., 2001. Airborne fungal spores colonising marbles exposed in the terrace of Mesina Museum, Sicily. Aerobiologica 17, 11-17.

Urzì, C., La Cono, V., De Leo, F., Donato, P., 2003. Fluorescent *In Situ* Hybridization (FISH) to study biodeterioration in cultural heritage. In: Saiz-Jimenez, C. (Ed), Molecular biology and cultural heritage, A.A. Balkema, Lisse, pp. 55-60.

Vicent Garcia, J.M., Montero Ruiz, I., Rodriguez Alcalde, A.L., Martinez Navarrete, M.I., Chapa Brunet, T., 1996. Aplicación de la imagen multiespectral al estudio y conservación del arte rupestre postpaleolítico. Trabajos de Prehistoria 53, 19-35.

Vollenweider, R.A., Talling, J.F., Westlake, D.F., (Eds), 1974. A Manual on Methods for Measuring Primary Production in Aquatic Environments, 2nd edition, Blackwell, Oxford, UK.

Wakefield, R.D., Jones, M.S., 1998. An introduction to stone colonizing micro-organisms and biodeterioration of building stone. Quarterly Journal of Engineering Geology 31, 301-313.

Walker, J.J., Spear, J.R., Pace, N.R., 2005. Geobiology of a microbial endolithic community in the Yellowstone geothermal environment. Nature 434, 1011-1014.

Ward, D.M., Weller, R., Bateson, M.M., 1990. 16S rRNA sequences reveal numerous uncultured microorganisms in a natural community. Nature 345, 63-65.

Warren-Rhodes, K., Rhodes, K., Pointing, S., Ewing, S., Lacap, D., Gómez-Silva, B., Amundson, R., Friedmann, E., McKay, P., 2006. Hypolithic cyanobacteria, dry limit of photosynthesis, and microbial ecology in the hyperarid Atacama Desert. Microbial Ecology 52, 389-398.

Warscheid, T., Oelting, M., Krumbein, W.E., 1991. Physico-chemical aspects of

biodeterioration processes on rocks with special regard to organic pollutants. International Biodeterioration 28, 37-48.

Warscheid, T., 2000. Integrated concepts for the protection of cultural artifacts against biodeterioration. In: Ciferri, O., Tiano, P., Mastromei, G. (Eds) Of microbes and Art – The role of microbial communities in the degradation and protection of cultural heritage, Kluwer Academic, New York, pp. 185-201.

Warscheid, T., Braams, J., 2000. Biodeterioration of stone: A review. International Biodeterioration and Biodegradation 46, 343-368.

Weisburg, W.G., Barns, S.M., Pelletier, D.A., Lane, D.J., 1991. 16S Ribosomal DNA Amplification for Phylogenetic Study. Journal of Bacteriology 173, 697-703.

Welton, R.G., Ribas Silva, M., Gaylarde, C., Herrera, L.K., Anleo, X., De Belie, N., Modrý, S., 2005. Techniques applied to the study of microbial impacto n building materials. Materials and Structures 38, 883-893.

Wierzchos, J., Ascaso, C., 1994. Application of backscattered electron imaging to the study of the lichen-rock interface. Journal of Microscopy-Oxford 175, 54-59.

Wierzchos, J., De los Rios, A., Sancho, L.G., Ascaso, C., 2004. Viability of endolithic micro-organisms in rocks from the McMurdo Dry Valleys of Antarctica established by confocal and fluorescence microscopy. Journal of Microscopy-Oxford 216, 57-61.

Wierzchos, J., Ascaso, C., McKay, C.P., 2006. Endolithic cyanobacteria in halite rocks from the hyperarid core of the Atacama Desert. Astrobiology 6, 1-8.

Wilderer, P.A., Characklis, W.G., 1989. Structure and function of biofilms. In: Characklis, W.G., Wildener, P.A. (Eds), Structure and Function of Biofilms, Wiley, Chichester, pp. 5-17.

Wilmotte, A., 1994. Molecular evolution and taxonomy of the cyanobacteria. In: Bryant, D.A. (Ed.), The Molecular Biology of Cyanobacteria. Kluwer, Dordrecht, pp. 1-25.

Wimpenny, J., Manz, W., Szewzyk, U., 2000. Heterogeneity in biofilms. FEMS Microbiology Reviews 24, 661-671.

Wollenzien, U., De Hoog, G.S., Krumbein, W.E., Urzi, C., 1995. On the isolation of microcolonial fungi occurring on and in marble and other calcareous rocks. Science of the Total Environment 167, 287-294.

Wun, C., Lltsky, W., 1982. Rapid Determination of Algal Chlorophyll by Gas-Liquid Chromatography. Environmental Science and Technology 16, 335-338.

Yentsch, C.S., Menzel, D.W., 1963. A method for determination of chlorophyll and phaeophytin by fluorescence. Deep-Sea Research 10, 221-31.

Young, M.E., Alakomi, H.L., Fortune, I., Gorbushina, A.A., Krumbein, W.E., Maxwell, I., McCullagh, C., Robertson, P., Saarela, M., Valero, J., Vendrell, M., 2008. Development of a biocidal treatment regime to inhibit biological growths on cultural heritage: BIODAM. Environmental Geology 56, 631-641.

Zagari, M., Antonelli, F., Urzi, C., 2000. Biological patinas on the limestone of the Loches Romanic Tower (Touraine, France). In: Fassina, V. (Ed), 9th International Congress on Deterioration and Conservation of Stone, Elsevier, Venice, pp. 445 - 451.

Zhang, X.Q., Bishop, P.L., Kupferle, M.J., 1998. Measurement of polysaccharides and proteins in biofilm extracellular polymers. Water Science and Technology 37, 345-348.

Zimmermann, J., Gonzalez, J.M., Saiz-Jimenez, C., Ludwig, W., 2005. Detection and phylogenetic relationships of highly diverse uncultured acidobacterial communities in Altamira Cave using 23S rRNA sequence analyses. Geomicrobiology Journal 22, 379-388.

Zurita, Y.P., Cultrone, G., Castillo, P.S., Sebastián, E., Bolívar, F.C., 2005. Microalgae associated with deteriorated stonework of the fountain of Bibatauín in Granada, Spain. International Biodeterioration and Biodegradation 55, 55-61.

APPENDICES

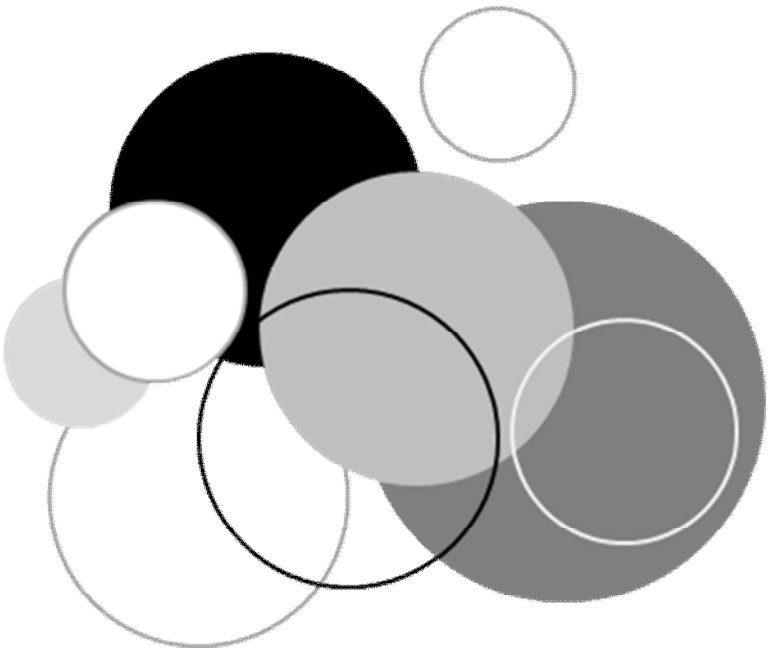

APPENDIX ONE

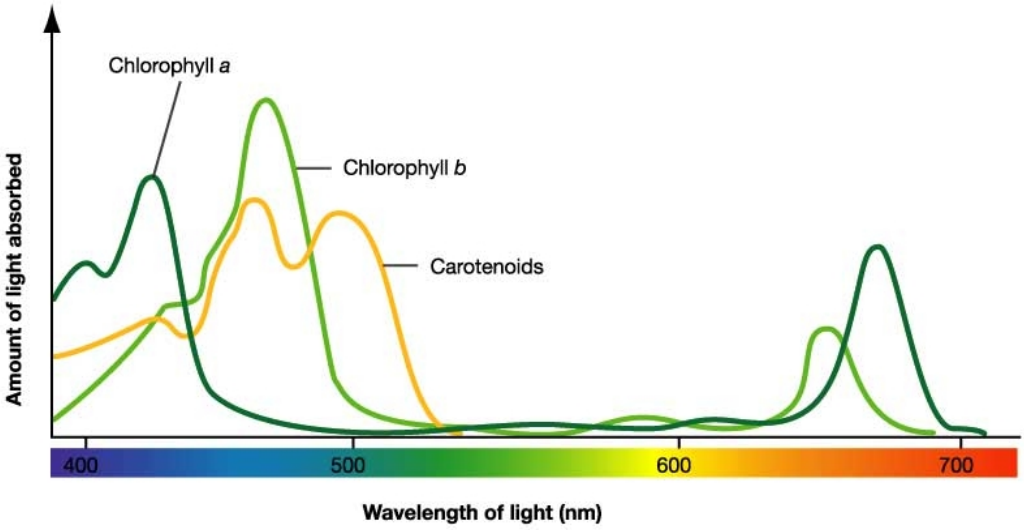

Figure 1. Absorption spectrum of chlorophyll *a*, chlorophyll *b* and carotenoids.

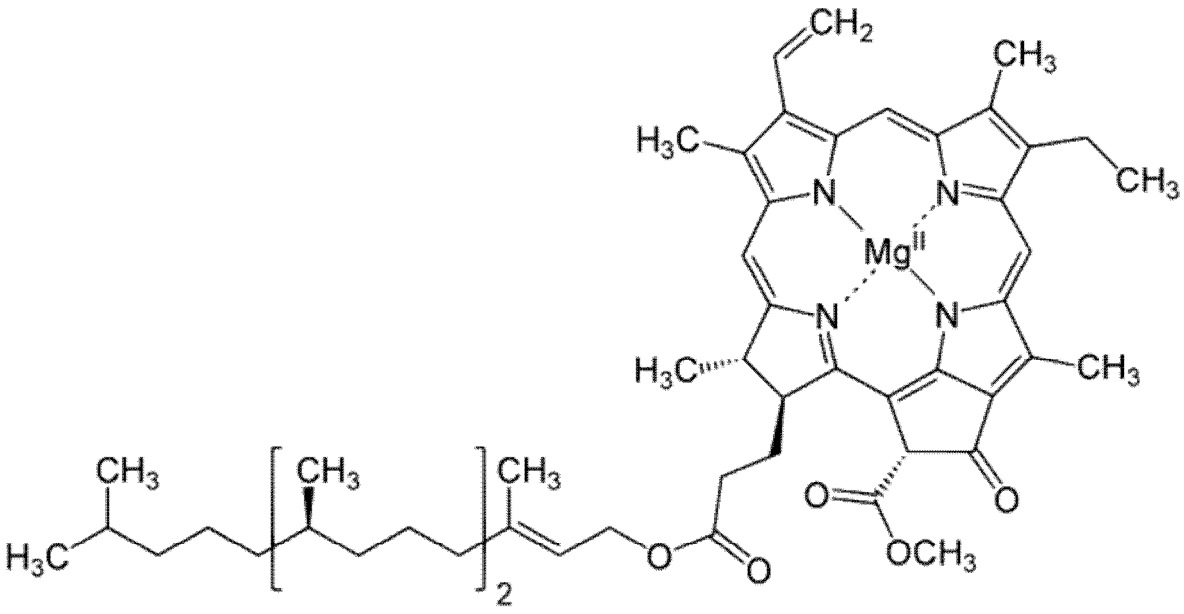

Figure 2. Chlorophyll *a* molecule.

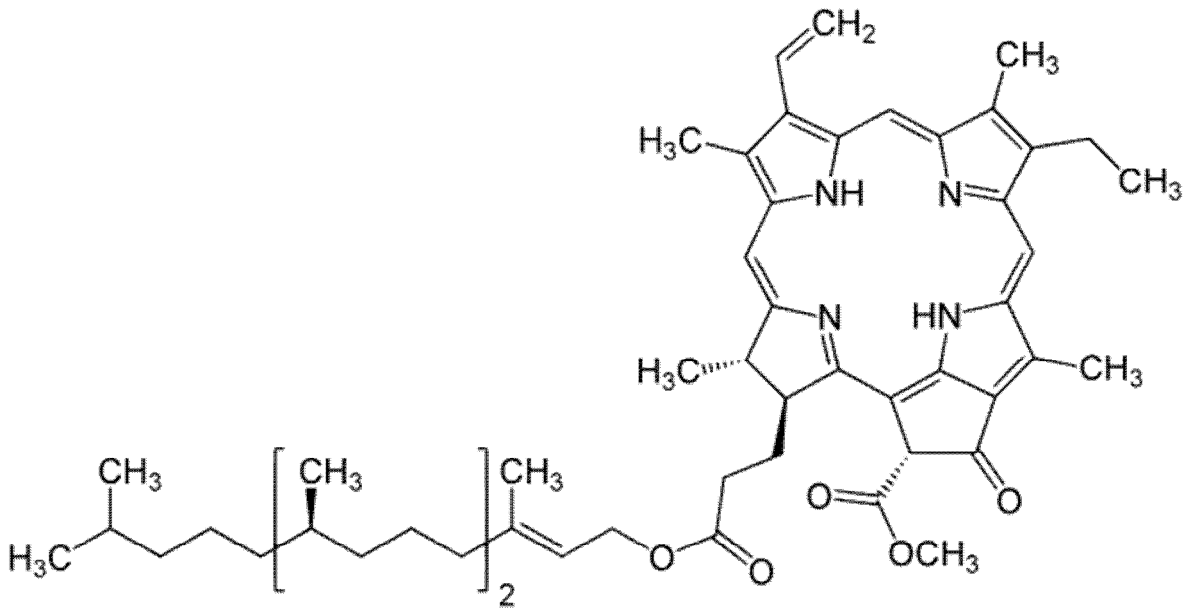

Figure 3. Pheophytin *a* molecule. Pheophytin *a* has the structure similar to chlorophyll *a*, but without the central magnesium metal atom that is substituted with two hydrogen atoms.

APPENDIX TWO

Buffers and solutions

EDTA 0.5M (pH 8.0) solution

- dilution of 0.5 mols (186.1 g) of EDTA (Sigma-Aldrich, MW = 372.24) in distilled water;
- pH is adjusted at 8 by adding NaOH;
- distilled water addition (final volume of 1 L);
- autoclave sterilisation at 121ºC during 15 min.

50x Tris-Acetate-EDTA (TAE) buffer

- Tris(hidroxymethil)-aminomethane 2 M
- Acetic acid glacial (pH 8.2) 1 M
- EDTA (Sigma-Aldrich) 0.1 M
- distilled water addition (final volume of 1 L);
- autoclave sterilisation at 121ºC during 15 min.

0.5x Tris-Acetate-EDTA (TAE) buffer

1:100 (v/v) dilution of 50x TAE buffer

DGGE loading buffer

- Glycerol 50% (v/v) 25 ml
- EDTA 0.5M (pH 8.0) solution 20 ml
- Bromphenol blue, sodium salt (AppliChem, USA) 0.05% (p/v) 25 mg

Agarose gel-loading buffer

- DGGE loading buffer 1 ml
- SYBR GREEN II (Molecular Probes, Eugene, USA) 1 or 2 µ

0% denaturant stock solution

- 40% Acrylamide/Bisacrylamide: 37.5:1; BioRad, Germany) 198 ml
- 50x TAE buffer 10 ml
- distilled water addition (final volume of 1 L)
- Storage at 4ºC

80% denaturant stock solution

- 40% Acrylamide/Bisacrylamide: 37.5:1; BioRad, Germany) 198 ml
- 50x TAE buffer 10 ml
- deionised formamide 32% (v/v)
- Urea (Sigma-Aldrich) 5.6 M
- distilled water addition (final volume of 1 L)
- Storage at 4ºC

10% (w/v) of ammonium persulfate (APS) solution

- APS (Panreac, Spain) 1 g
- Distilled water 10 ml
- Storage at 4ºC

N,N,N',N'-tetramethylethylenediamine (*TEMED)* (Sigma-Aldrich)

- Storage at 4ºC

Culture media

LB medium

- Tryptone 10 g
- Yeast extract 5g
- NaCl 10g
- Agar 20g
- distilled water addition (final volume of 1 L);
- pH is adjusted at 8 by adding NaOH
- autoclave sterilisation at 121ºC during 15 min.

BG11 medium

Macronutrients

- $NaNO_3$ 1.5 g
- $MgSO_4.7H_2O$ 0.075 g
- $CaCl_2.2H_2O$ 0.036 g
- Na citrate 0.006 g
- Na_2CO_3 0.02 g
- K_2HPO_4 0.4 g

Micronutrients

- H_3BO_3 0.0286 g
- $MnCl_2.4H_2O$ 0.018 g
- $ZnSO_4.7H_2O$ 0.0022 g
- $NaMoO_4.2H_2O$ 0.0039 g
- $CuSO_4.5H_2O$ 0.00079 g
- $Co(NO_3)_2.6H_2O$ 0.000494 g

- Agar 20 g
- distilled water addition (final volume of 1 L);

APPENDIX THREE

Concentration of pheophytin present on the studied lithotypes after 30, 60 and 90 days of incubation.

Lithotype	Amount of pheophytin ($\mu g.cm^{-3}$)		
	After 30 days	After 60 days	After 90 days
CA	- 0.95 ± 0.32	- 0.67 ± 0.46	- 0.86 ± 0.09
CL	- 0.70 ± 0.04	- 0.22 ± 0.06	- 0.19 ± 0.12
SC	- 1.17 ± 0.26	- 1.31 ± 0.88	- 1.60 ± 0.48
PF	- 0.87 ± 0.24	- 1.87 ± 0.30	- 2.05 ± 0.64
PL	- 1,47 ± 0.17	- 0.84 ± 0.05	- 0.64 ± 0.14